RAIO-0419-65098

April 05, 2019

Docket No. 52-048

U.S. Nuclear Regulatory Commission
ATTN: Document Control Desk
One White Flint North
11555 Rockville Pike
Rockville, MD 20852-2738

SUBJECT: NuScale Power, LLC Supplemental Response to NRC Request for Additional Information No. 110 (eRAI No. 8932) on the NuScale Design Certification Application

REFERENCES:
1. U.S. Nuclear Regulatory Commission, "Request for Additional Information No. 110 (eRAI No. 8932)," dated July 30, 2017
2. NuScale Power, LLC Response to NRC "Request for Additional Information No. 110 (eRAI No.8932)," dated April 30, 2018
3. NuScale Power, LLC Response to NRC "Request for Additional Information No. 110 (eRAI No.8932)," dated May 22, 2018

The purpose of this letter is to provide the NuScale Power, LLC (NuScale) supplemental response to the referenced NRC Request for Additional Information (RAI).

The Enclosure to this letter contains NuScale's supplemental response to the following RAI Questions from NRC eRAI No. 8932:

- 03.07.02-4
- 03.07.02-6

This letter and the enclosed response make no new regulatory commitments and no revisions to any existing regulatory commitments.

If you have any questions on this response, please contact Marty Bryan at 541-452-7172 or at mbryan@nuscalepower.com.

Sincerely,

Zackary W. Rad
Director, Regulatory Affairs
NuScale Power, LLC

Distribution: Gregory Cranston, NRC, OWFN-8H12
Samuel Lee, NRC, OWFN-8H12
Marieliz Vera, NRC, OWFN-8H12

Enclosure 1: NuScale Supplemental Response to NRC Request for Additional Information eRAI No. 8932

D111
NRO

Enclosure 1:

NuScale Supplemental Response to NRC Request for Additional Information eRAI No. 8932

NuScale Power, LLC
1100 NE Circle Blvd., Suite 200 Corvalis, Oregon 97330, Office: 541.360.0500, Fax: 541.207.3928
www.nuscalepower.com

NUSCALE
Power for all humankind

Response to Request for Additional Information
Docket No. 52-048

eRAI No.: 8932
Date of RAI Issue: 07/30/2017

NRC Question No.: 03.07.02-4

10 CFR 50 Appendix S requires that the safety functions of structures, systems, and components (SSCs) must be assured during and after the vibratory ground motion associated with the Safe Shutdown Earthquake (SSE) through design, testing, or qualification methods.

On Page 3.7-22 of the FSAR, in the second paragraph, to discuss the adequacy of 7P Extended Subtraction Method (ESM) model, the applicant provided 7P versus 9P ISRS comparisons for the Capitola time histories in Figures 3.7.2-8 to10. However, the FSAR does not provide a comparison of transfer functions for the 7P and 9P models. The review of transfer functions is essential to ensure that the numerical implementation of the SSI analysis methods is acceptable and consistent with the guidance in DSRS Section 3.7.2. In the same paragraph, the applicant also states, "This level of agreement justifies using a 7P versus a 9P model and, because the results are similar, demonstrates the acceptability of using the extended subtraction method as an alternative to the direct method." The staff believes that 7P vs 9P ESM comparison captures only an "incremental" enhancement between the two models. The adequacy of an ESM model should be established against the direct method (DM). Therefore, in addition to a comparison of the 7P and 9P ESM models, the applicant is requested to provide a comparison of the transfer functions for the 7P ESM and the DM models at selected nodes of the critical sections and other important locations in the RXB and CRB, or, provide technical justification for why a 7P vs 9P comparison is sufficient and acceptable. Guidance in DSRS Section 3.7.2 allows the use of reduced-size models in comparing the solutions of the subtraction or modified subtraction method (SM/MSM) with those of the DM to gain insight into the adequacy of SM/MSM.

NuScale Response:

The NRC provided the following feedback regarding the August 24, 2018 supplement (ML18236A927) to this request for additional information (RAI) question during the audit of FSAR Sections 3.7 and 3.8 in December of 2018.

1. For the Reactor Building (RXB), benchmarking results appear to show that extended subtraction method (ESM) in-structure response spectra (ISRS) results exceed the direct method (DM) results at few locations by more than 15% (e.g., RAI Figures 67 and 70). Please provide ESM/DM ISRS comparisons at the following locations: NuScale Power Module (NPM) lug and skirt support, Reactor Building crane (RBC) support, spent fuel pool rack locations, and Bioshield support. If the exceedances are greater than 15%, provide a comparison of the DM ISRS with the design basis ISRS.

2. For the RXB, provide a comparison of NPM design basis support loads with those obtained from the DM.

3. For the Control Building (CRB), benchmarking results appear to show that ESM ISRS results exceed the DM results at the technical support center (TSC) (e.g., RAI Figure 8). Please provide ESM/DM ISRS comparisons at the following locations: TSC (Node 38298) and the emergency equipment room (Node 35713). If exceedances are greater than 15%, provide a comparison of the DM ISRS with the design basis ISRS.

4. Include a COL item for the COLA to establish appropriate number of planes for the ESM.

The NRC provided additional feedback during a public meeting on February 26, 2019 as follows:

5. ISRS exceedances should be checked at the following additional locations (other than those already covered in the previous RAI responses):

    a. RXB Crane Support
    b. RXB Bioshield Support
    c. CRB Emergency Equipment Room
    d. CRB TSC Room/MCR

6. It is difficult to accurately quantify the extent and level of ISRS exceedances by looking at Figures only. Therefore, the applicant is requested to provide numerical Tables that indicate

exceedances in terms of percentage (%) of the control cases.

7. Please indicate in the RAI response, a description of the analysis cases involved in the sensitivity study.

Response to Question 1

Background Information, Methodology, and Approach

The methodology used for comparison of the in-structure response spectra (ISRS) data is presented here. The Reactor Building (RXB) direct method (DM) ISRS plots are developed based on 4 percent structural damping and do not require scaling in order to be compared with the corresponding design basis ISRS.

The first step is to compare the DM ISRS with 1.15 times the 7P extended subtraction method (ESM) ISRS. If the DM ISRS plots are bounded by 1.15 times the 7P ESM ISRS, no further action is needed, as this shows an exceedance of less than 15 percent. However, if the DM ISRS is greater than 1.15 times the 7P ESM ISRS, a comparison between the DM ISRS and 1.15 times the peak-broadened 7P ESM ISRS is performed. Subsequently, if the DM ISRS is greater than 1.15 times the peak-broadened 7P ESM ISRS, then comparison with 1.15 times the design basis ISRS is provided. Finally, if the DM ISRS is not bounded by 1.15 times the design basis ISRS, the design basis ISRS plots are updated to account for the identified exceedances.

These steps are summarized in the following flowchart.

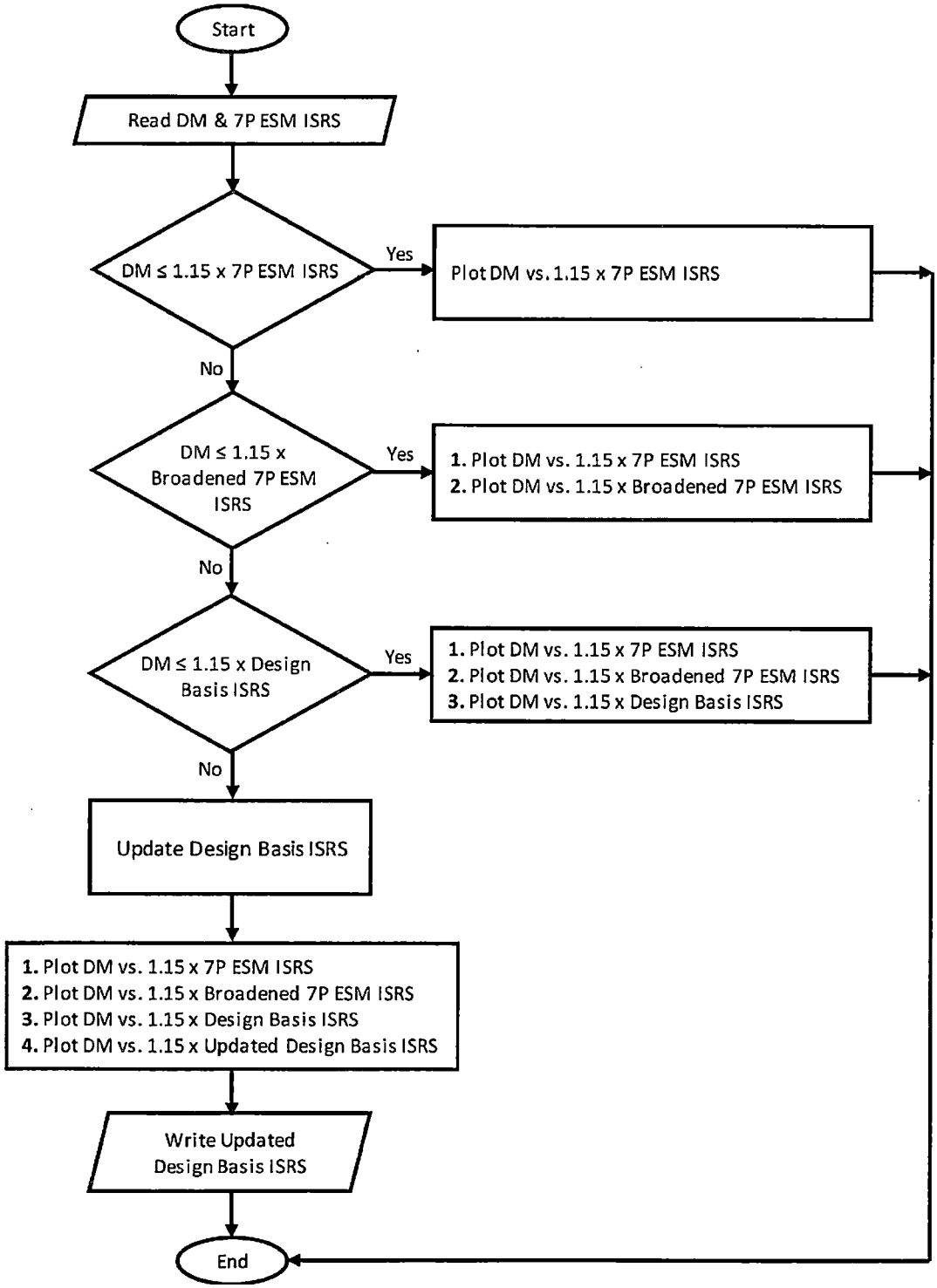

Figure 1. Flowchart for In-Structure Response Spectra Comparison, Direct Method vs. 7P Extended Subtraction Method

Direct Method and 7P Extended Subtraction Method In-Structure Response Spectra Comparison

The following table provides a list of locations where ISRS comparison is performed, as well as a description of the locations.

Table 1. Locations for Direct Method vs. 7P Extended Subtraction Method In-Structure Response Spectra Comparison

Node Number	Direction(s)	Location
4831	X, Y, Z	Top of Basemat within Grid Lines A, B, 4, 5
5642	X, Y, Z	Northeast Corner on Top of Basemat
5846	X, Y, Z	Top of Basemat within Grid Lines B, C, 2, 3
6145	X, Y, Z	RXM 3 Floor Node under Module
16257	Y	RXM 1 Lug Support Locations
16271	X	RXM 1 Lug Support Locations
16287	Y	RXM 1 Lug Support Locations
16621	Y	RXM 6 Lug Support Locations
16635	X	RXM 6 Lug Support Locations
16651	Y	RXM 6 Lug Support Locations
26345	X, Y, Z	Northeast Corner of Bioshield
27649	X, Y, Z	Crane Rail Slab at Grid Line RX-4 at El. 145'-6"

Figure 2 through Figure 12 show the locations of the nodes in the RXB for which DM vs. 7P ESM ISRS comparisons are performed.

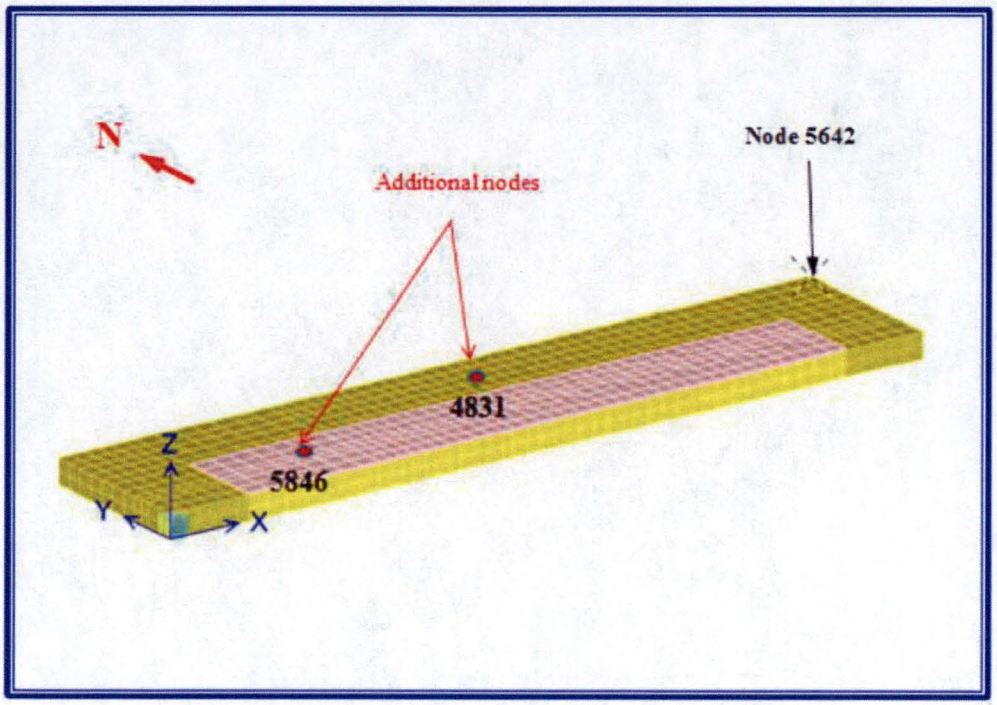

Figure 2. Three Nodes on Top of Basemat

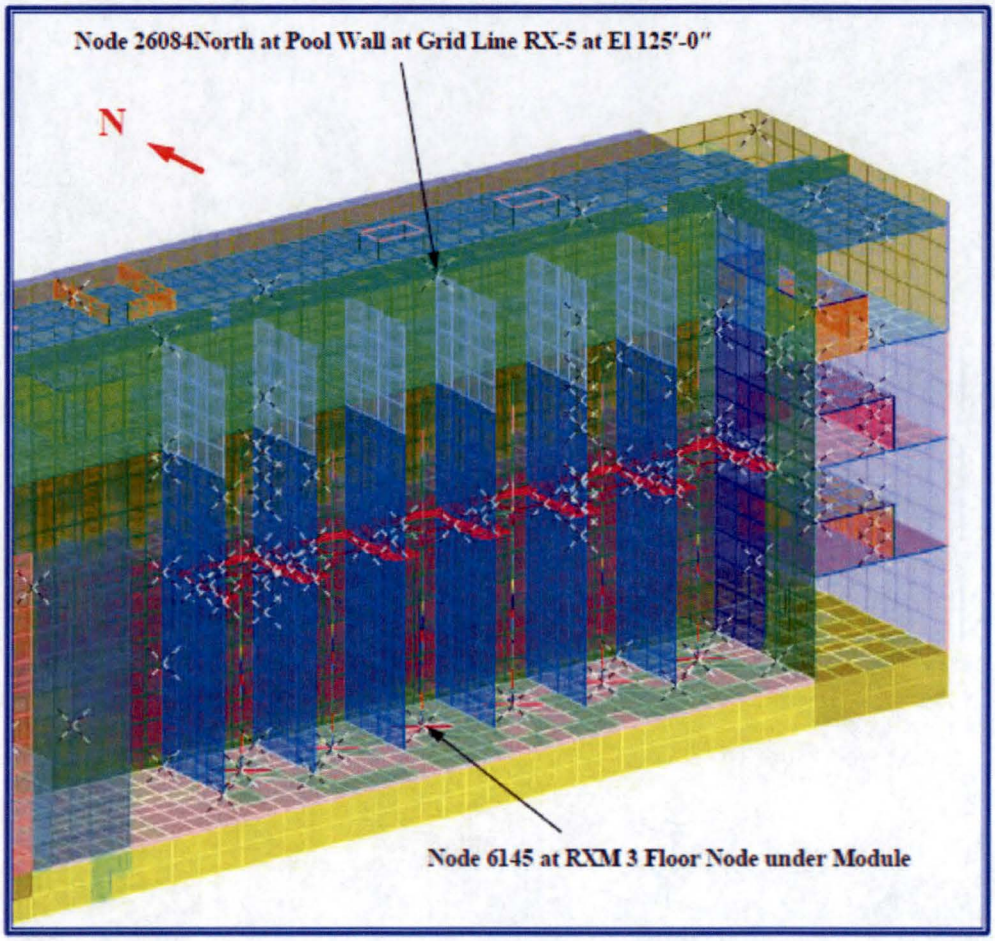

Figure 3. Node 6145 and Node 26084, under Module 3 (Z=132") and at Pool Wall (Z=1320")

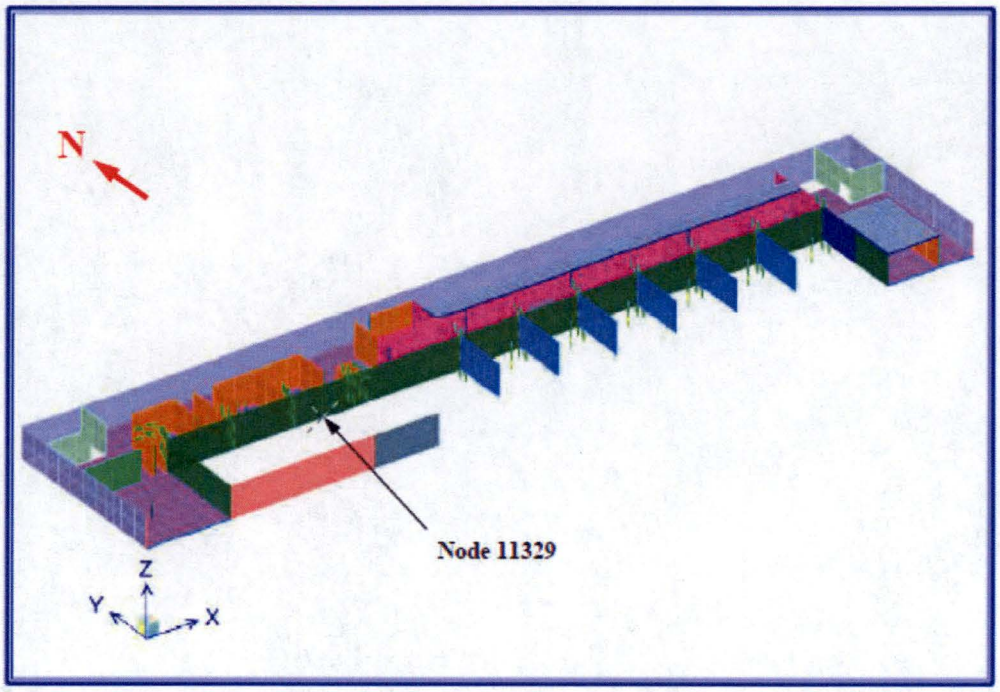

Figure 4. Node 11329 at East Dry Dock Wall, El. 50'-0"- Northeast Corner (Z=420")

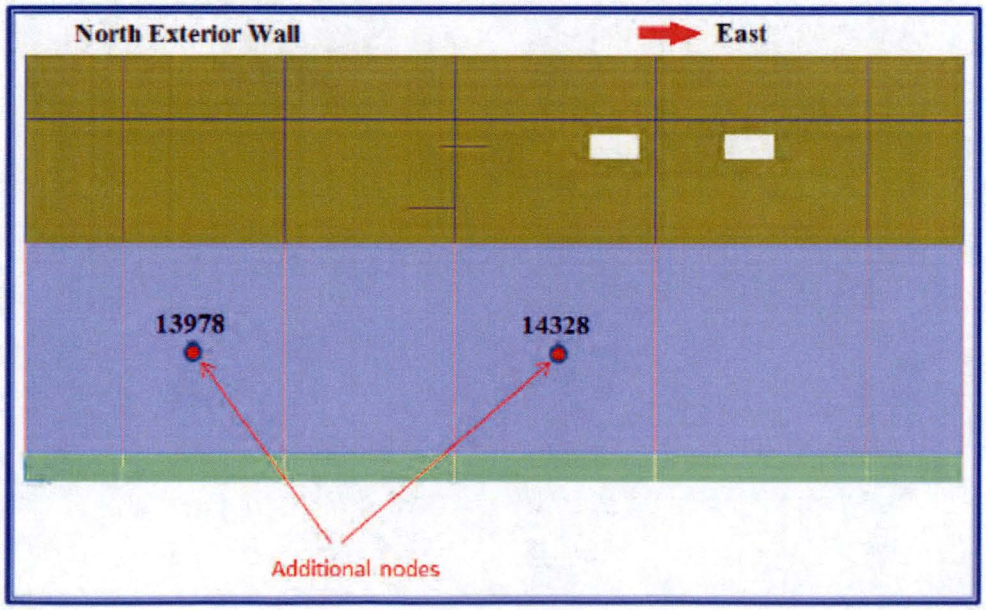

Figure 5. Nodes 13978 and 14328 at North Wall (Z=570")

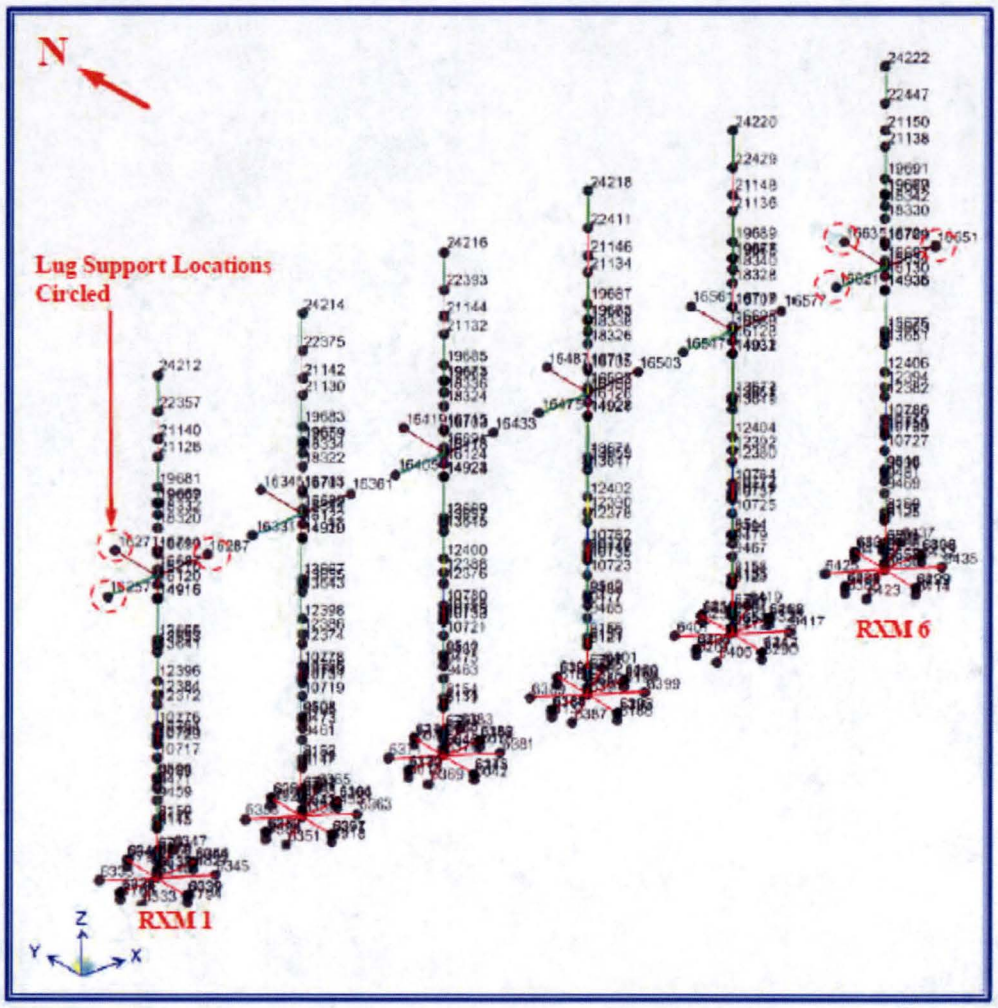

Figure 6. Lug Support Locations at RXM 1 and RXM 6 (Z=673.73")

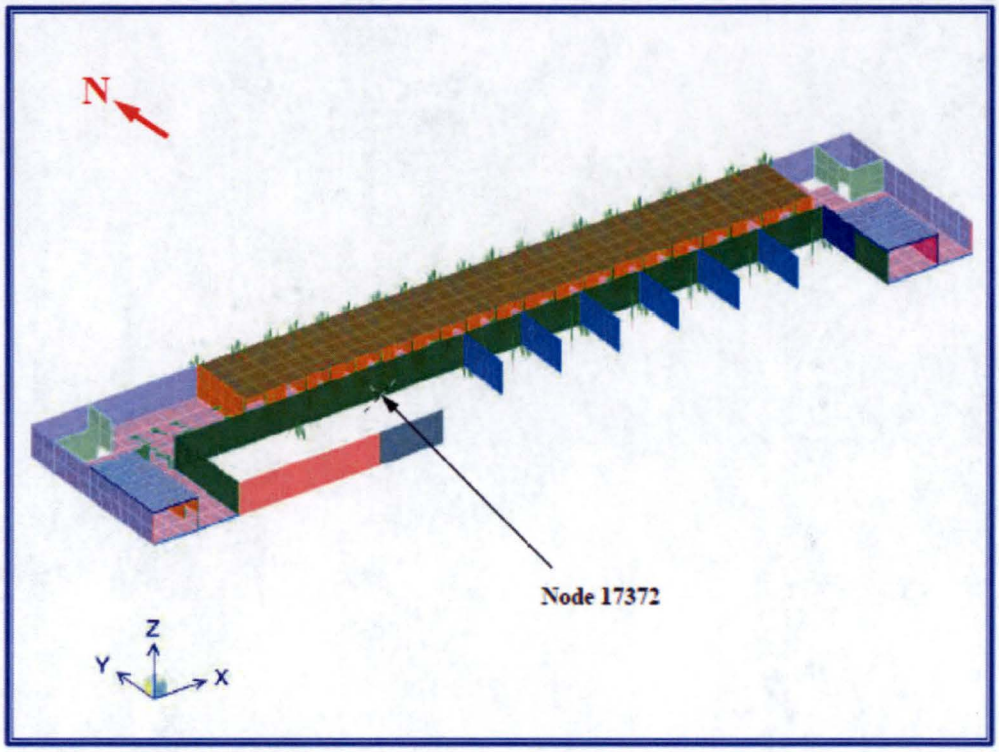

Figure 7. Node 17372 at North Pool Wall between Grid Lines RX-3 and RX-4, El. 75'-0" (Z=720")

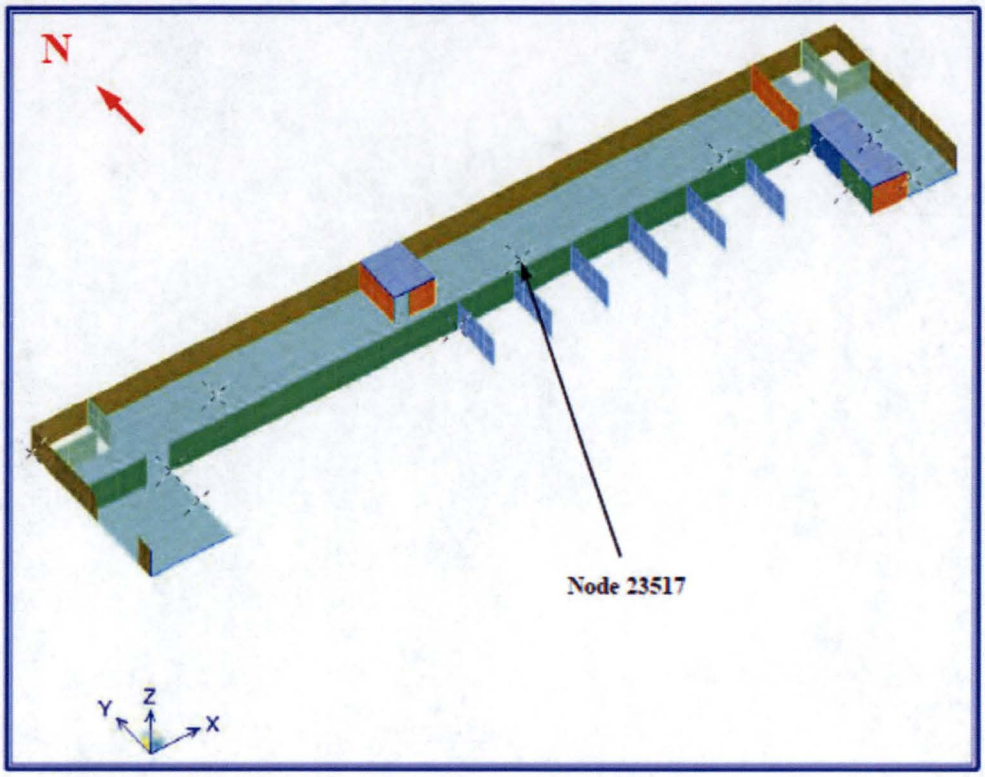

Figure 8. Node 23517 at Mid-Span of North Slab between Grid Lines RX-4 and RX-5, El. 100′-0″ (Z=1020")

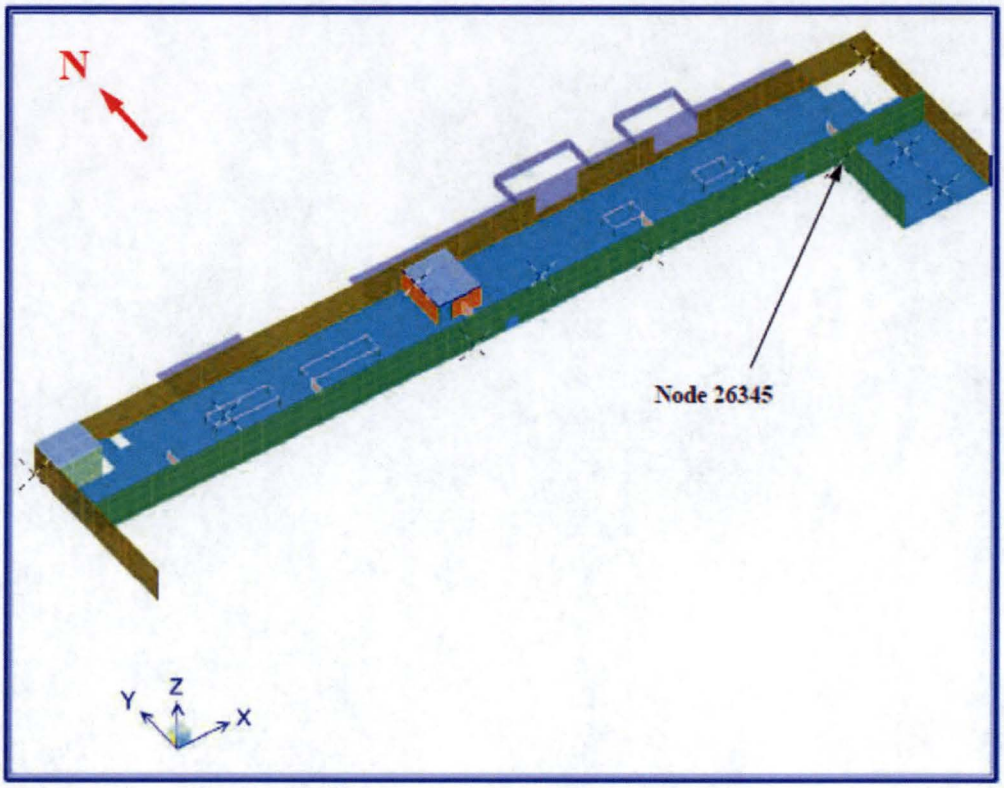

Figure 9. Node 26435 Located at Northeast Corner of Bioshield (Z=1320")

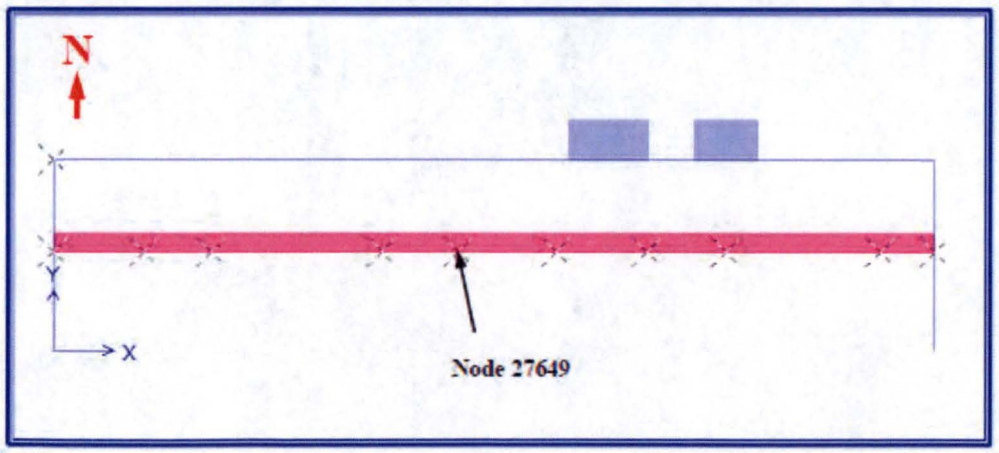

Figure 10. Node 27649 at Crane Rail Slab at Grid Line RX-4, El. 145′-6″ (Z=1548")

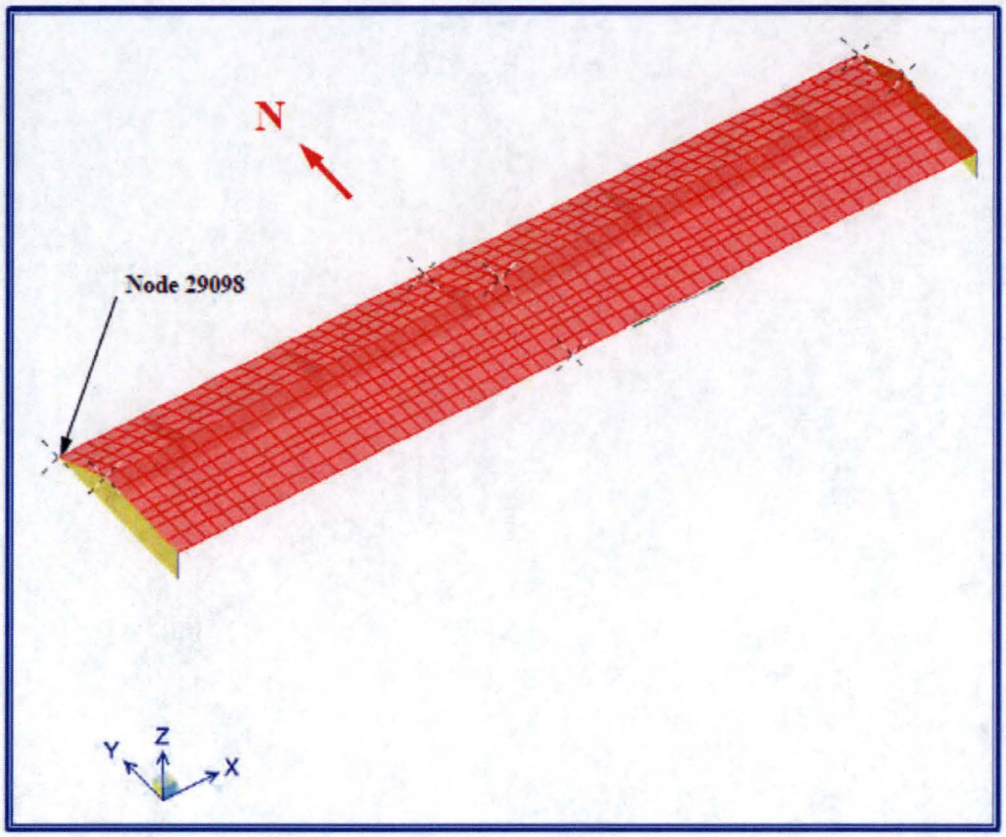

Figure 11. Node 29098 Located at Northwest Corner on Top of North Exterior Wall (Z=1824")

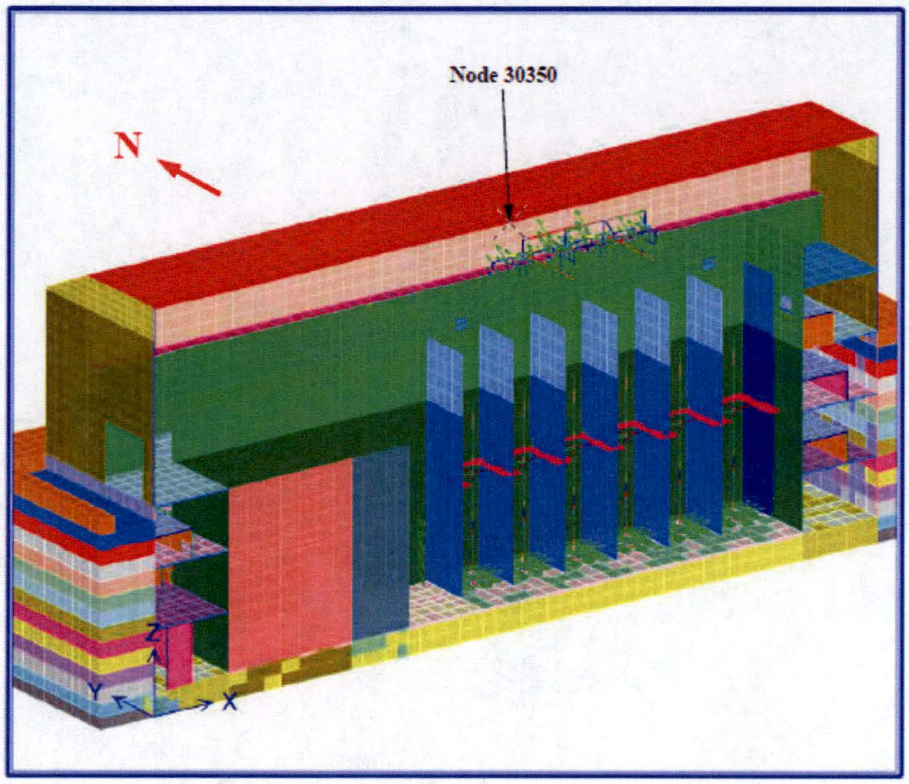

Figure 12. Node 30350, at Center of Roof Slab

Direct Method and 7P Extended Subtraction Method In-Structure Response Spectra Comparison Results

Figure 13 through Figure 45 present the results of the RXB ISRS comparison between DM and 7P ESM methods. As shown in Table 2, six cases show exceedances above 1.15 times the 7P ESM ISRS, with one above 1.15 times the peak-broadened 7P ESM ISRS and 1.15 times the design basis. For this location, 26345 X, the design basis ISRS is updated to account for the identified exceedances, as shown in Figure 37.

Table 2. Summary of the Direct Method and 7P Extended Subtraction Method In-Structure Response Spectra Comparison Results

	Number of Cases	Node/ Direction	Location
DM > 7P ESM x1.15	6	16271, X 16635, X 27649, X 26345, X 26345, Y 26345, Z	RXM 1 Lug Support Locations RXM 6 Lug Support Locations Crane Rail Slab Northeast Corner of Bioshield Northeast Corner of Bioshield Northeast Corner of Bioshield
DM > Broadened 7P ESM x1.15	1	26345, X	Northeast Corner of Bioshield
DM > Design Basis ISRS x1.15	1	26345, X	Northeast Corner of Bioshield

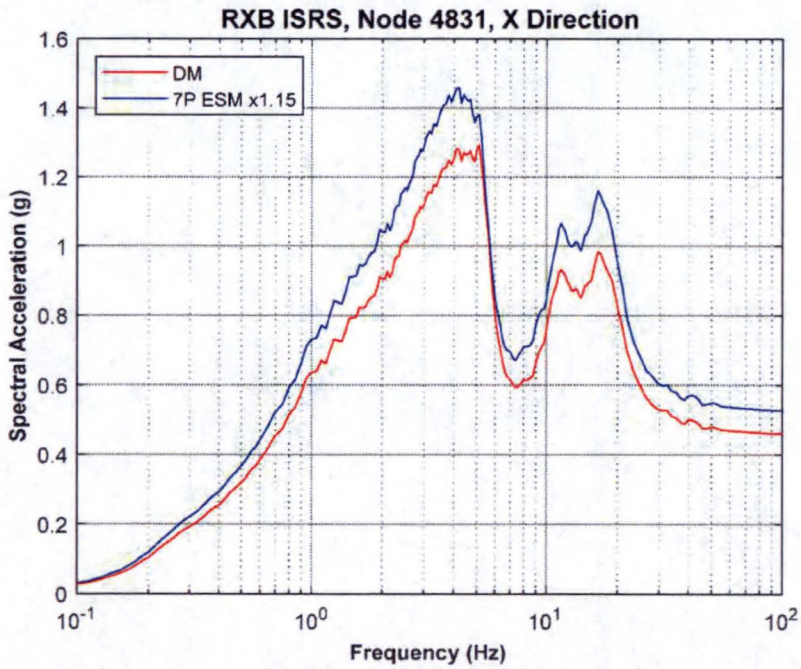

Figure 13. Reactor Building In-Structure Response Spectra Comparison, Node 4831, X-Direction

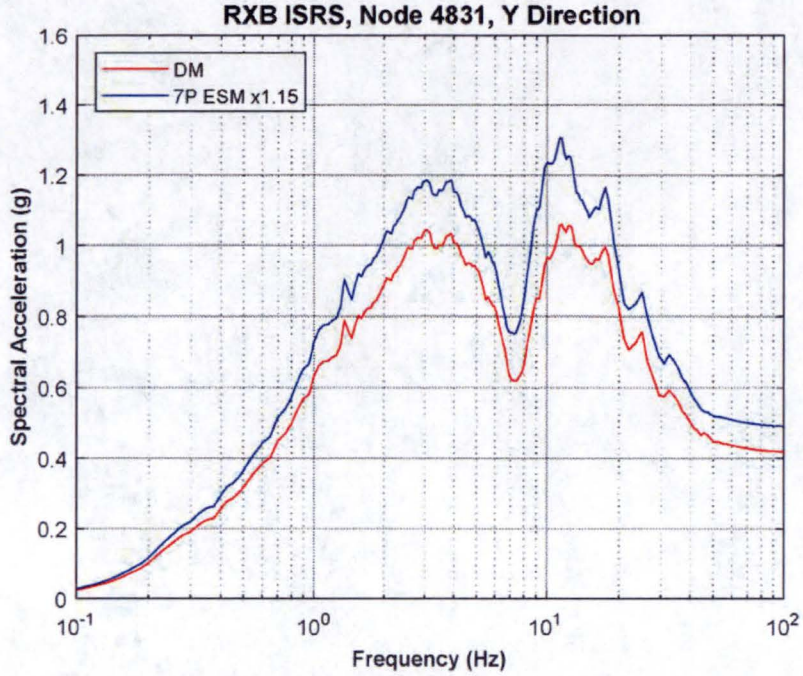

Figure 14. Reactor Building In-Structure Response Spectra Comparison, Node 4831, Y-Direction

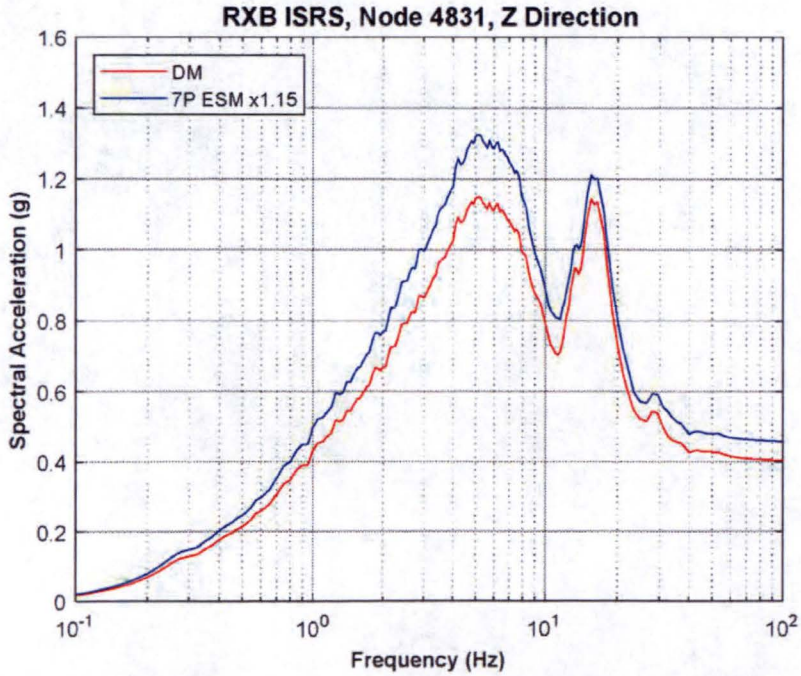

Figure 15. Reactor Building In-Structure Response Spectra Comparison, Node 4831, Z-Direction

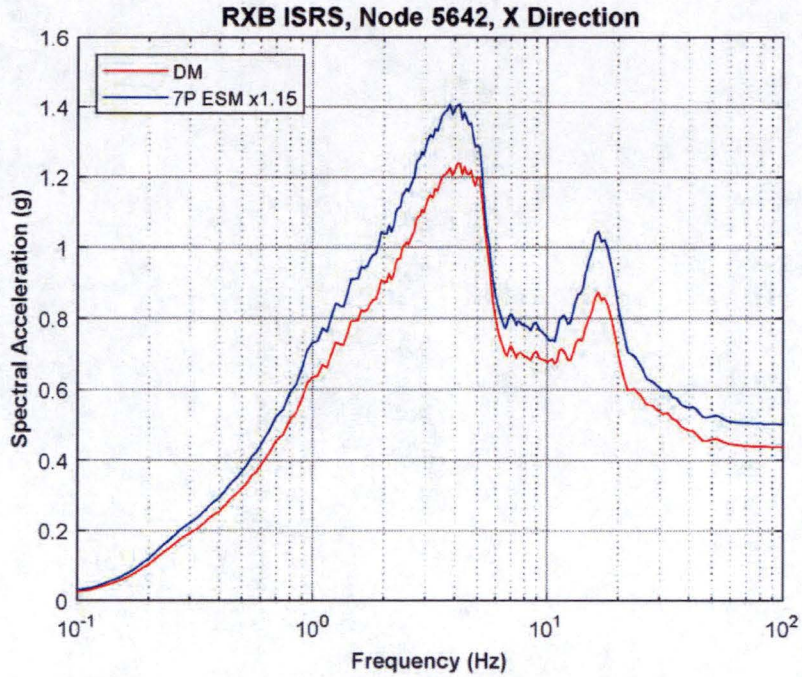

Figure 16. Reactor Building In-Structure Response Spectra Comparison, Node 5642, X-Direction

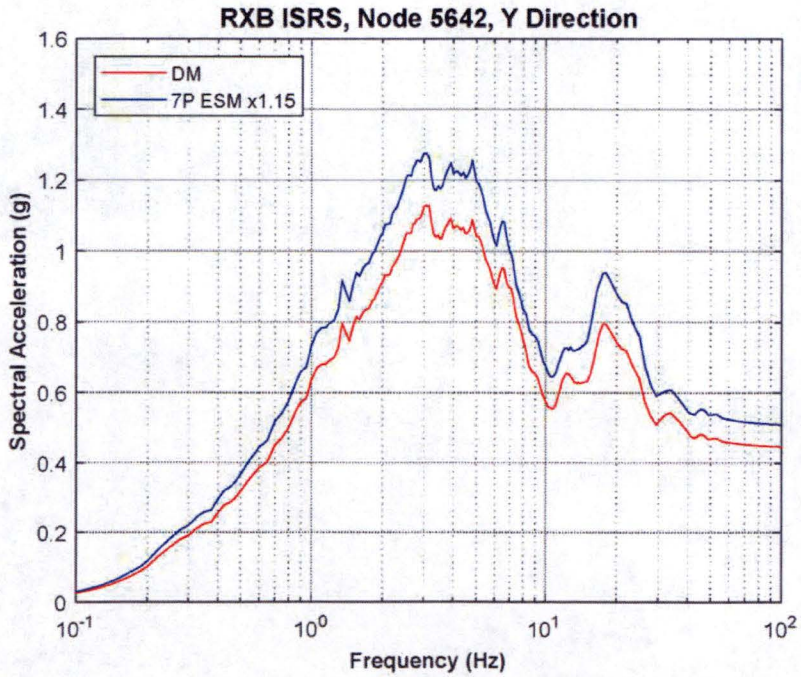

Figure 17. Reactor Building In-Structure Response Spectra Comparison, Node 5642, Y-Direction

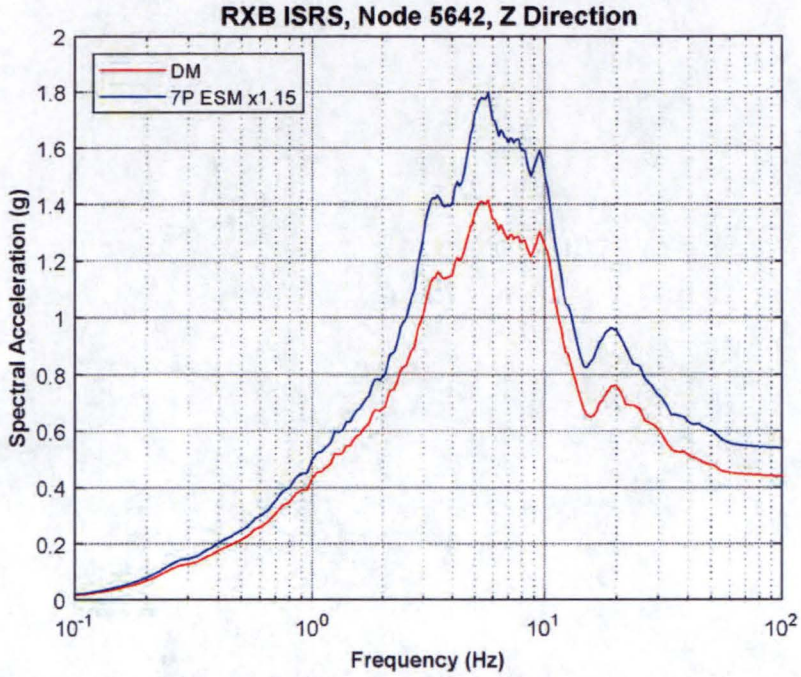

Figure 18. Reactor Building In-Structure Response Spectra Comparison, Node 5642, Z-Direction

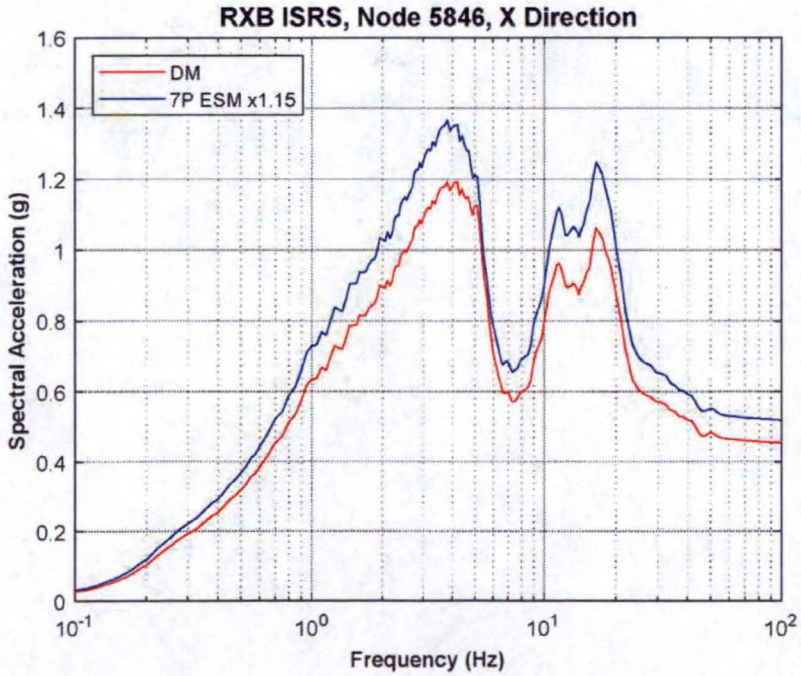

Figure 19. Reactor Building In-Structure Response Spectra Comparison, Node 5846, X-Direction

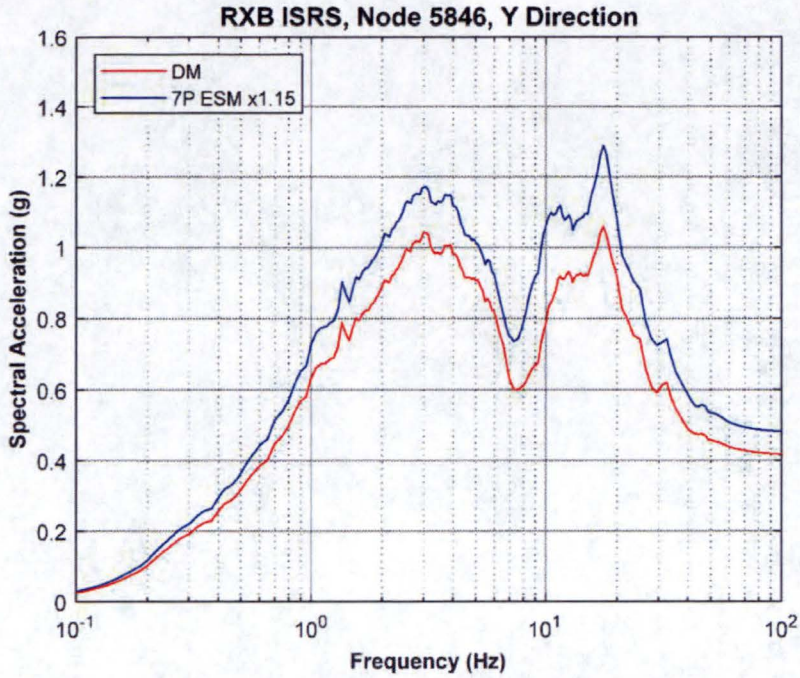

Figure 20. Reactor Building In-Structure Response Spectra Comparison, Node 5846, Y-Direction

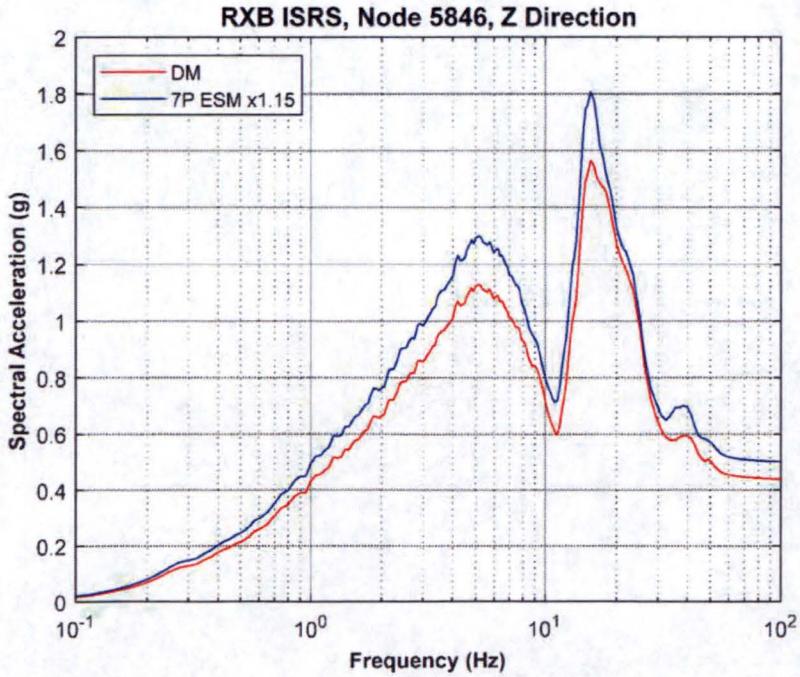

Figure 21. Reactor Building In-Structure Response Spectra Comparison, Node 5846, Z-Direction

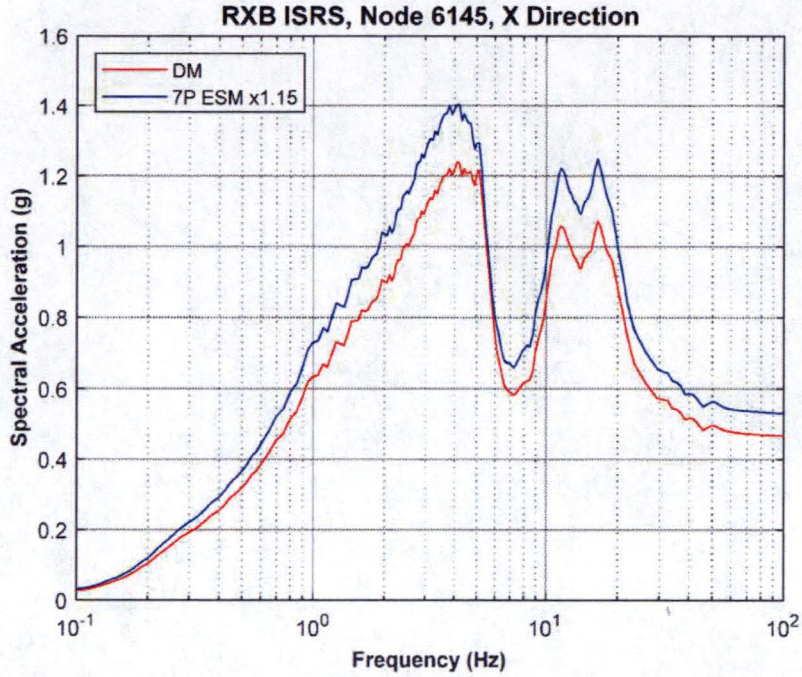

Figure 22. Reactor Building In-Structure Response Spectra Comparison, Node 6145, X-Direction

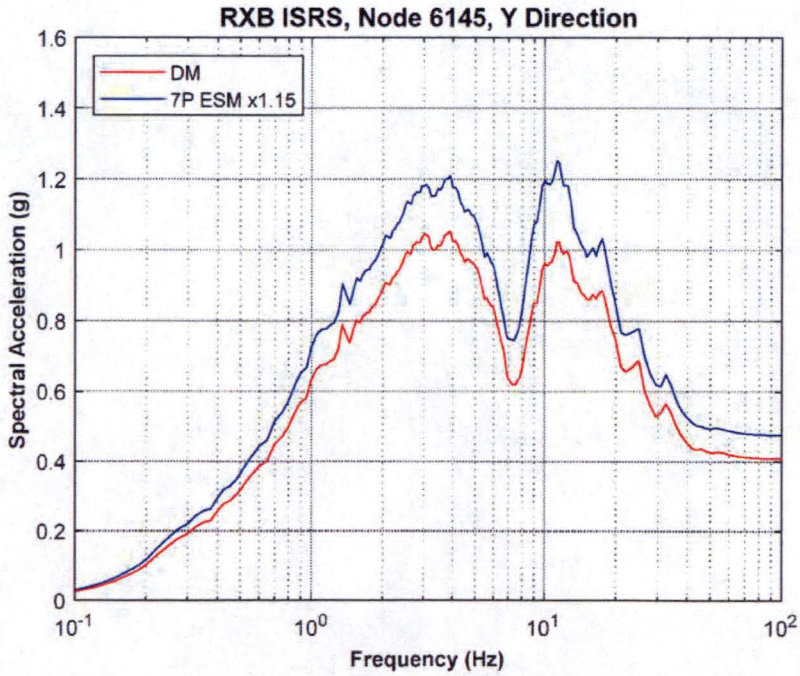

Figure 23. Reactor Building In-Structure Response Spectra Comparison, Node 6145, Y-Direction

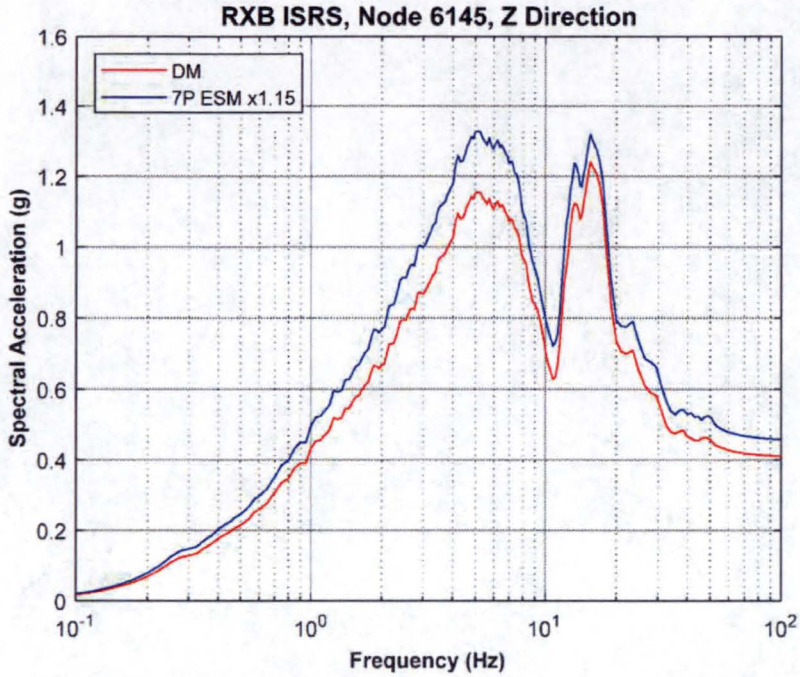

Figure 24. Reactor Building In-Structure Response Spectra Comparison, Node 6145, Z-Direction

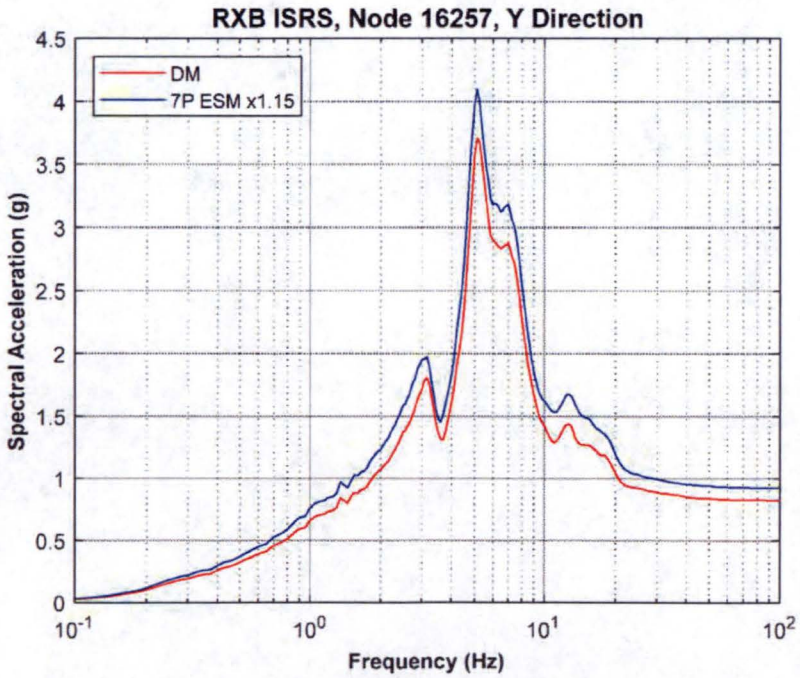

Figure 25. Reactor Building In-Structure Response Spectra Comparison, Node 16257, Y-Direction

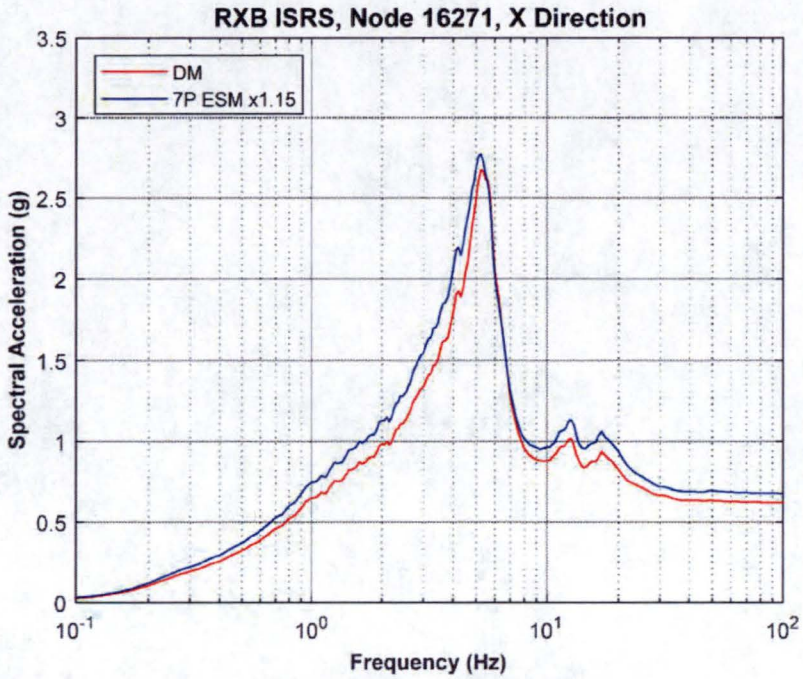

Figure 26. Reactor Building In-Structure Response Spectra Comparison, Node 16271, X-Direction (a)

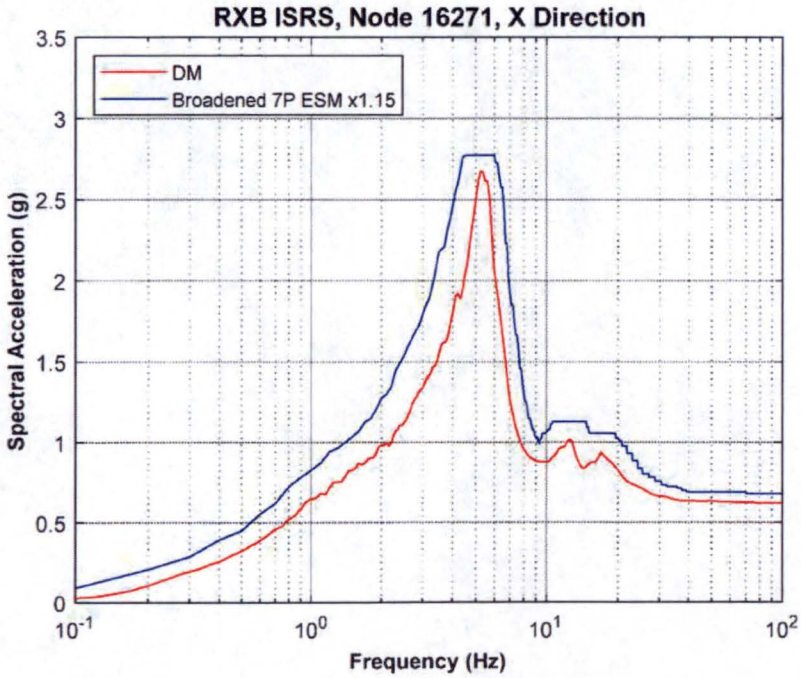

Figure 27. Reactor Building In-Structure Response Spectra Comparison, Node 16271, X-Direction (b)

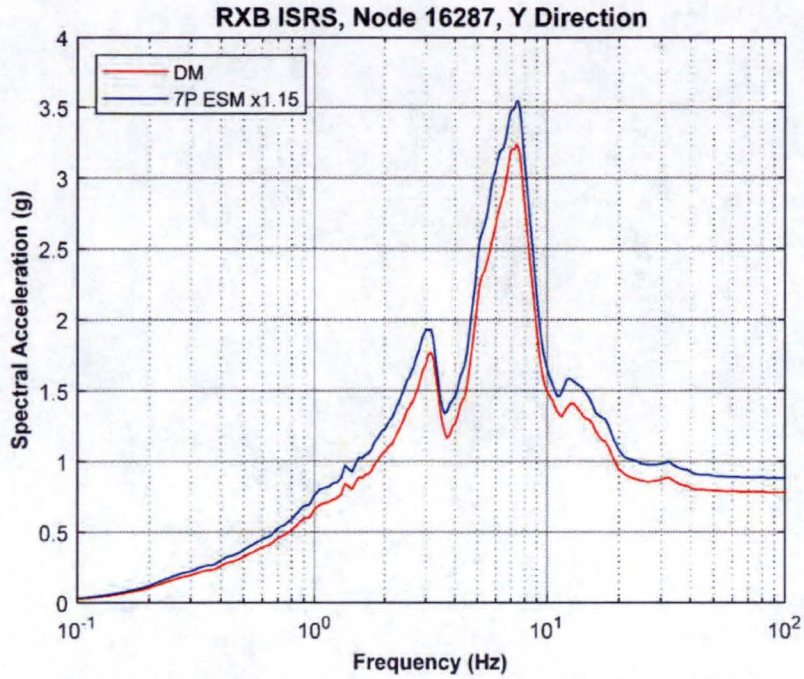

Figure 28. Reactor Building In-Structure Response Spectra Comparison, Node 16287, Y-Direction

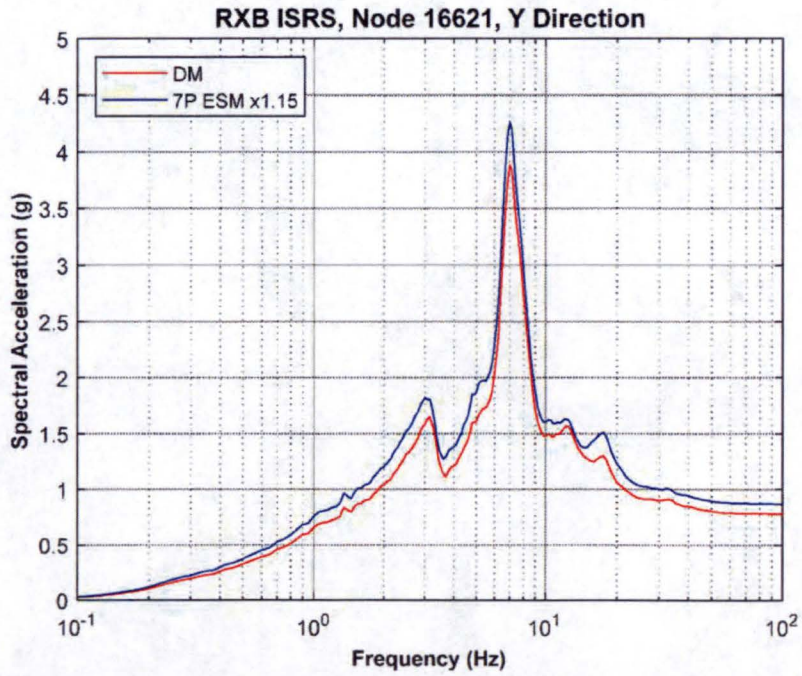

Figure 29. Reactor Building In-Structure Response Spectra Comparison, Node 16621,

Y-Direction

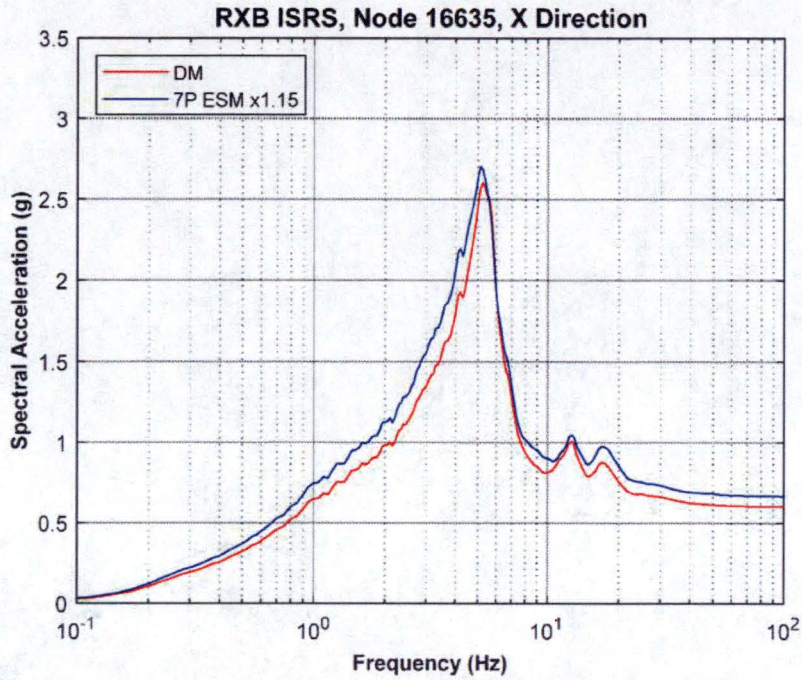

Figure 30. Reactor Building In-Structure Response Spectra Comparison, Node 16635, X-Direction (a)

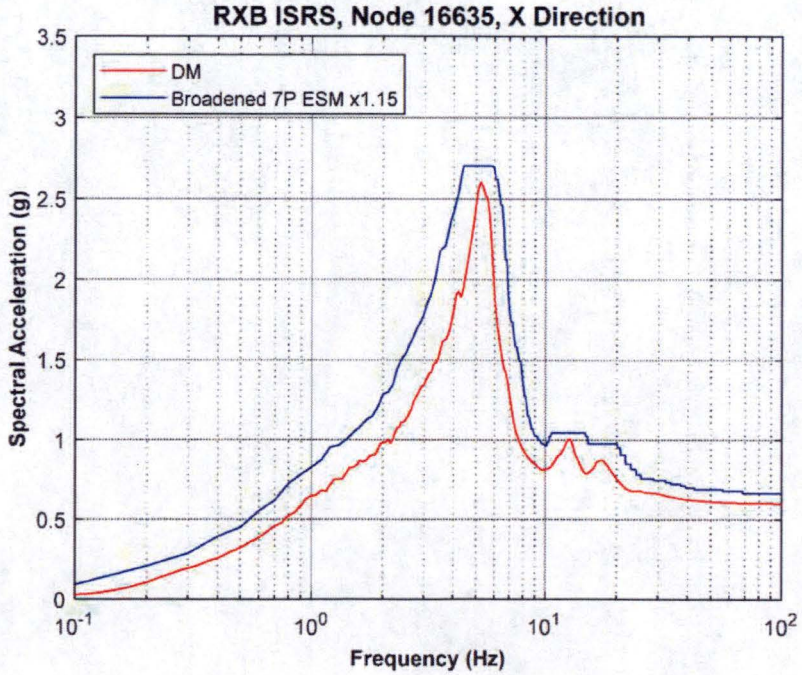

Figure 31. Reactor Building In-Structure Response Spectra Comparison, Node 16635, X-Direction (b)

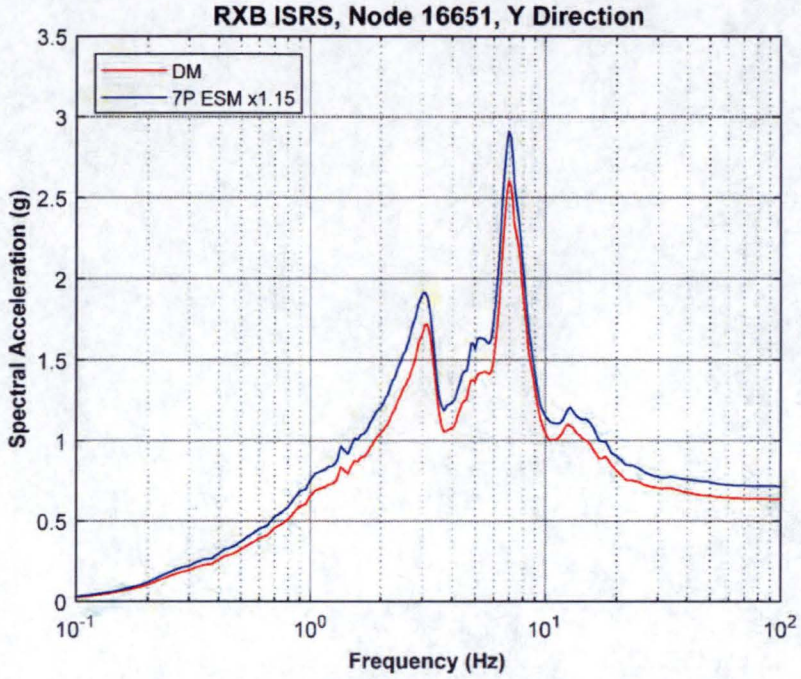

Figure 32. Reactor Building In-Structure Response Spectra Comparison, Node 16651, Y-Direction

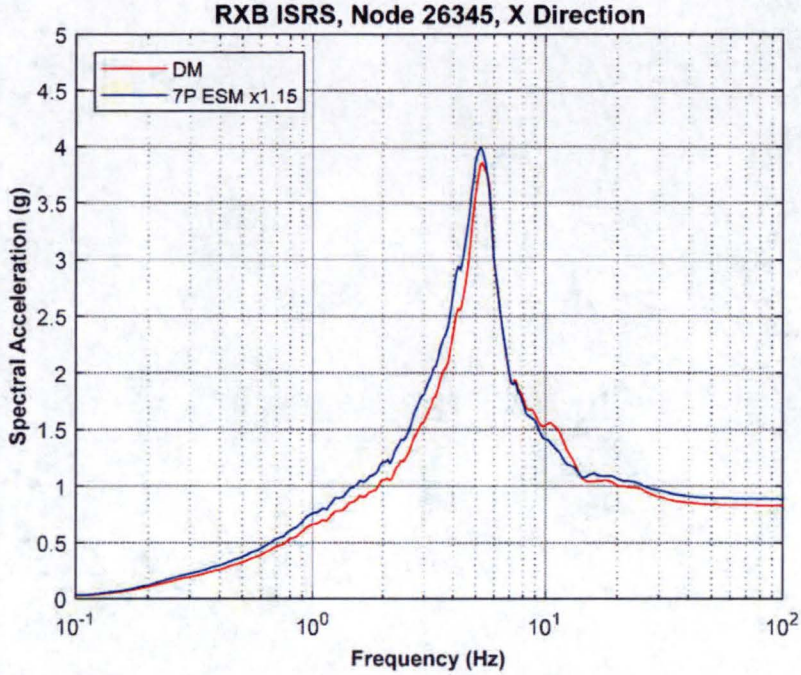

Figure 33. Reactor Building In-Structure Response Spectra Comparison, Node 26345, X-Direction (a)

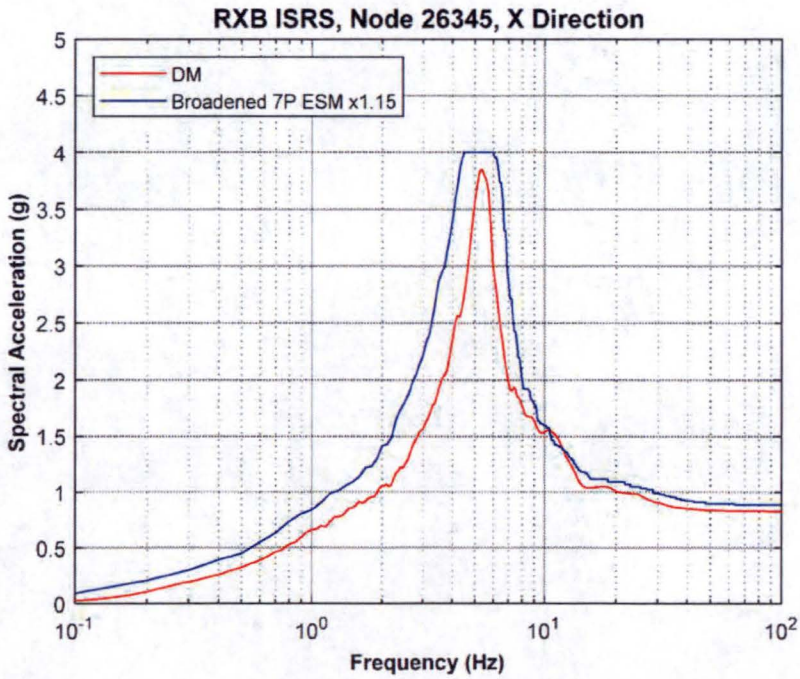

Figure 34. Reactor Building In-Structure Response Spectra Comparison, Node 26345, X-Direction (b)

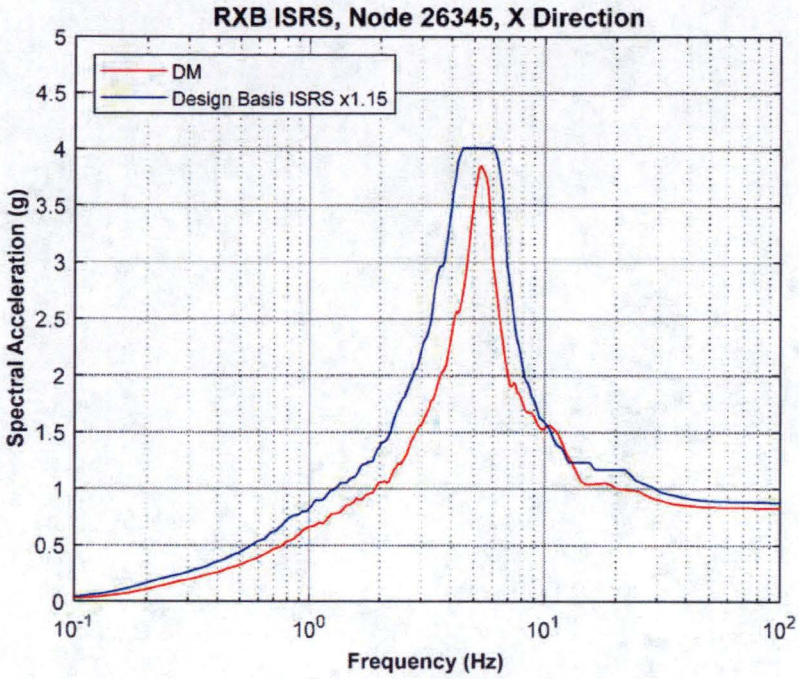

Figure 35. Reactor Building In-Structure Response Spectra Comparison, Node 26345, X-Direction (c)

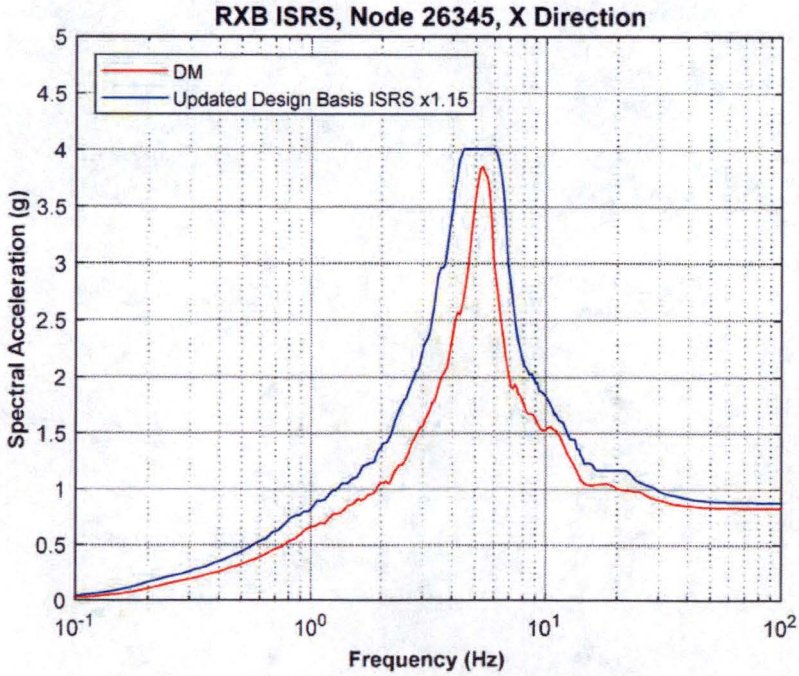

Figure 36. Reactor Building In-Structure Response Spectra Comparison, Node 26345, X-Direction (d)

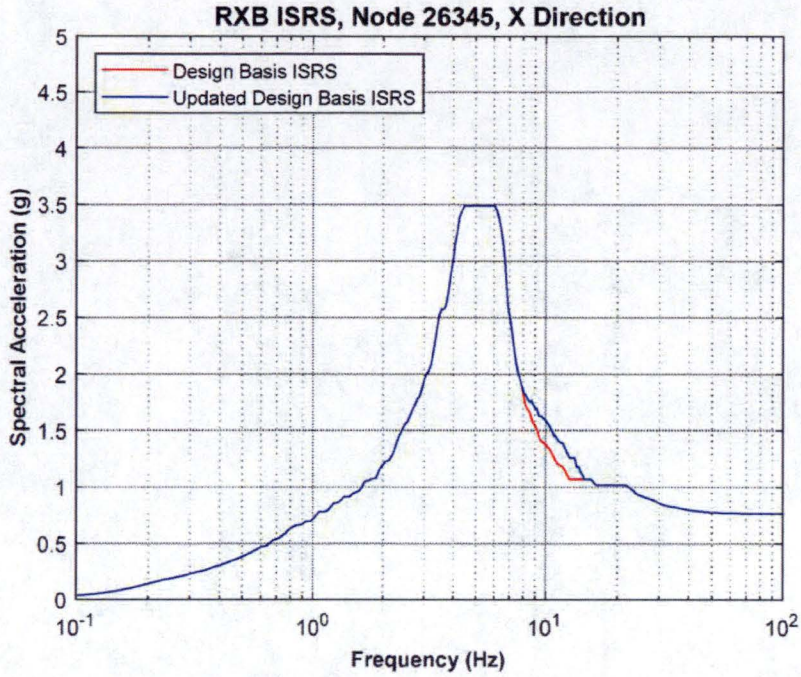

Figure 37. Reactor Building In-Structure Response Spectra Comparison, Node 26345, X-Direction (e)

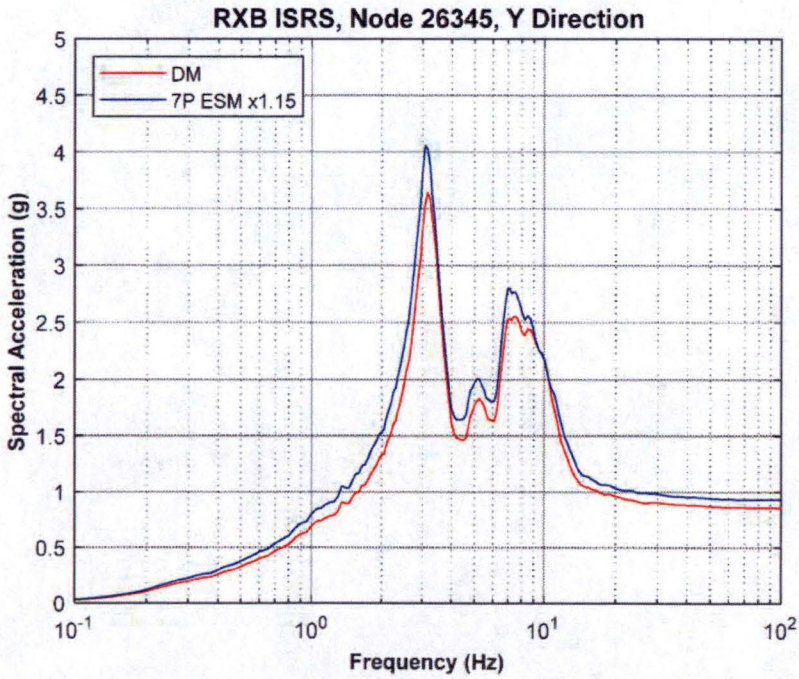

Figure 38. Reactor Building In-Structure Response Spectra Comparison, Node 26345, Y-Direction (a)

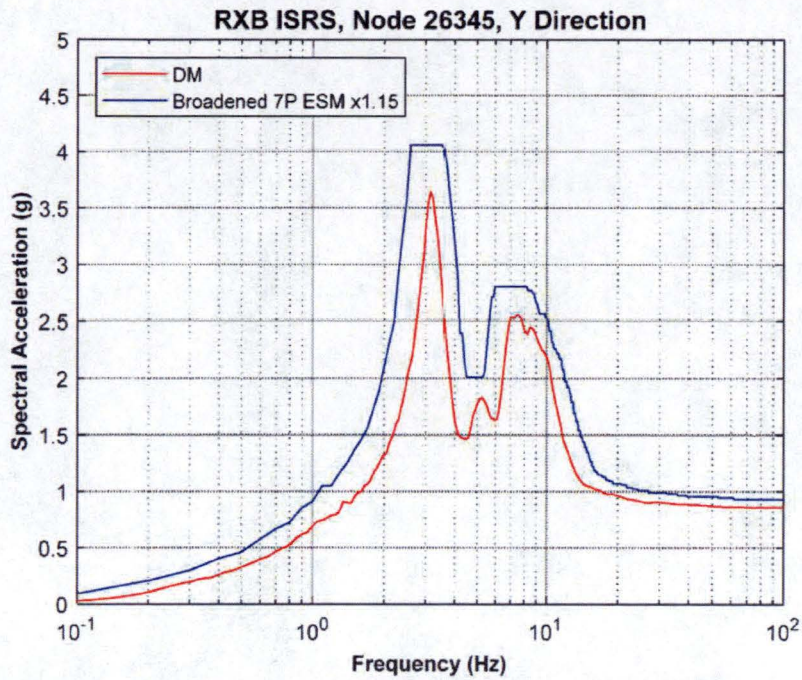

Figure 39. Reactor Building In-Structure Response Spectra Comparison, Node 26345, Y-Direction (b)

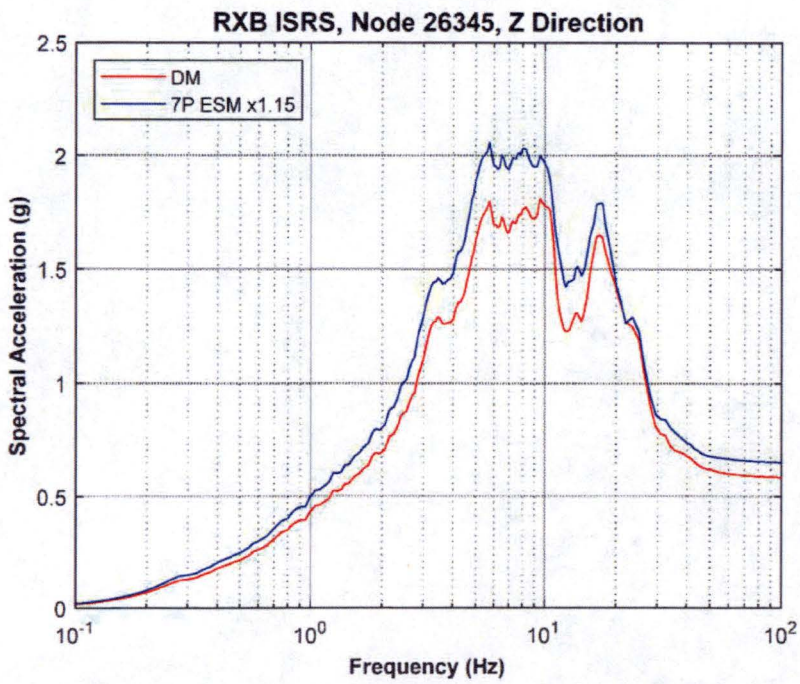

Figure 40. Reactor Building In-Structure Response Spectra Comparison, Node 26345, Z-Direction (a)

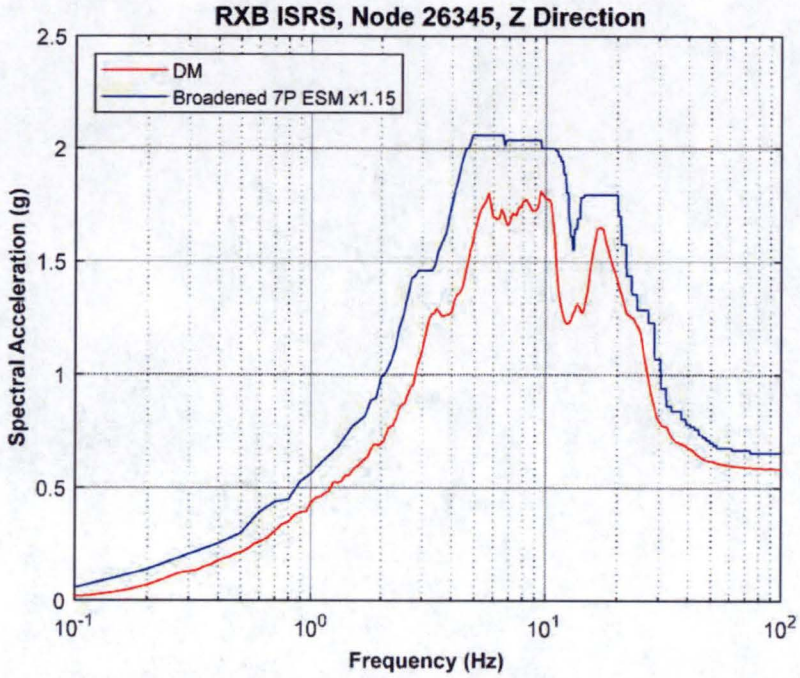

Figure 41. Reactor Building In-Structure Response Spectra Comparison, Node 26345, Z-Direction (b)

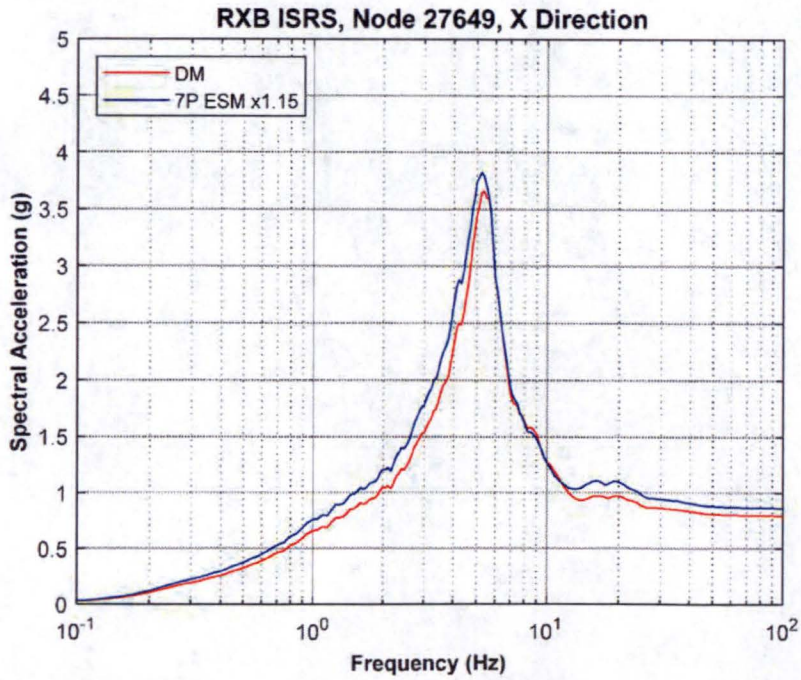

Figure 42. Reactor Building In-Structure Response Spectra Comparison, Node 27649, X-Direction (a)

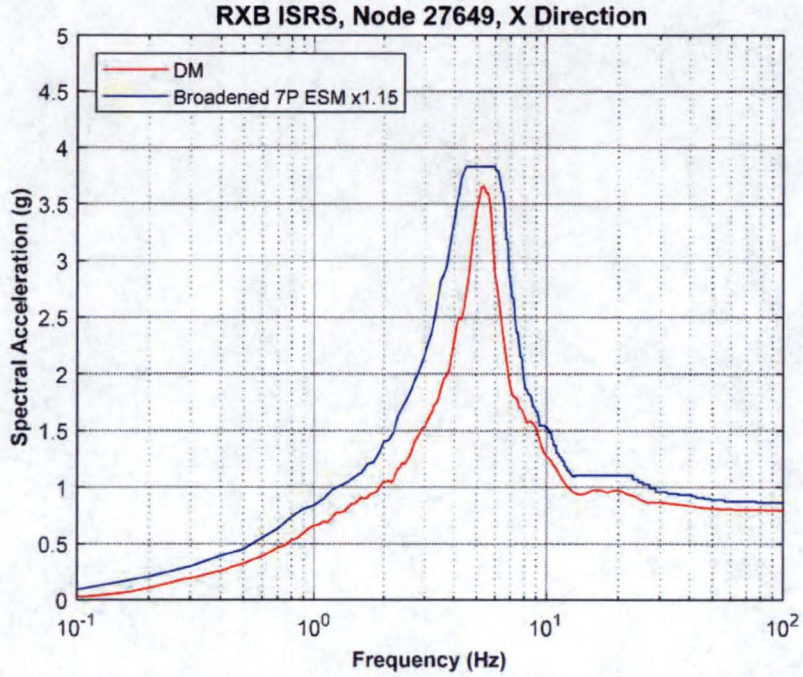

Figure 43. Reactor Building In-Structure Response Spectra Comparison, Node 27649, X-Direction (b)

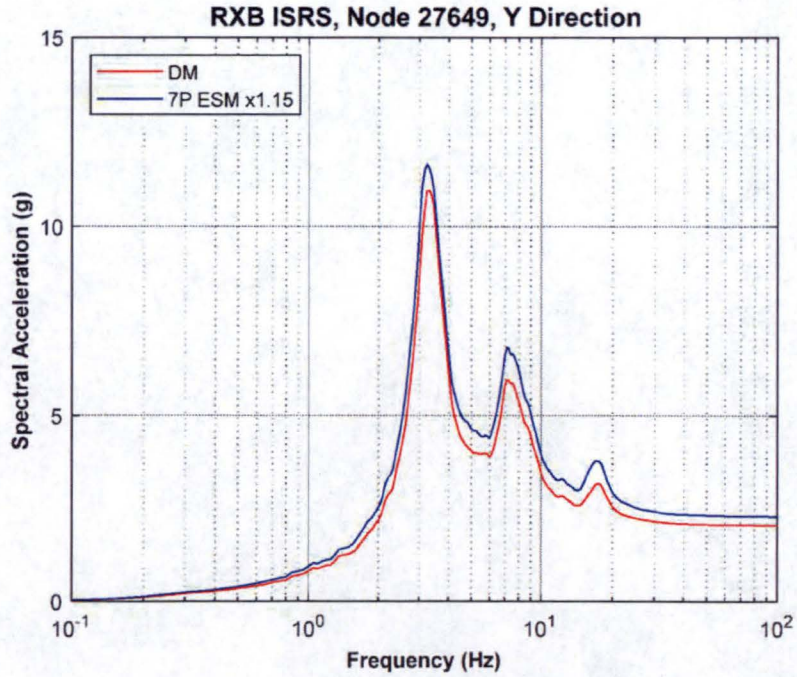

Figure 44. Reactor Building In-Structure Response Spectra Comparison, Node 27649, Y-Direction

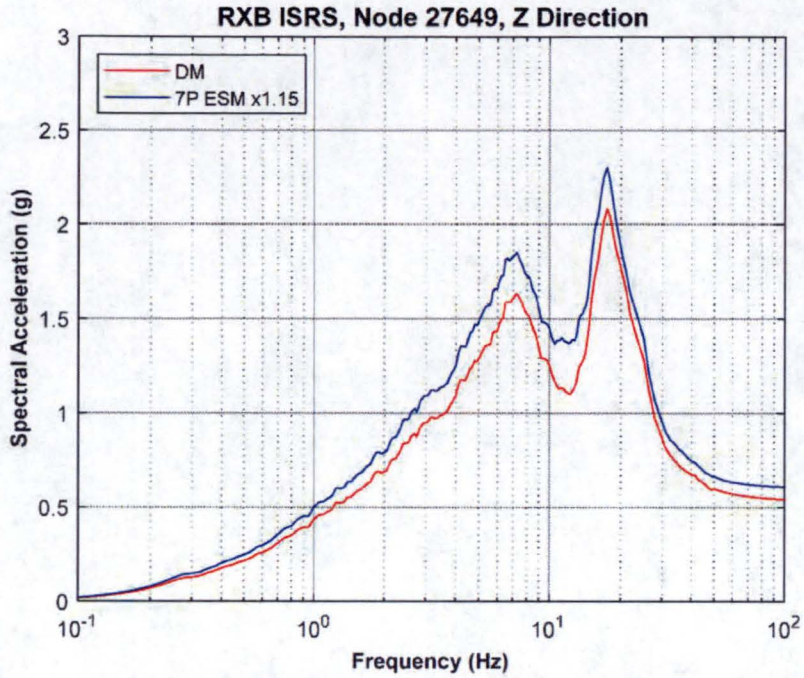

Figure 45. Reactor Building In-Structure Response Spectra Comparison, Node 27649, Z-Direction

Updated Design Basis In-Structure Response Spectra for Floor Elevations

Node 26345, shown in Figure 46, is used to develop the design basis ISRS for floor elevation 126 ft. Therefore, any changes to this node's design basis ISRS should be examined and compared with the enveloped ISRS for floor elevation 126 ft. Figure 47 provides this comparison for the X-direction. As shown, the floor's enveloped ISRS bounds the updated ISRS for node 26345 in the X-direction. Thus, updating the design basis ISRS for the enveloped floor elevation 126 ft ISRS is not necessary.

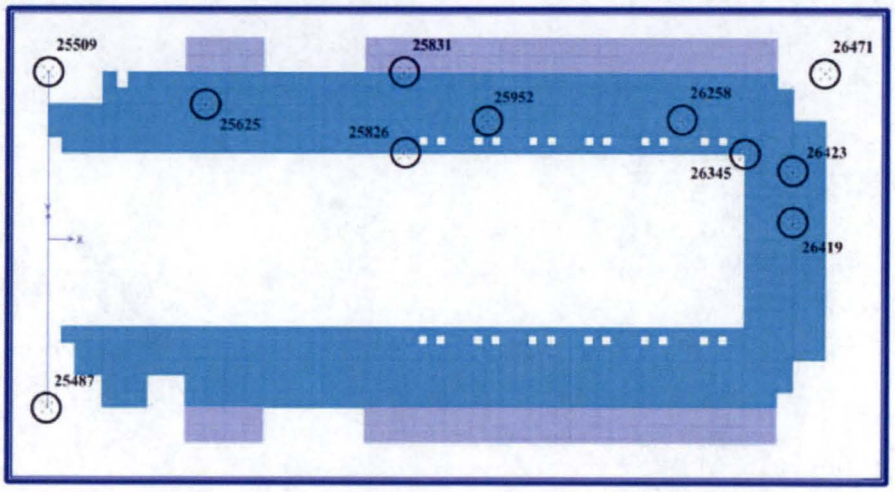

Figure 46. Node Numbers for Floor El. 126' In-Structure Response Spectra Generation

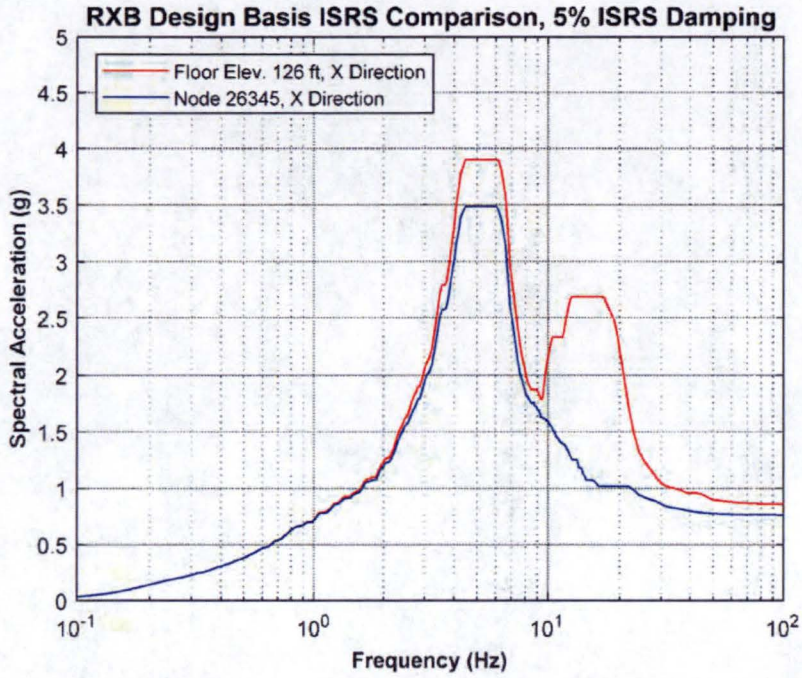

Figure 47. Reactor Building Design Basis In-Structure Response Spectra Comparison, Floor El. 126' vs. Node 26345, X-Direction

Response to Question 2

Forces and moments in the north pool wall are provided in Table 4, below. The NPM1 bay walls, including the pool wall and two wing walls, are shown in Figure 48. The 16 elements in the pool wall around the north lug support of NPM1 are selected to compare forces and moments. The maximum forces and moments among the 16 elements are compared in Table 4 and the percent differences are included.

The percent difference is calculated using the formula

$$\% \text{ difference} = (ESM-DM)/DM \times 100\%$$

A positive difference indicates the ESM value is greater than the corresponding DM value. A negative difference indicates the DM result is greater than the ESM result. If a negative difference is not more than 15 percent, the ESM value associated with the negative difference is deemed acceptable. As shown in Table 4 all the ESM values in the pool wall elements are acceptable because the differences are less than 15 percent.

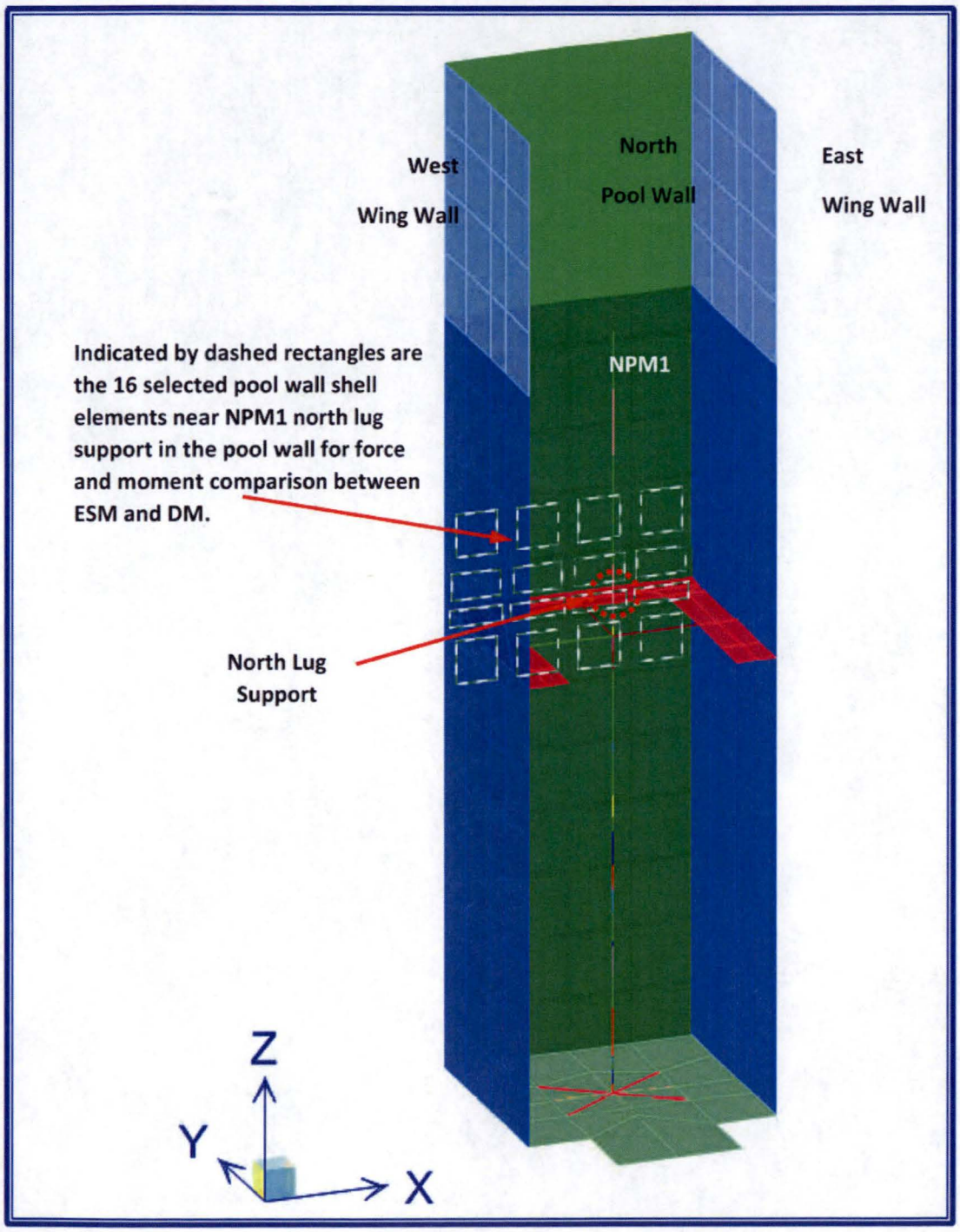

Figure 48. Selected Shell Elements in North Pool Wall near NPM1 Lug Support

Table 4. Comparison of Maximum Forces and Moments in the North Pool Wall near the North Lug Support of NPM1 between ESM and DM

Force or Moment Compared	Description	Maximum Values		
		ESM	DM	Difference (%)†
Sxx (kip/ft)	In-plane force in the EW direction	182	186	**-2.3%**
Syy (kip/ft)	In-plane force in the vertical direction	164	172	**-4.9%**
Sxy (kip/ft)	In-plane shear force	211	221	**-4.6%**
Mxx (kip-ft/ft)‡	Bending about the vertical axis	326	347	**-6.1%**
Myy (kip-ft/ft)‡	Bending about EW axis	372	393	**-5.2%**
Vxz (kip/ft)	Out-of-plane shear in the vertical section	214	228	**-6.1%**
Vyz (kip/ft)	Out-of-plane shear in the horizontal (EW) section	92	97	**-4.4%**

† % = (ESM-DM)/DM*100. A negative % indicates the ESM value is less than the DM value

‡ The twisting moment Mxy was added to Mxx and Myy.

Response to Question 3

Background Information, Methodology, and Approach

This section presents the methodology used for comparing the ISRS data, as well as the methodology for scaling ISRS acceleration data from 7 percent structural damping to 4 percent structural damping.

ISRS Acceleration Comparison Methodology

The approach used for comparing the DM vs. 7P ESM ISRS is presented here. The DM ISRS plots are developed based on 7 percent structural damping and require scaling in order to be compared with the corresponding design basis ISRS.

The first step is to compare the DM ISRS with 1.15 times the 7P ESM ISRS. If the DM ISRS plots are bounded by 1.15 times the 7P ESM ISRS, no further action is needed, as this shows an exceedance of less than 15 percent. However, if the DM ISRS is greater than 1.15 times the 7P ESM ISRS, a comparison between the SS ISRS and 1.15 times the peak-broadened 7P ESM ISRS is performed. Subsequently, if the DM ISRS is greater than 1.15 times the peak-broadened 7P ESM ISRS, comparison with 1.15 times the design basis ISRS is provided. Finally, if the damping-scaled DM ISRS is not bounded by 1.15 times the design basis ISRS, the design basis ISRS plots are updated to account for the identified exceedances.

These steps are summarized in the flowchart below.

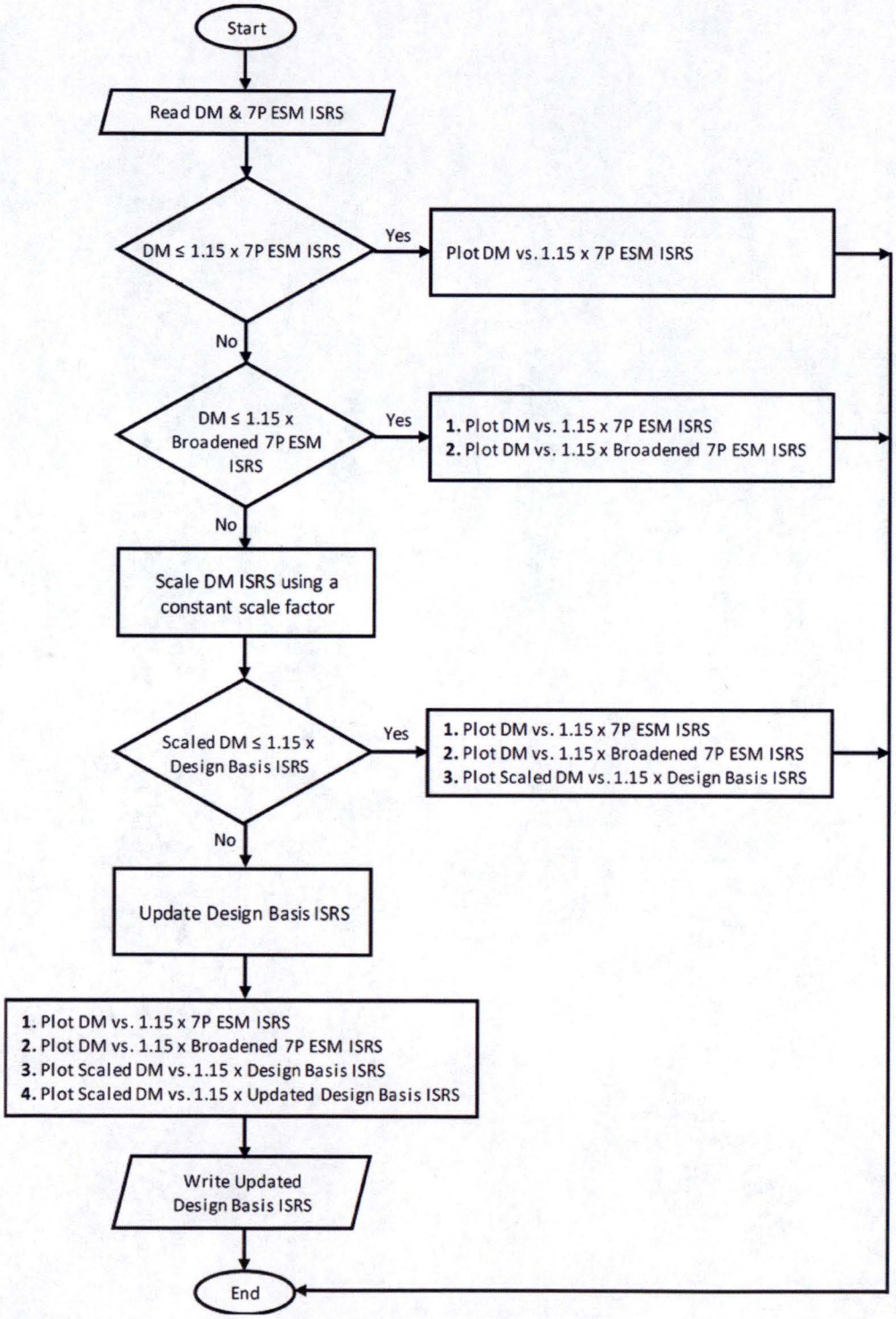

Figure 49. Flowchart for In-Structure Response Spectra Comparison, Direct Method vs. 7P Extended Subtraction Method

Direct Method and 7P Extended Subtraction Method In-Structure Response Spectra Comparison

Table 3 provides a list of locations where ISRS comparison is performed and a description of the locations.

Table 3. Locations for Direct Method vs. 7P Extended Subtraction Method In-Structure Response Spectra Comparison

Node Number	Direction(s)	Location
35713	X, Y, Z	Emergency Equipment Room Between Grid Lines CB-D and CB-E at El. 76'-6"
38298	X, Y, Z	Slab between Grid Lines CB-A and CB-B (Technical Support Center) at El. 100'-0"

The following figures show the locations of the nodes in the CRB for which DM vs. 7P ESM ISRS comparisons are performed.

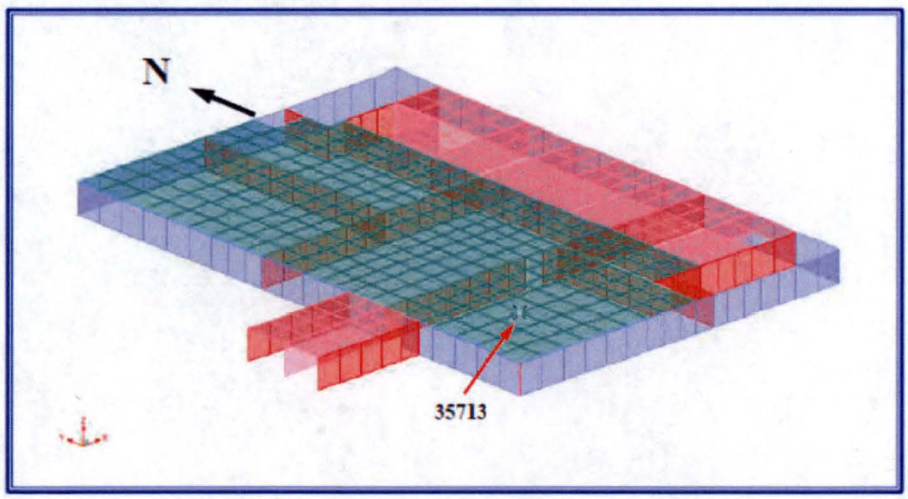

Figure 50. Selected Node for In-Structure Response Spectra Comparison at Top of Concrete, El. 76'-6"

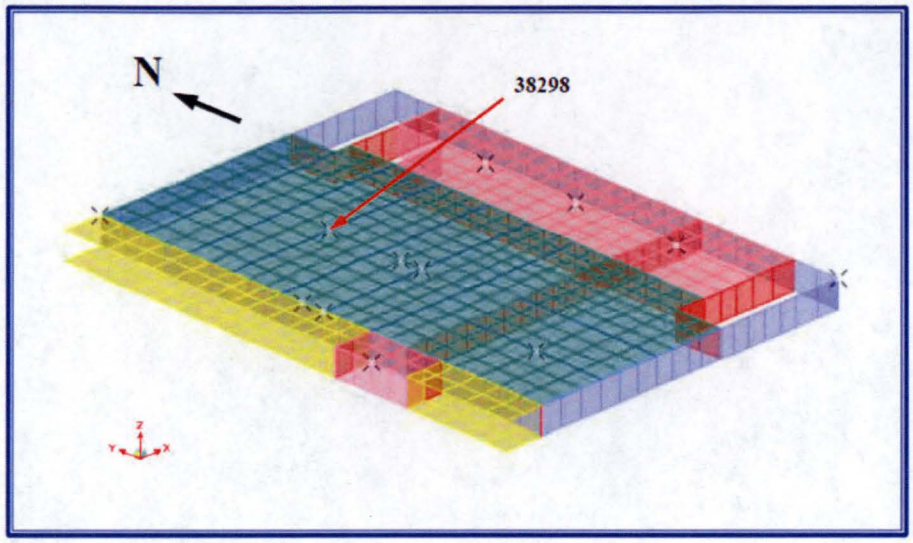

Figure 51. Top of Concrete at Technical Center and Grade El. 100'-0" In-Structure Response Spectra Node Locations

Direct Method and 7P Extended Subtraction Method In-Structure Response Spectra Comparison Results

None of the scaled DM ISRS plots show exceedances above 1.15 times the peak-broadened 7P ESM ISRS. Therefore, ISRS scaling and comparison with the design basis ISRS is not required.

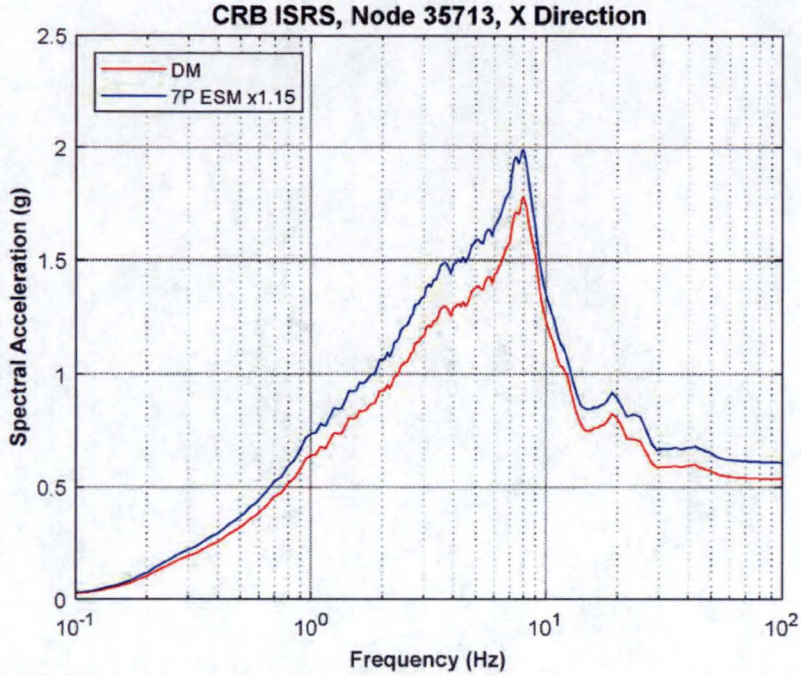

Figure 52. Control Building In-Structure Response Spectra Comparison, Node 35713, X-Direction

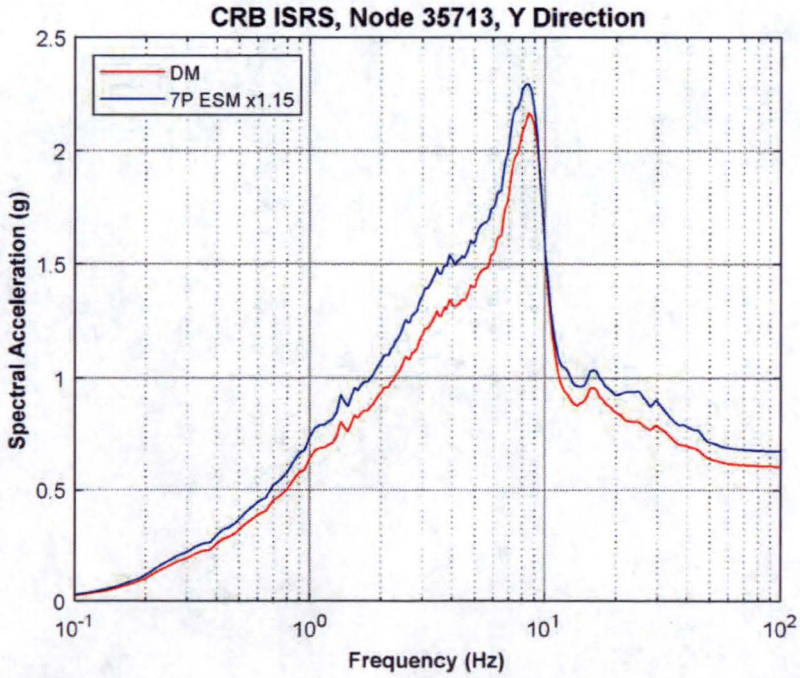

Figure 53. Control Building In-Structure Response Spectra Comparison, Node 35713, Y-Direction

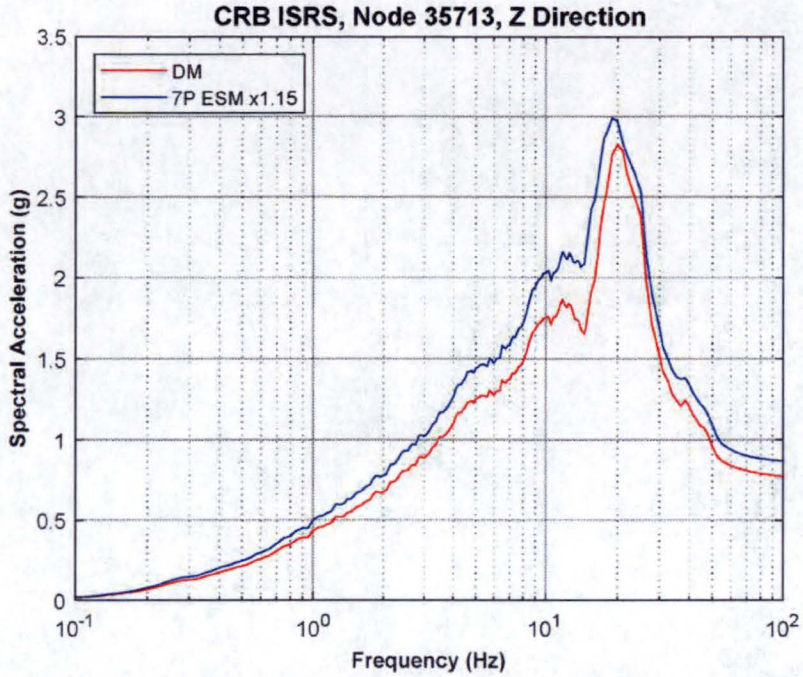

Figure 54. Control Building In-Structure Response Spectra Comparison, Node 35713, Z-Direction

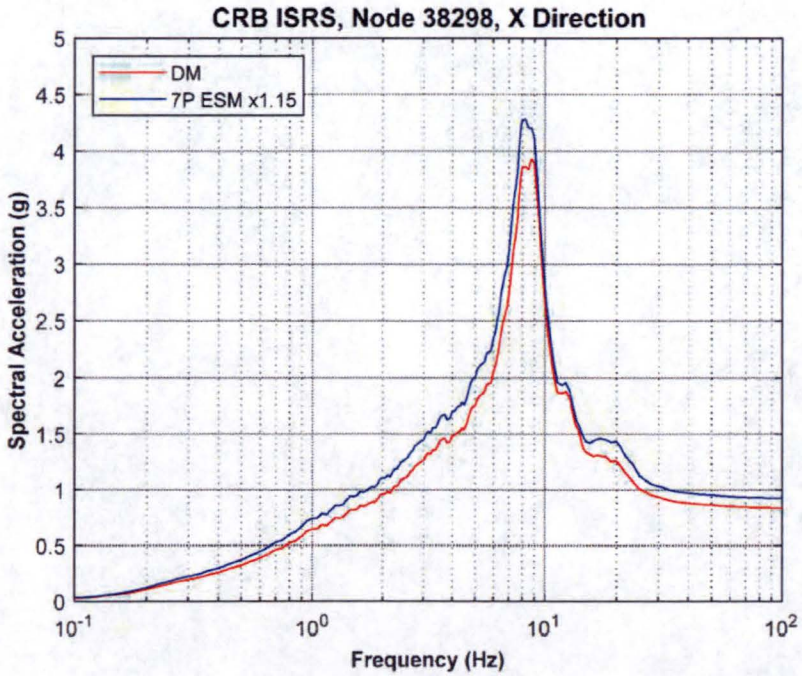

Figure 55. Control Building In-Structure Response Spectra Comparison, Node 38298, X-Direction

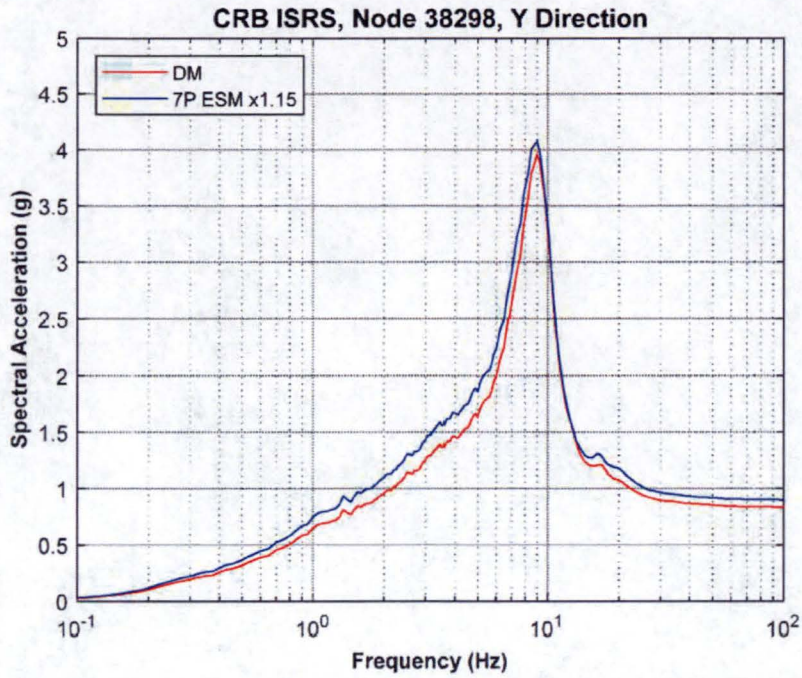

Figure 56. Control Building In-Structure Response Spectra Comparison, Node 38298, Y-Direction

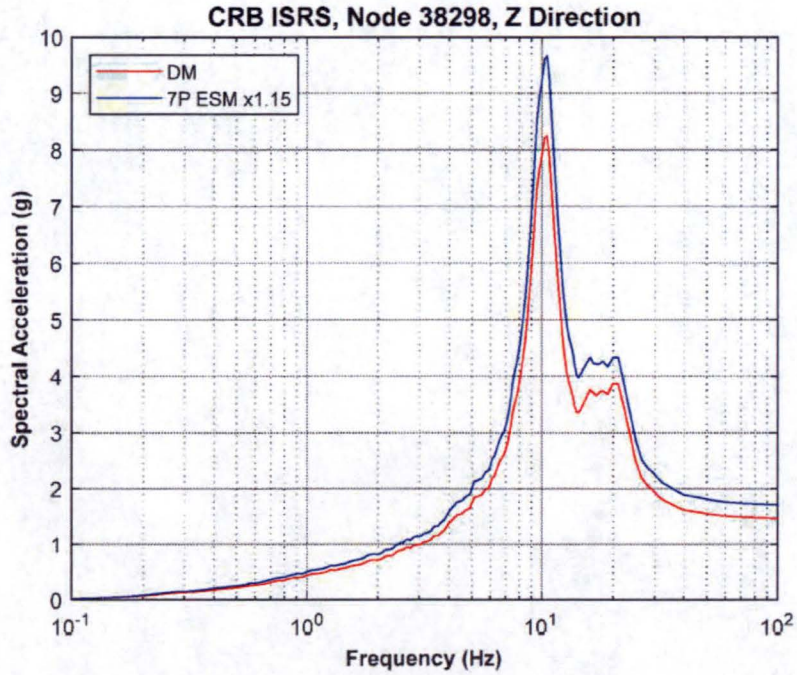

Figure 57. Control Building In-Structure Response Spectra Comparison, Node 38298, Z-Direction

Responses to Questions 4, 5, 6, and 7

4. NuScale has included COL Item 3.7-15 in the attached FSAR markup.

5. The information has been provided as a part of Responses 1 and 3 above.

6. As discussed with the NRC on February 26, 2019, in lieu of providing tables, NuScale has provided plots of 1.15 times ESM to show where or if there are exceedances greater than 15 percent. This allows clear inspection of the data.

7. The following describes the analysis cases involved in the sensitivity study.

   Two models were used for the RXB. The first model using the 7P ESM for the FSAR is a full, three-dimensional model. The term '7P' indicates the nodes in seven selected planes of the excavated soil model are used as the interaction nodes for soil impedance calculation. The seven planes include four side planes, top and bottom planes, and an intermediate horizontal plane. In order to analyze the RXB with the DM, a half RXB model must be used so the number of interaction nodes is within the capability of the SASSI2010 program. Therefore, a half model of the north half of the RXB was analyzed for the DM. Both models were then analyzed for Soil Type 7, cracked concrete condition with 4 percent concrete damping. The five certified seismic design response spectra (CSDRS)-compatible time histories (i.e., Capitola, Chi-Chi, El Centro, Izmit, and Yermo) are used as the seismic input by averaging the results from the five inputs.

   Similarly, two models were used for the CRB. The first model uses the ESM and generates the FSAR results. The second model is the same model, but uses the DM. Both models were analyzed for Soil Type 7, cracked concrete condition with 4 percent concrete damping. The same five CSDRS-compatible time histories are used by averaging the results from the five inputs.

Impact on DCA:

The FSAR Section 3.7.2, Tables 1.8-2 and 3.7.2-56, and Figures 3.72-114, 3.7.2-118a and 3.7.2-119a have been revised as described in the response above and as shown in the markup provided with the response to question 03.07.02-6.

Response to Request for Additional Information
Docket No. 52-048

eRAI No.: 8932
Date of RAI Issue: 07/31/2017

NRC Question No.: 03.07.02-6

10 CFR 50 Appendix S requires that the safety functions of structures, systems, and components (SSCs) must be assured during and after the vibratory ground motion associated with the Safe Shutdown Earthquake (SSE) through design, testing, or qualification methods.

a. DSRS 3.7.2 provides guidance that effects of potential separation or loss of contact between the structure and the soil during the earthquake should be considered in SSI analysis. On Page 3.7-23 of the FSAR, in the second paragraph from the bottom, the applicant states, "To model the soil separation, the Young's modulus of the backfill elements down to a depth of 25' (the top four layers of backfill elements) was decreased by a factor of 100." The applicant is requested to provide a basis for 25 ft of separation depth. Also, please clarify if the modulus reduction by a factor of 100 applies only to the backfill elements interfacing with the exterior walls or to all the backfill elements outside the exterior walls.

b. On Page 3.7-23 of the FSAR, in the bottom paragraph, the applicant states, "Soil separation has negligible effect on the response of the structure. The primary point of comparison is at the NPM. The study showed that the maximum reaction force at the base of the NPMs decreased by approximately 5 percent, and the maximum reaction force at the NPM lug restraints decreased by more than 15 percent." The applicant is requested to provide information on soil separation effect on computed transfer functions and seismic demands (forces, ISRS) at critical section locations and external walls. Please provide comparison plots for results between the intact and soil-separated cases. When soil- separation results in increased seismic demands, such increased demands should be taken into account in establishing the design basis seismic demands.

c. The staff notes that a soil-separation study was conducted for the RXB but not for the CRB. The applicant is requested to provide a technical justification for not conducting a similar study for the CRB.

NuScale Response:

The NRC provided the following feedback regarding the August 24, 2018 supplement (ML18236A573) to this request for additional information (RAI) question during the audit of FSAR Sections 3.7 and 3.8 in December of 2018.

1. For the Reactor Building (RXB), a soil-separation/nonsoil-separation (SS/NSS) in-structure response spectra (ISRS) comparison is needed at the following locations: NuScale Power Module (NPM) lug and skirt support, Reactor Building crane (RBC) support, spent fuel pool (SFP) rack locations, and bioshield support. An NPM support and the RBC support load comparison is also required.

2. For the Control Building (CRB), benchmarking results appear to show that SS ISRS results exceed the NSS results at few locations by more than 25 percent (e.g., FSAR Figures 3.7.2-136 and 138. RAI Figures 75, 78, and 90). At these locations, provide a comparison of SS cases with the design basis demand.

The NRC provided additional feedback during a public meeting on February 26, 2019, as follows:

3. ISRS exceedances should be checked at the following additional locations (other than those already covered in the previous RAI responses):

    a. RXB Crane Support
    b. RXB Bioshield Support
    c. CRB Emergency Equipment Room
    d. CRB TSC Room/MCR

4. It is difficult to accurately quantify the extent and level of ISRS exceedances by looking at Figures only. Therefore, the applicant is requested to provide numerical Tables that indicate exceedances in terms of percentage (%) of the control cases.

5. Please indicate in the RAI response, a description of the analysis cases involved in the sensitivity study.

Response to Question 1

The NPM support reactions were provided in Table 1 of the May 22, 2018 RAI response submittal (ML18142C204), which shows close agreement in the soil-separation case and the design basis.

Background Information, Methodology, and Approach

This section presents the methodology used for comparing the ISRS data and the methodology for scaling ISRS acceleration data from 7 percent structural damping to 4 percent structural damping.

In-Structure Response Spectra Acceleration Comparison Methodology

The approaches used for comparing the direct method (DM) vs. 7P extended subtraction method (ESM) ISRS and the SS versus NSS ISRS are almost identical. The difference is the DM ISRS plots are based on 4 percent structural damping and do not require scaling in order to be compared with the corresponding design basis ISRS.

The first step is to compare the SS ISRS with 1.15 times the NSS ISRS. If the SS ISRS plots are bounded by 1.15 times the NSS ISRS, no further action is needed, as this shows an exceedance of less than 15 percent. However, if the SS ISRS is greater than 1.15 times the NSS ISRS, a comparison between the SS ISRS and 1.15 times the peak-broadened NSS ISRS is performed. Subsequently, if the SS ISRS is greater than 1.15 times the peak-broadened NSS ISRS, comparison with 1.15 times the design basis ISRS is provided. Finally, if the damping-scaled SS ISRS is not bounded by 1.15 times the design basis ISRS, the design basis ISRS plots are updated to account for the identified exceedances.

These steps are summarized in the following flowchart.

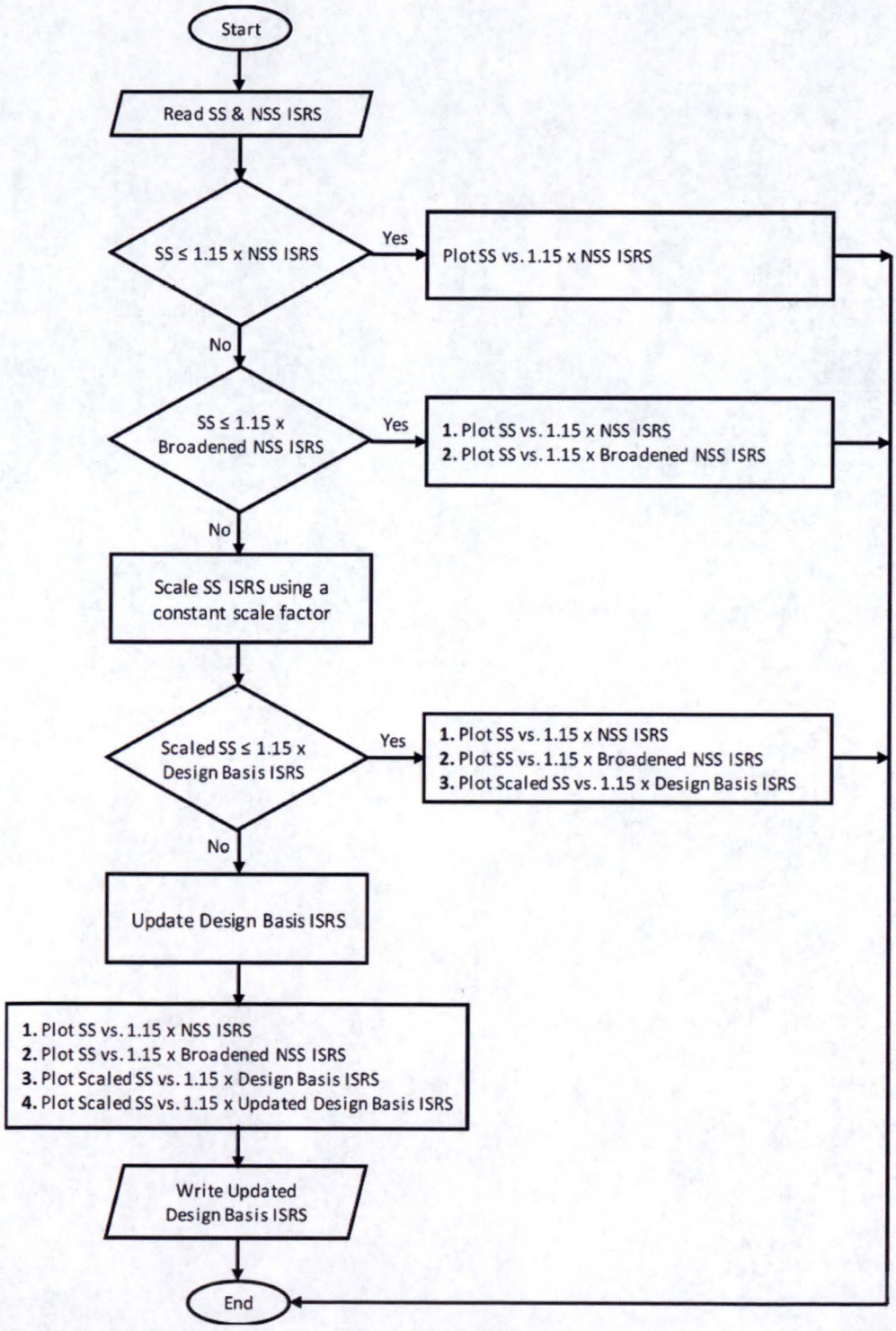

Figure 1. Flowchart for In-Structure Response Spectra Comparison, Soil-Separation vs. Nonsoil-Separation

In-Structure Response Spectra Damping Scaling Methodology

Soil-separation ISRS acceleration plots are based on 7 percent structural damping, whereas design basis ISRS plots are based on 4 percent damping. Therefore, SS ISRS plots are scaled to 4 percent damping in order to be equivalent and are compared with the design basis ISRS, if needed. Hence, a scaling methodology has been developed and a constant scale factor is selected through comparison of the results of three different methods.

The ISRS damping scaling methodology is summarized in the following steps:

1. Identify all node and direction combinations where ISRS scaling is needed.
2. Run a SAP2000 fixed-base time history analysis using certified seismic design response spectra (CSDRS)-compatible, Capitola time history input in east-west, north-south, and vertical directions, with 4, 5, 7 percent structural damping.
3. For each node and direction identified in step 1, calculate the square root of the sum of the squares ISRS using 5 percent ISRS damping.
4. Calculate $a = \frac{ISRS_{(SAP2000,\,4\%\,Damping)}}{ISRS_{(SAP2000,\,7\wedge Damping)}}$.
5. Generate ISRS for 4 percent structural damping using the NUREG/CR-6728 method based on the SAP2000 fixed-base analysis and 5 percent structural damping from step 3.
6. Calculate $b = \frac{ISRS_{(NUREG,\,4\%\,Damping)}}{ISRS_{(SAP2000,\,7\%\,Damping)}}$.
7. Generate ISRS for 4 percent structural damping using the White-Noise Method (Reference 1) based on the SAP2000 fixed-base analysis and 5 percent structural damping from step 3.
8. Calculate $c = \frac{ISRS_{(¿-Noise,\,4\%\,Damping)}}{ISRS_{(SAP2000,\,7\%\,Damping)}}$.
9. Compare $a, b,$ and c to determine a constant damping scaling factor.

NUREG/CR-6728 Method

Section 4.9 of NUREG/CR-6728 provides several methods for estimating design response spectra for damping values other than 5 percent based on the 5 percent damped spectrum. The random vibration method is described as the most theoretically consistent method to account for damping. The procedure presented below is used for scaling the ISRS acceleration plots.

$$SA\,(f,\xi) = SA\,(f,0.05)\left[\frac{1+4.9\,\xi\,f\,D}{1+4.9\,x\,0.05\,f\,D}\right]^{-0.41} \qquad 1 \le f < 5\,Hz \qquad \text{Equation 1}$$

$$SA\,(f,\xi) = \left\{PGA^2 + [SA\,(f,0.05)^2 - PGA^2]\left[\frac{1+4.9\,\xi\,f\,D}{1+4.9\,x\,0.05\,f\,D}\right]^{-0.82}\right\}^{1/2} \qquad 5\,Hz < f \qquad \text{Equation 2}$$

Where:

SA:	Spectral Acceleration
f:	Frequency
ξ:	Damping
D:	Strong Motion Duration
PGA:	Peak Ground Acceleration

Per NUREG/CR-6728, in Equation 2, the second term on the right-hand-side (involving subtraction) should not be less than 0.

The following assumptions are made while using Equations 1 and 2:

- PGA for horizontal and vertical directions is 0.5g
- Duration of strong motion is 7 sec
- CSDRS-compatible Capitola acceleration time history input is used

White-Noise Method

The White-Noise Method, shown below, uses the square root of the damping ratio as the scale factor.

$$DSF \cong \sqrt{\frac{5}{\beta}} \qquad \text{Equation 3}$$

Where:

DSF:	Damping Scaling Factor
β:	Damping ratio (%)

As shown in the following sections, SS ISRS accelerations exceed 1.15 times the peak-broadened NSS ISRS at one location only, i.e., 27529 Z, requiring the damping scaling factor to be developed. In accordance with the damping scaling methodology described above, a SAP2000 fixed-base time history analysis using CSDRS-compatible, Capitola time history input in the east-west, north-south, and vertical directions is performed for structural damping of 4, 5, and 7 percent. Then, ISRS plots are generated as shown in Figure 2.

Damping scaling factors, described in steps 4, 6, and 8 of the methodology, are plotted in Figure 3. After comparing these plots, a constant damping scaling factor of 1.15 is selected to scale the ISRS accelerations from 7 percent structural damping to 4 percent structural damping.

For verification purposes, a comparison is made between the ISRS plot generated by the SAP2000 fixed-base analysis and three ISRS plots calculated based on the scaling methods described in this section. As seen in Figure 4, the estimated ISRS accelerations reasonably match the calculated SAP2000 ISRS.

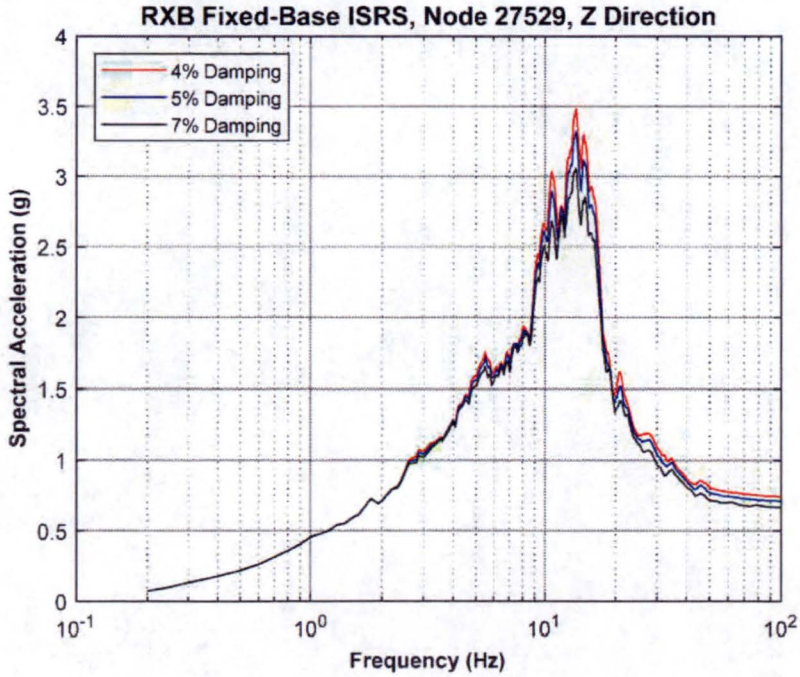

Figure 2. Reactor Building Fixed-Base In-Structure Response Spectra, Node 27529, Z-Direction

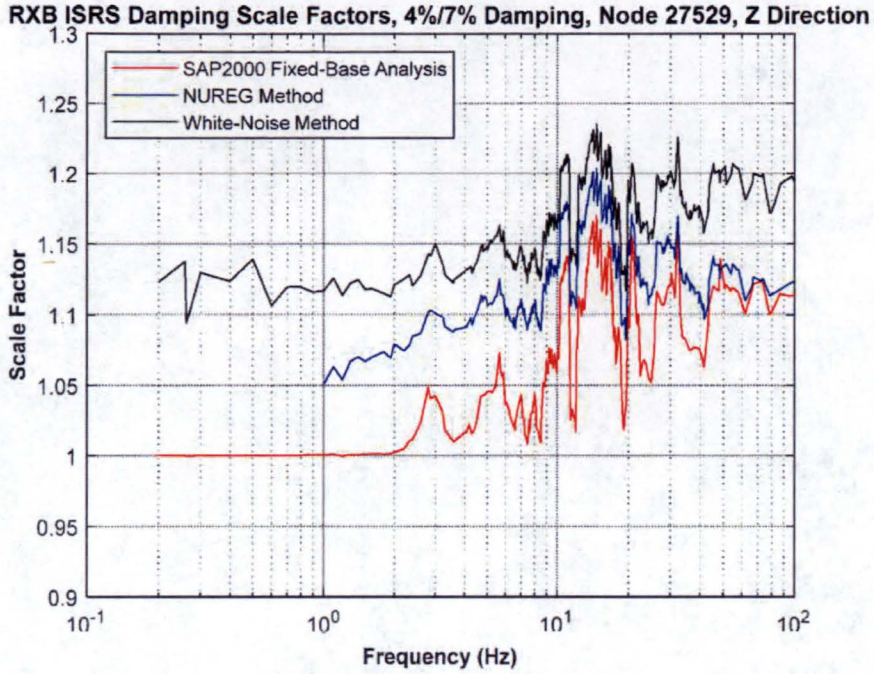

Figure 3. Reactor Building In-Structure Response Spectra Damping Ratios for 4 Percent to 7 Percent Damping, Node 27529, Z-Direction

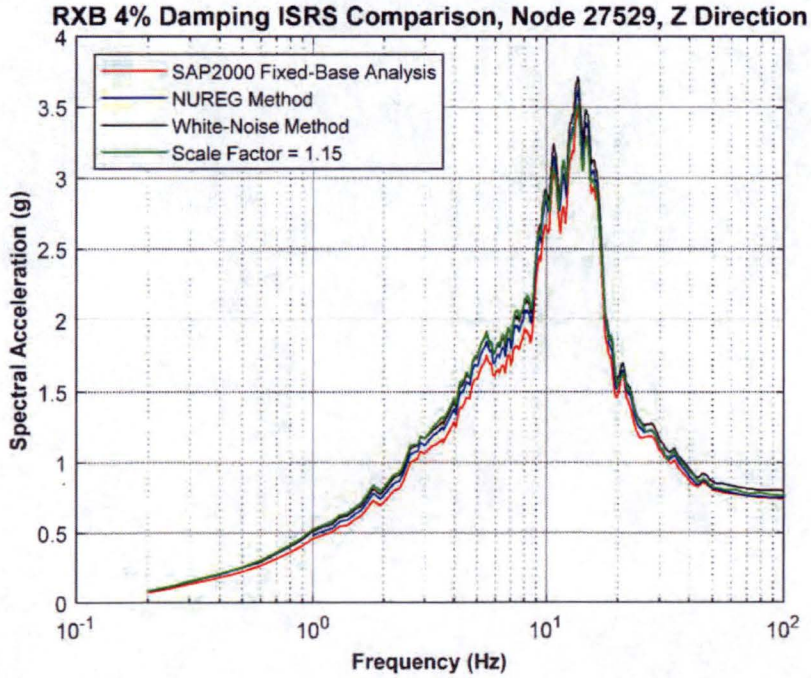

Figure 4. Reactor Building In-Structure Response Spectra for 4 Percent Damping, Node 27529, Z-Direction

Note that the constant damping scaling factor of 1.15 is selected based on the comparison between several scaling factors derived from various methods.

Soil-Separation and Nonsoil-Separation In-Structure Response Spectra Comparison

Table 1 provides a list of locations where ISRS comparison is performed and a description of the locations.

Table 1. Locations for Soil-Separation vs. Nonsoil-Separation In-Structure Response Spectra Comparison

Node Number	Direction(s)	Location
3996	X, Y, Z	NW Corner on Top of Basemat
4741	X, Y, Z	Mid-Span of North Exterior Wall on Top of Basemat
5642	X, Y, Z	NE Corner on Top of Basemat
6013	X, Y, Z	RXM 1 West Pool Wall at Floor - SW Corner
6017	X, Y, Z	RXM 1 West Pool Wall at Floor - NW Corner
6065	X, Y, Z	RXM 1 East Pool Wall at Floor - SE Corner
6069	X, Y, Z	RXM 1 East Pool Wall at Floor - NE Corner
6273	X, Y, Z	RXM 6 West Pool Wall at Floor - SW Corner
6277	X, Y, Z	RXM 6 West Pool Wall at Floor - NW Corner
6325	X, Y, Z	RXM 6 East Pool Wall at Floor - SE Corner
6329	X, Y, Z	RXM 6 East Pool Wall at Floor - NE Corner
6340	X, Y, Z	RXM Module 1 Base Node
6430	X, Y, Z	RXM Module 6 Base Node
16257	Y	RXM 1 at West Lug Support Location
16271	X	RXM 1 at North Lug Support Location
16287	Y	RXM 1 at East Lug Support Location
16621	Y	RXM 6 at West Lug Support Location
16635	X	RXM 6 at North Lug Support Location
16651	Y	RXM 6 at East Lug Support Location
25826	X, Y, Z	Northwest Corner of Bioshield
26345	X, Y, Z	Northeast Corner of Bioshield
27529	X, Y, Z	Crane Rail Slab at Grid Line RX-2 at El. 145′-6″
27885	X, Y, Z	Crane Rail Slab between Grid Lines RX-6 and RX-7 at El. 145′-6″

The following figures show the locations of the nodes in the RXB for which SS vs. NSS ISRS comparisons are performed.

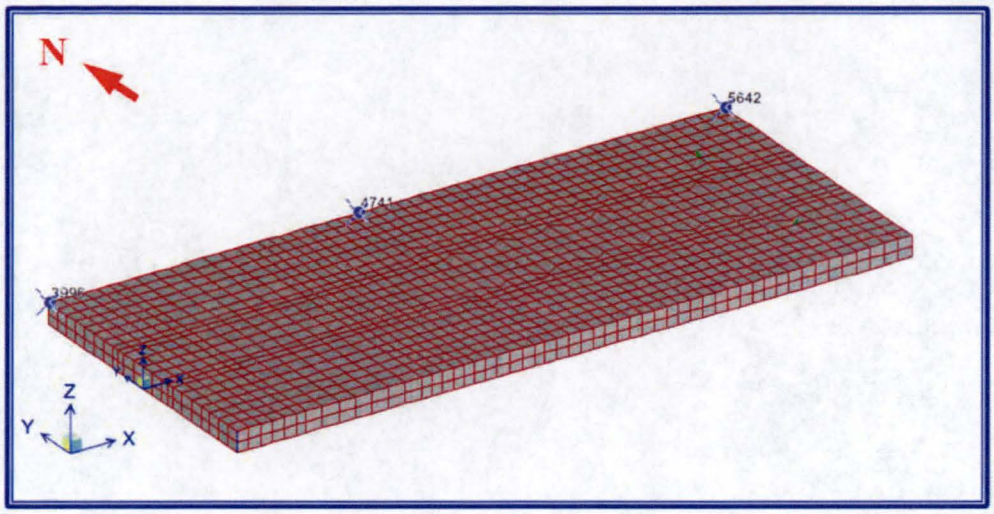

Figure 5. Nodes Selected on Basemat for In-Structure Response Spectra Comparison

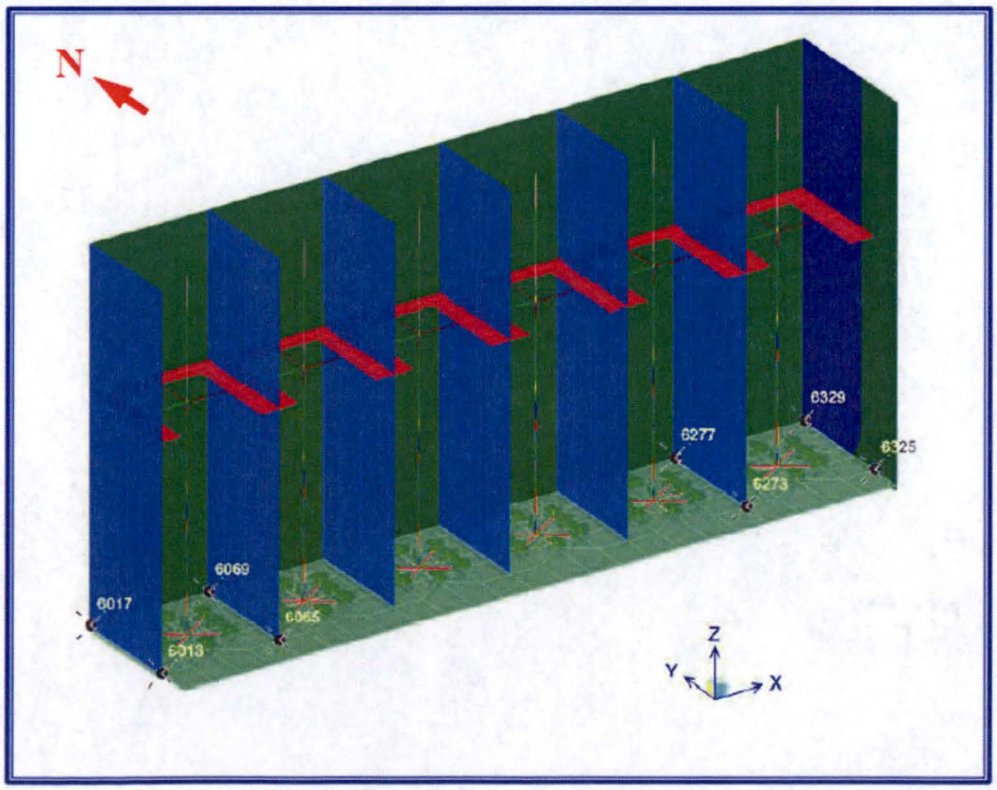

Figure 6. Nodes Selected on NuScale Power Module Pool Floor for In-Structure Response Spectra Comparison

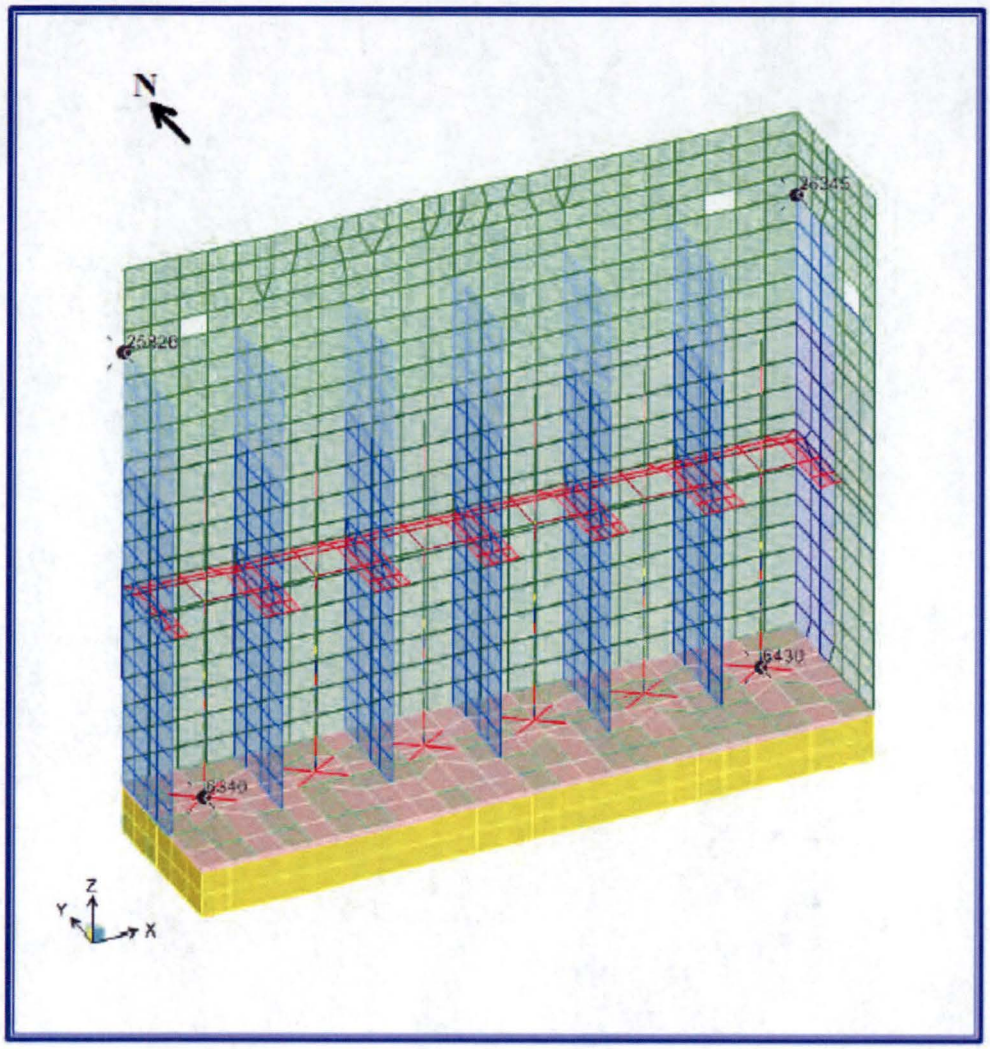

Figure 7. Nodes Selected for In-Structure Response Spectra Comparison at RXM 1 Base, RXM 6 Base, and Bioshields

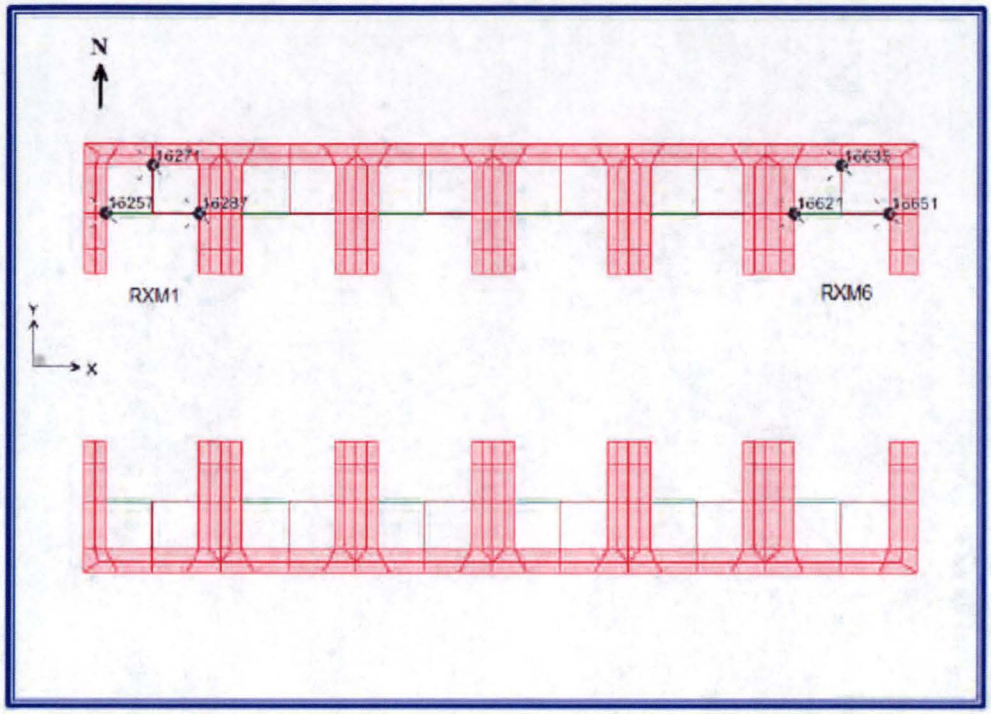

Figure 8. Nodes Selected for In-Structure Response Spectra Comparison at RXM 1 and RXM 6 Lug Supports

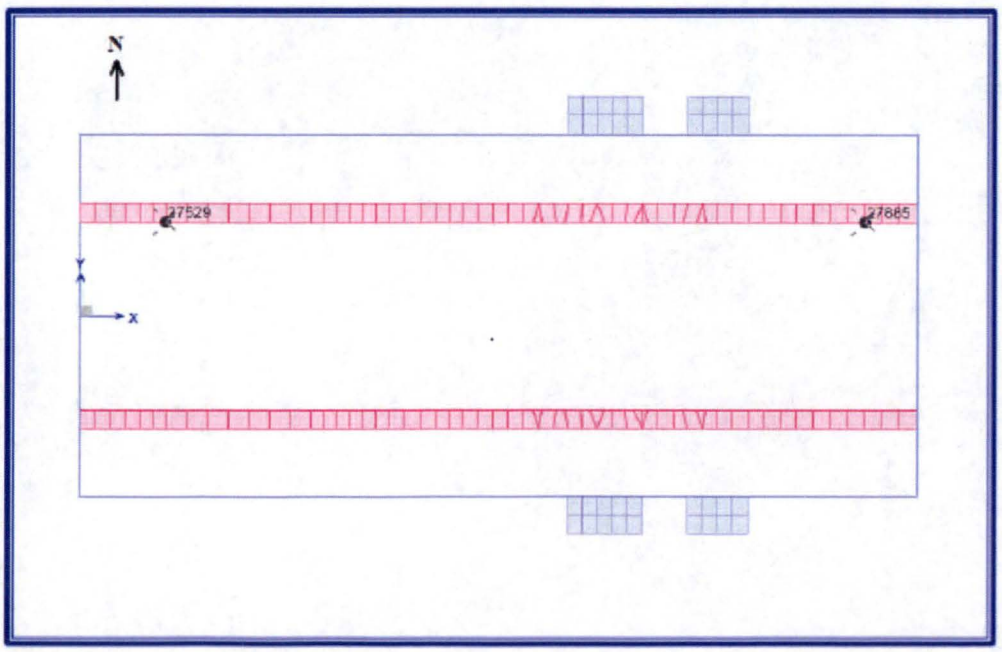

Figure 9. Nodes Selected for In-Structure Response Spectra Comparison at Crane Rail

Soil-Separation and Nonsoil-Separation In-Structure Response Spectra Comparison Results

Figure 10 through Figure 85 present the results of the comparison between SS and NSS ISRS. One case shows exceedances above 1.15 times the peak-broadened NSS ISRS and 1.15 times the design basis. For this location, 27529 Z, the design basis ISRS is updated to account for the identified exceedances, as shown in Figure 80.

Table 2. Summary of the Soil-Separation and Nonsoil-Separation In-Structure Response Spectra Comparison Results

	Number of Cases	**Node/ Direction**	**Location**
SS > NSS x 1.15	18	3996, Z 6017, Z 6069, Z 6277, Z 6325, Z 16257, Y 16287, Y 16621, Y 16651, Y 25826, Y 25826, Z 26345, Y 27529, Y 27529, Z 27885, Y 27885, Z	NW Corner on Top of Basemat RXM 1 West Pool Wall at Floor - NW Corner RXM 1 East Pool Wall at Floor - NE Corner RXM 6 West Pool Wall at Floor - NW Corner RXM 6 East Pool Wall at Floor - SE Corner RXM 1 at West Lug Support Location RXM 1 at East Lug Support Location RXM 6 at West Lug Support Location RXM 6 at East Lug Support Location Northwest Corner of Bioshield Northwest Corner of Bioshield Northeast Corner of Bioshield Crane Rail Slab Crane Rail Slab Crane Rail Slab Crane Rail Slab
SS > Peak-Broadened NSS x 1.15	1	27529, Z	Crane Rail Slab
Scaled SS > Design Basis ISRS x 1.15	1	27529, Z	Crane Rail Slab

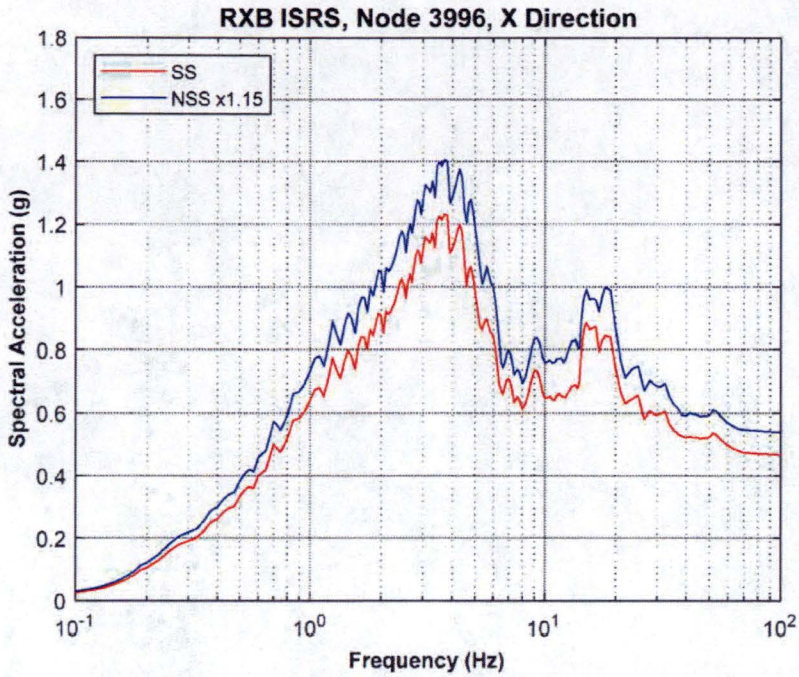

Figure 10. Reactor Building In-Structure Response Spectra Comparison, Node 3996, X-Direction

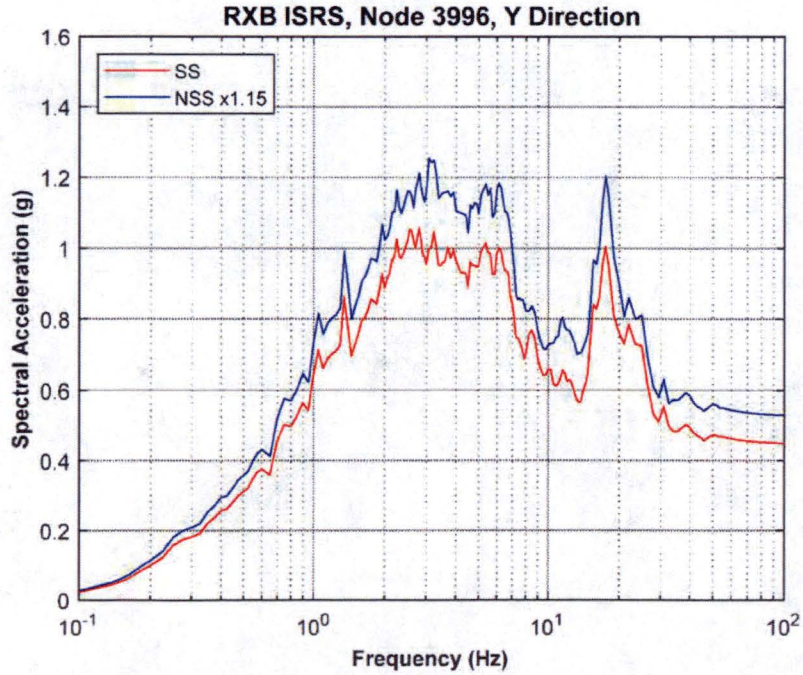

Figure 11. Reactor Building In-Structure Response Spectra Comparison, Node 3996, Y-Direction

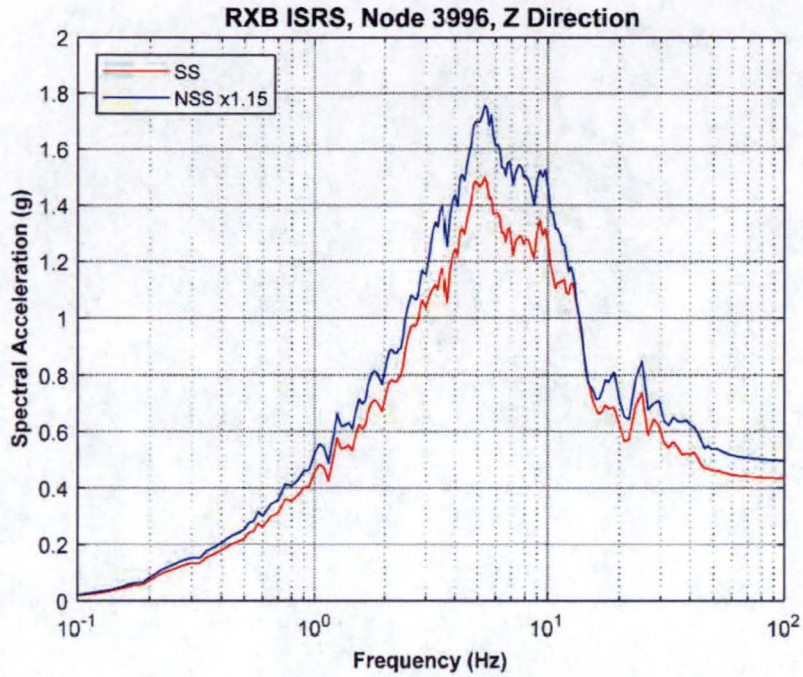

Figure 12. Reactor Building In-Structure Response Spectra Comparison, Node 3996, Z-Direction (a)

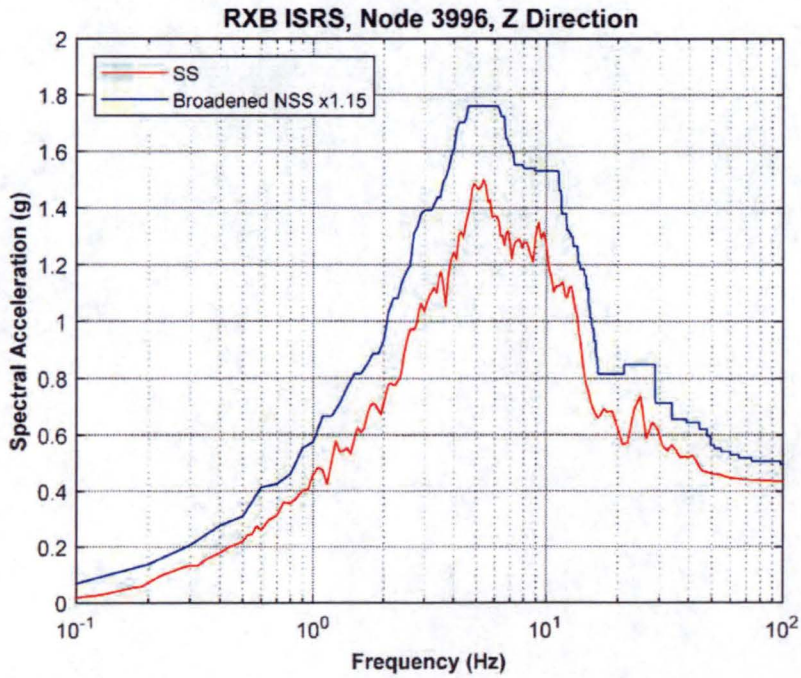

Figure 13. Reactor Building In-Structure Response Spectra Comparison, Node 3996, Z-Direction (b)

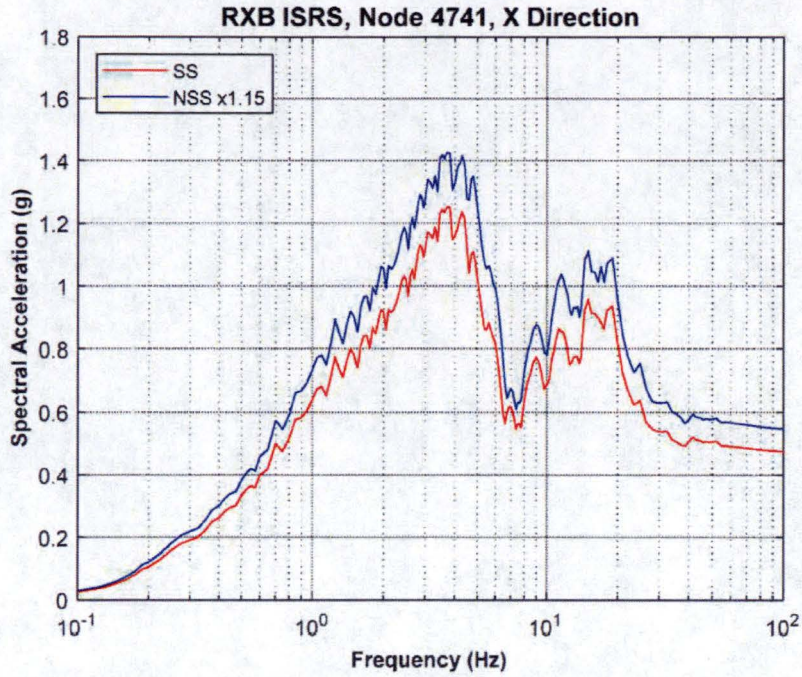

Figure 14. Reactor Building In-Structure Response Spectra Comparison, Node 4741, X-Direction

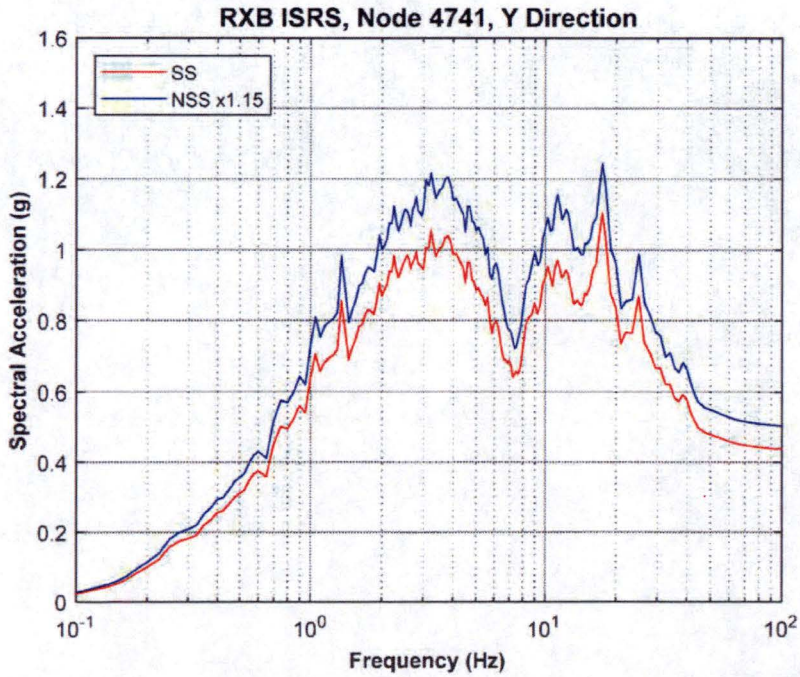

Figure 15. Reactor Building In-Structure Response Spectra Comparison, Node 4741, Y-Direction

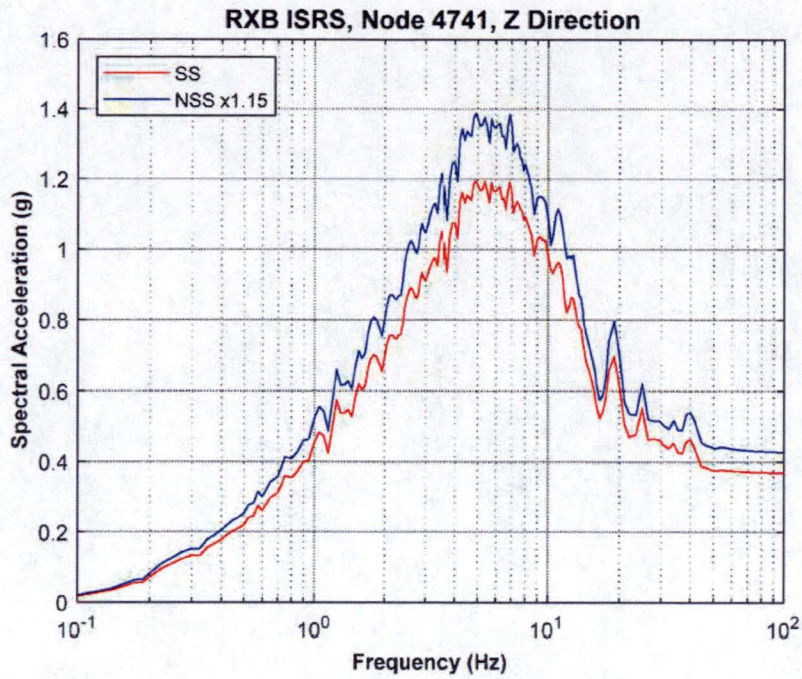

Figure 16. Reactor Building In-Structure Response Spectra Comparison, Node 4741, Z-Direction

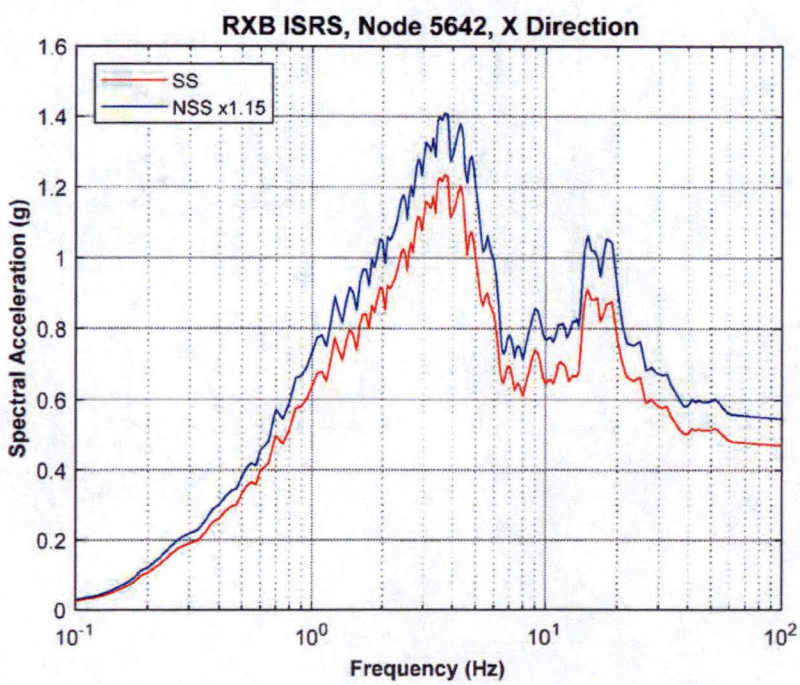

Figure 17. Reactor Building In-Structure Response Spectra Comparison, Node 5642, X-Direction

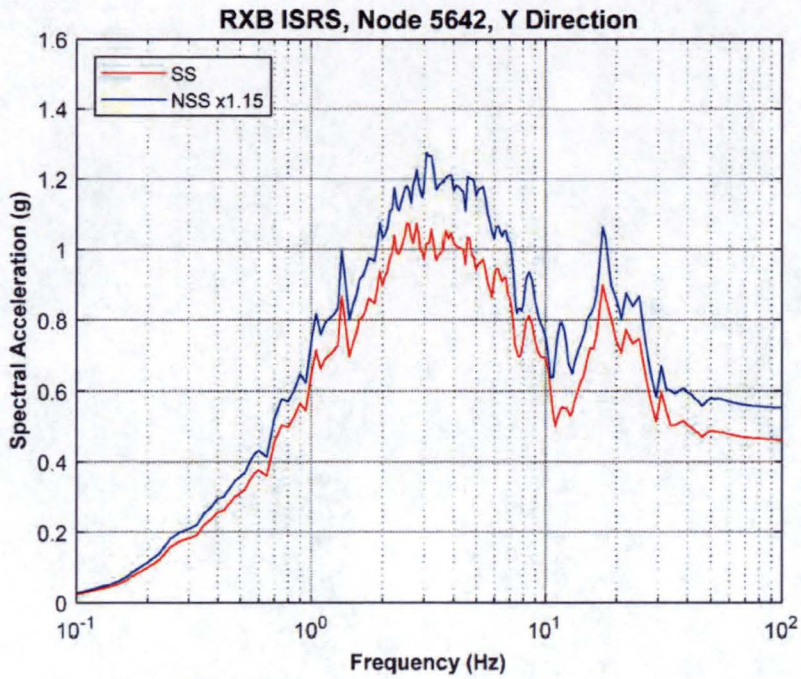

Figure 18. Reactor Building In-Structure Response Spectra Comparison, Node 5642, Y-Direction

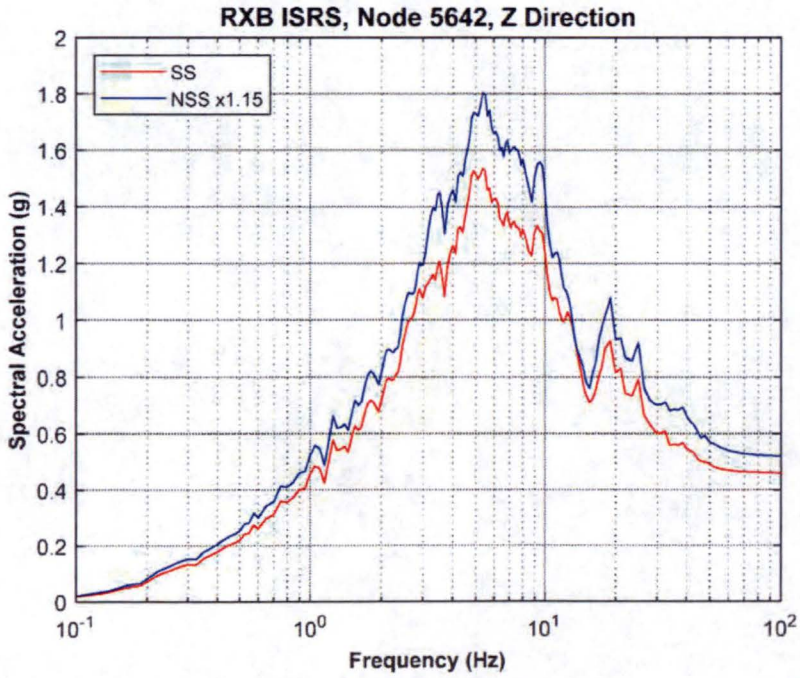

Figure 19. Reactor Building In-Structure Response Spectra Comparison, Node 5642, Z-Direction

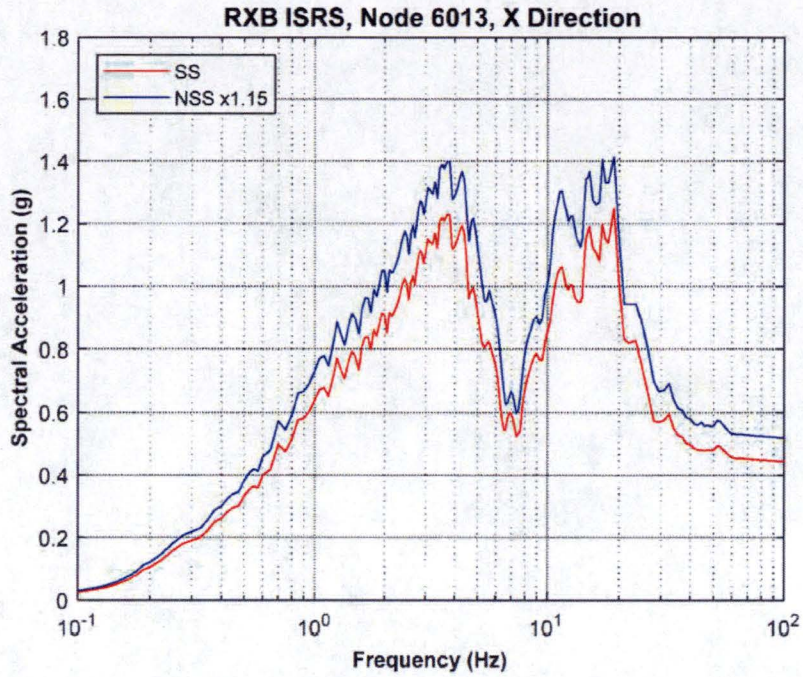

Figure 20. Reactor Building In-Structure Response Spectra Comparison, Node 6013, X-Direction

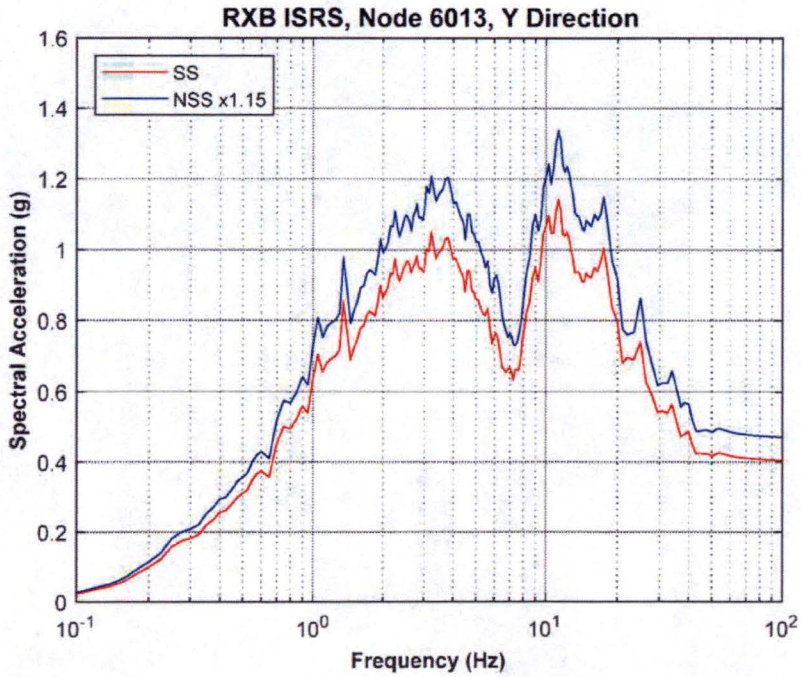

Figure 21. Reactor Building In-Structure Response Spectra Comparison, Node 6013, Y-Direction

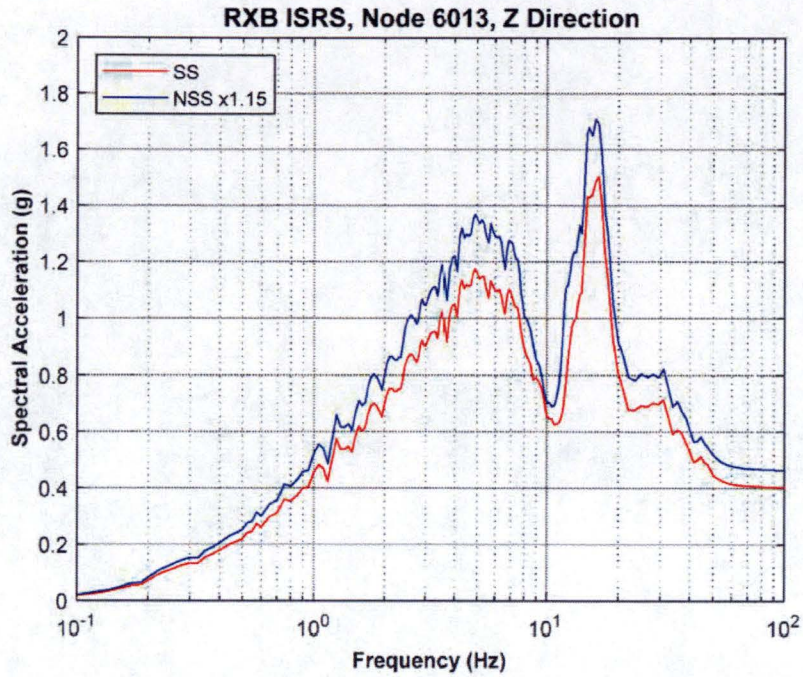

Figure 22. Reactor Building In-Structure Response Spectra Comparison, Node 6013, Z-Direction

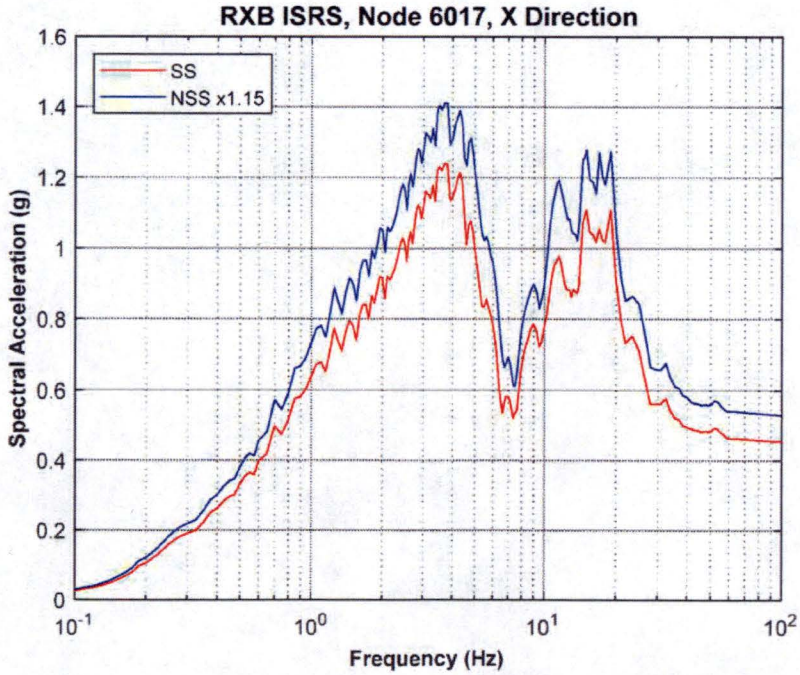

Figure 23. Reactor Building In-Structure Response Spectra Comparison, Node 6017, X-Direction

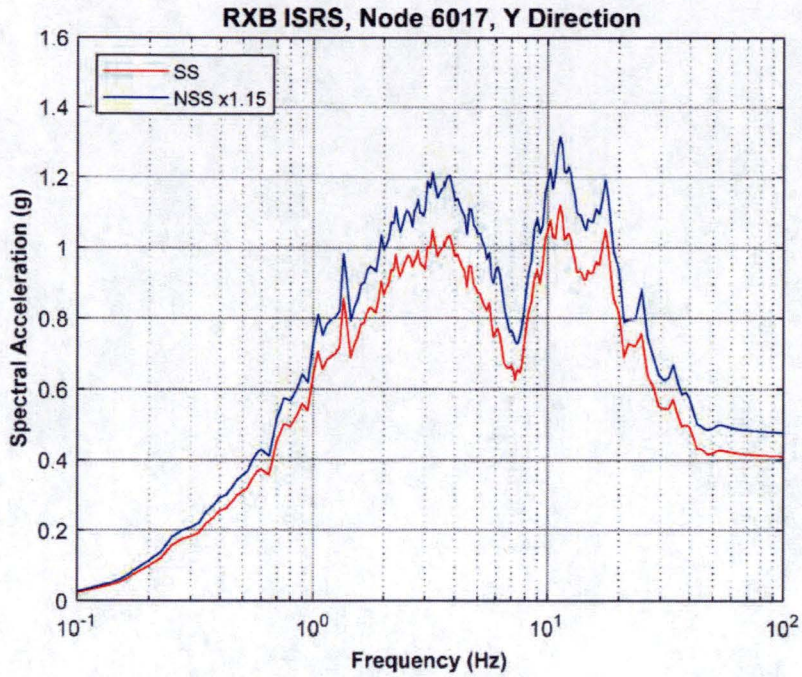

Figure 24. Reactor Building In-Structure Response Spectra Comparison, Node 6017, Y-Direction

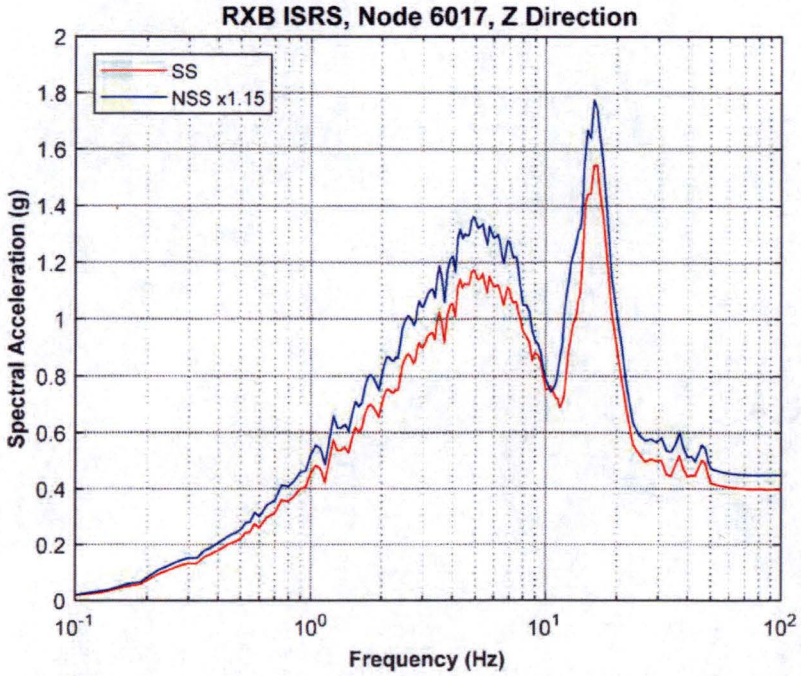

Figure 25. Reactor Building In-Structure Response Spectra Comparison, Node 6017, Z-Direction (a)

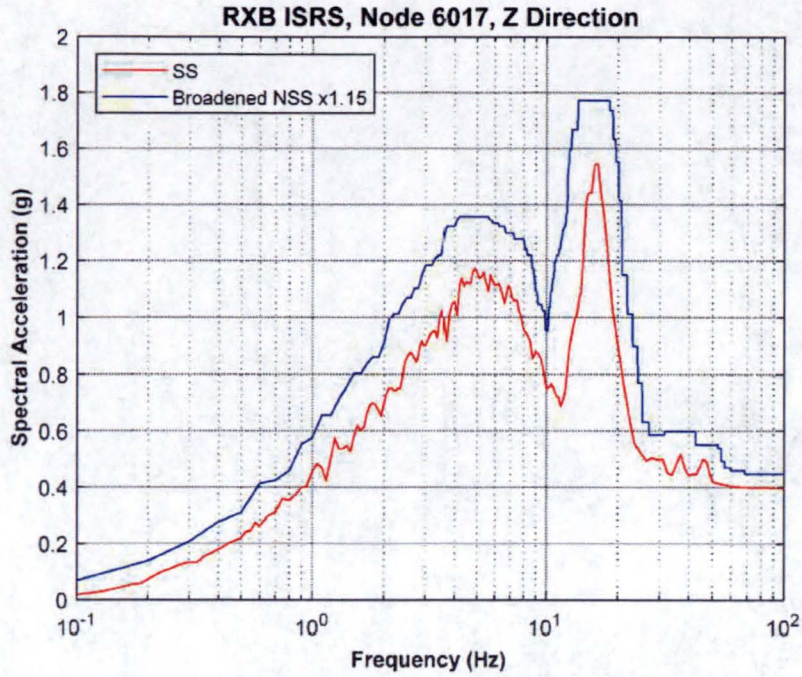

Figure 26. Reactor Building In-Structure Response Spectra Comparison, Node 6017, Z-Direction (b)

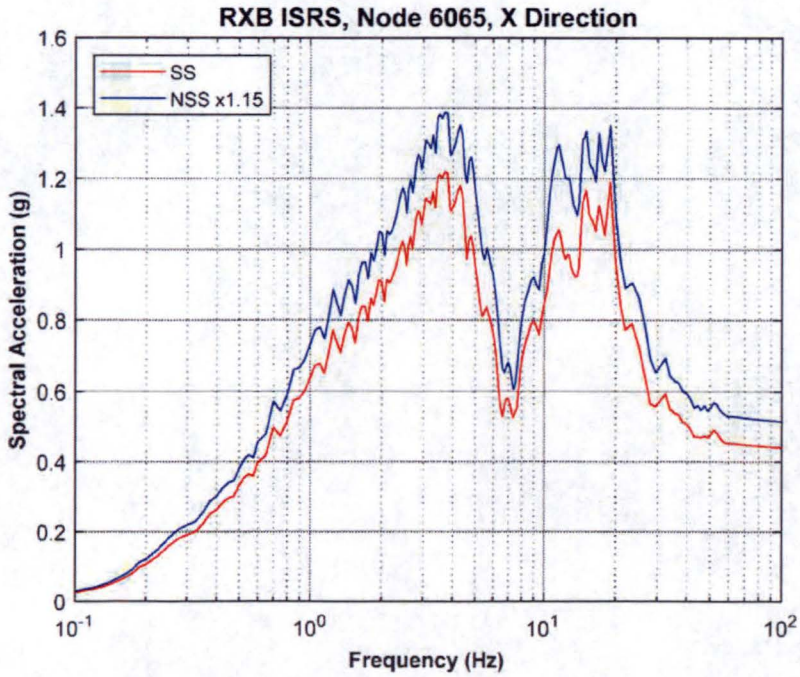

Figure 27. Reactor Building In-Structure Response Spectra Comparison, Node 6065, X-Direction

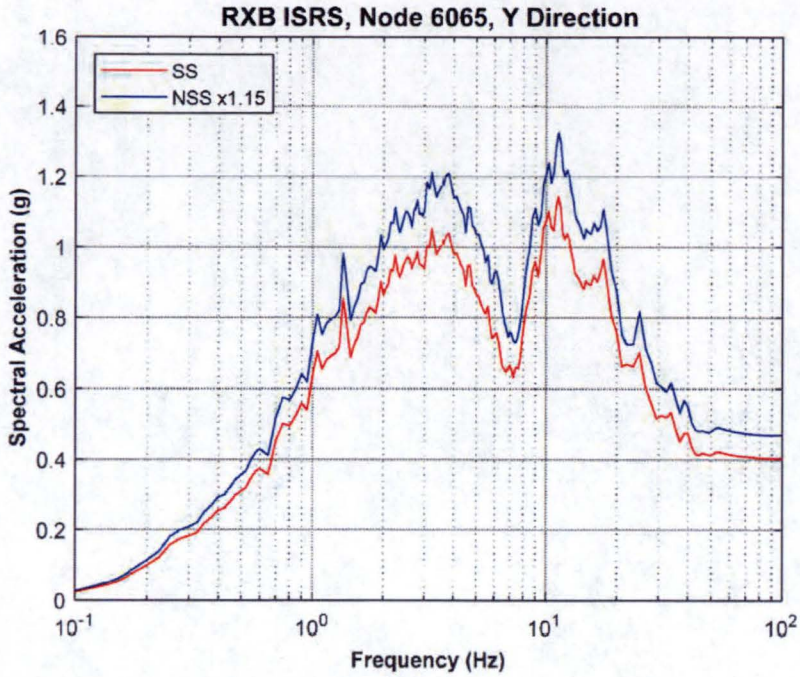

Figure 28. Reactor Building In-Structure Response Spectra Comparison, Node 6065, Y-Direction

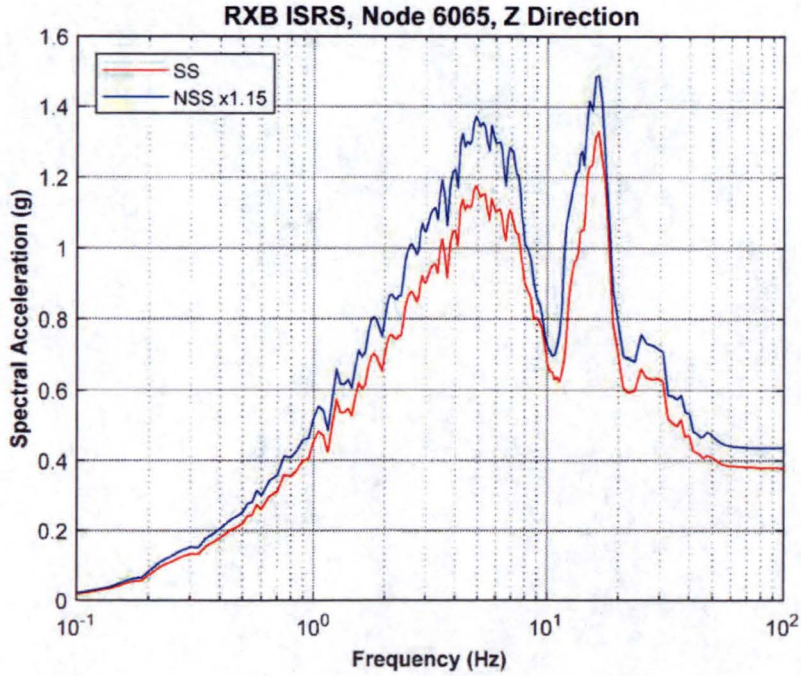

Figure 29. Reactor Building In-Structure Response Spectra Comparison, Node 6065, Z-Direction

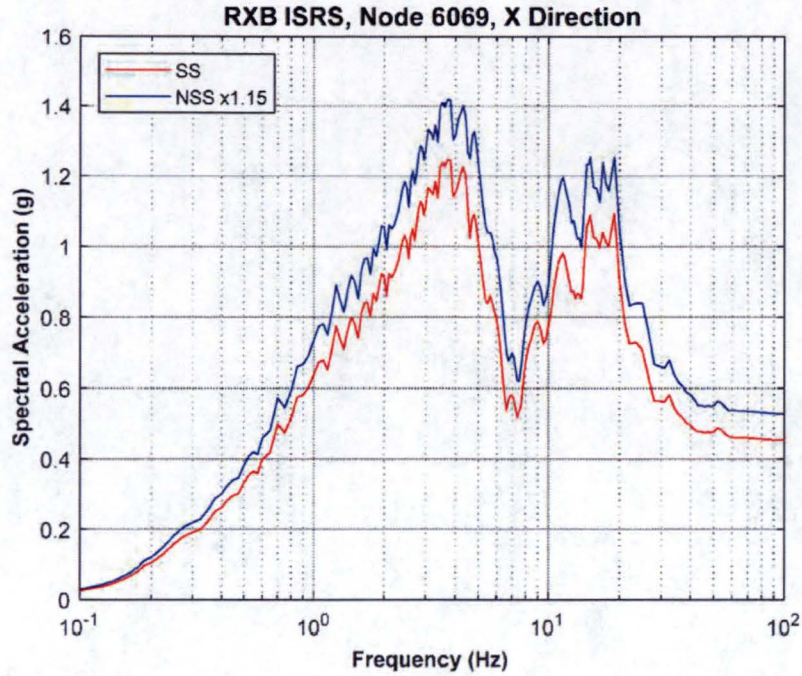

Figure 30. Reactor Building In-Structure Response Spectra Comparison, Node 6069, X-Direction

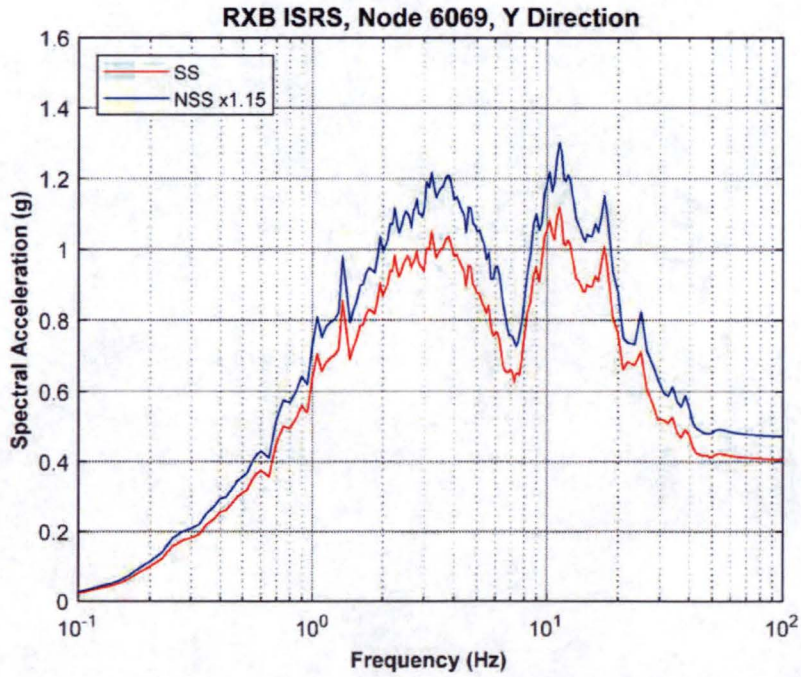

Figure 31. Reactor Building In-Structure Response Spectra Comparison, Node 6069, Y-Direction

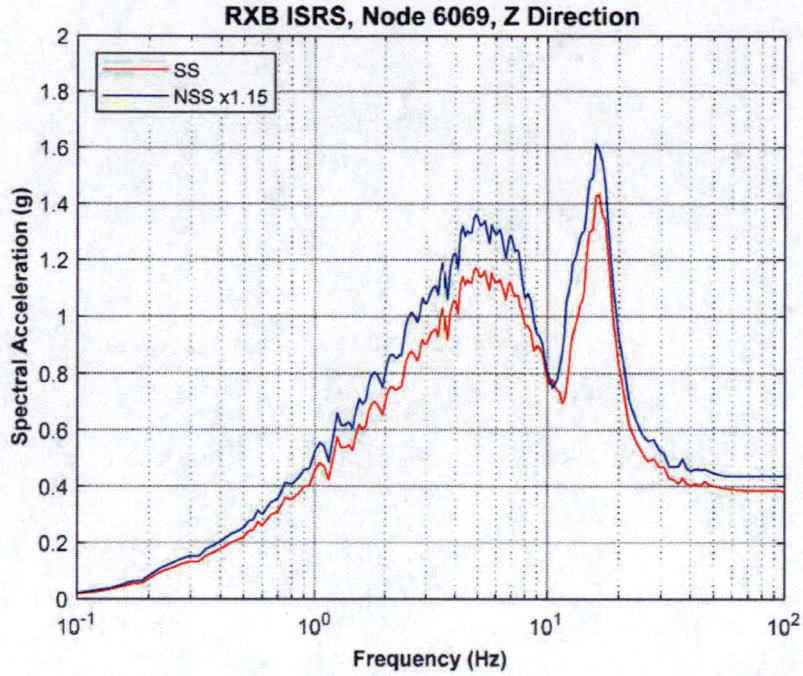

Figure 32. Reactor Building In-Structure Response Spectra Comparison, Node 6069, Z-Direction (a)

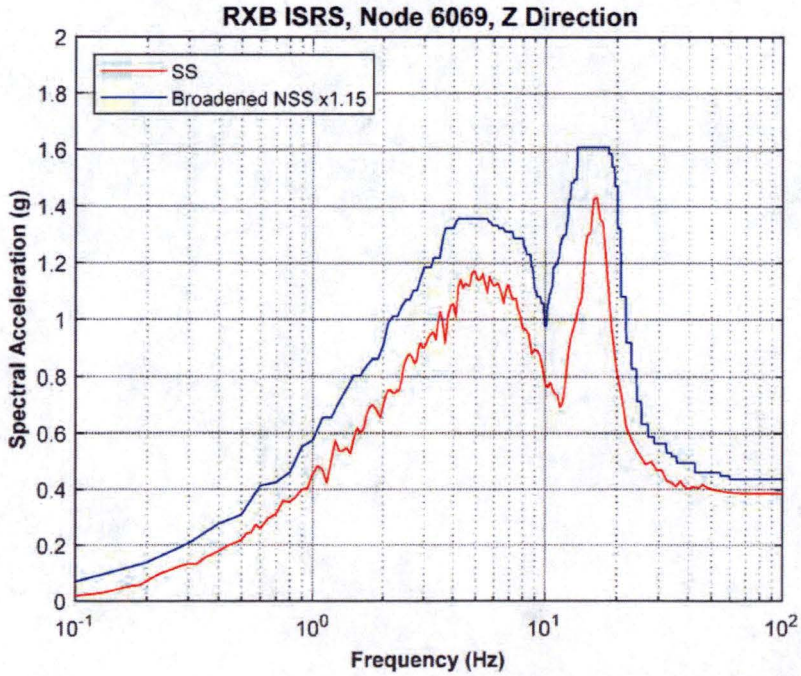

Figure 33. Reactor Building In-Structure Response Spectra Comparison, Node 6069, Z-Direction (b)

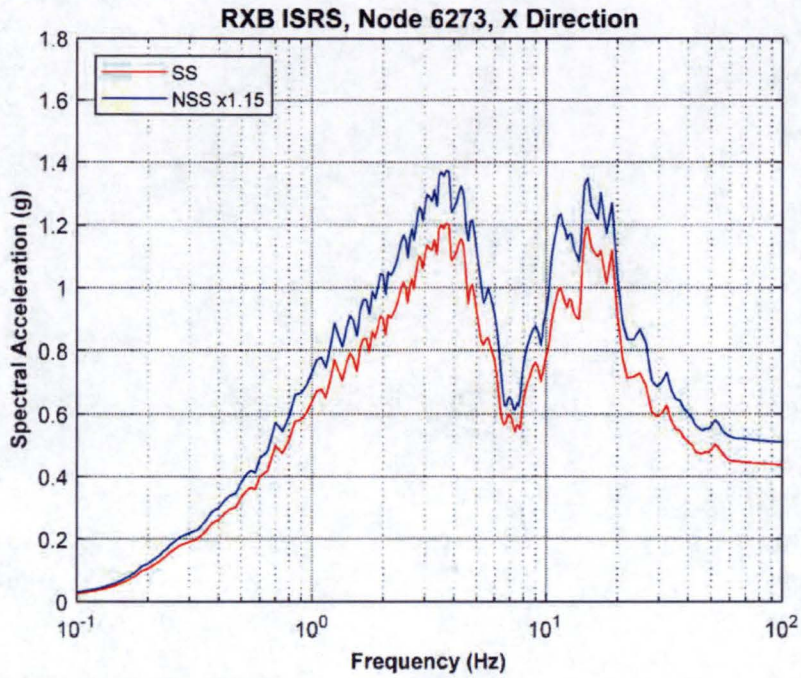

Figure 34. Reactor Building In-Structure Response Spectra Comparison, Node 6273, X-Direction

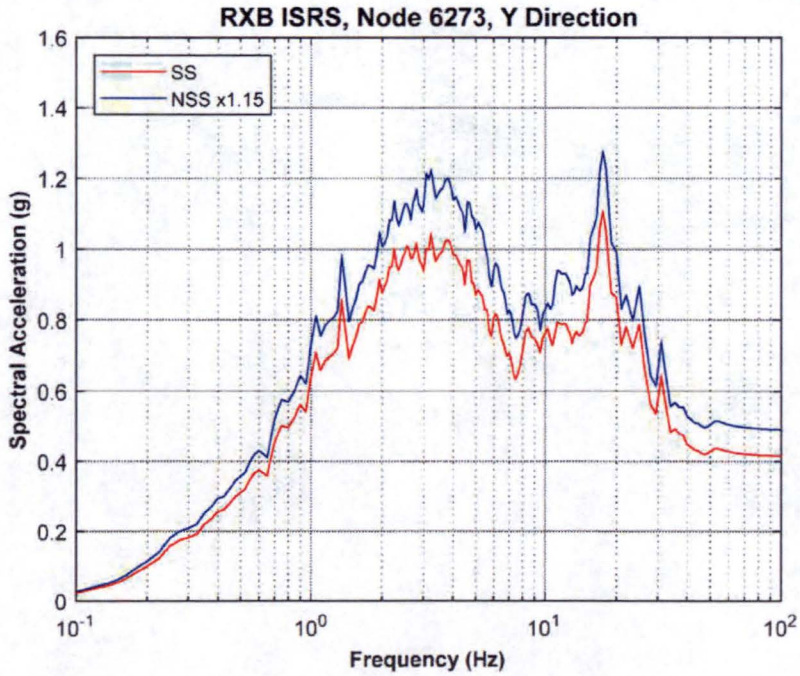

Figure 35. Reactor Building In-Structure Response Spectra Comparison, Node 6273, Y-Direction

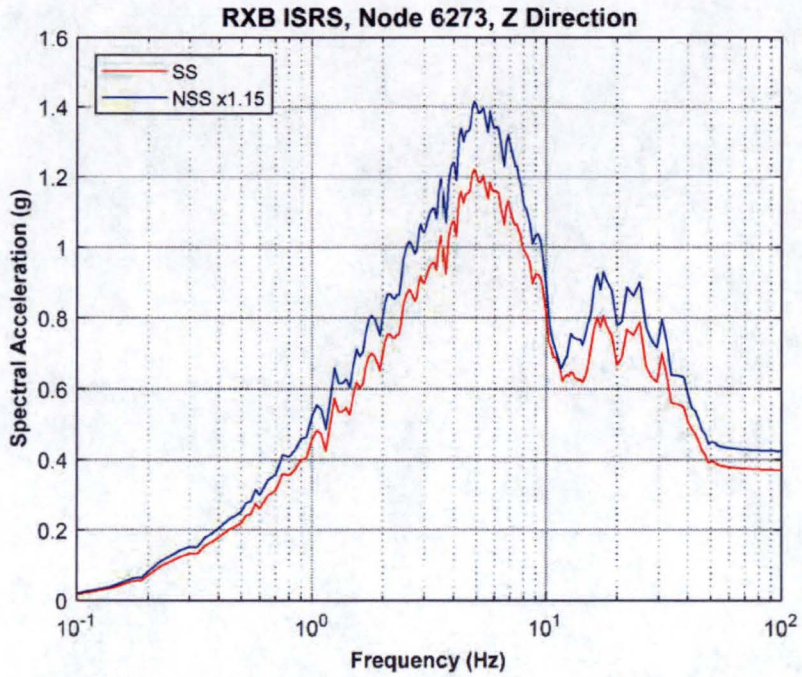

Figure 36. Reactor Building In-Structure Response Spectra Comparison, Node 6273, Z-Direction

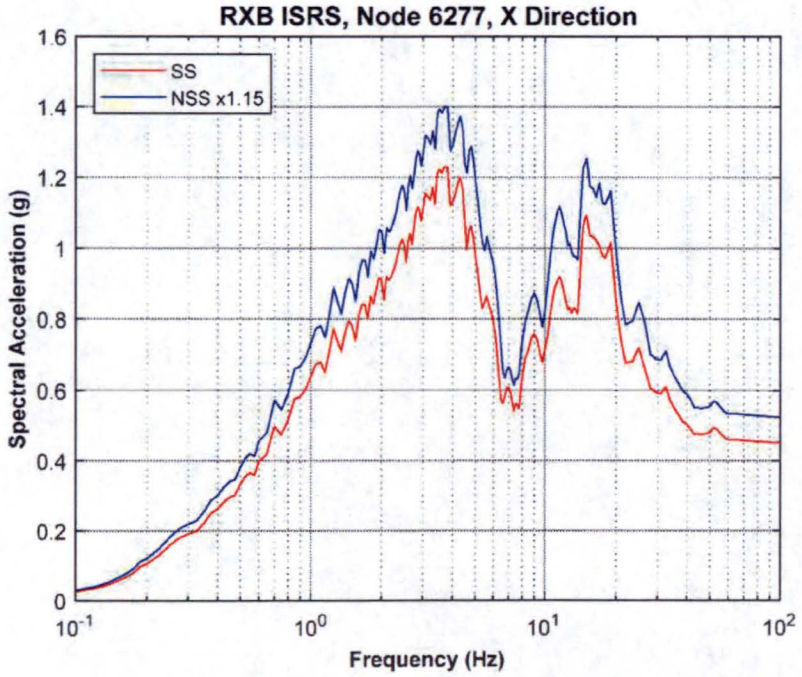

Figure 37. Reactor Building In-Structure Response Spectra Comparison, Node 6277, X-Direction

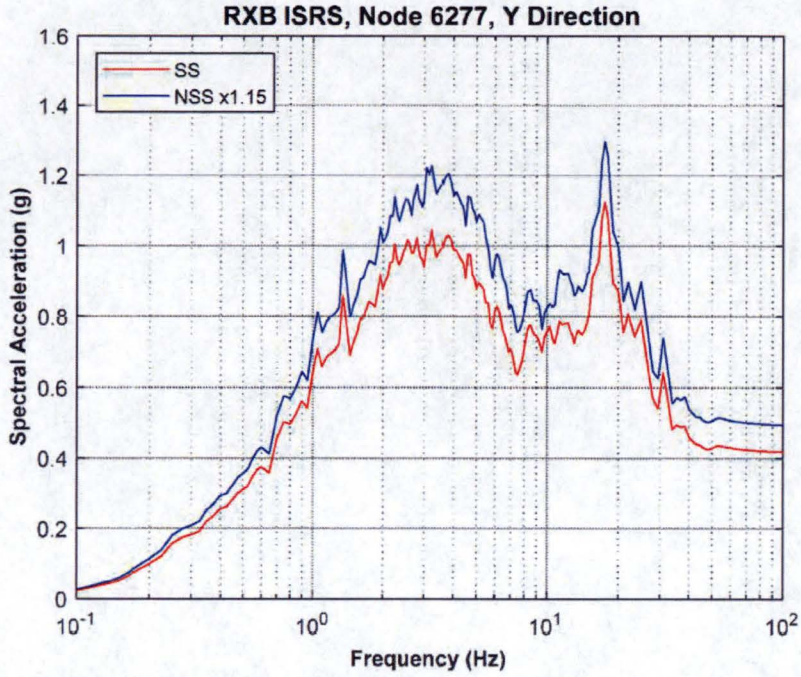

Figure 38. Reactor Building In-Structure Response Spectra Comparison, Node 6277, Y-Direction

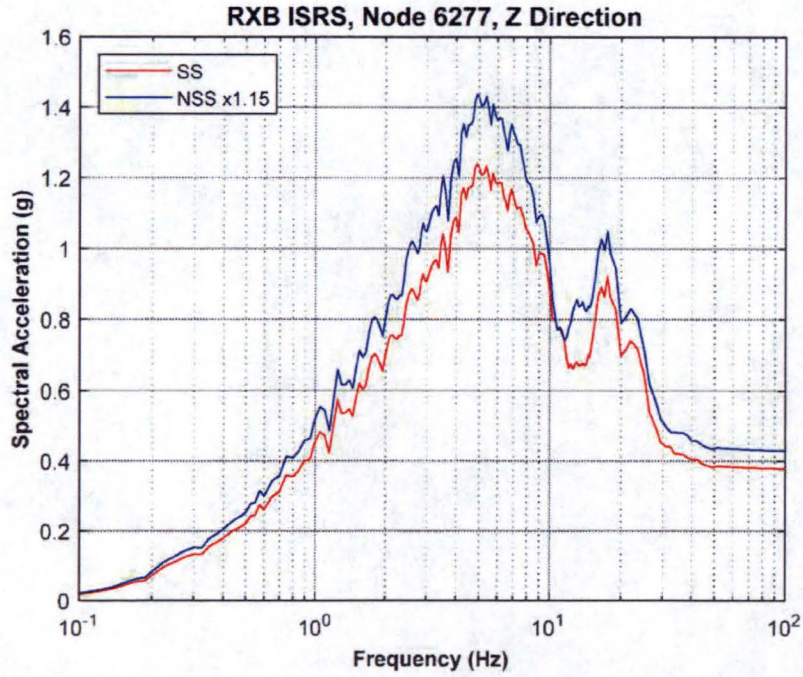

Figure 39. Reactor Building In-Structure Response Spectra Comparison, Node 6277, Z-Direction (a)

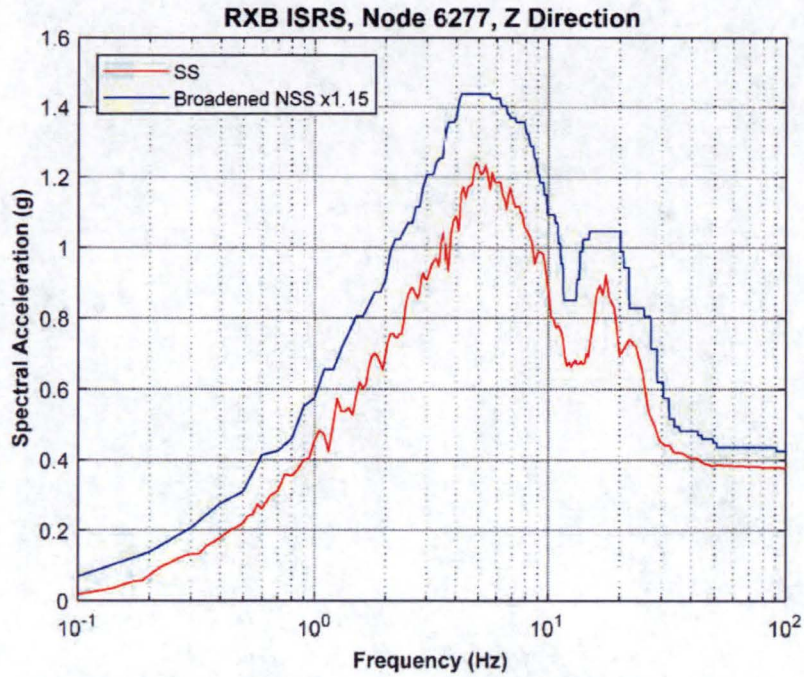

Figure 40. Reactor Building In-Structure Response Spectra Comparison, Node 6277, Z-Direction (b)

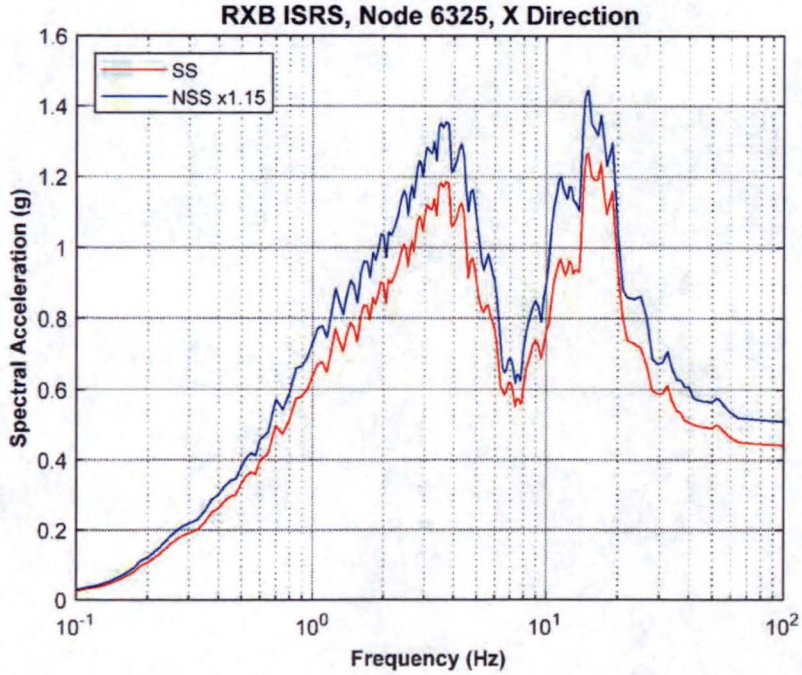

Figure 41. Reactor Building In-Structure Response Spectra Comparison, Node 6325, X-Direction

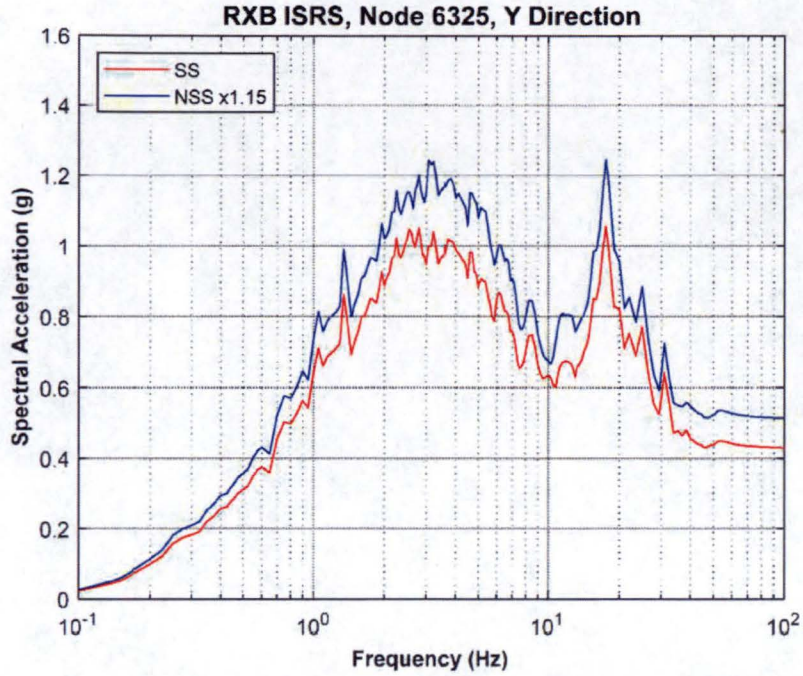

Figure 42. Reactor Building In-Structure Response Spectra Comparison, Node 6325, Y-Direction

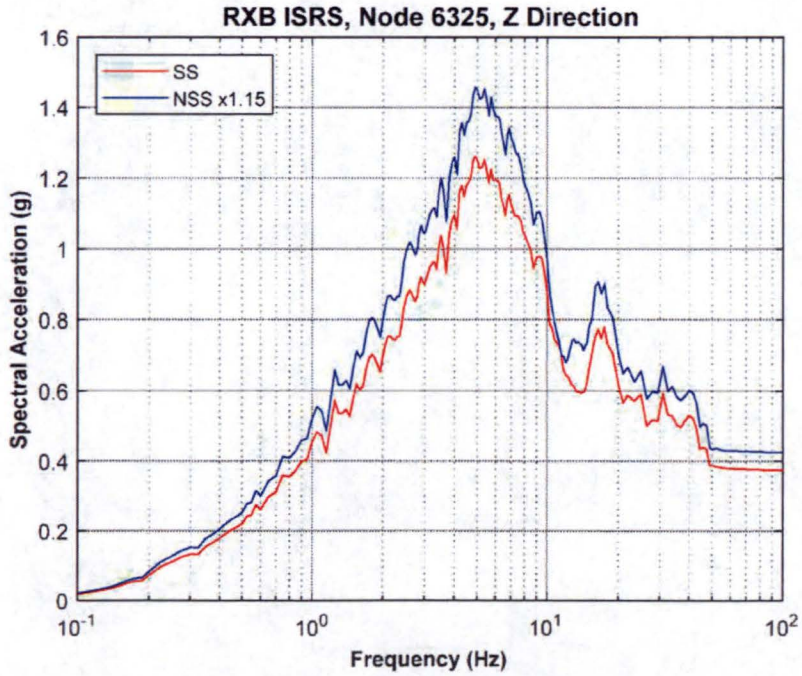

Figure 43. Reactor Building In-Structure Response Spectra Comparison, Node 6325, Z-Direction (a)

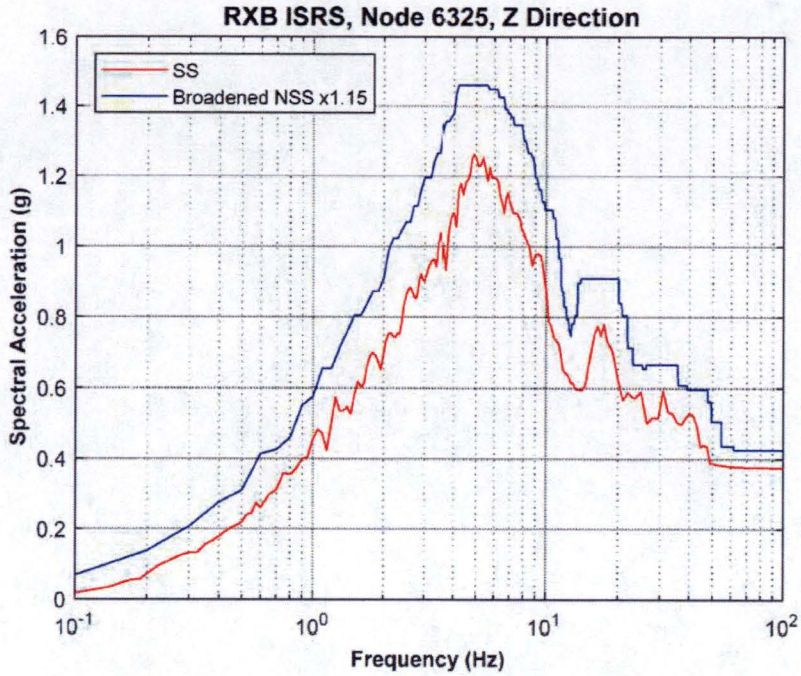

Figure 44. Reactor Building In-Structure Response Spectra Comparison, Node 6325, Z-Direction (b)

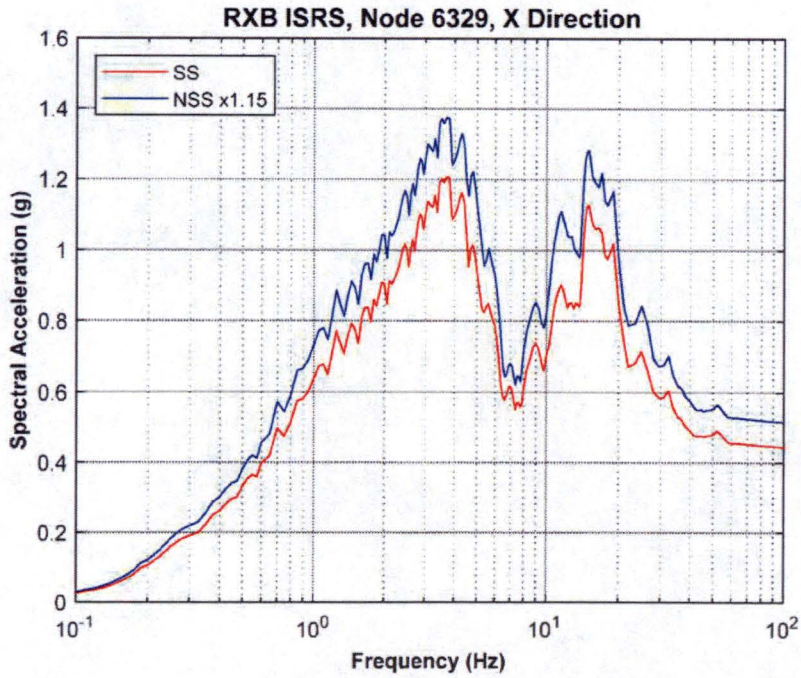

Figure 45. Reactor Building In-Structure Response Spectra Comparison, Node 6329, X-Direction

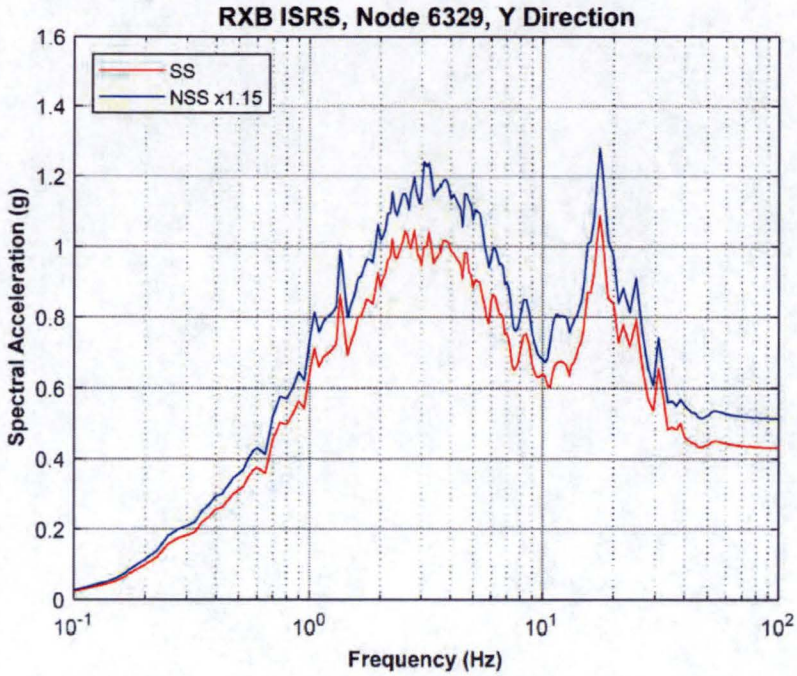

Figure 46. Reactor Building In-Structure Response Spectra Comparison, Node 6329, Y-Direction

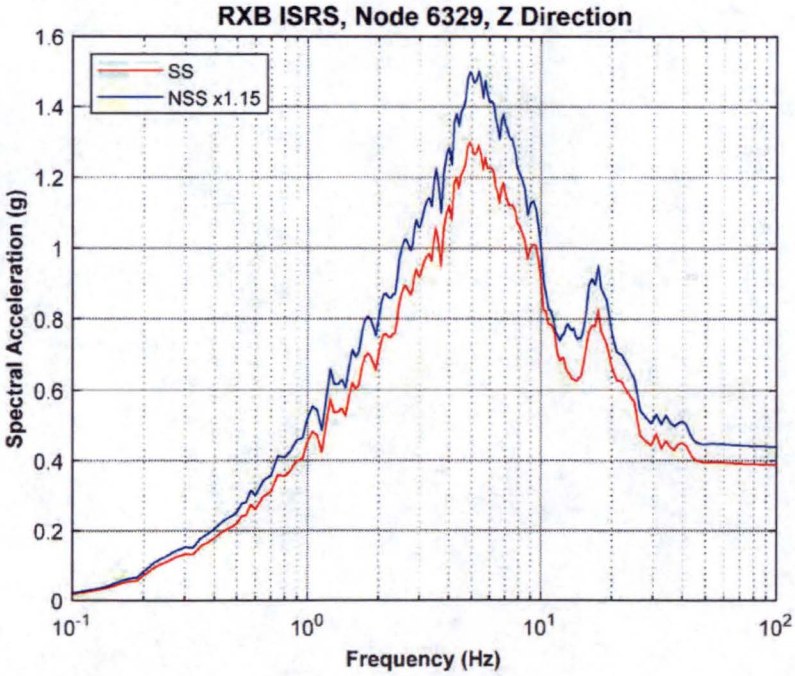

Figure 47. Reactor Building In-Structure Response Spectra Comparison, Node 6329, Z-Direction

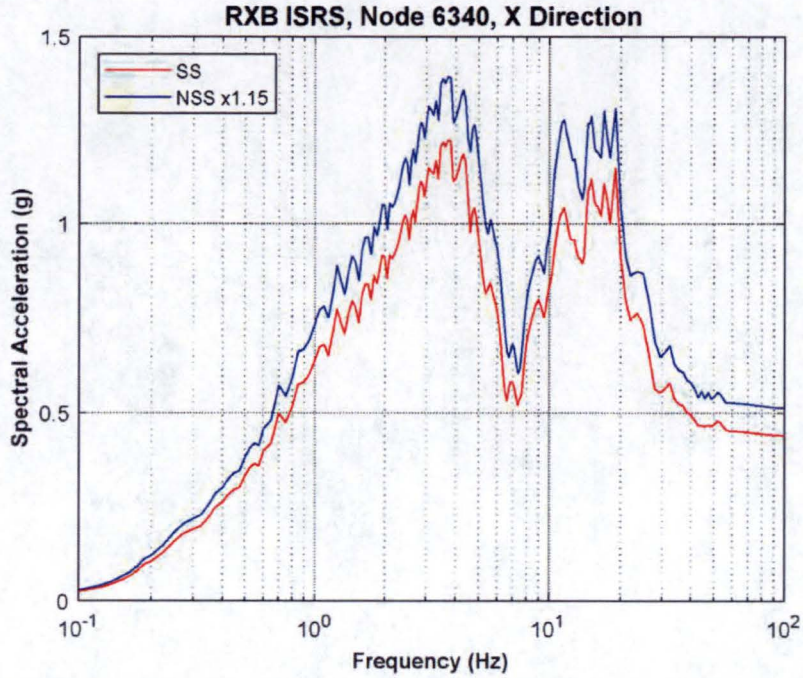

Figure 48. Reactor Building In-Structure Response Spectra Comparison, Node 6340, X-Direction

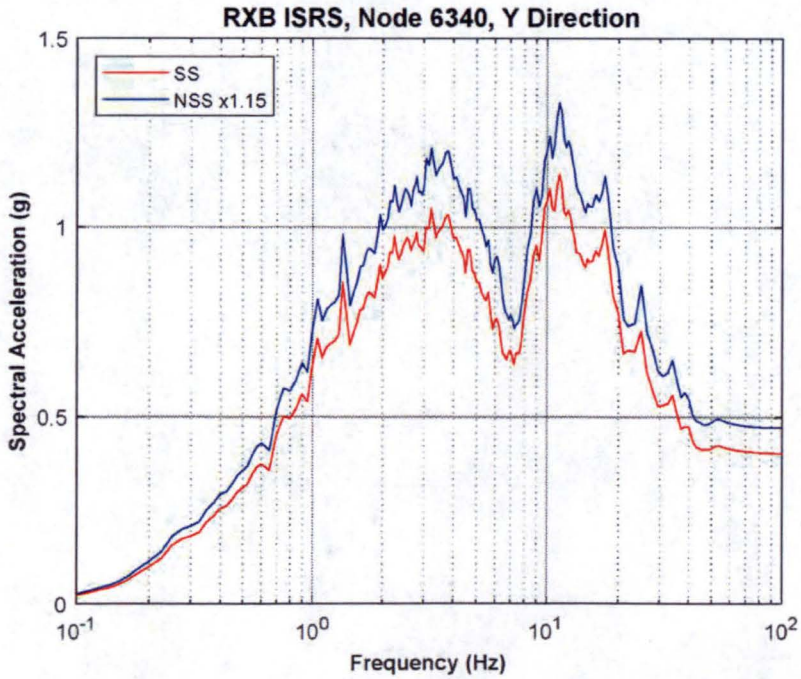

Figure 49. Reactor Building In-Structure Response Spectra Comparison, Node 6340, Y-Direction

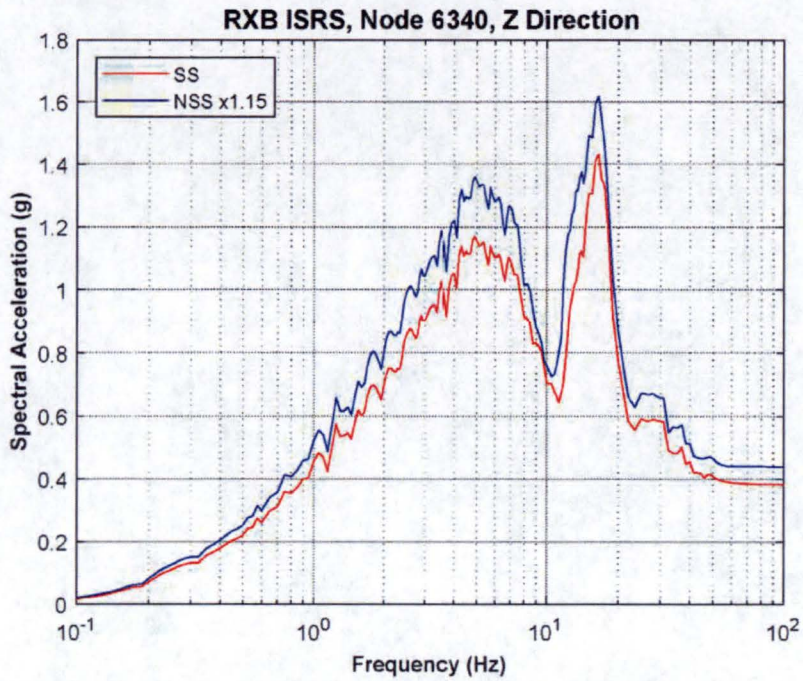

Figure 50. Reactor Building In-Structure Response Spectra Comparison, Node 6340, Z-Direction

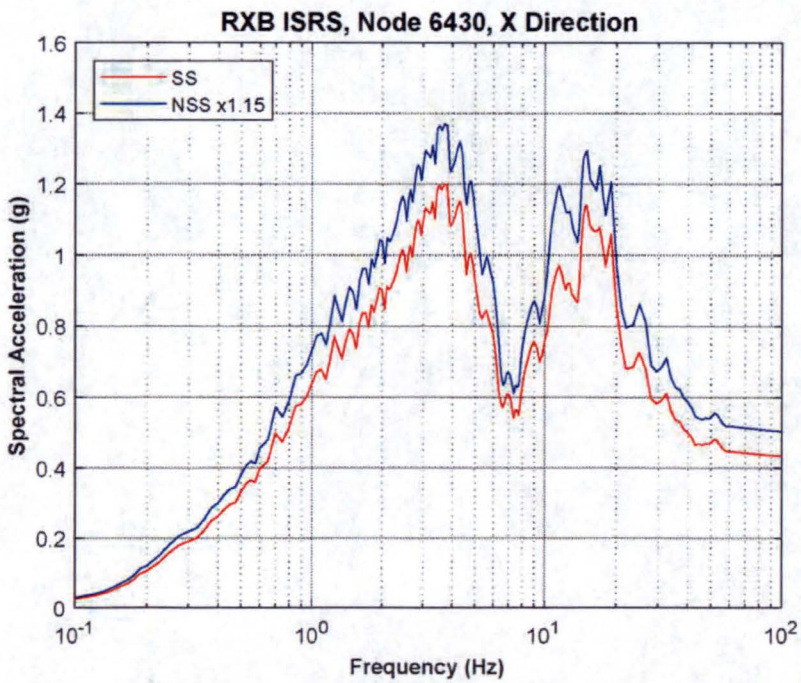

Figure 51. Reactor Building In-Structure Response Spectra Comparison, Node 6430, X-Direction

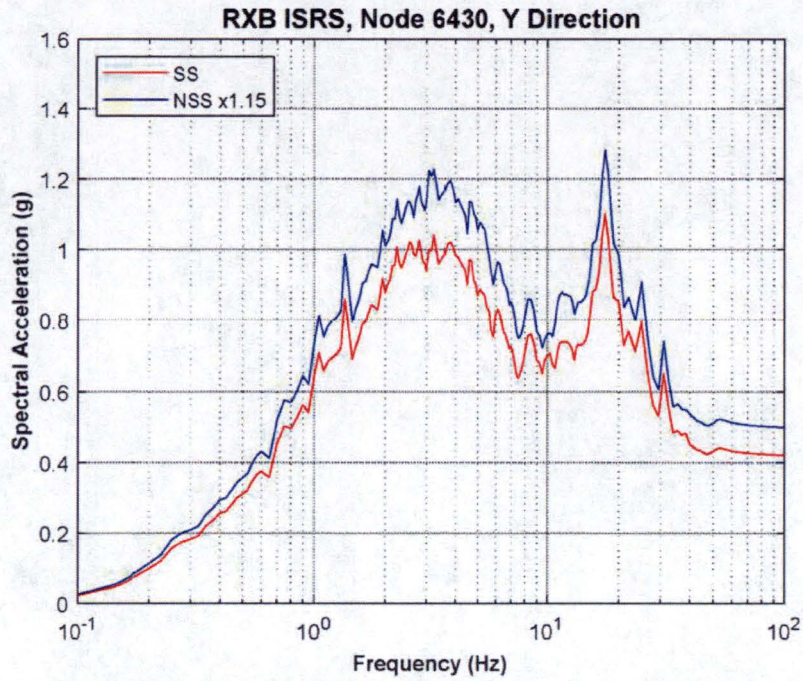

Figure 52. Reactor Building In-Structure Response Spectra Comparison, Node 6430, Y-Direction

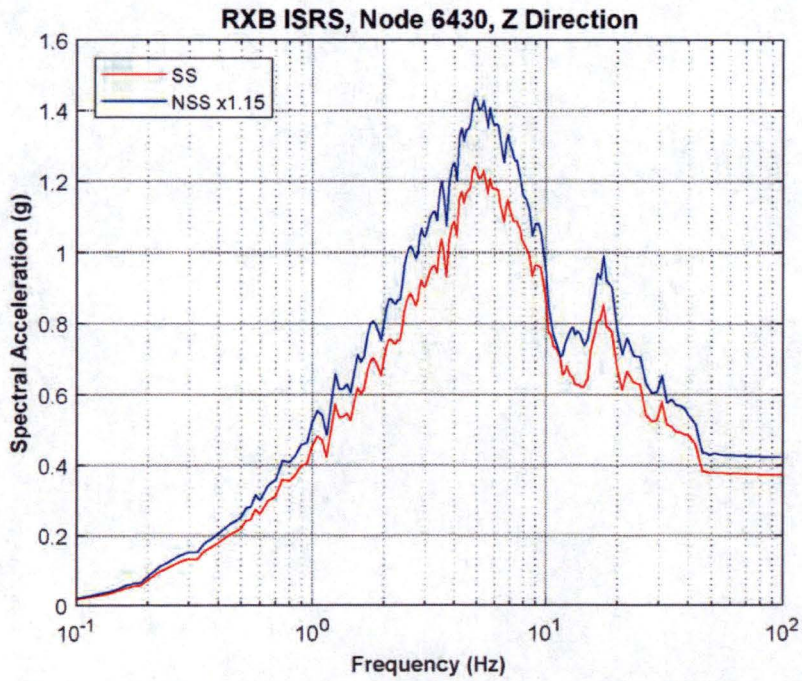

Figure 53. Reactor Building In-Structure Response Spectra Comparison, Node 6430, Z-Direction

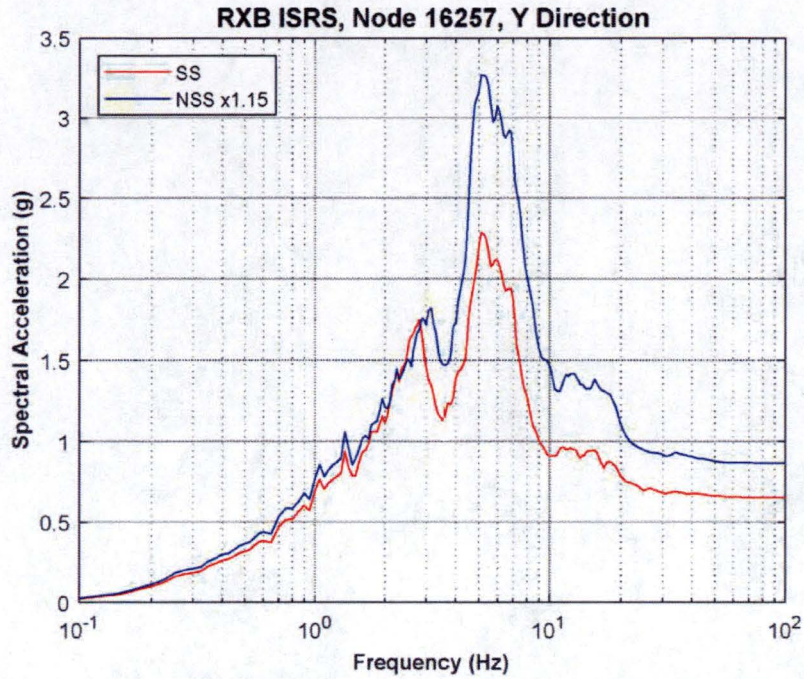

Figure 54. Reactor Building In-Structure Response Spectra Comparison, Node 16257, Y-Direction (a)

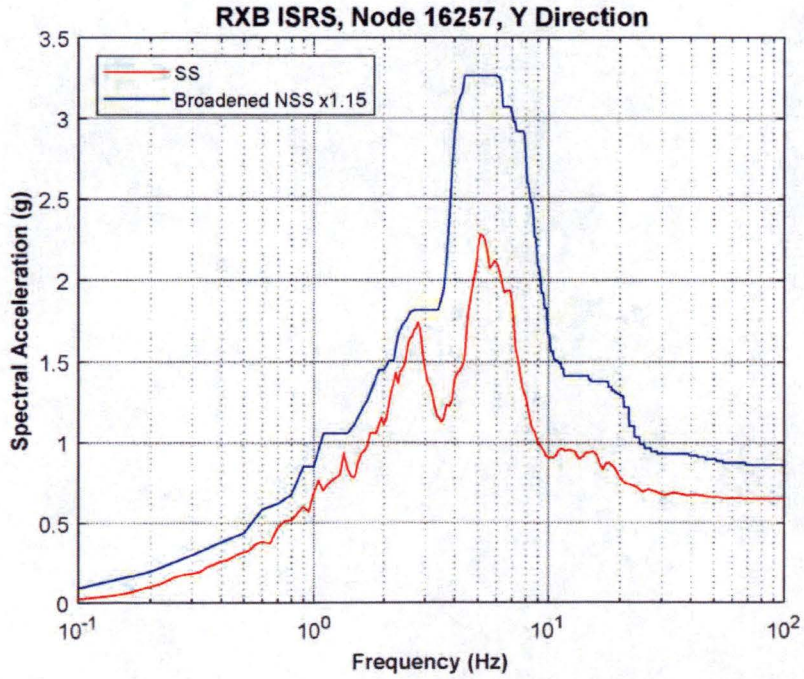

Figure 55. Reactor Building In-Structure Response Spectra Comparison, Node 16257, Y-Direction (b)

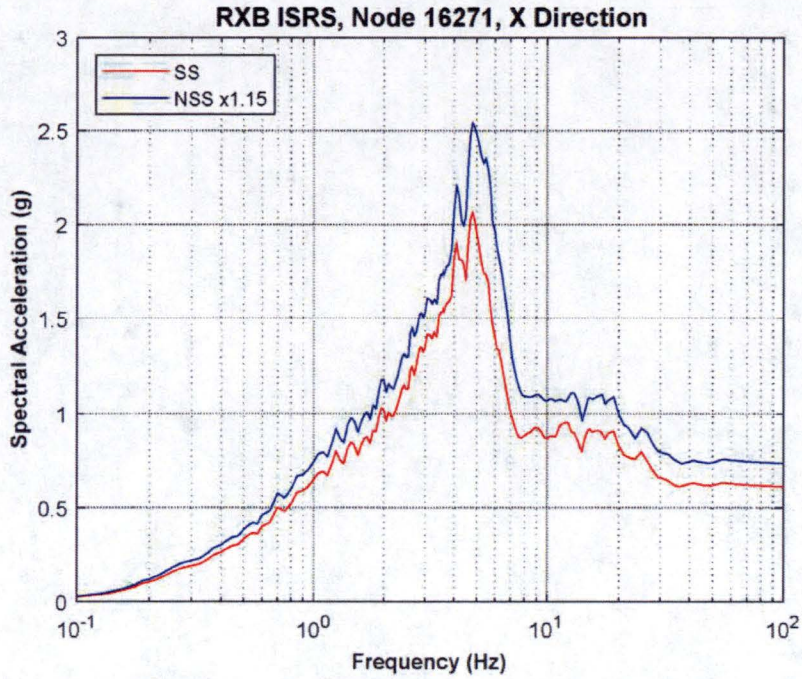

Figure 56. Reactor Building In-Structure Response Spectra Comparison, Node 16271, X-Direction

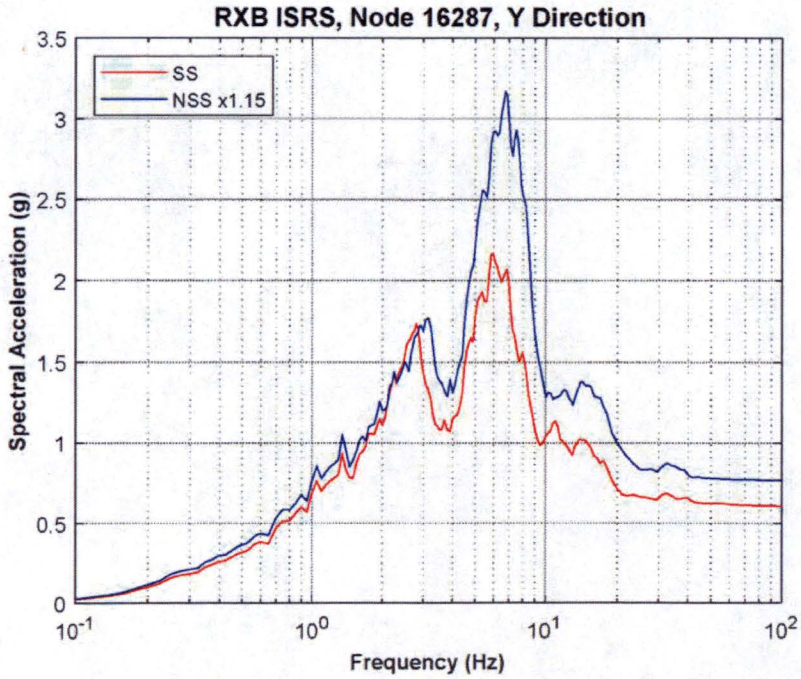

Figure 57. Reactor Building In-Structure Response Spectra Comparison, Node 16287, Y-Direction (a)

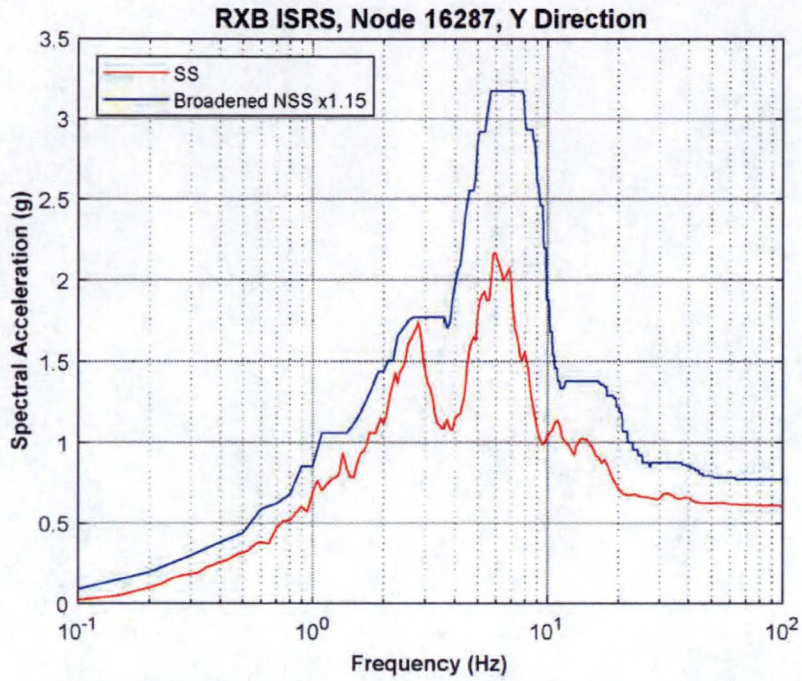

Figure 58. Reactor Building In-Structure Response Spectra Comparison, Node 16287, Y-Direction (b)

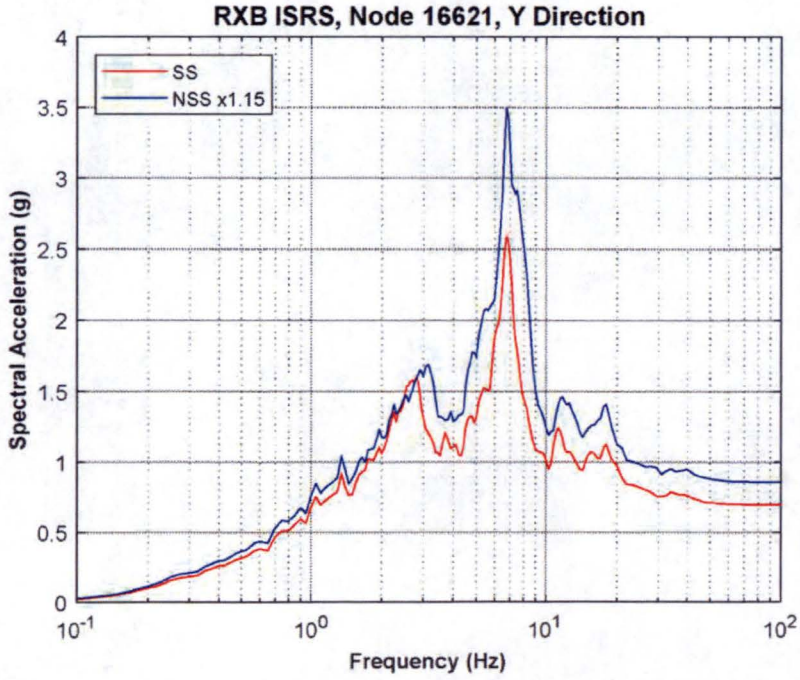

Figure 59. Reactor Building In-Structure Response Spectra Comparison, Node 16621, Y-Direction (a)

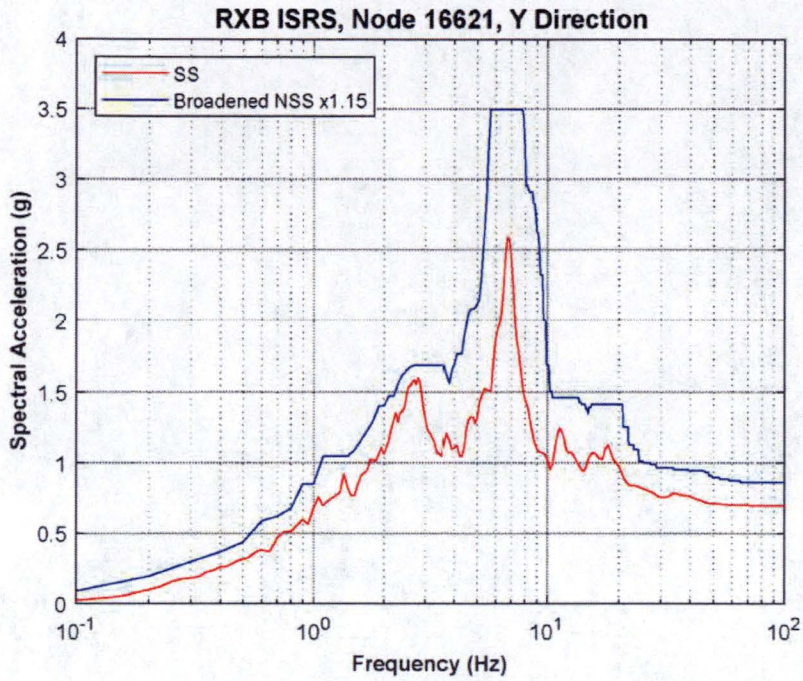

Figure 60. Reactor Building In-Structure Response Spectra Comparison, Node 16621, Y-Direction (b)

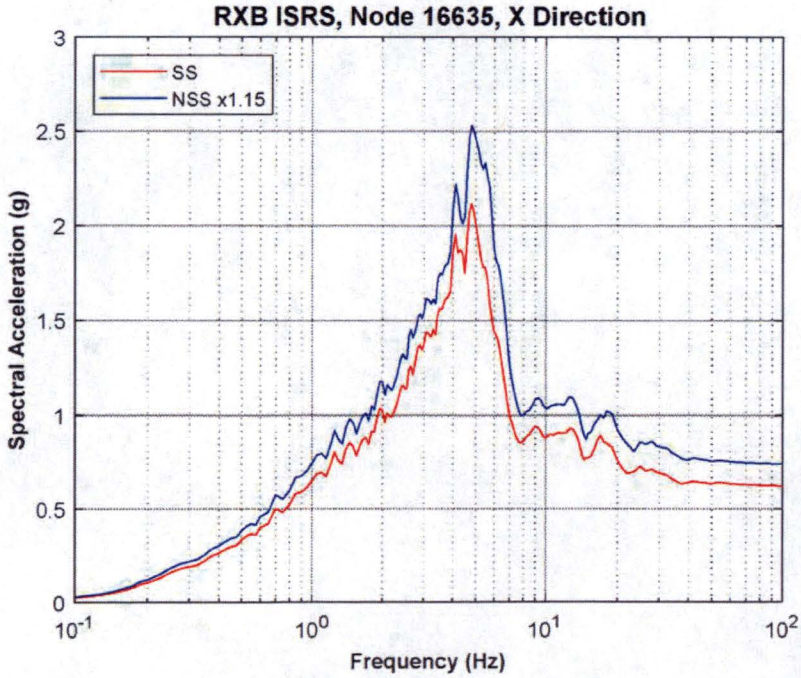

Figure 61. Reactor Building In-Structure Response Spectra Comparison, Node 16635, X-Direction

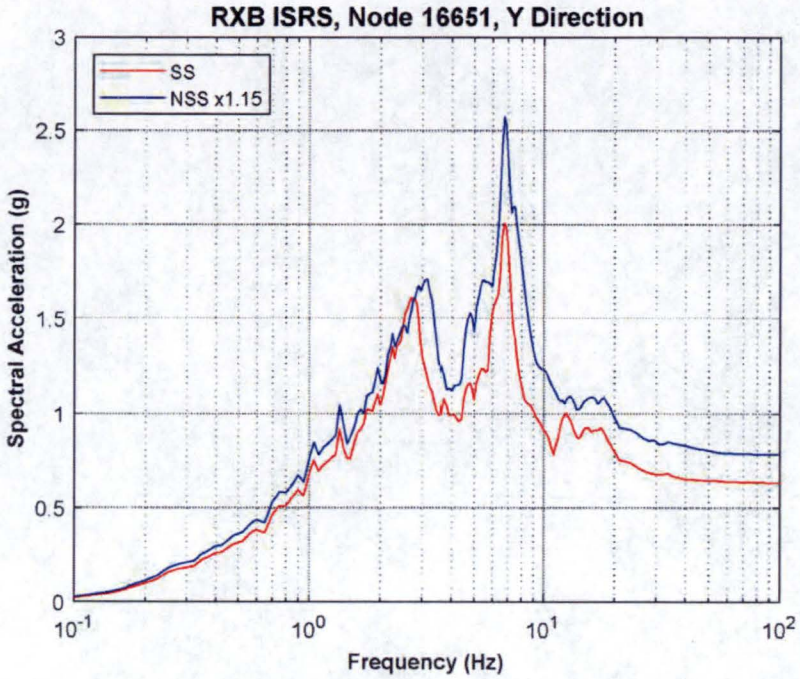

Figure 62. Reactor Building In-Structure Response Spectra Comparison, Node 16651, Y-Direction (a)

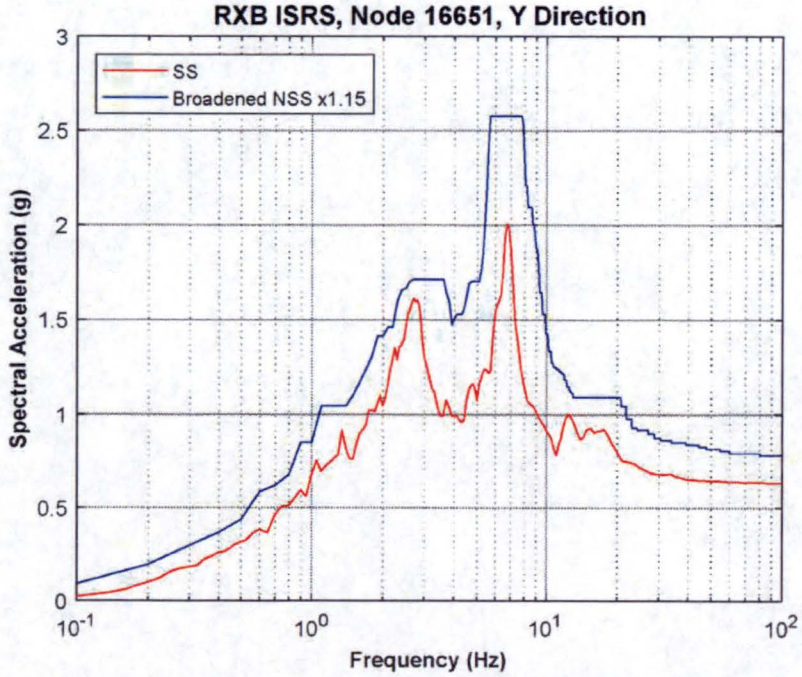

Figure 63. Reactor Building In-Structure Response Spectra Comparison, Node 16651, Y-Direction (b)

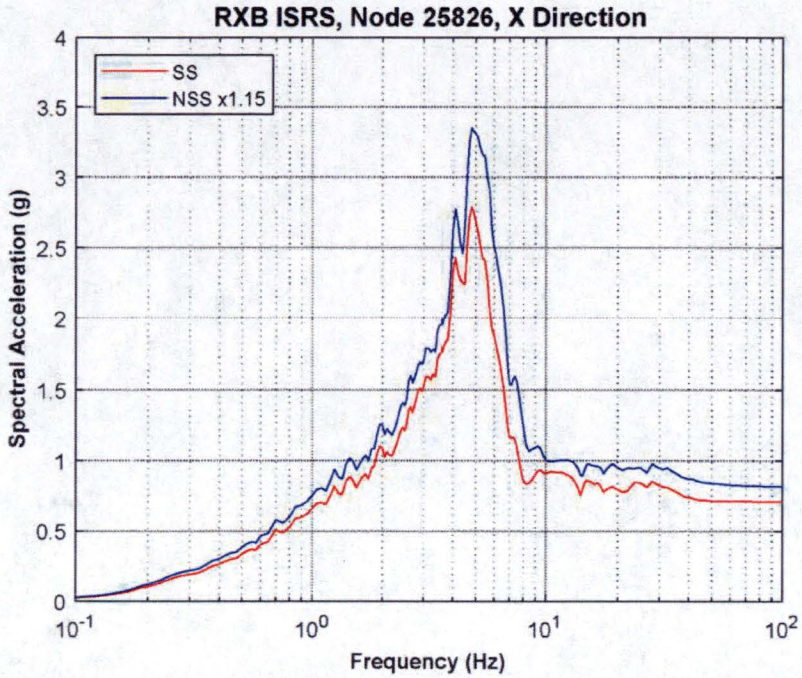

Figure 64. Reactor Building In-Structure Response Spectra Comparison, Node 25826, X-Direction

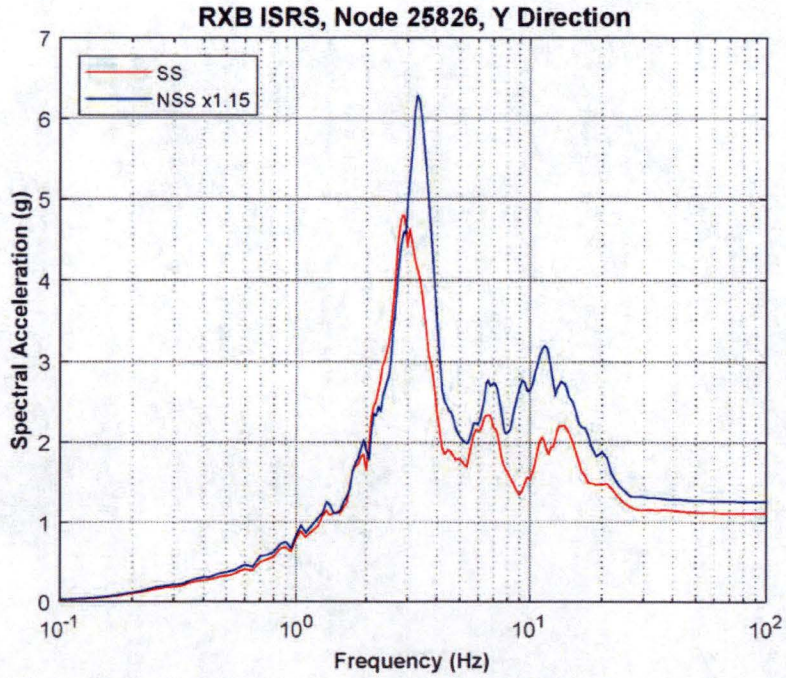

Figure 65. Reactor Building In-Structure Response Spectra Comparison, Node 25826, Y-Direction (a)

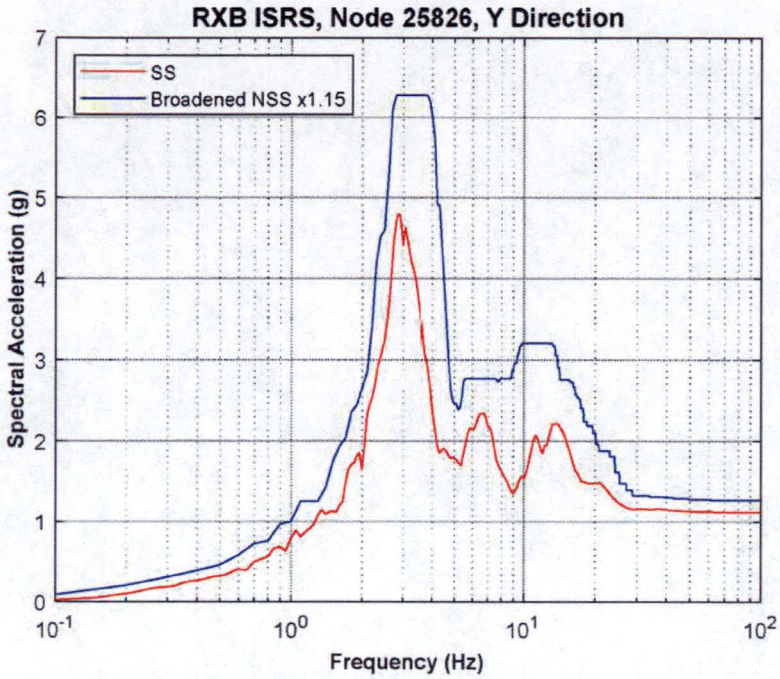

Figure 66. Reactor Building In-Structure Response Spectra Comparison, Node 25826, Y-Direction (b)

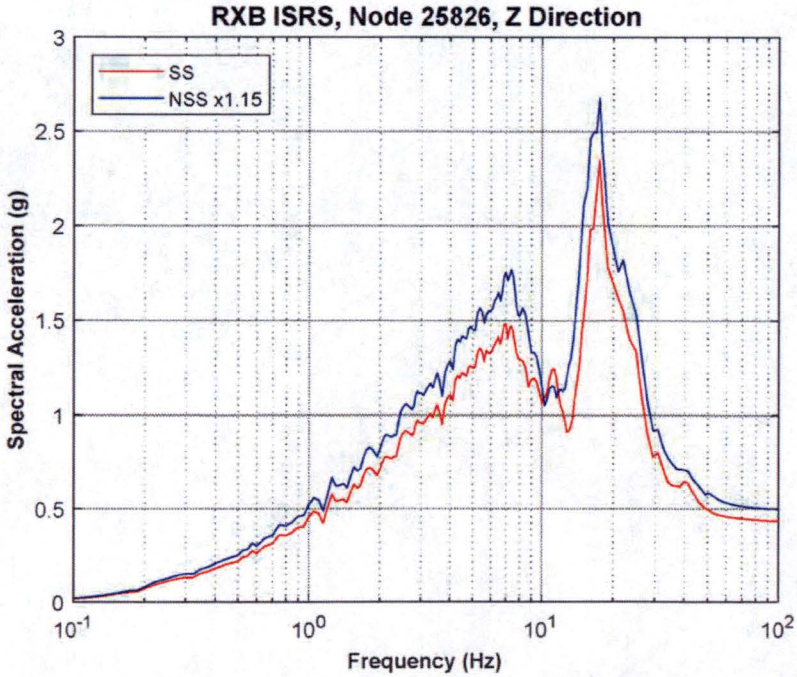

Figure 67. Reactor Building In-Structure Response Spectra Comparison, Node 25826, Z-Direction (a)

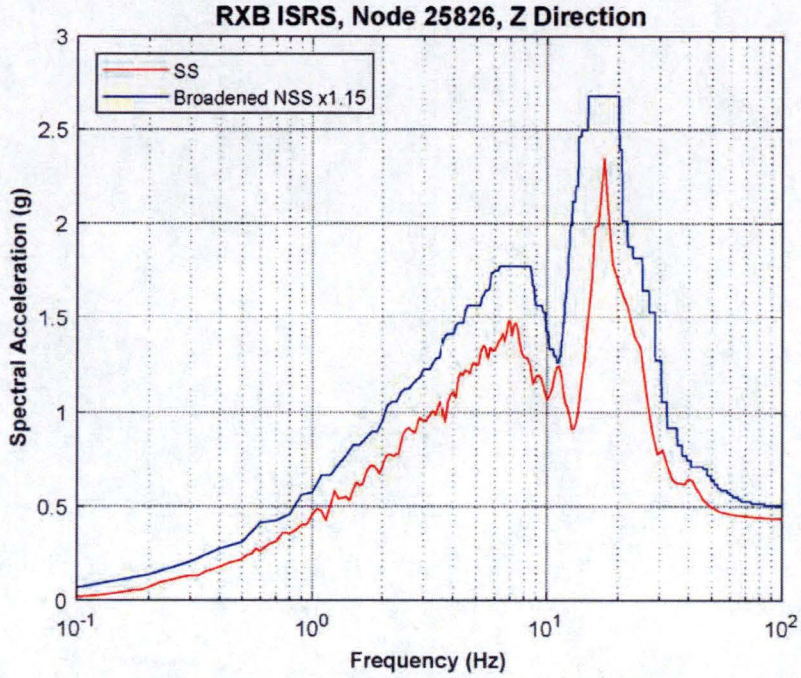

Figure 68. Reactor Building In-Structure Response Spectra Comparison, Node 25826, Z-Direction (b)

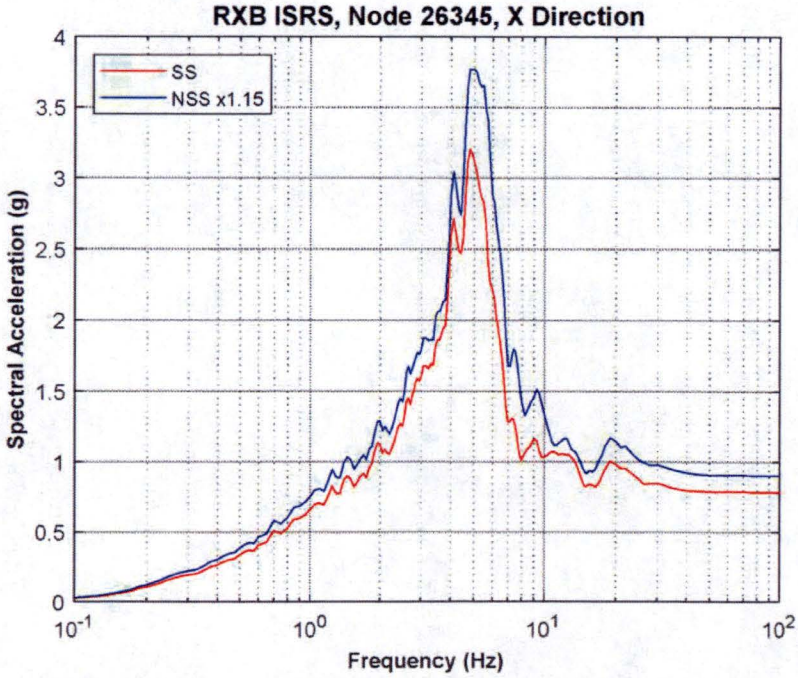

Figure 69. Reactor Building In-Structure Response Spectra Comparison, Node 26345, X-Direction

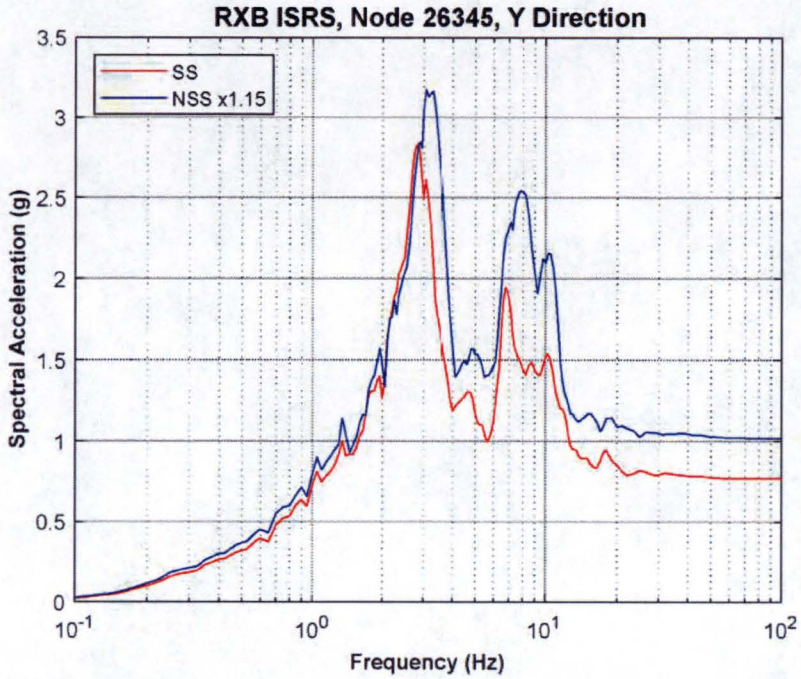

Figure 70. Reactor Building In-Structure Response Spectra Comparison, Node 26345, Y-Direction (a)

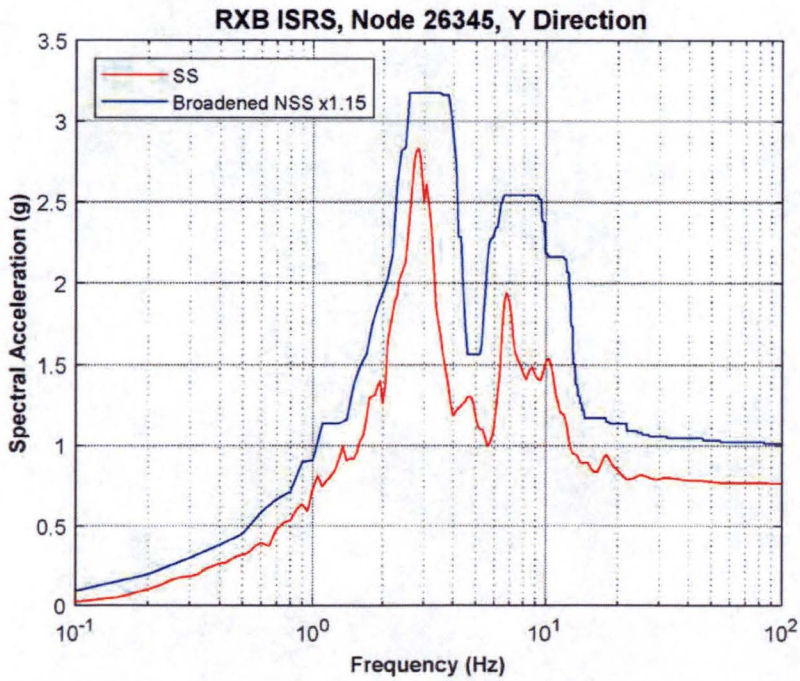

Figure 71. Reactor Building In-Structure Response Spectra Comparison, Node 26345, Y-Direction (b)

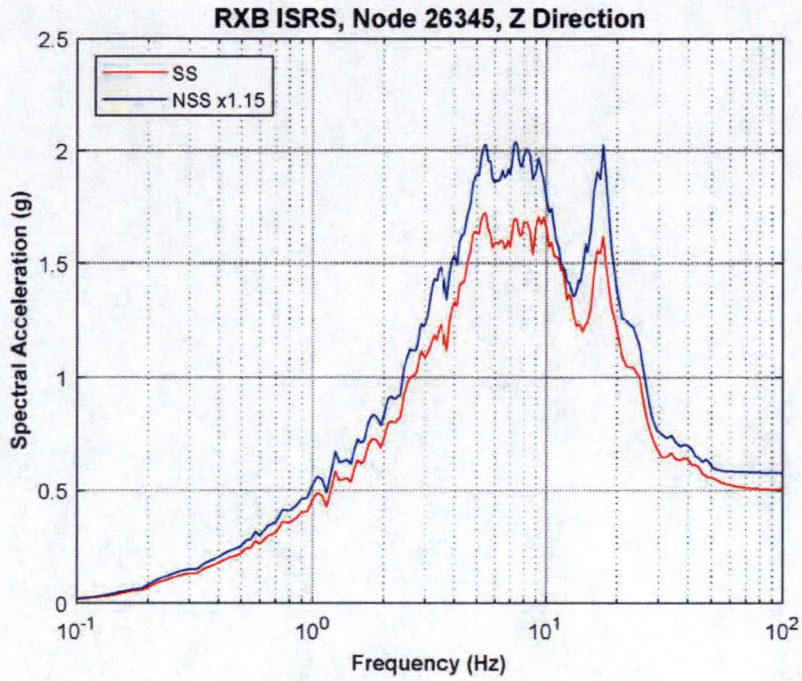

Figure 72. Reactor Building In-Structure Response Spectra Comparison, Node 26345, Z-Direction

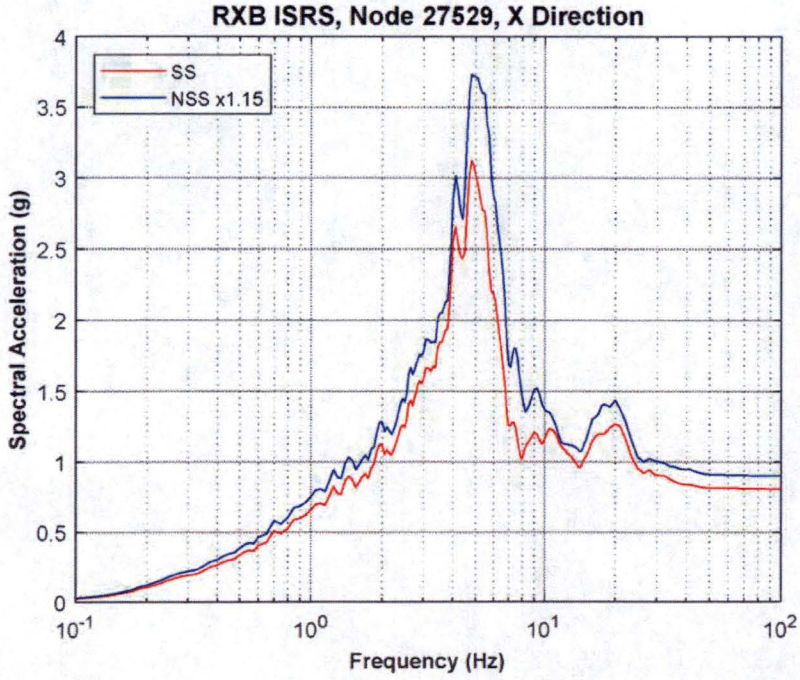

Figure 73. Reactor Building In-Structure Response Spectra Comparison, Node 27529, X-Direction

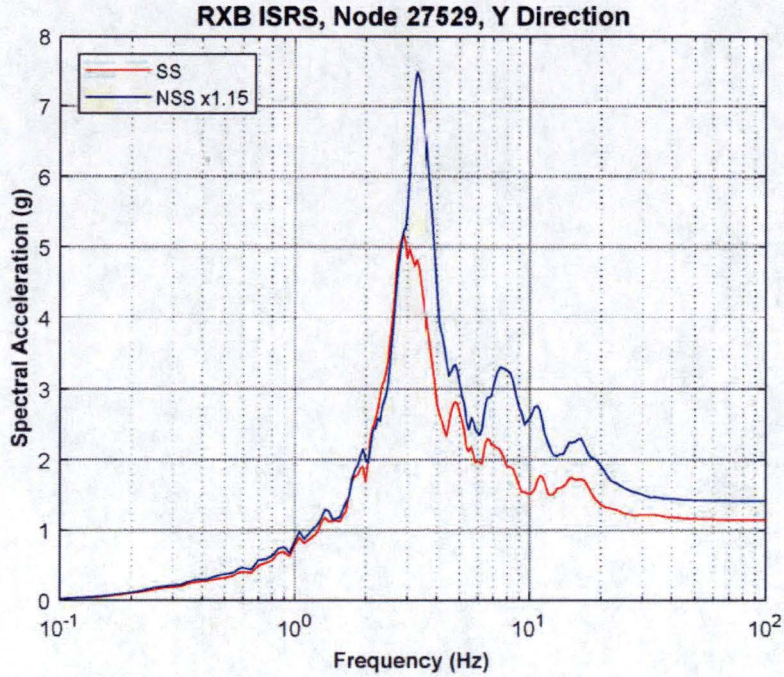

Figure 74. Reactor Building In-Structure Response Spectra Comparison, Node 27529, Y-Direction (a)

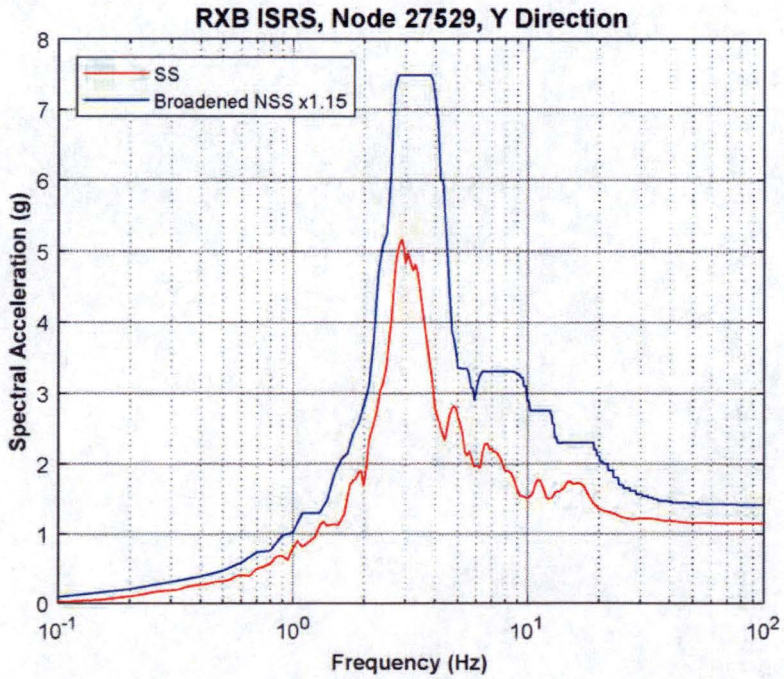

Figure 75. Reactor Building In-Structure Response Spectra Comparison, Node 27529, Y-Direction (b)

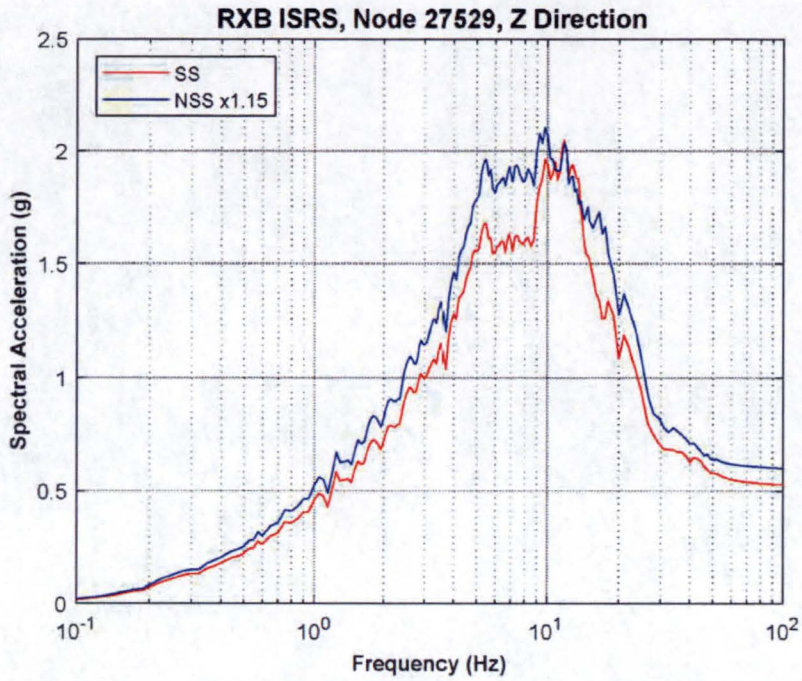

Figure 76. Reactor Building In-Structure Response Spectra Comparison, Node 27529, Z-Direction (a)

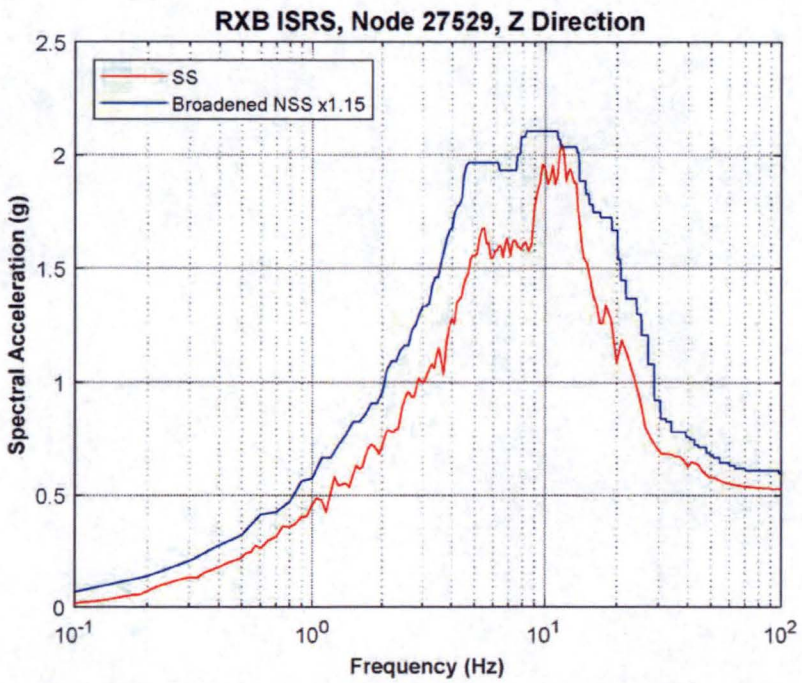

Figure 77. Reactor Building In-Structure Response Spectra Comparison, Node 27529, Z-Direction (b)

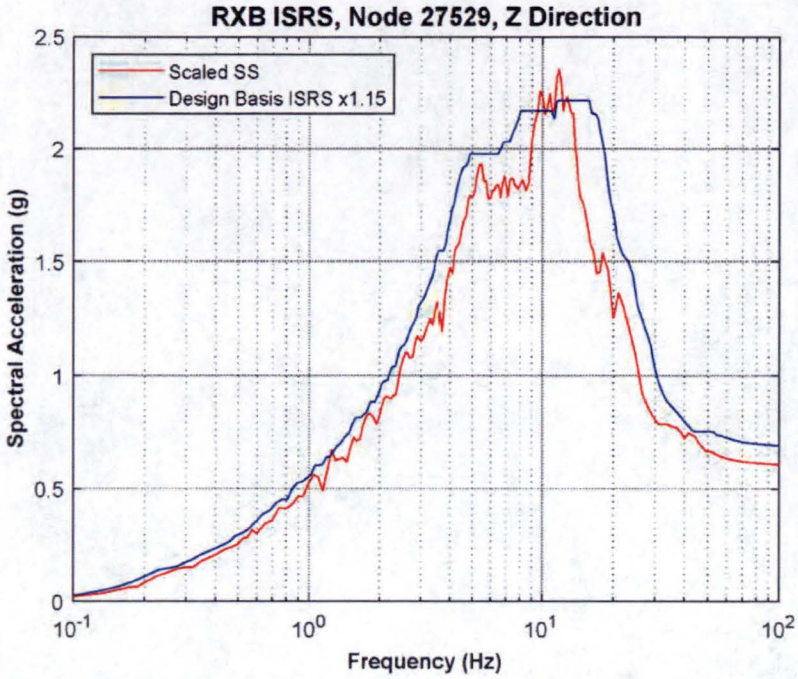

Figure 78. Reactor Building In-Structure Response Spectra Comparison, Node 27529, Z-Direction (c)

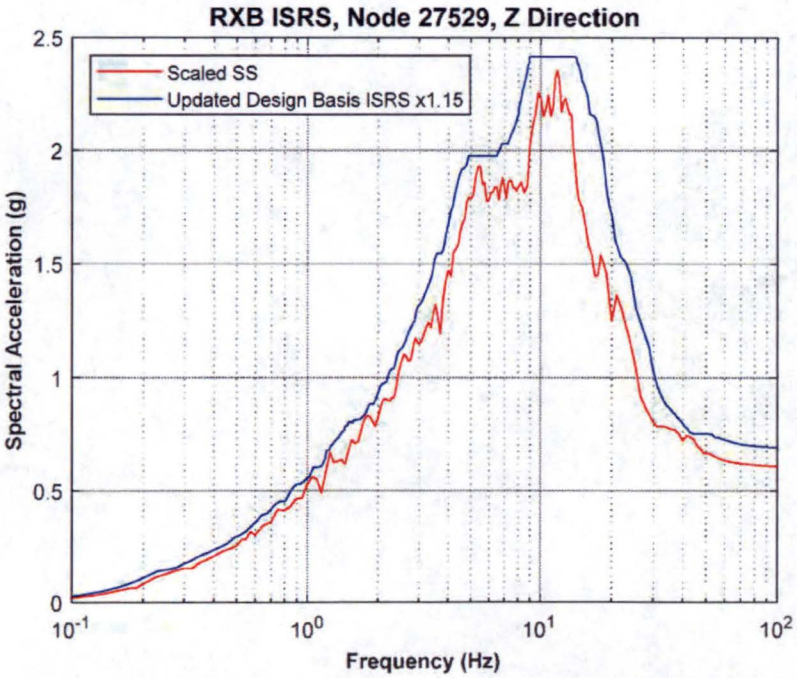

Figure 79. Reactor Building In-Structure Response Spectra Comparison, Node 27529, Z-Direction (d)

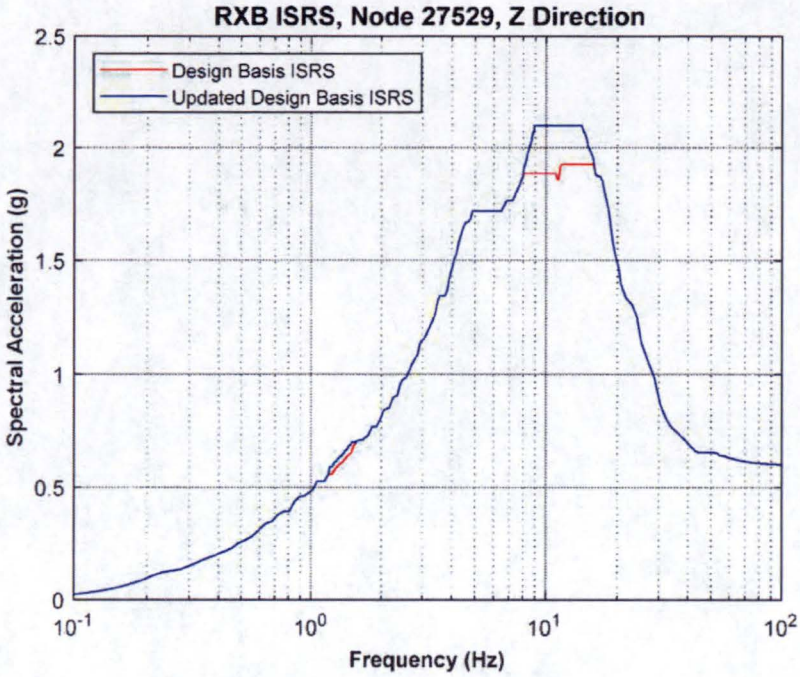

Figure 80. Reactor Building In-Structure Response Spectra Comparison, Node 27529, Z-Direction (e)

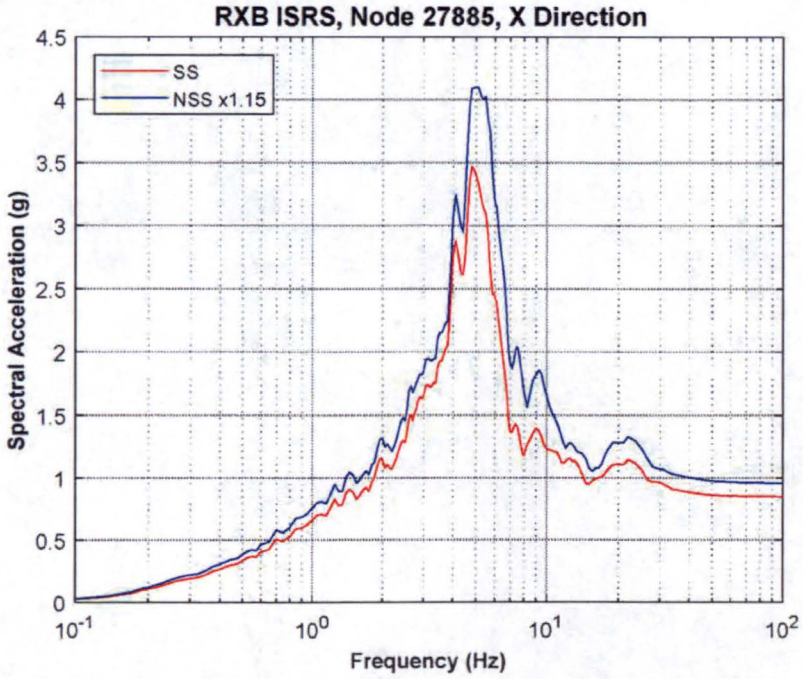

Figure 81. Reactor Building In-Structure Response Spectra Comparison, Node 27885, X-Direction

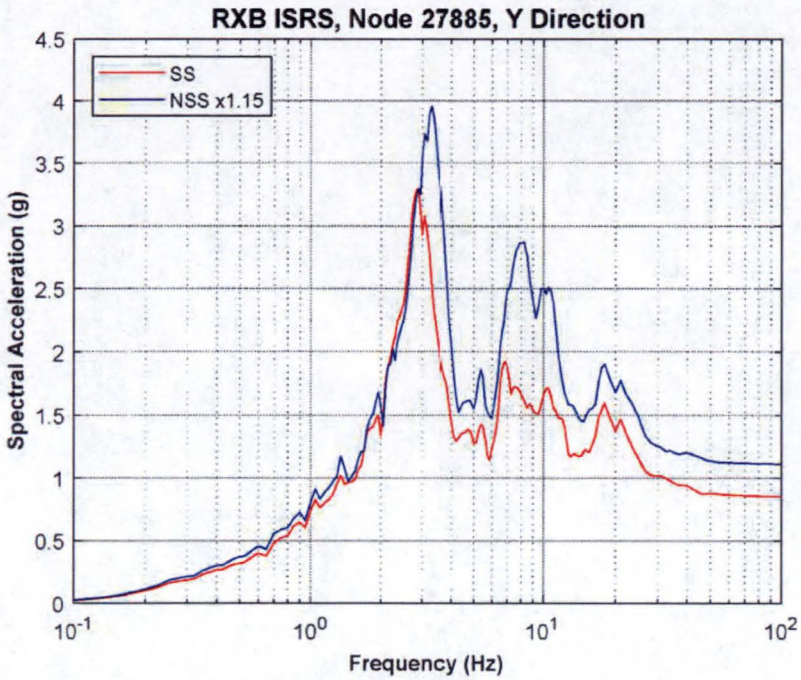

Figure 82. Reactor Building In-Structure Response Spectra Comparison, Node 27885, Y-Direction (a)

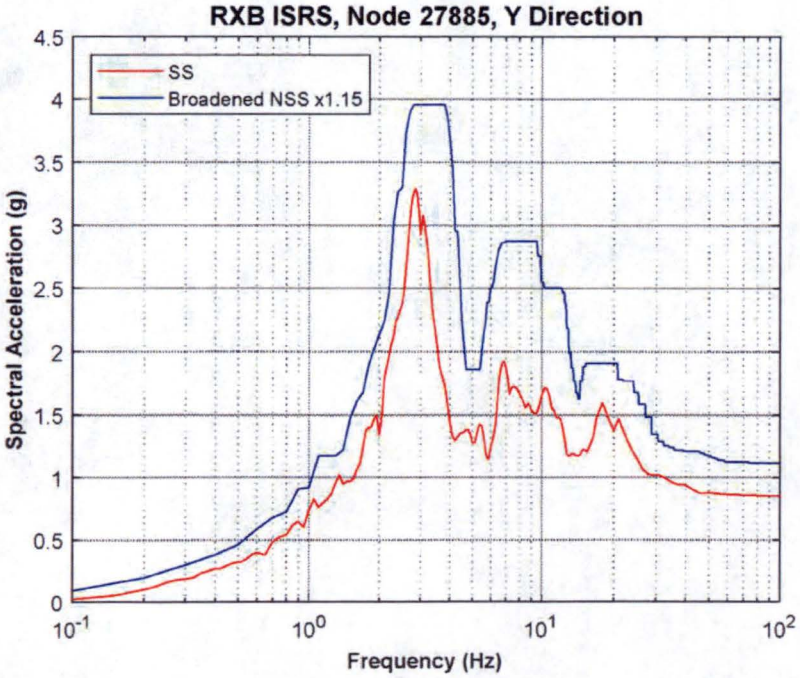

Figure 83. Reactor Building In-Structure Response Spectra Comparison, Node 27885, Y-Direction (b)

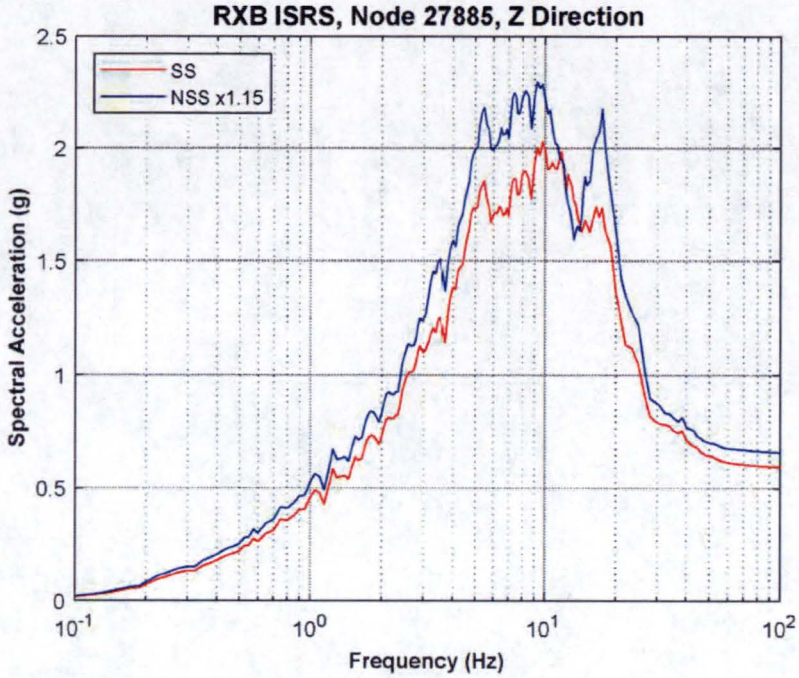

Figure 84. Reactor Building In-Structure Response Spectra Comparison, Node 27885, Z-Direction (a)

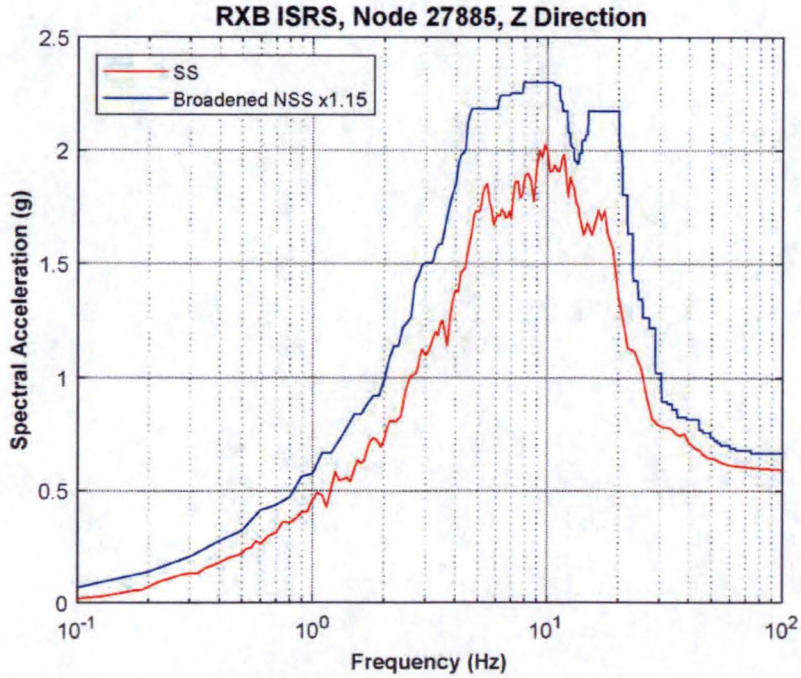

Figure 85. Reactor Building In-Structure Response Spectra Comparison, Node 27885, Z-Direction (b)

Updated Design Basis In-Structure Response Spectra for Crane Wheels

Table 3 provides a list of the node numbers used to develop the crane wheels' enveloped ISRS. As shown in the table, crane slab node 27529 is not listed as a location used to generate the crane wheel nodes' enveloped ISRS. Figure 86 shows the comparison between the crane wheels' enveloped ISRS and updated design basis ISRS for node 27529. As shown in the figure, the 5 percent damped, crane wheels' enveloped ISRS does not bound the ISRS for node 27529. Therefore, a new enveloped design basis ISRS, as shown in Figure 87, is developed to take this exceedance into account.

Table 3. Crane Wheel Locations for In-Structure Response Spectra Presentation

Location No.	Node No.	Nodal Coordinates (inch)			Location Description
		X (E-W)	Y (N-S)	Z (VT)	
1	27679	2215.00	-453.00	1548.00	SW crane wheel
2	27680	2215.00	453.00	1548.00	NW crane wheel
3	27797	3067.25	-453.00	1548.00	SE crane wheel
4	27798	3067.25	453.00	1548.00	NE crane wheel

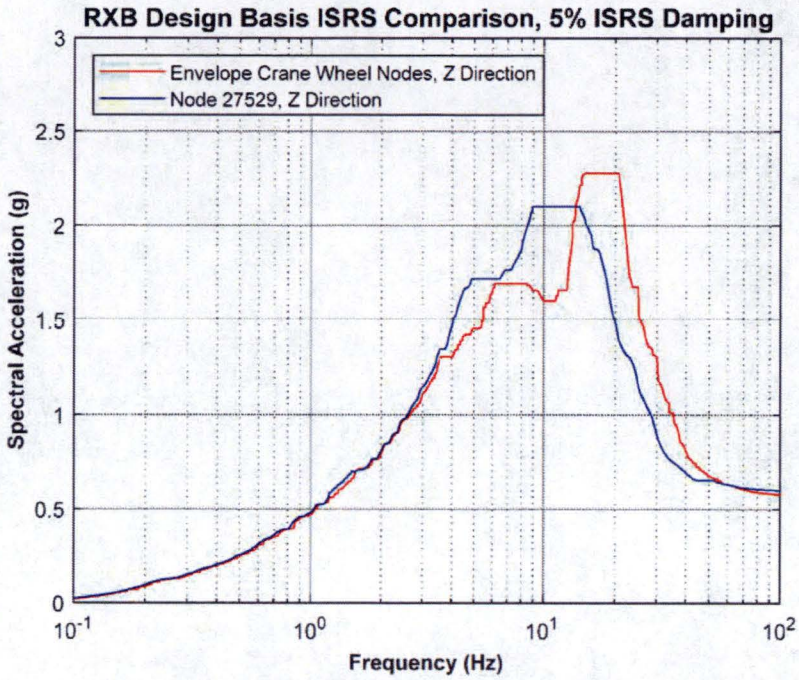

Figure 86. Reactor Building Design Basis In-Structure Response Spectra Comparison, Crane Wheels' Enveloped ISRS vs. Node 27529, Z-Direction

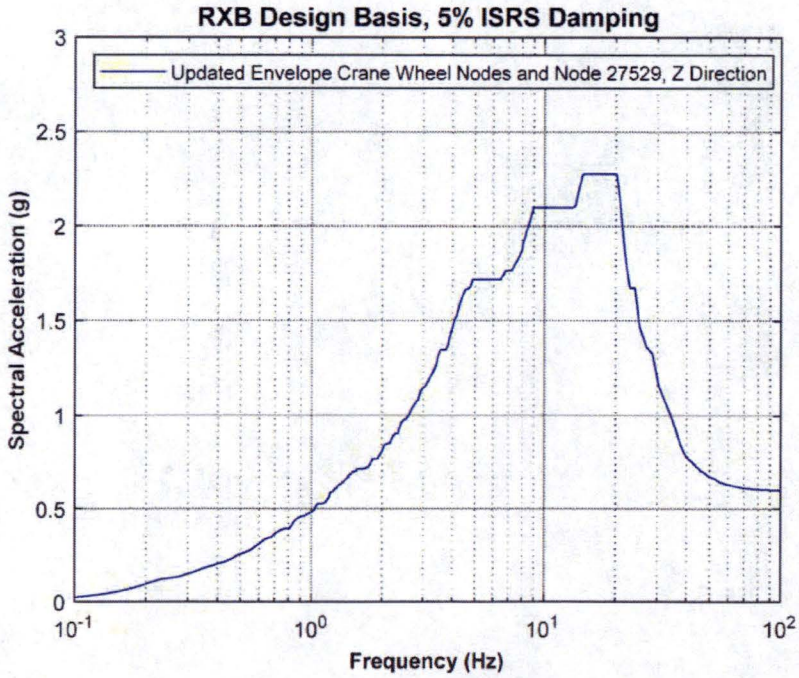

Figure 87. Reactor Building Design Basis In-Structure Response Spectra, Updated Envelope of Crane Wheels and Node 27529, Z-Direction

A frequency-dependent scale factor, α_{fi} is presented to modify the ISRS plots for other damping ratios, as shown below:

$$\alpha_{f_i} = \left(\frac{Updated\ Design\ Basis\ ISRS, 5\%\ Damping)}{Design\ Basis\ ISRS, 5\%\ Damping}\right)_{f_i} \qquad \text{Equation 4}$$

Where, for each frequency point, f_i , the scale factor, α_{fi} is calculated by dividing the updated 5 percent damped design basis ISRS by the 5 percent damped design basis ISRS. Then, ISRS plots for each damping ratio are scaled in accordance with Equation 5

$$Updated\ Design\ Basis\ ISRS, \xi\ Damping = \alpha_{f_i}(Design\ Basis\ ISRS, \xi\ \ Damping) \qquad \text{Equation 5}$$

Figure 88 shows the updated enveloped ISRS of crane wheels and node 27529 in the Z-Direction for all damping ratios.

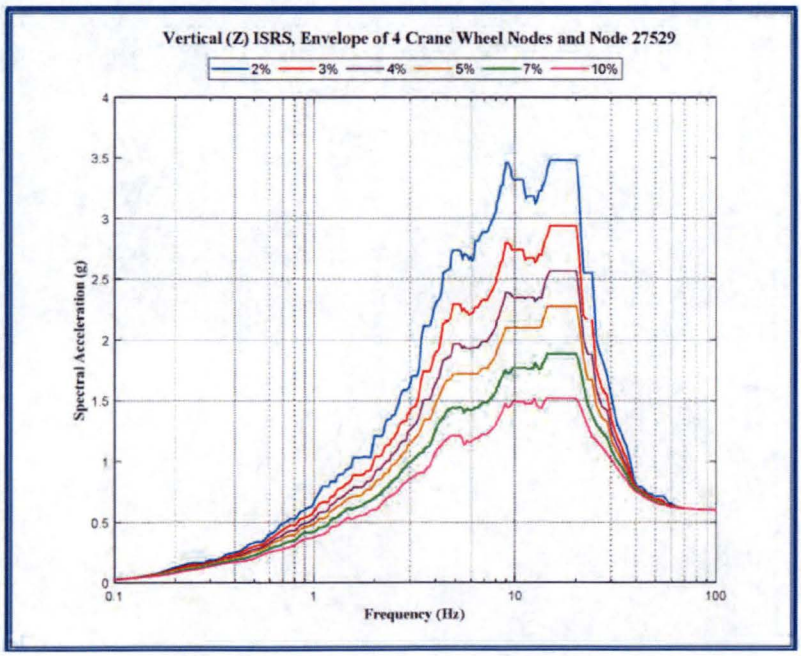

Figure 88. Updated Enveloped In-Structure Response Spectra of Crane Wheels and Node 27529, Z-Direction

Response to Question 2

Background Information, Methodology, and Approach

The methodology, approach, and steps taken for comparing the Control Building (CRB) ISRS data are similar to those for the RXB, described in the Response to Question 1.

As subsequently shown, SS ISRS accelerations exceed 1.15 times the peak-broadened NSS ISRS at two locations, i.e., 34380 Z and 35713 Z, requiring the damping scaling factor to be developed. In accordance with the damping scaling methodology, a SAP2000 fixed-base time history analysis using CSDRS-compatible Capitola time history input in the east-west, north-south, and vertical directions is performed for structural damping values of 4, 5, and 7 percent. Then, ISRS plots are generated, as shown in Figure 89 and Figure 90.

Damping scaling factors, described in steps 4, 6, and 8 of the methodology, are plotted in Figure 91 and Figure 92. After comparing these plots, a constant damping scaling factor of 1.25 is selected to scale the ISRS accelerations from 7 percent structural damping to 4 percent structural damping.

For verification purposes, a comparison is made between the ISRS plot generated by the SAP2000 fixed-base analysis and three ISRS plots calculated based on the scaling methods described in this section. As seen in Figure 93 and Figure 94, the estimated ISRS accelerations reasonably match the calculated SAP2000 ISRS.

Using a larger constant damping scaling factor would excessively overestimate the ISRS accelerations at lower frequencies. It is expected that the underestimation of the peak response for node 35713 Z would not adversely impact the results of the comparison made here. As seen in Figure 131, the scaled SS ISRS obtained from soil-structure interaction analysis is bounded by the updated design basis ISRS, with substantial margin.

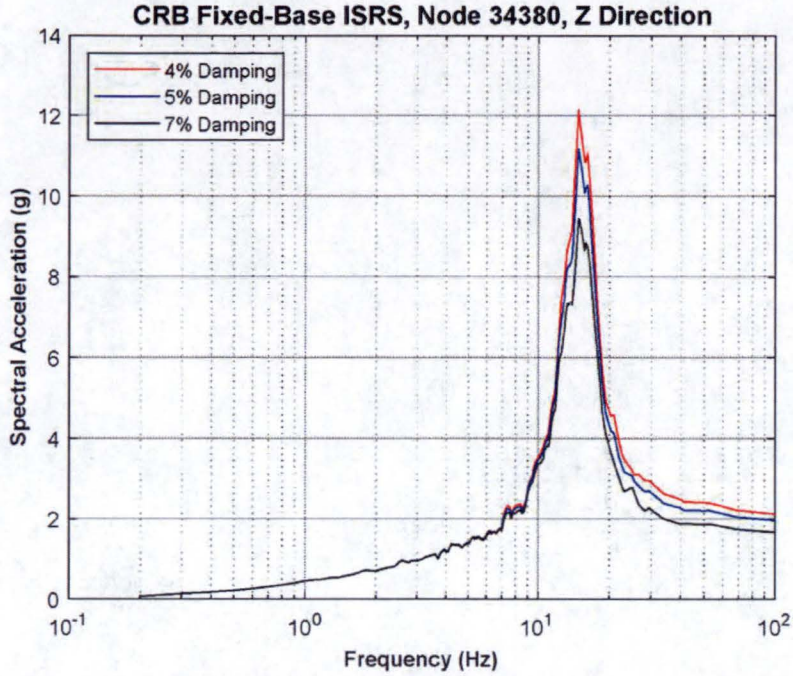

Figure 89. Control Building Fixed-Base In-Structure Response Spectra, Node 34380, Z-Direction

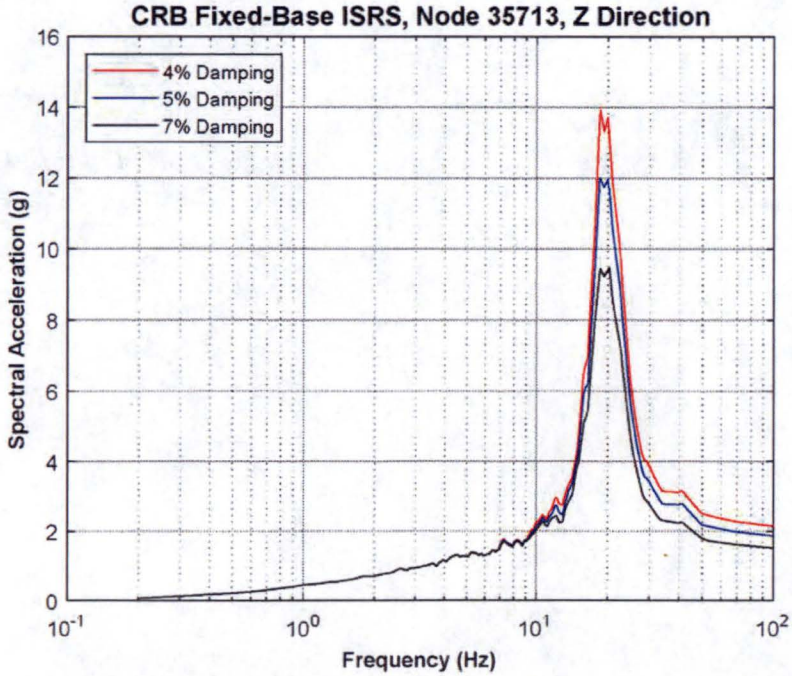

Figure 90. Control Building Fixed-Base In-Structure Response Spectra, Node 35713, Z-Direction

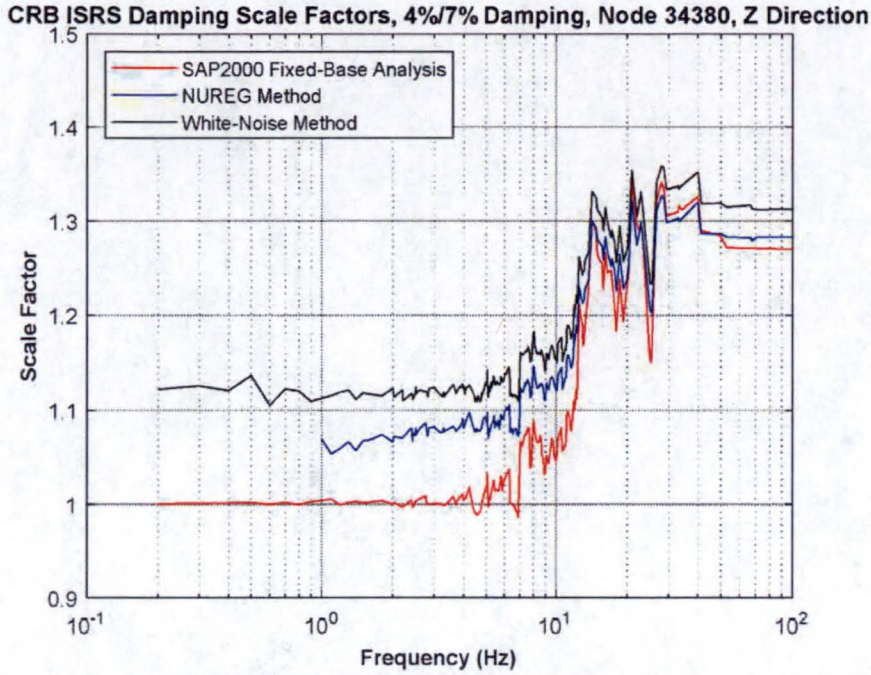

Figure 91. Control Building In-Structure Response Spectra Damping Ratios for 4 Percent to 7 Percent Damping, Node 34380, Z-Direction

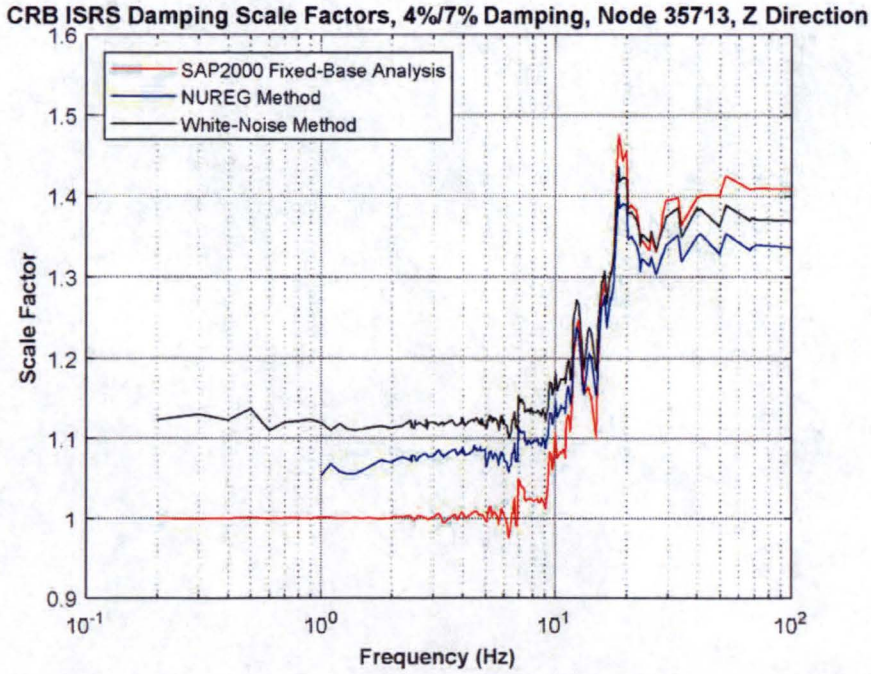

Figure 92. Control Building In-Structure Response Spectra Damping Ratios for 4 Percent to 7 Percent Damping, Node 35713, Z-Direction

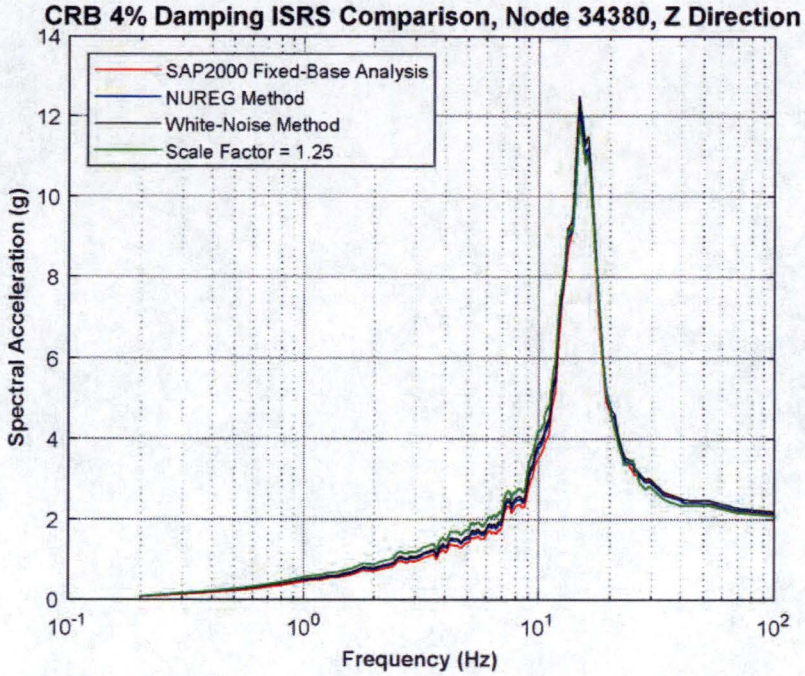

Figure 93. Control Building In-Structure Response Spectra for 4 Percent Damping, Node 34380, Z-Direction

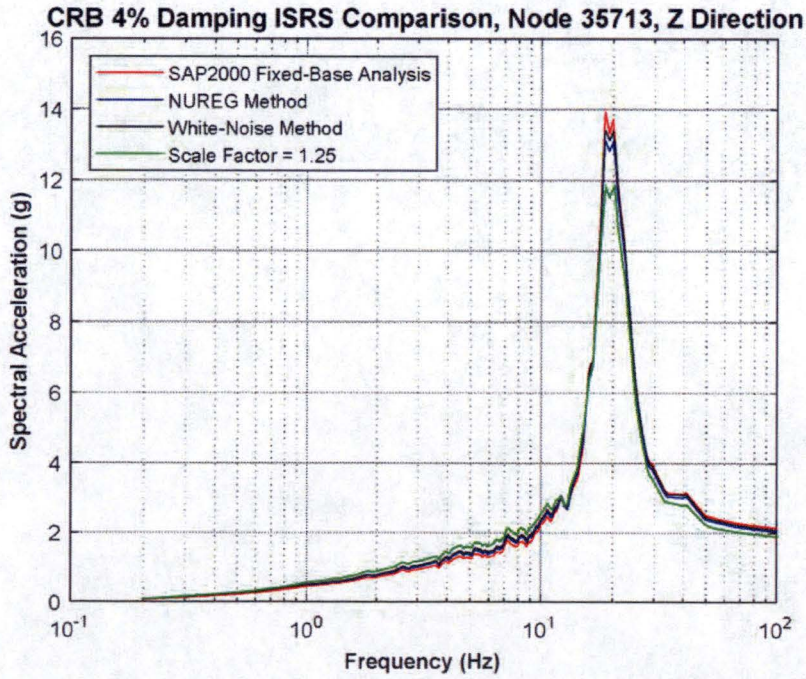

Figure 94. Control Building In-Structure Response Spectra for 4 Percent Damping, Node 35713, Z-Direction

Soil-Separation and Nonsoil-Separation In-Structure Response Spectra Comparison

Table 4 provides a list of locations where ISRS comparison is performed, as well as a description of the locations.

Table 4. Locations for Soil-Separation vs. Nonsoil-Separation In-Structure Response Spectra Comparison

Node Number	Direction(s)	Location
32345	X, Y, Z	Northwest Corner at Top of Basemat (El. 50'-0")
32526	X, Y, Z	Center of Basemat at El. 50'-0"
34320	X, Y, Z	Northwest Corner at El. 63'-3"
34380	X, Y, Z	Slab Between Grid Line CB-D and CB-E at El. 63'-3"
35637	X, Y, Z	Northwest Corner at El. 76'-6"
35713	X, Y, Z	Emergency Equipment Room Between Grid Lines CB-D and CB-E at El. 76'-6"
38144	X, Y, Z	Northwest Corner at El. 100'-0"
38298	X, Y, Z	Slab between Grid Line CB-A and CB-B (Technical Support Center) at El. 100'-0"
39105	X, Y, Z	Northwest Corner at El. 120'-0"
39214	X, Y, Z	Mid-span of Slab Between Grid Lines CB-B and CB-C at El. 120'-0"
39715	X, Y, Z	Northwest Corner of Roof at El. 140'-0"

Figure 95 through Figure 100 show the locations of the nodes in the CRB for which SS vs. NSS ISRS comparisons are performed.

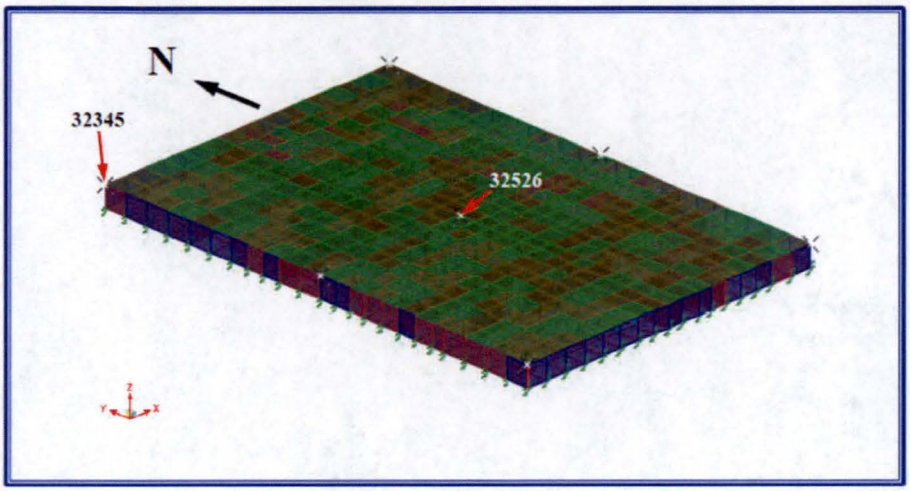

Figure 95. Top of Concrete at Basemat El. 50'-0" In-Structure Response Spectra Node Locations

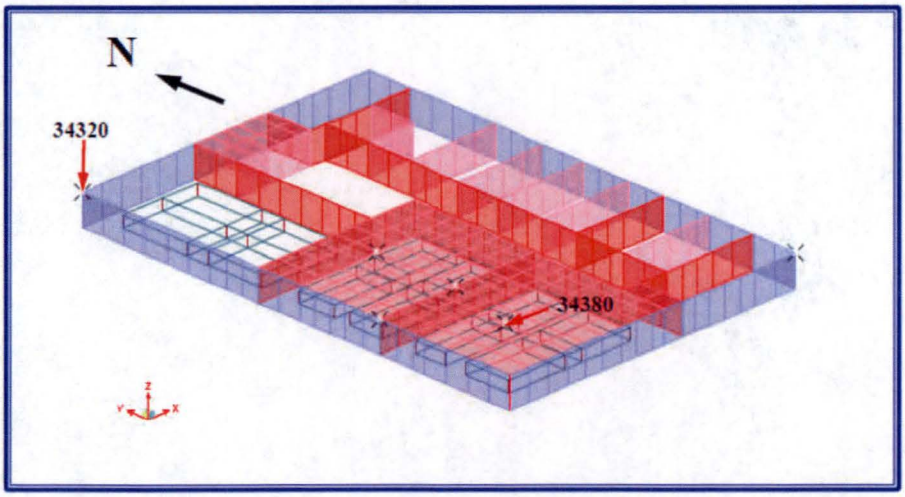

Figure 96. El. 63'-3" In-Structure Response Spectra Node Locations

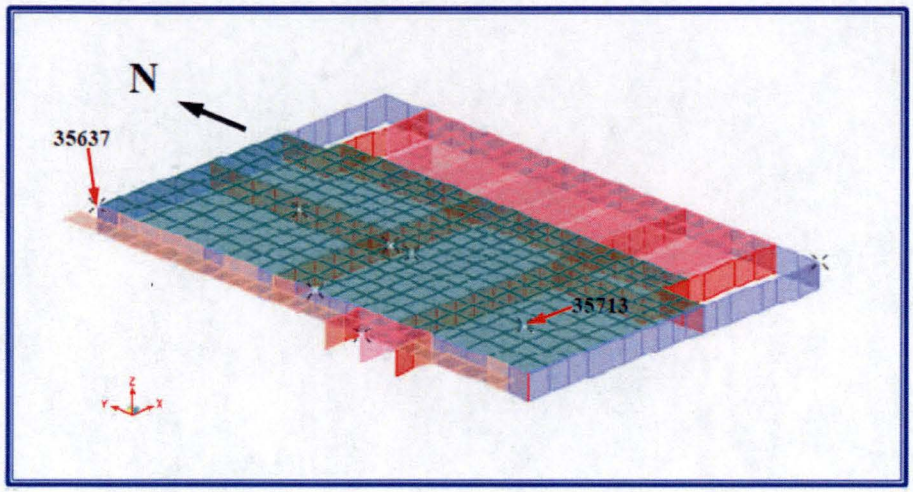

Figure 97. Top of Concrete at Main Control Room El. 76'-6" In-Structure Response Spectra Node Locations

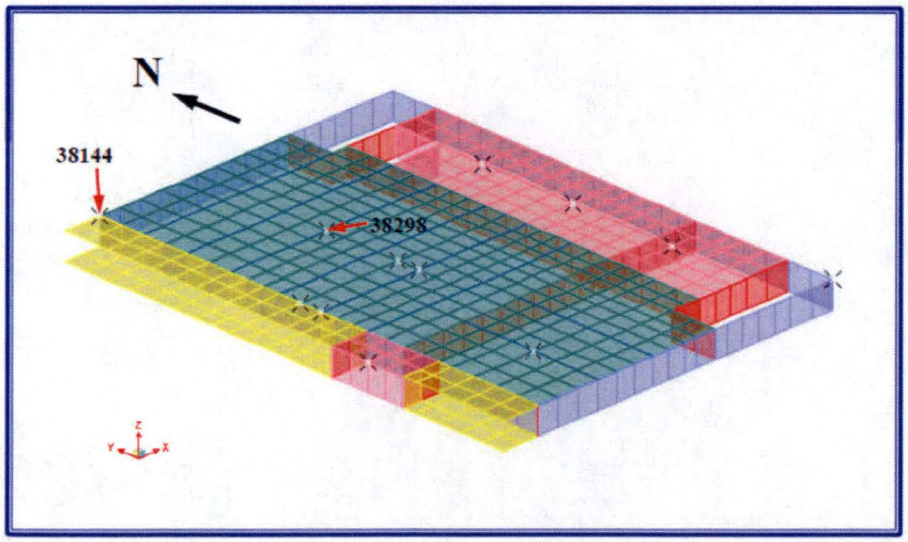

Figure 98. Top of Concrete at Technical Center and Grade El. 100'-0" In-Structure Response Spectra Node Locations

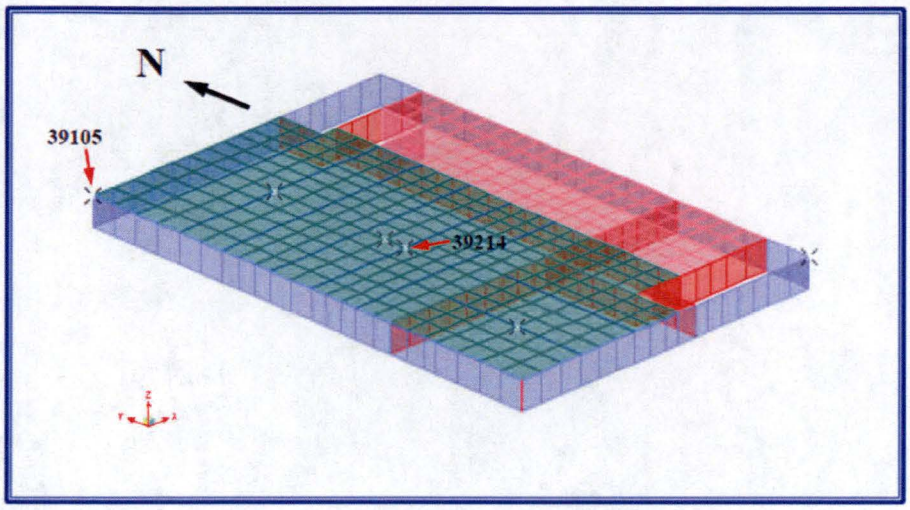

Figure 99. Top of Concrete at Mechanical Room and Base of Steel Structure El. 120'-0" In-Structure Response Spectra Node Locations

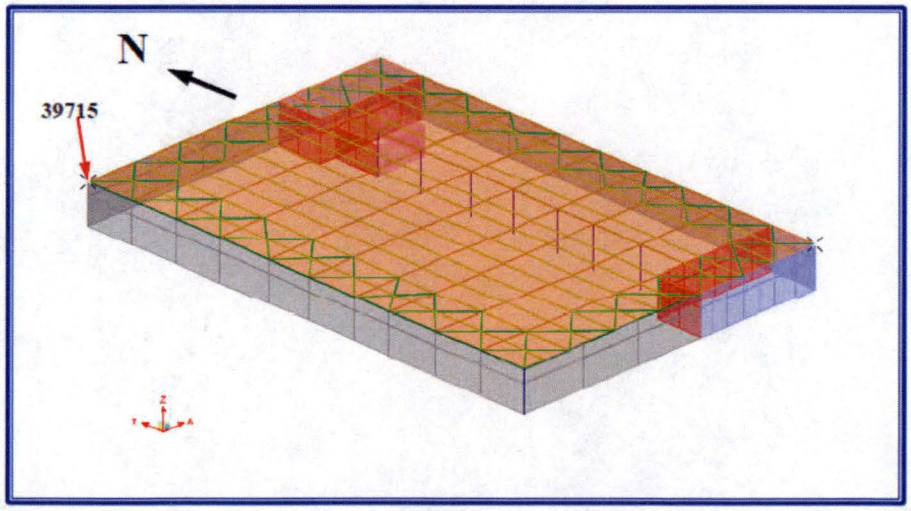

Figure 100. Roof El. 140'-0" In-Structure Response Spectra Node Location

Soil-Separation and Nonsoil-Separation In-Structure Response Spectra Comparison Results

Figure 101 through Figure 154 present the results of the comparison between SS and NSS ISRS. As shown in the following table, 15 cases show exceedances above 1.15 times the NSS ISRS, with two above 1.15 times the peak-broadened NSS ISRS and 1.15 times the design basis. For these locations, 34380 Z and 35713 Z, the design basis ISRS is updated to account for the identified exceedances, as shown in Figure 120 and Figure 132.

Table 5. Summary of the Soil-Separation and Nonsoil-Separation In-Structure Response Spectra Comparison Results

	# of Cases	**Node/ Direction**	**Location**
SS > NSS x1.15	15	32345, Z 32526, Z 34320, Z 34380, X 34380, Z 35637, Z 35713, X 35713, Z 38144, Z 38298, X 38298, Z 39105, X 39105, Z 39715, X 39715, Z	Northwest Corner at Top of Basemat Center of Basemat Northwest Corner at El. 63'-3" Slab Between Grid Line CB-D and CB-E at El. 63-3" Slab Between Grid Line CB-D and CB-E at El. 63-3" Northwest Corner at El. 76'-6" Emergency Equipment Room Emergency Equipment Room Northwest Corner at El. 100'-0" Technical Support Center Technical Support Center Northwest Corner at El. 120'-0" Northwest Corner at El. 120'-0" Northwest Corner of Roof at El. 140'-0" Northwest Corner of Roof at El. 140'-0"
SS > Peak-Broadened NSS x1.15	2	34380, Z 35713, Z	Slab Between Grid Line CB-D and CB-E at El. 63-3 Emergency Equipment Room
Scaled SS > Design Basis ISRS x1.15	2	34380, Z 35713, Z	Slab Between Grid Line CB-D and CB-E at El. 63-3 Emergency Equipment Room

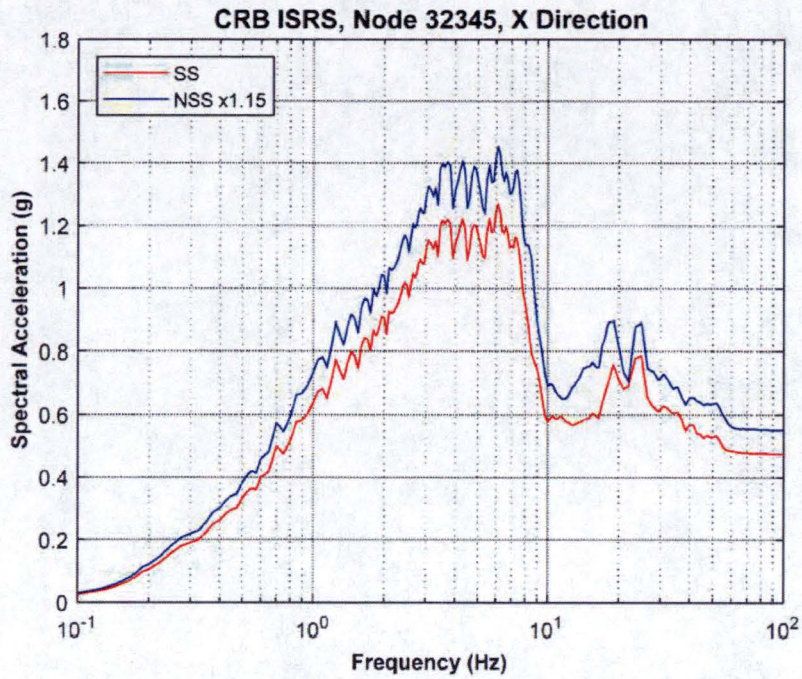

Figure 101. Control Building In-Structure Response Spectra Comparison, Node 32345, X-Direction

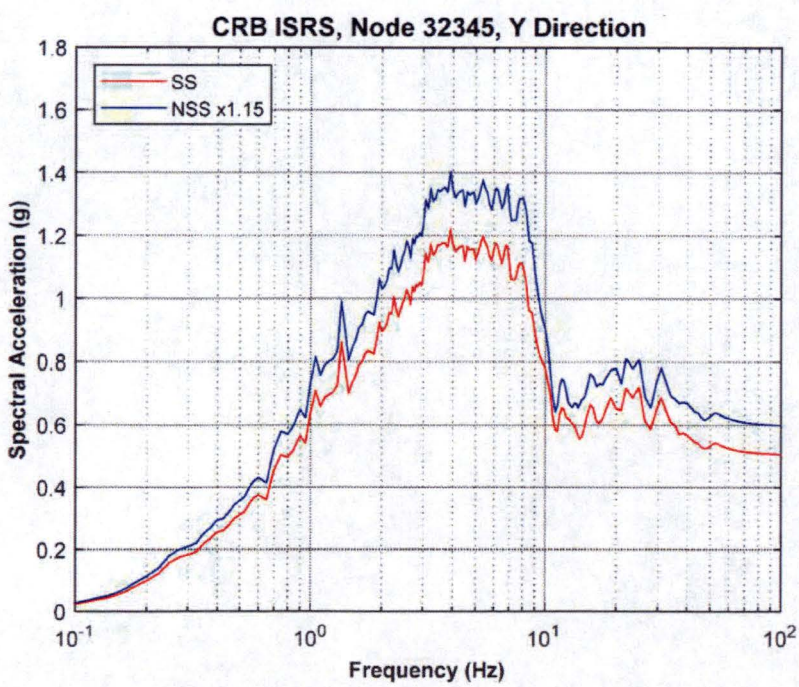

Figure 102. Control Building In-Structure Response Spectra Comparison, Node 32345, Y-Direction

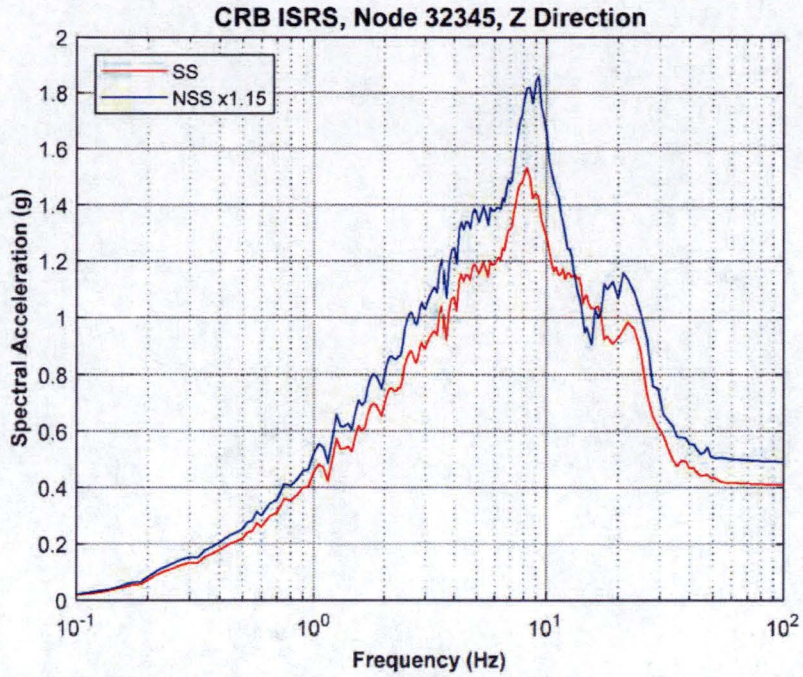

Figure 103. Control Building In-Structure Response Spectra Comparison, Node 32345, Z-Direction (a)

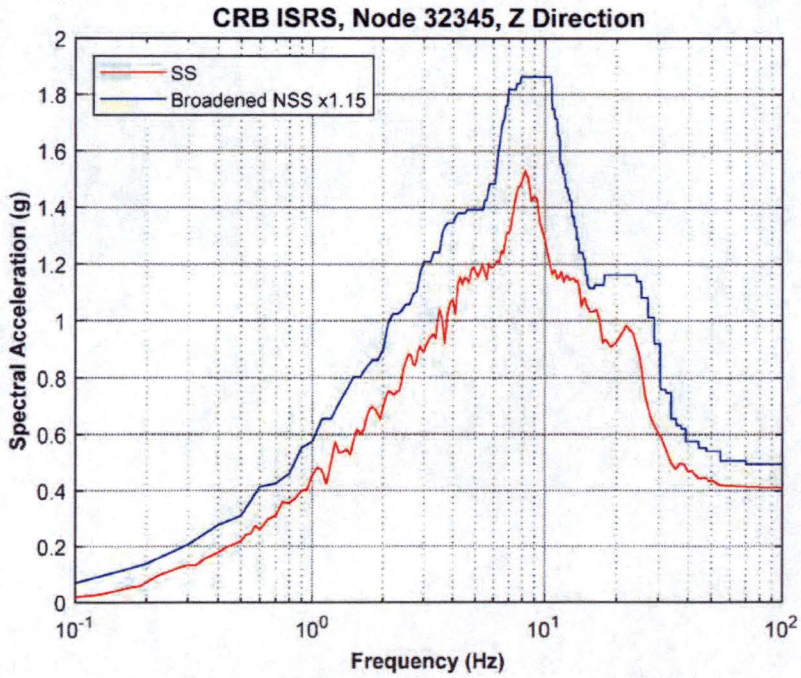

Figure 104. Control Building In-Structure Response Spectra Comparison, Node 32345, Z-Direction (b)

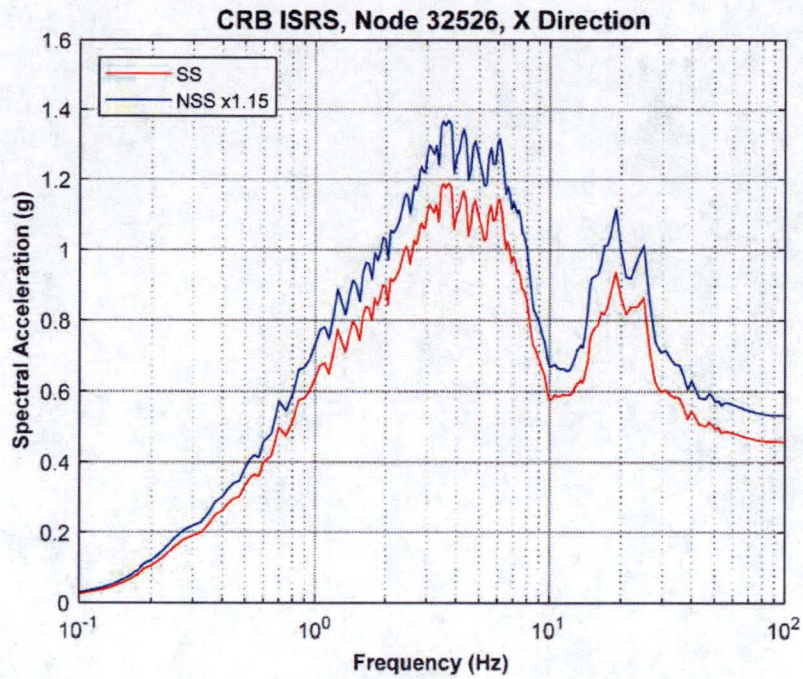

Figure 105. Control Building In-Structure Response Spectra Comparison, Node 32526, X-Direction

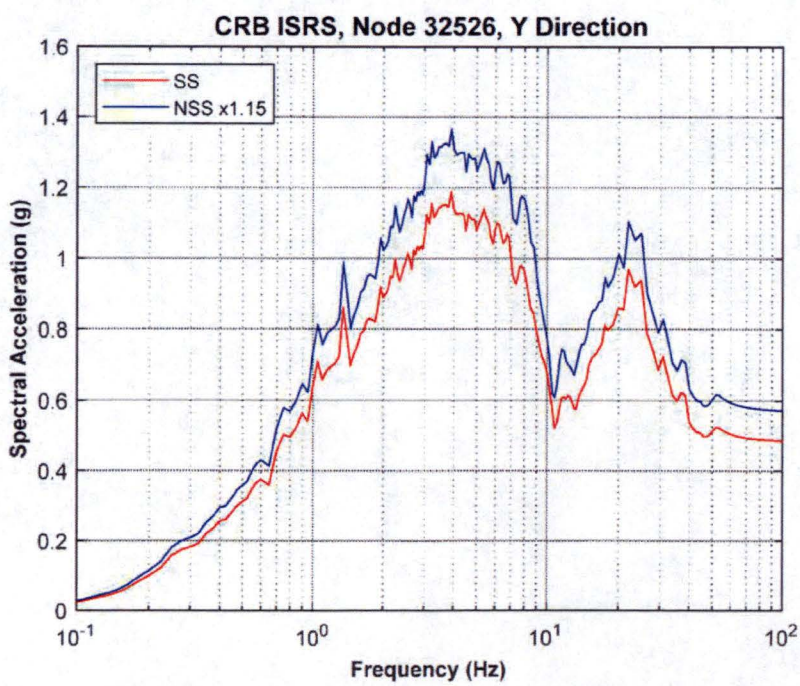

Figure 106. Control Building In-Structure Response Spectra Comparison, Node 32526, Y-Direction

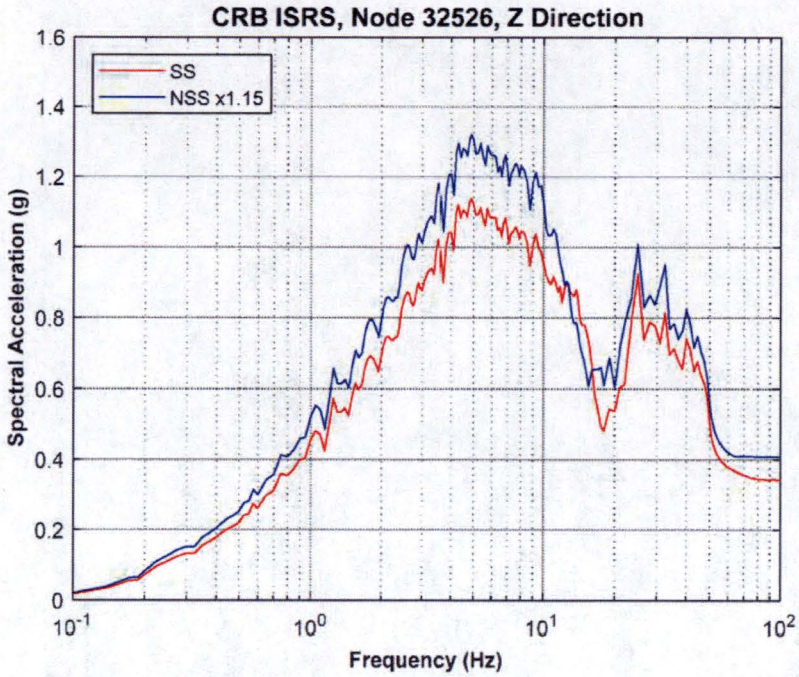

Figure 107. Control Building In-Structure Response Spectra Comparison, Node 32526, Z-Direction (a)

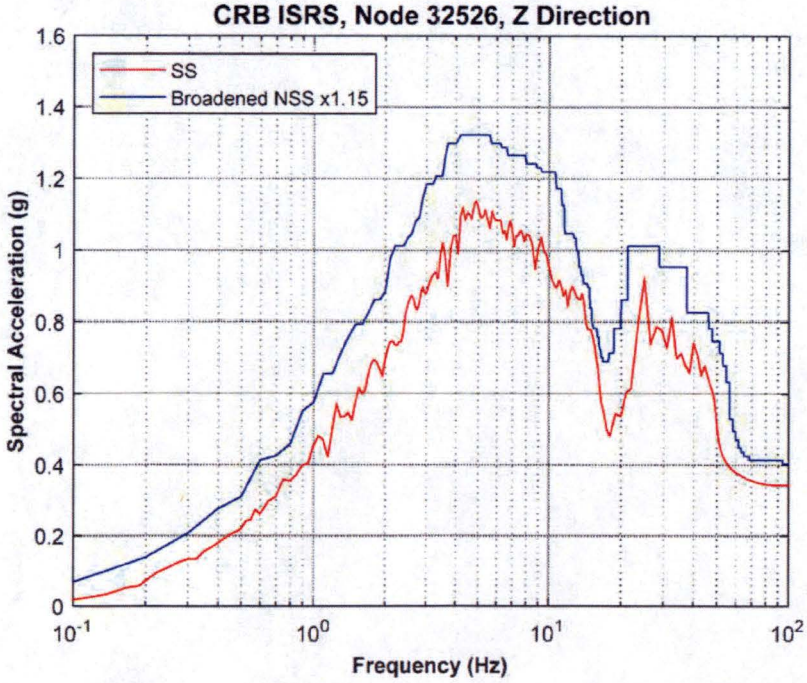

Figure 108. Control Building In-Structure Response Spectra Comparison, Node 32526, Z-Direction (b)

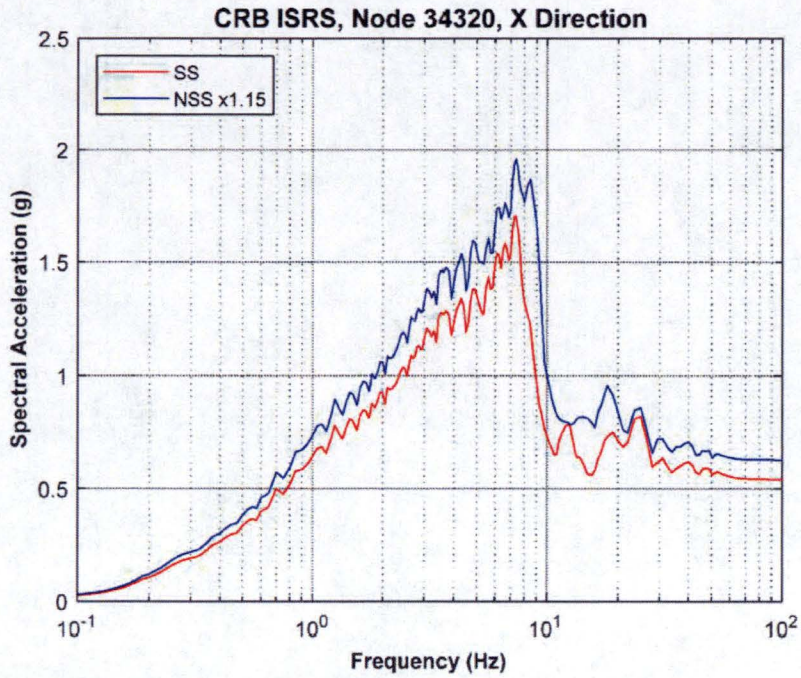

Figure 109. Control Building In-Structure Response Spectra Comparison, Node 34320, X-Direction

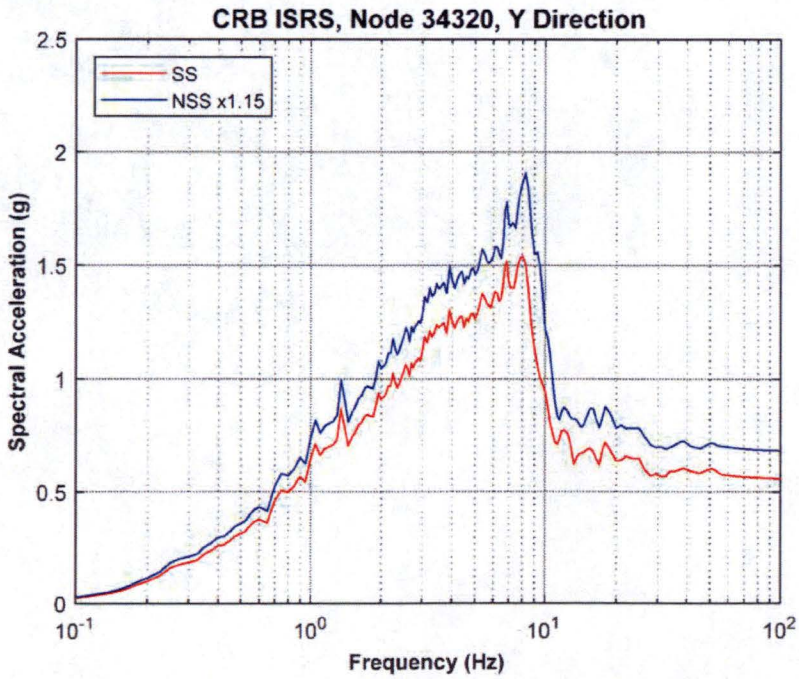

Figure 110. Control Building In-Structure Response Spectra Comparison, Node 34320, Y-Direction

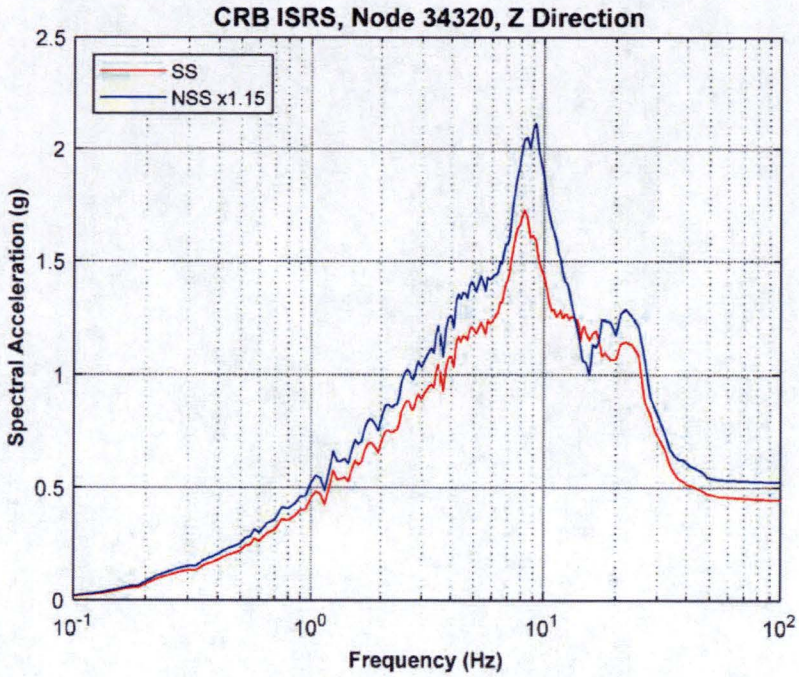

Figure 111. Control Building In-Structure Response Spectra Comparison, Node 34320, Z-Direction (a)

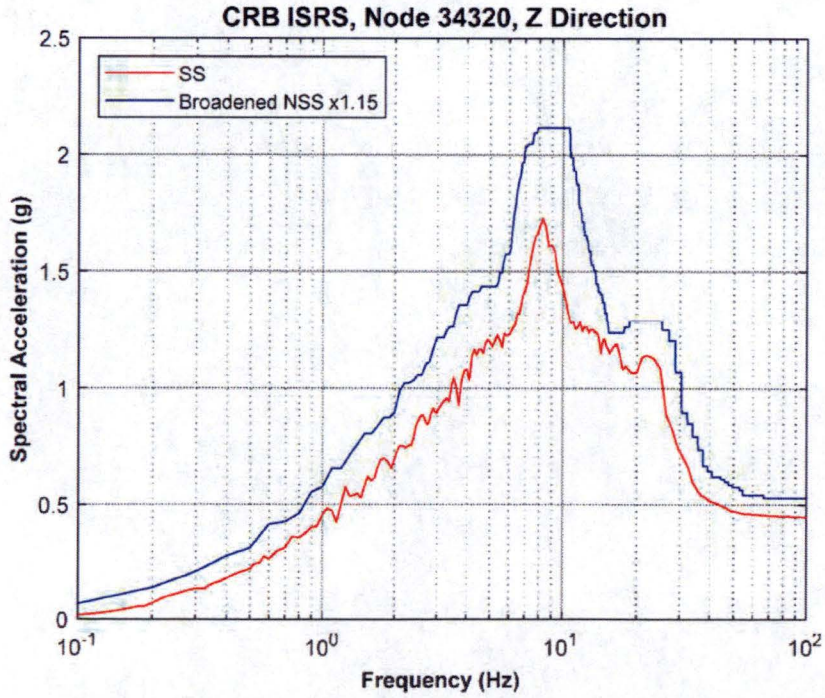

Figure 112. Control Building In-Structure Response Spectra Comparison, Node 34320, Z-Direction (b)

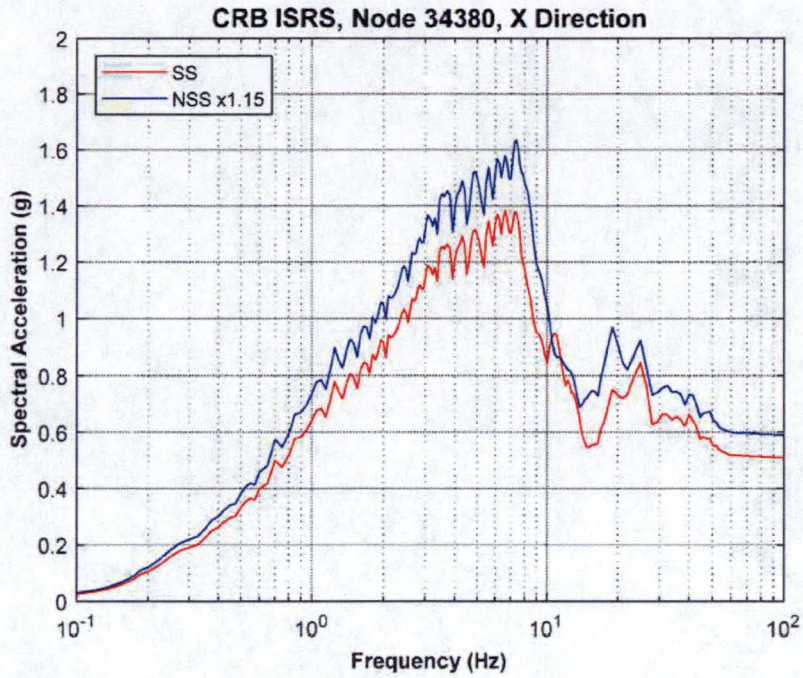

Figure 113. Control Building In-Structure Response Spectra Comparison, Node 34380, X-Direction (a)

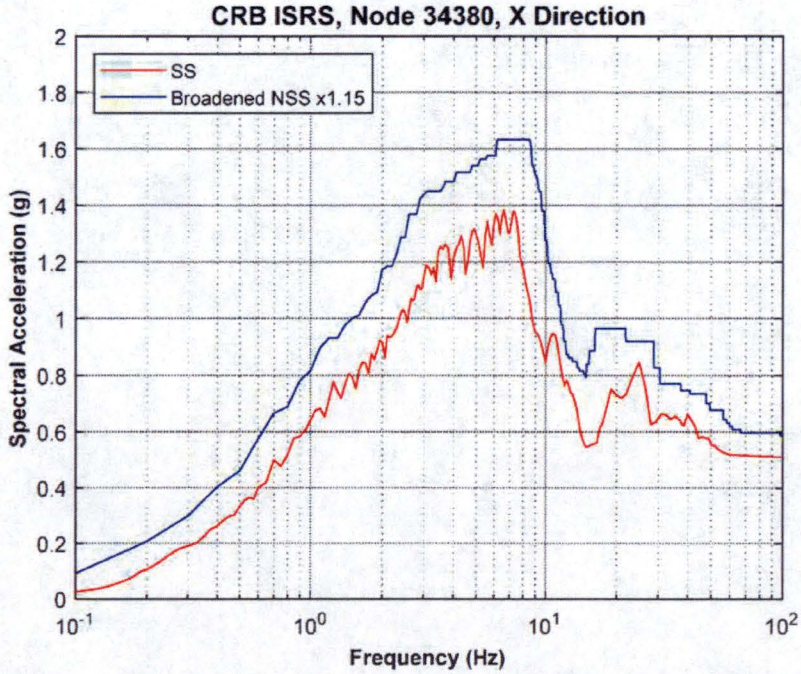

Figure 114. Control Building In-Structure Response Spectra Comparison, Node 34380, X-Direction (b)

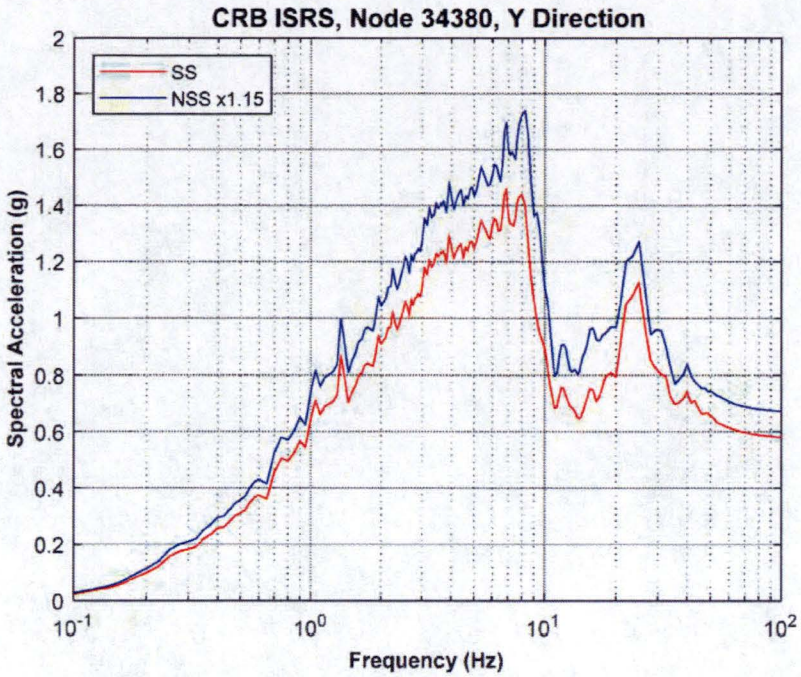

Figure 115. Control Building In-Structure Response Spectra Comparison, Node 34380, Y-Direction

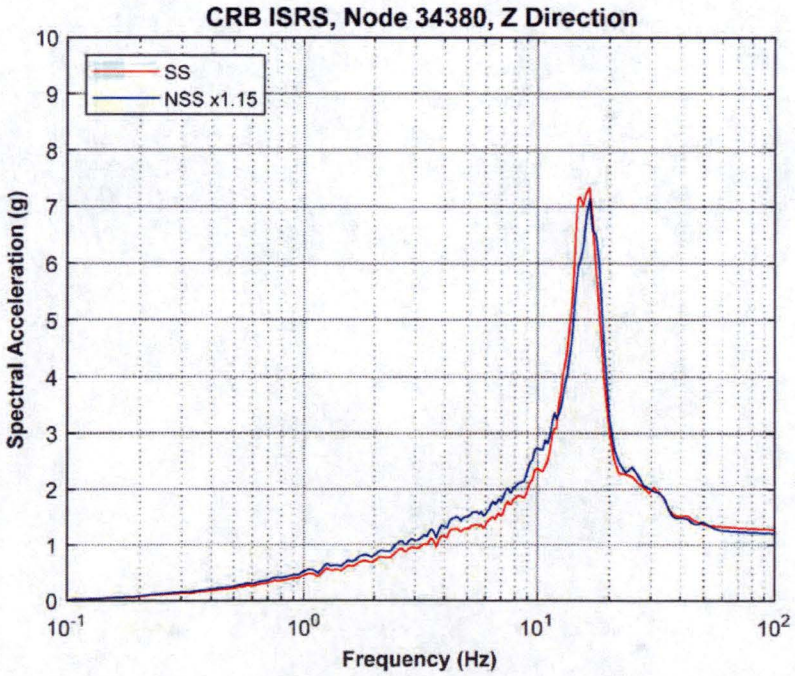

Figure 116. Control Building In-Structure Response Spectra Comparison, Node 34380, Z-Direction (a)

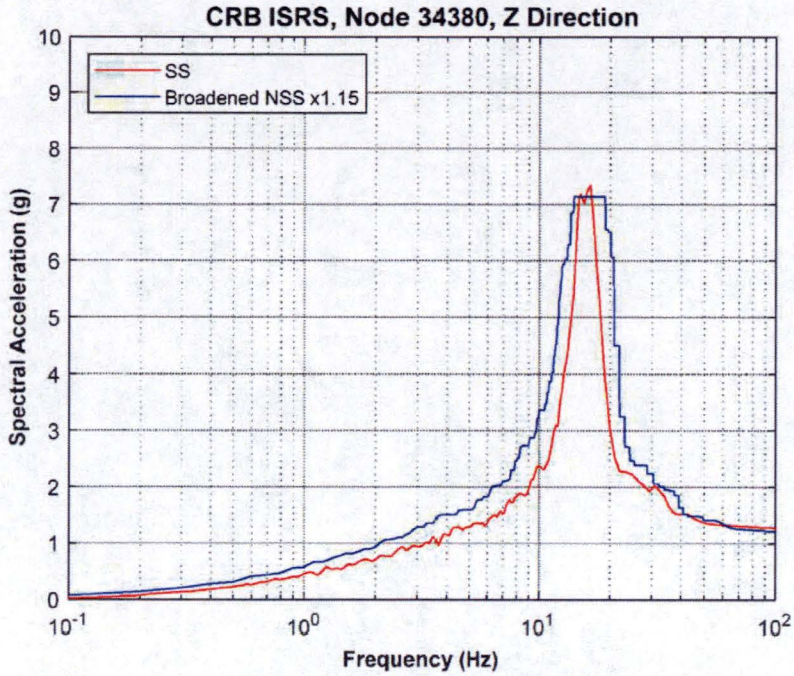

Figure 117. Control Building In-Structure Response Spectra Comparison, Node 34380, Z-Direction (b)

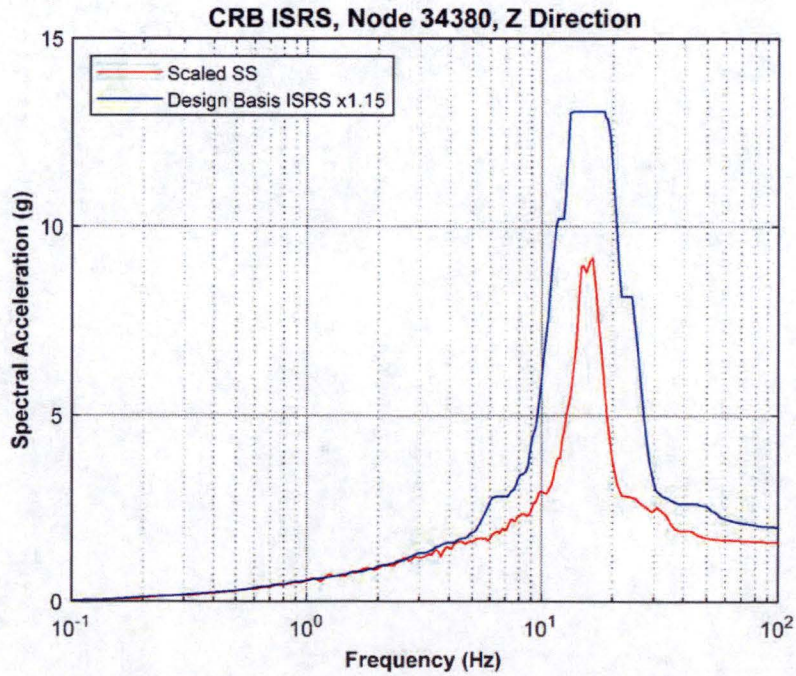

Figure 118. Control Building In-Structure Response Spectra Comparison, Node 34380, Z-Direction (c)

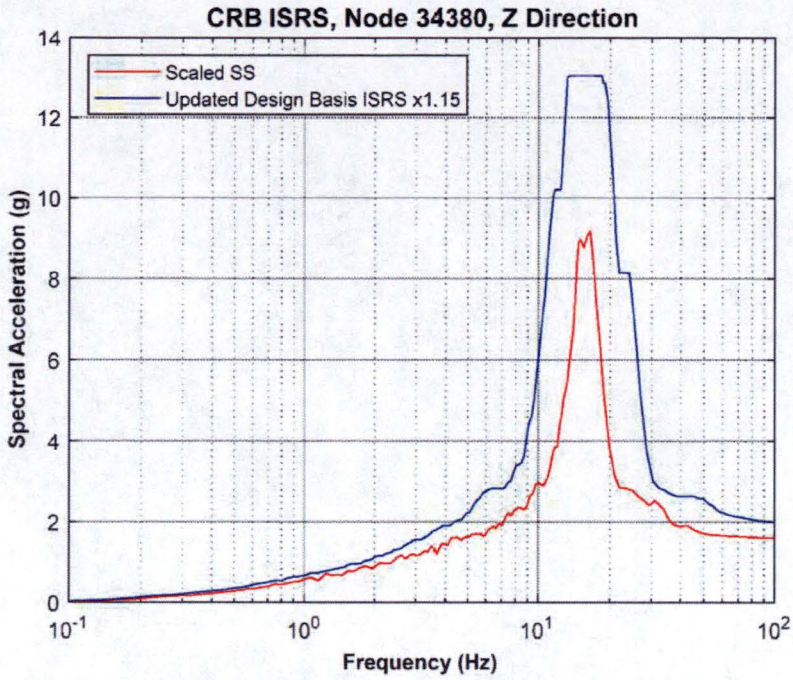

Figure 119. Control Building In-Structure Response Spectra Comparison, Node 34380, Z-Direction (d)

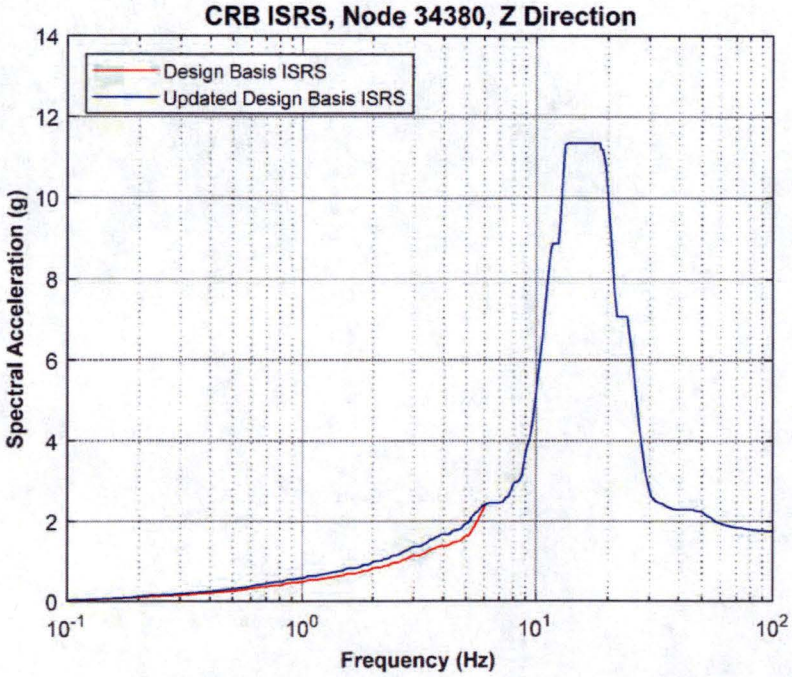

Figure 120. Control Building In-Structure Response Spectra Comparison, Node 34380, Z-Direction (e)

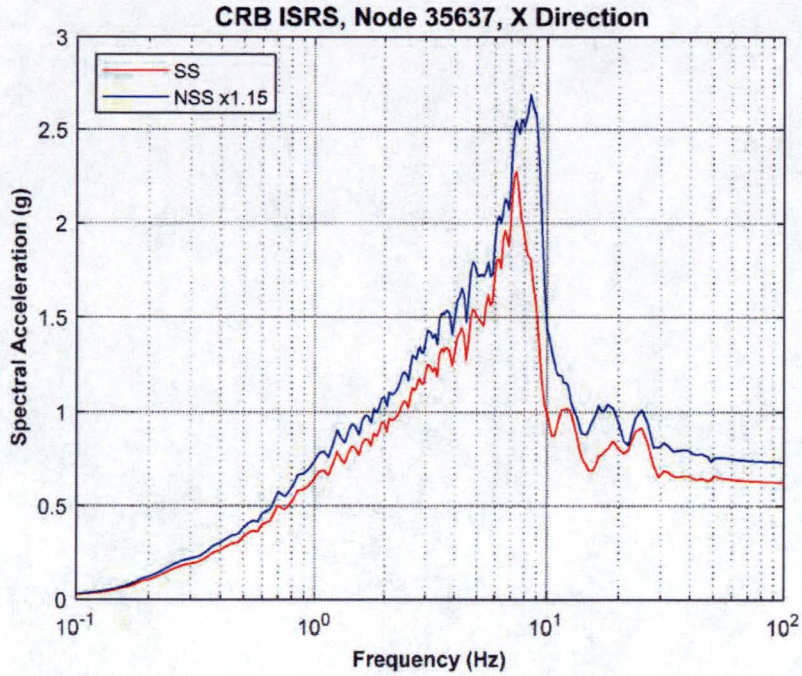

Figure 121. Control Building In-Structure Response Spectra Comparison, Node 35637, X-Direction

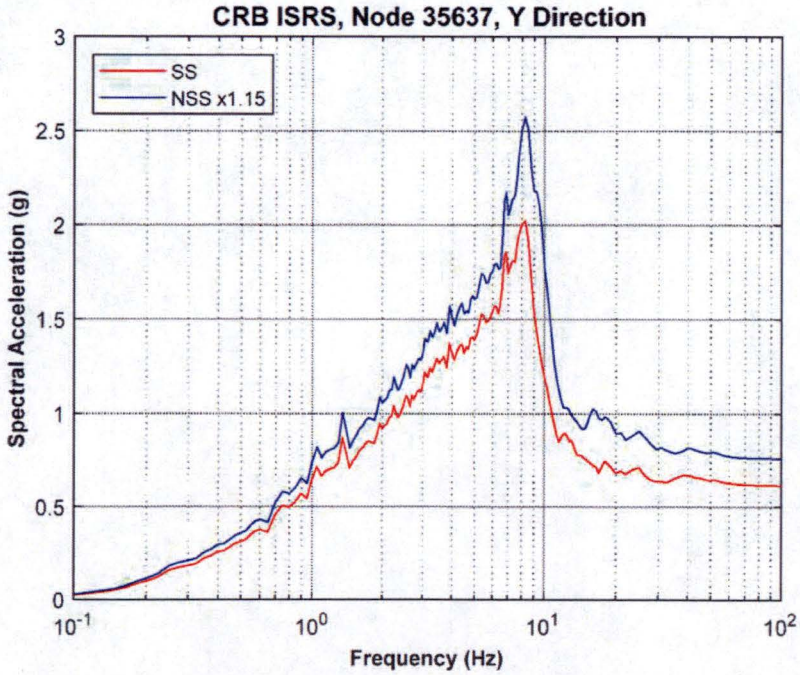

Figure 122. Control Building In-Structure Response Spectra Comparison, Node 35637, Y-Direction

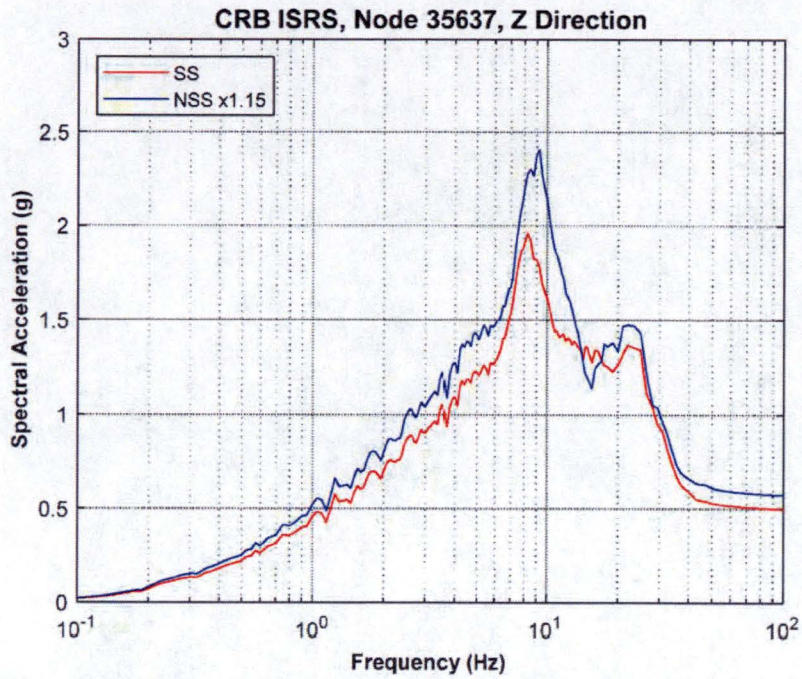

Figure 123. Control Building In-Structure Response Spectra Comparison, Node 35637, Z-Direction (a)

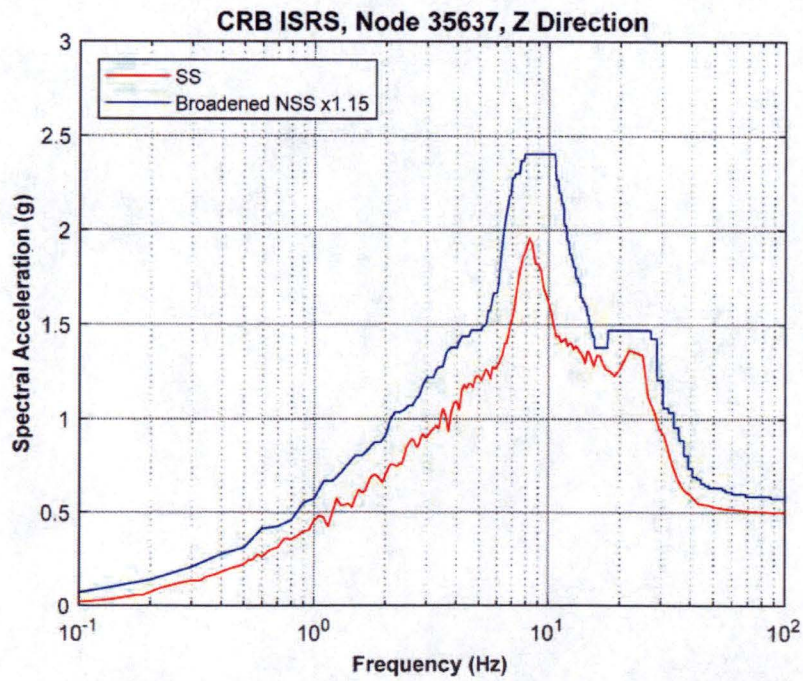

Figure 124. Control Building In-Structure Response Spectra Comparison, Node 35637, Z-Direction (b)

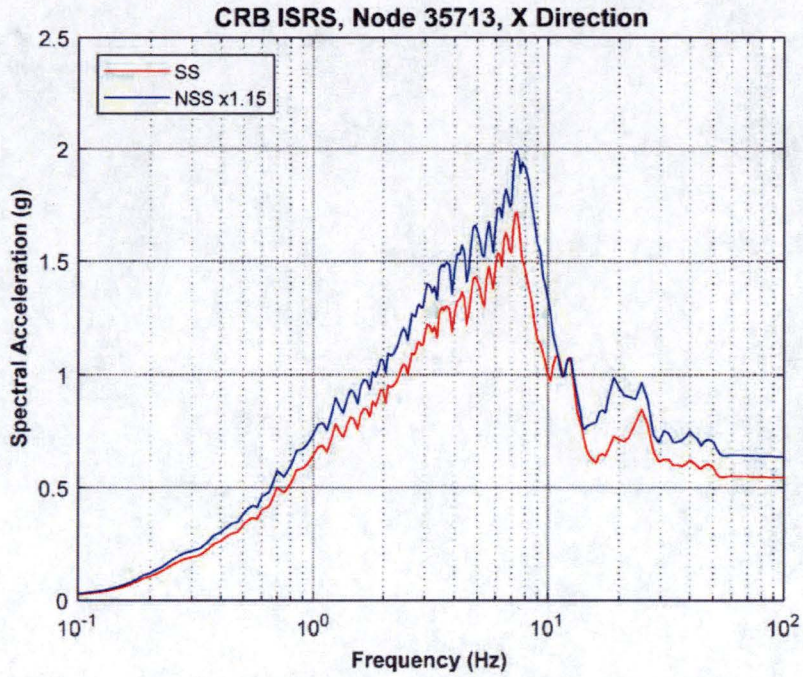

Figure 125. Control Building In-Structure Response Spectra Comparison, Node 35713, X-Direction (a)

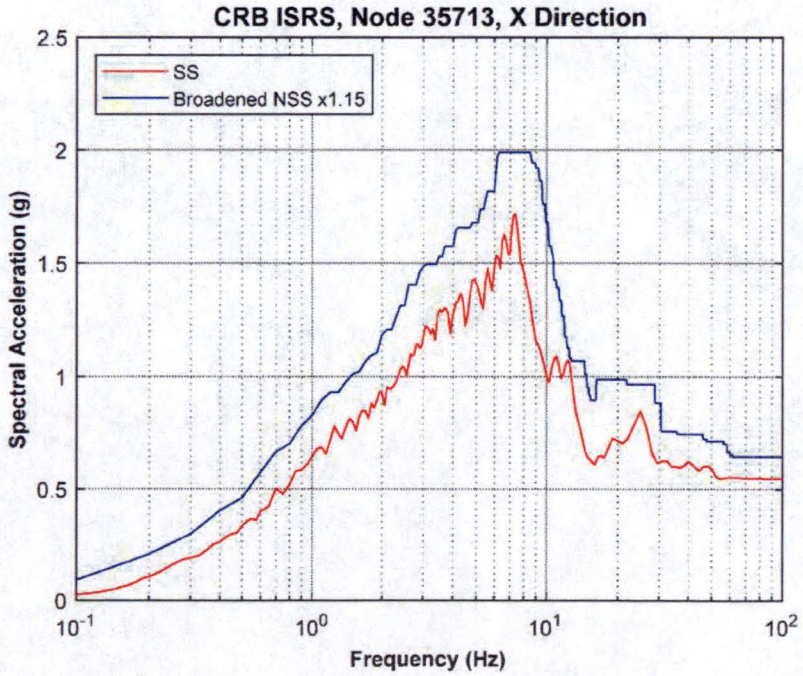

Figure 126. Control Building In-Structure Response Spectra Comparison, Node 35713, X-Direction (b)

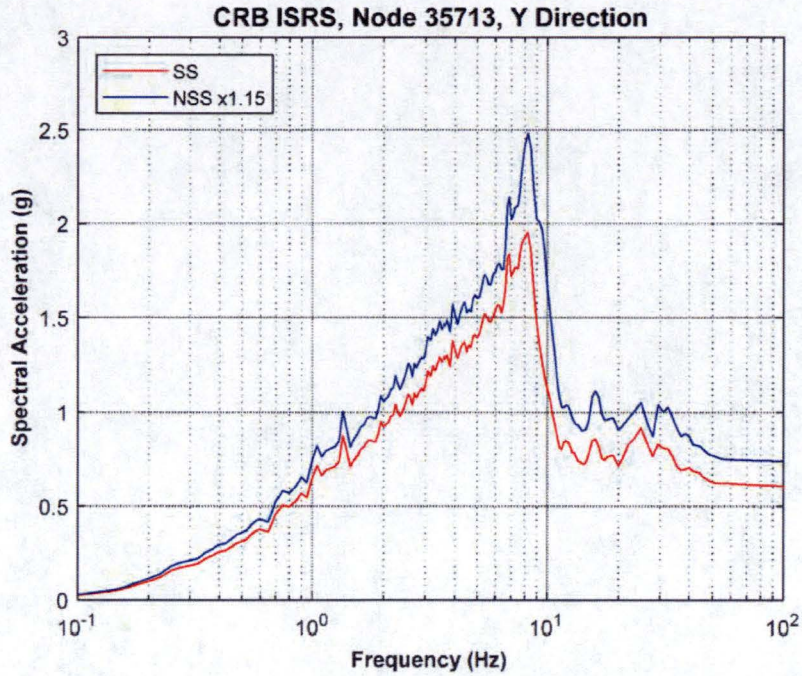

Figure 127. Control Building In-Structure Response Spectra Comparison, Node 35713, Y-Direction

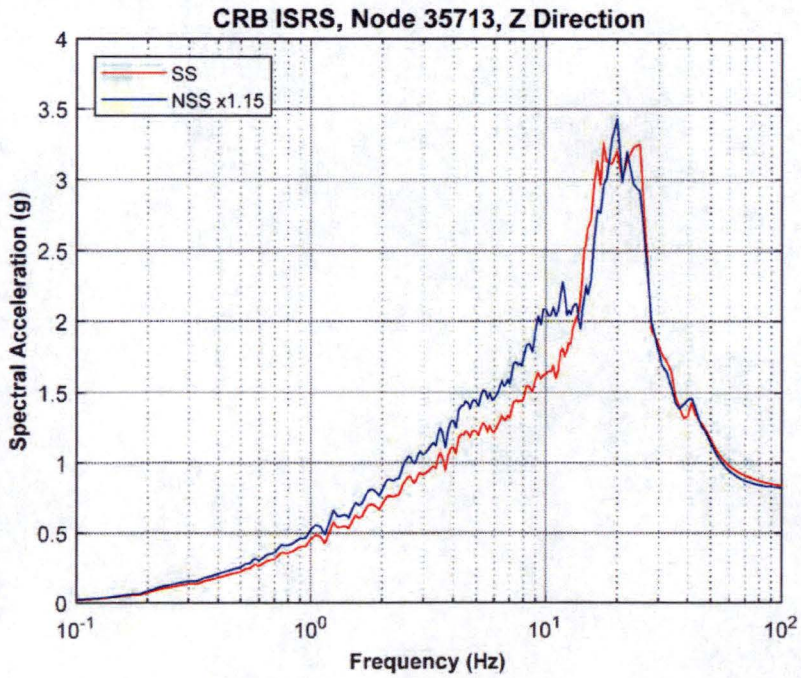

Figure 128. Control Building In-Structure Response Spectra Comparison, Node 35713, Z-Direction (a)

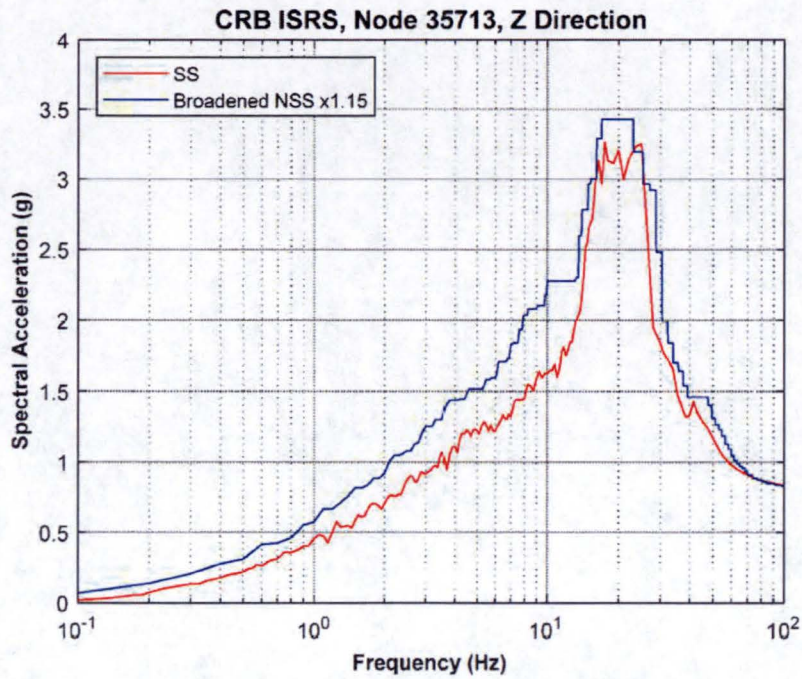

Figure 129. Control Building In-Structure Response Spectra Comparison, Node 35713, Z-Direction (b)

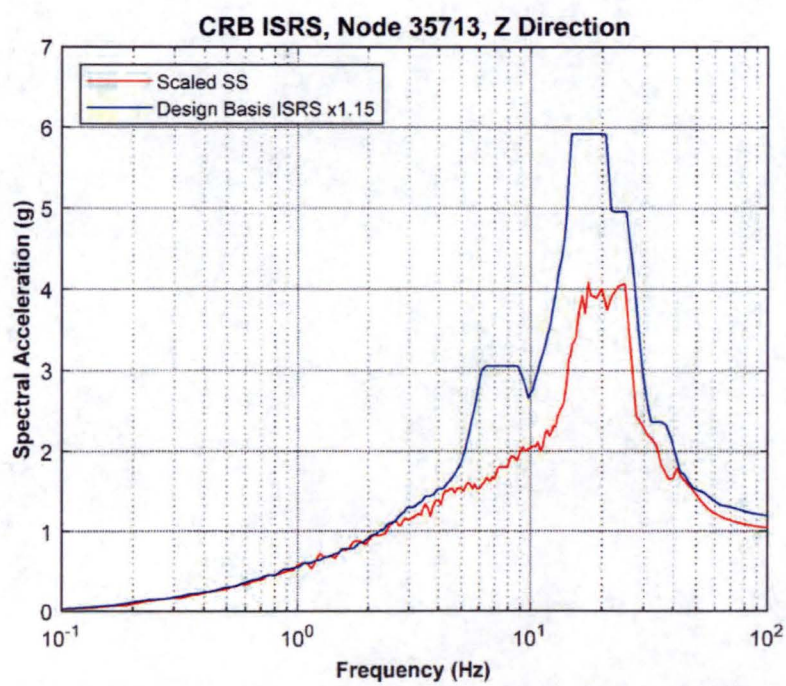

Figure 130. Control Building In-Structure Response Spectra Comparison, Node 35713, Z-Direction (c)

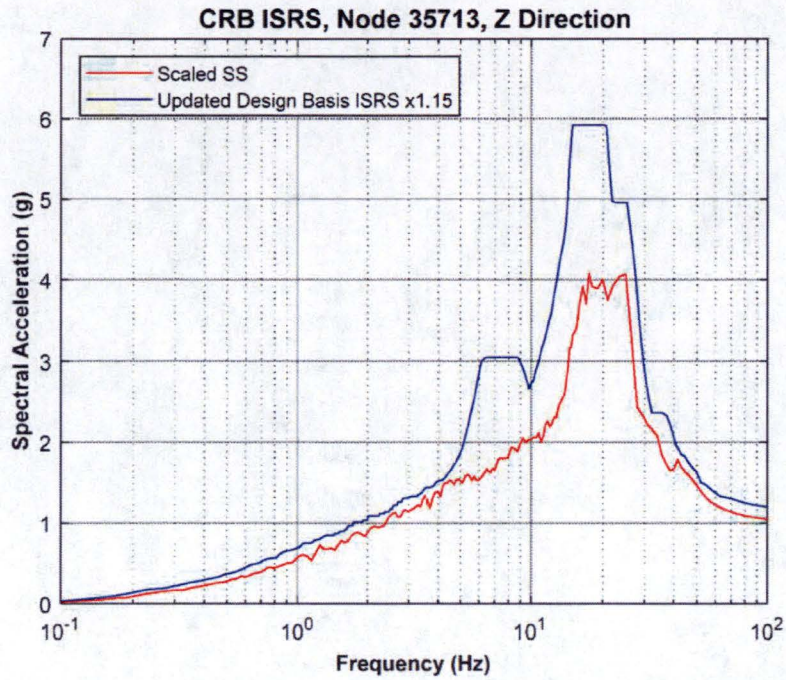

Figure 131. Control Building In-Structure Response Spectra Comparison, Node 35713, Z-Direction (d)

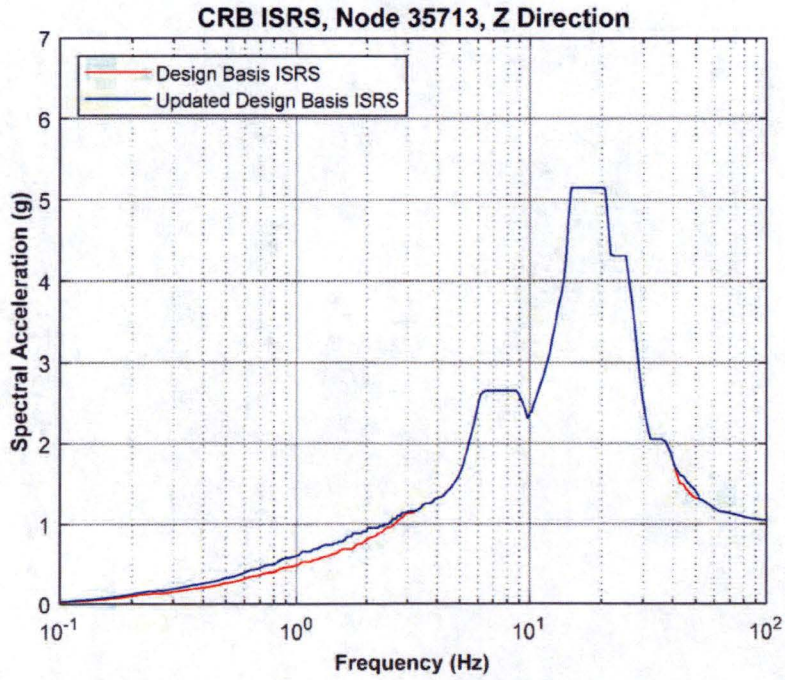

Figure 132. Control Building In-Structure Response Spectra Comparison, Node 35713, Z-Direction (e)

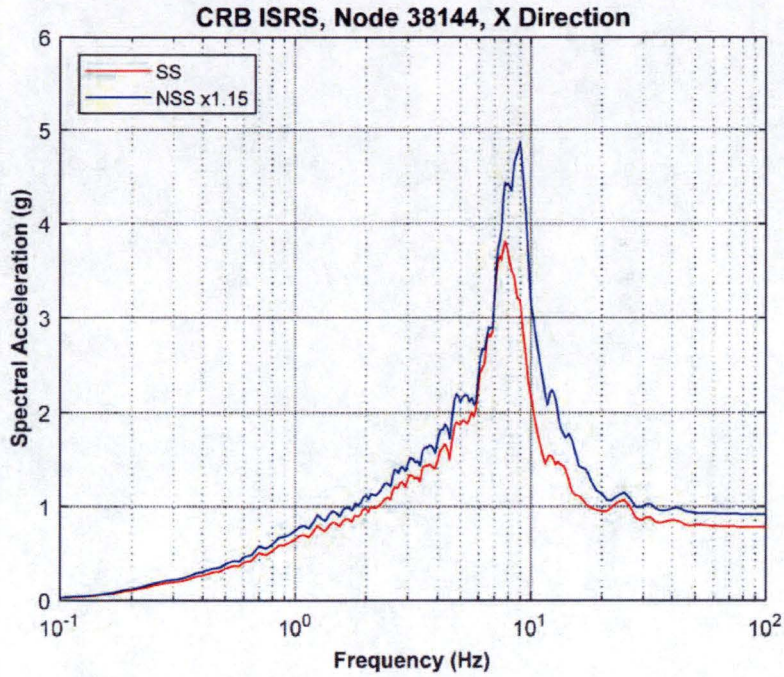

Figure 133. Control Building In-Structure Response Spectra Comparison, Node 38144, X-Direction

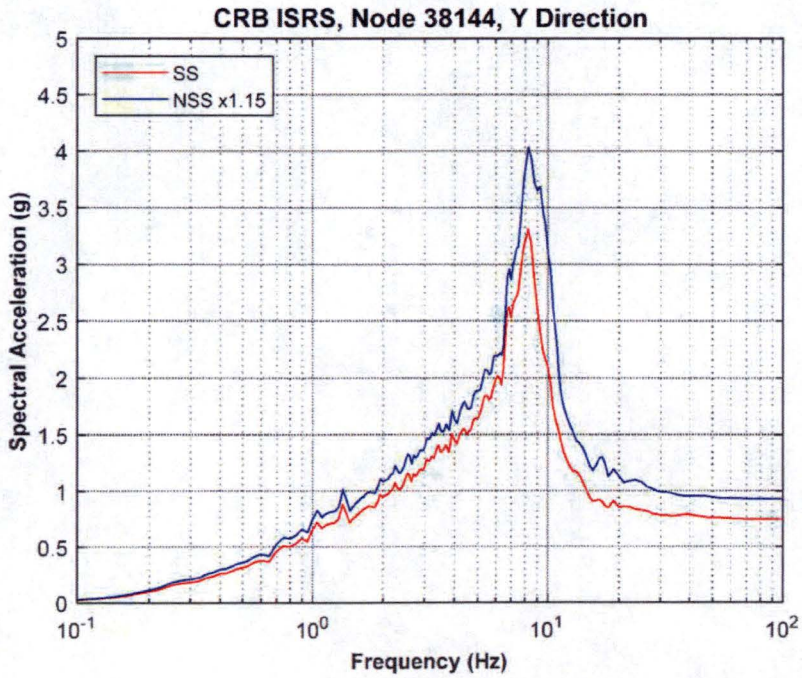

Figure 134. Control Building In-Structure Response Spectra Comparison, Node 38144, Y-Direction

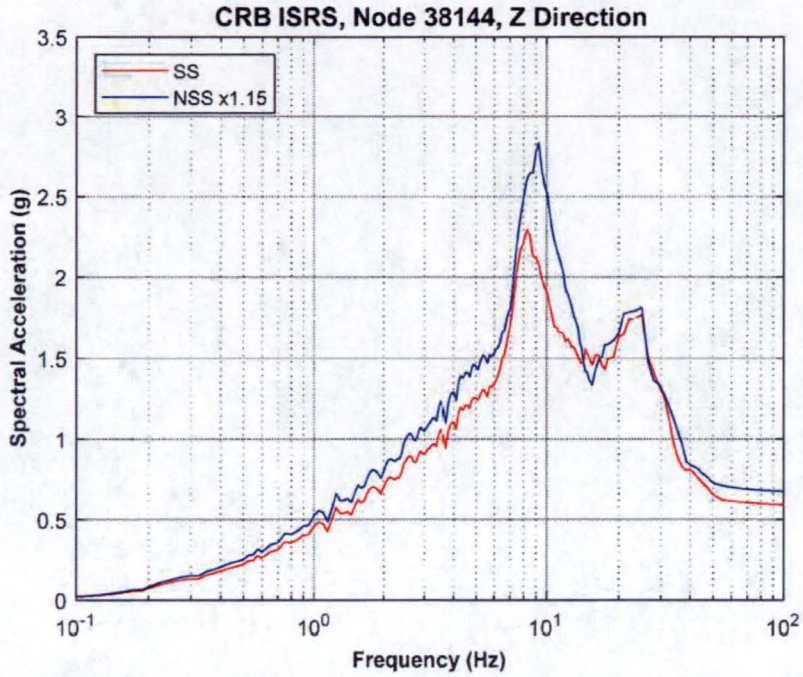

Figure 135. Control Building In-Structure Response Spectra Comparison, Node 38144, Z-Direction (a)

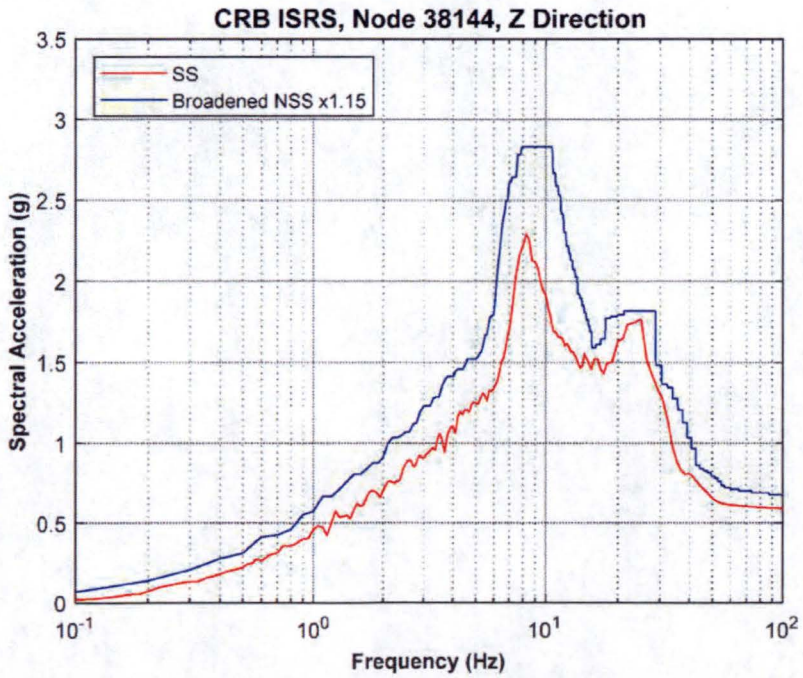

Figure 136. Control Building In-Structure Response Spectra Comparison, Node 38144, Z-Direction (b)

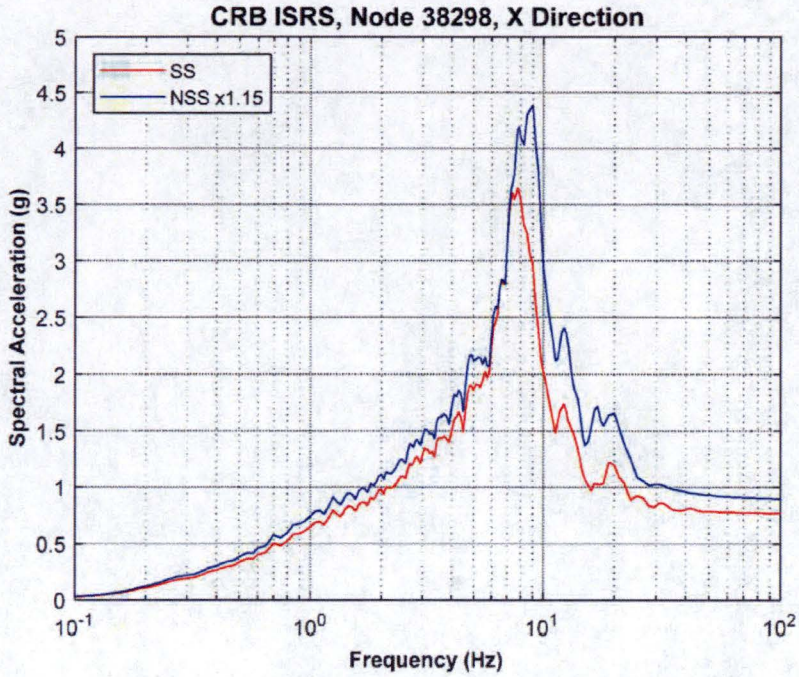

Figure 137. Control Building In-Structure Response Spectra Comparison, Node 38298, X-Direction (a)

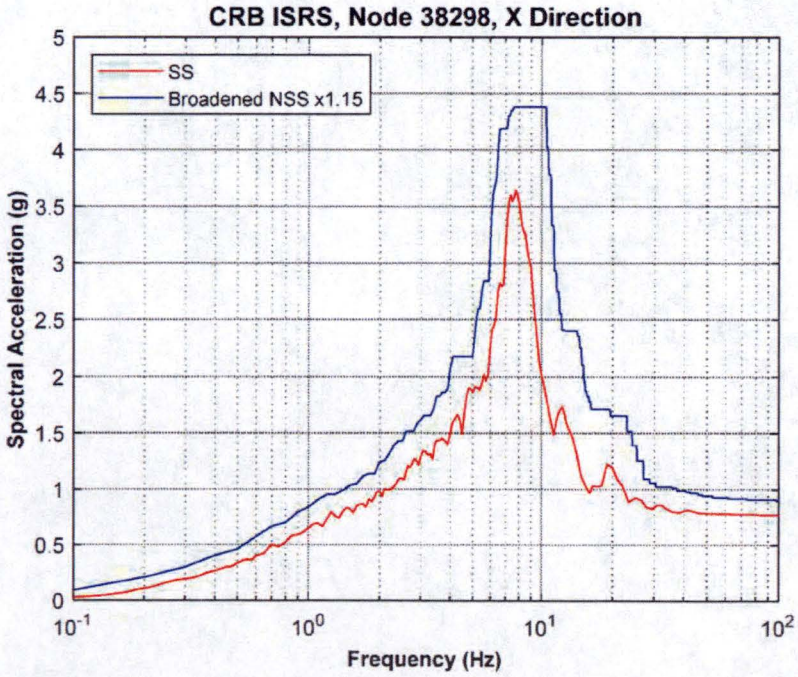

Figure 138. Control Building In-Structure Response Spectra Comparison, Node 38298, X-Direction (b)

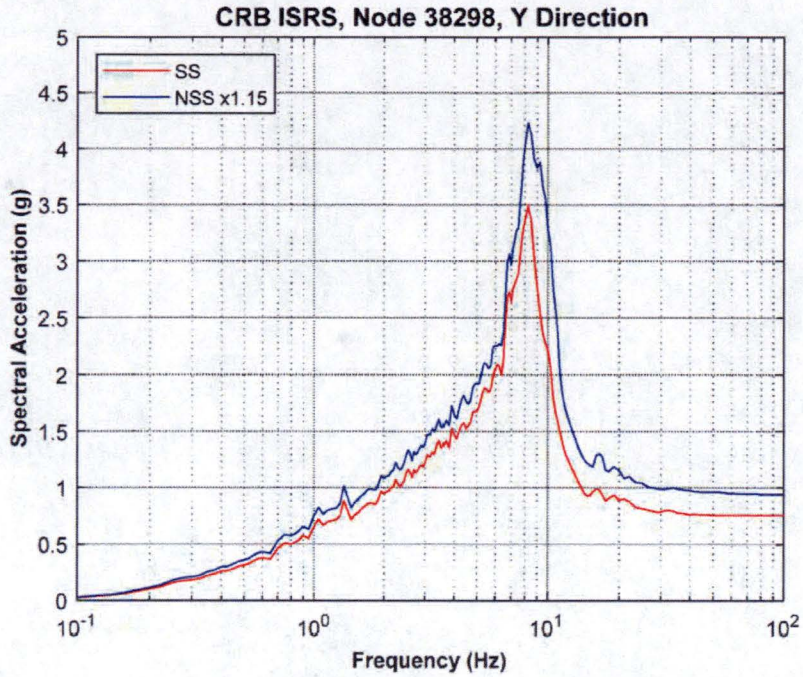

Figure 139. Control Building In-Structure Response Spectra Comparison, Node 38298, Y-Direction

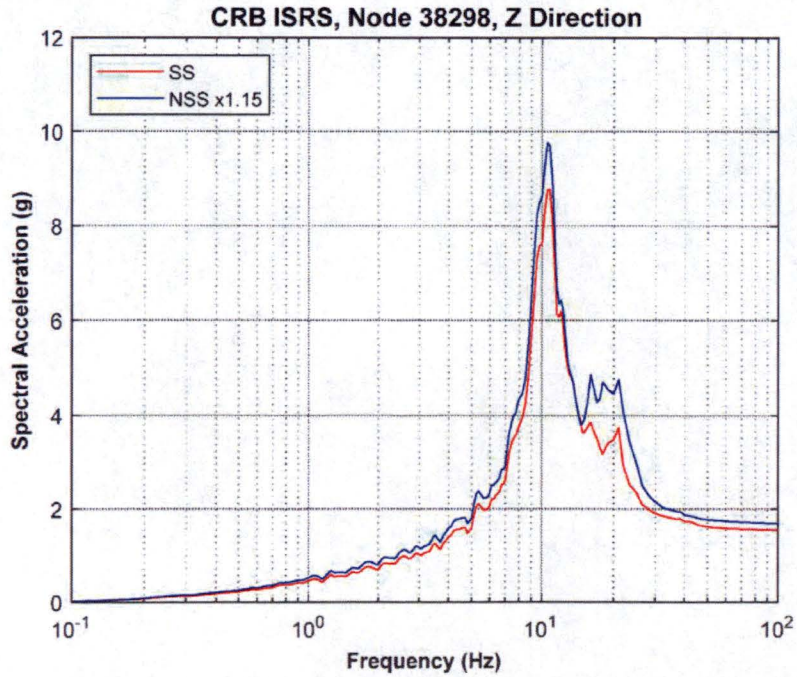

Figure 140. Control Building In-Structure Response Spectra Comparison, Node 38298, Z-Direction (a)

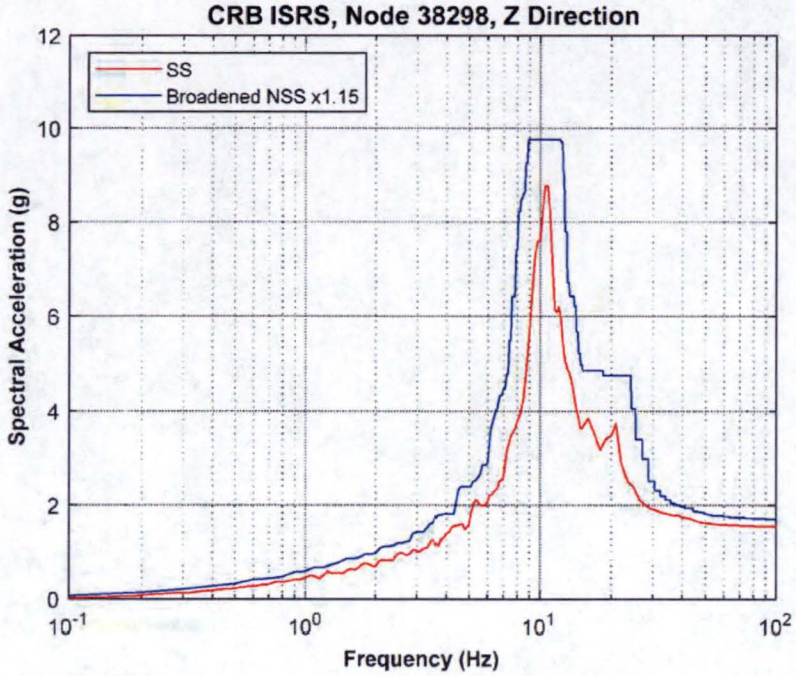

Figure 141. Control Building In-Structure Response Spectra Comparison, Node 38298, Z-Direction (b)

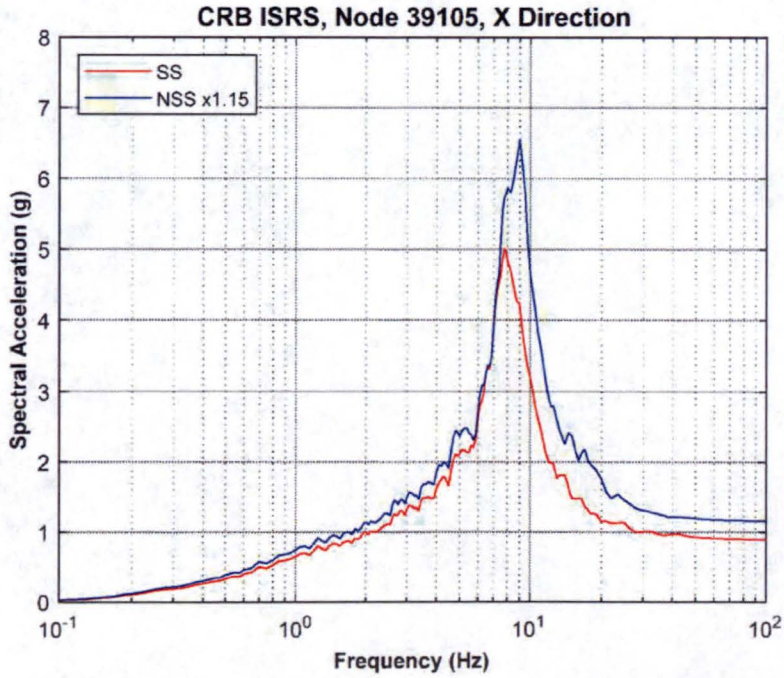

Figure 142. Control Building In-Structure Response Spectra Comparison, Node 39105, X-Direction (a)

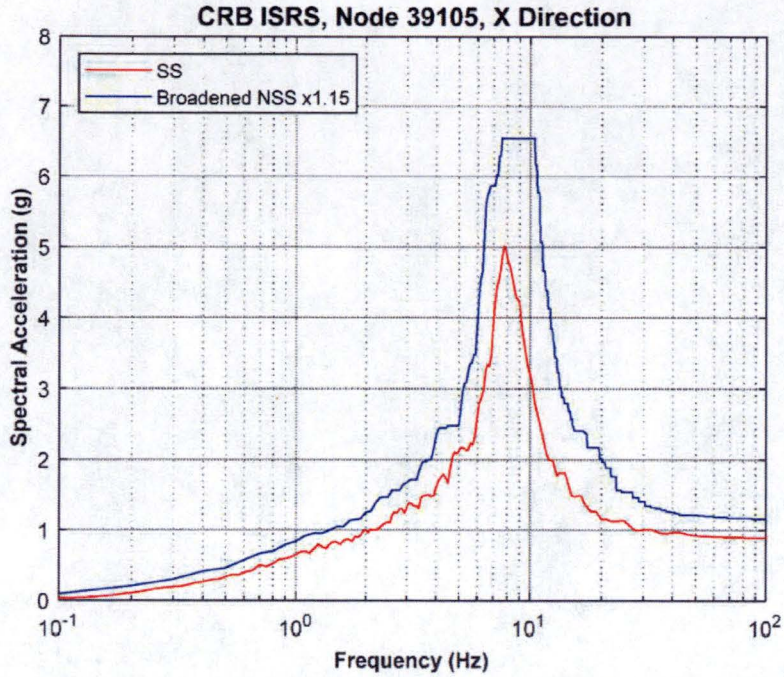

Figure 143. Control Building In-Structure Response Spectra Comparison, Node 39105, X-Direction (b)

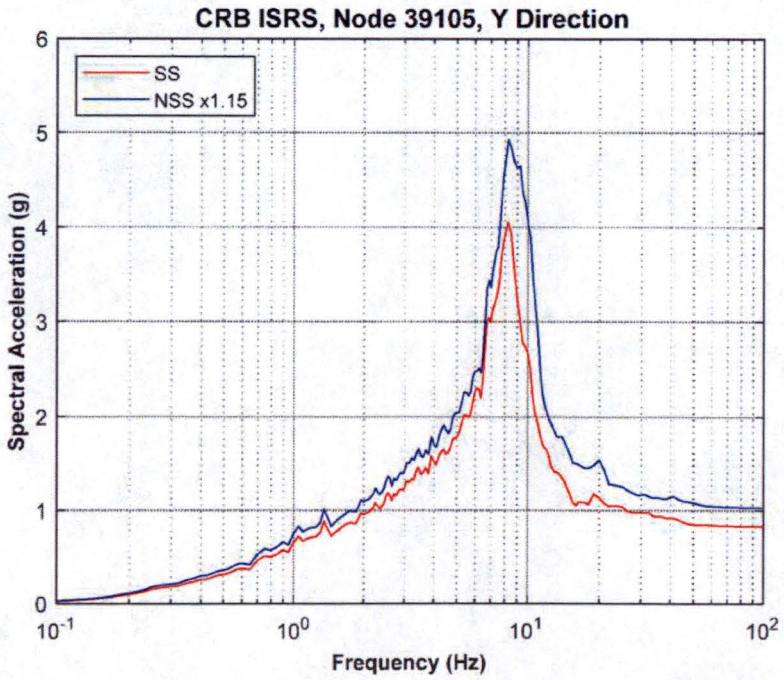

Figure 144. Control Building In-Structure Response Spectra Comparison, Node 39105, Y-Direction

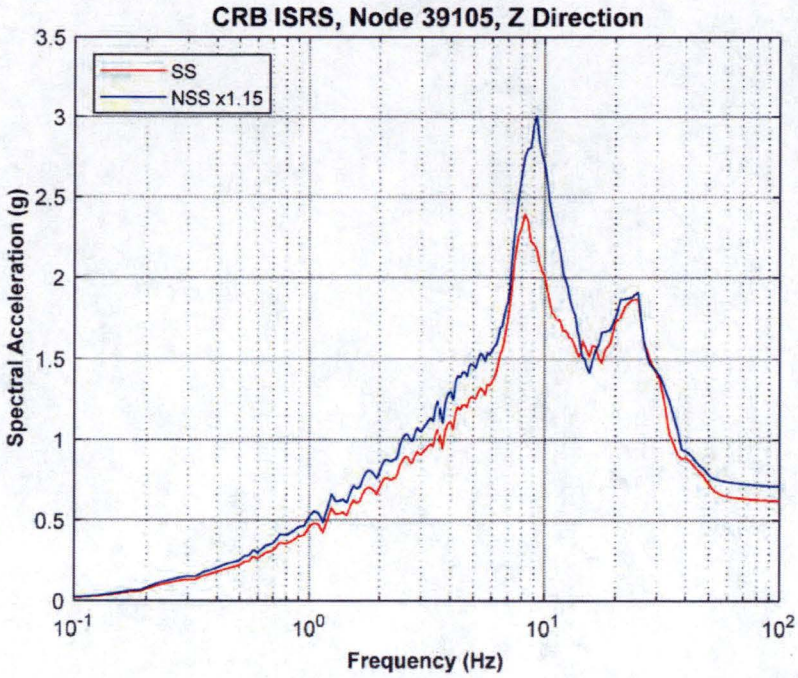

Figure 145. Control Building In-Structure Response Spectra Comparison, Node 39105, Z-Direction (a)

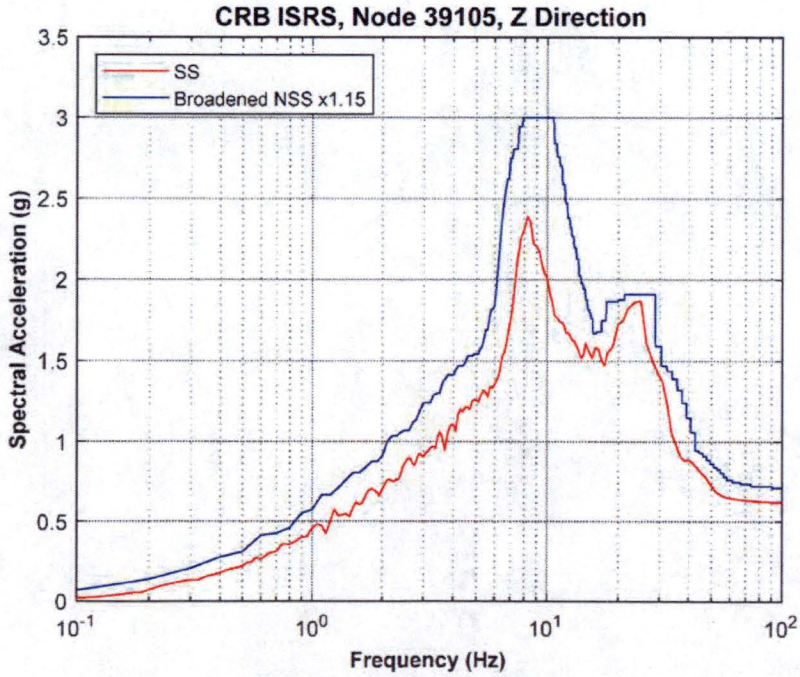

Figure 146. Control Building In-Structure Response Spectra Comparison, Node 39105, Z-Direction (b)

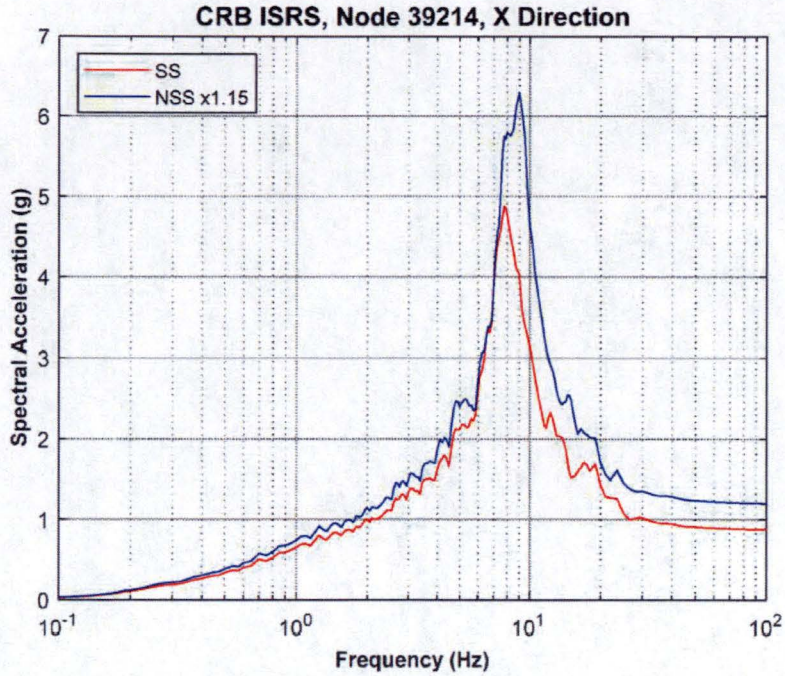

Figure 147. Control Building In-Structure Response Spectra Comparison, Node 39214, X-Direction

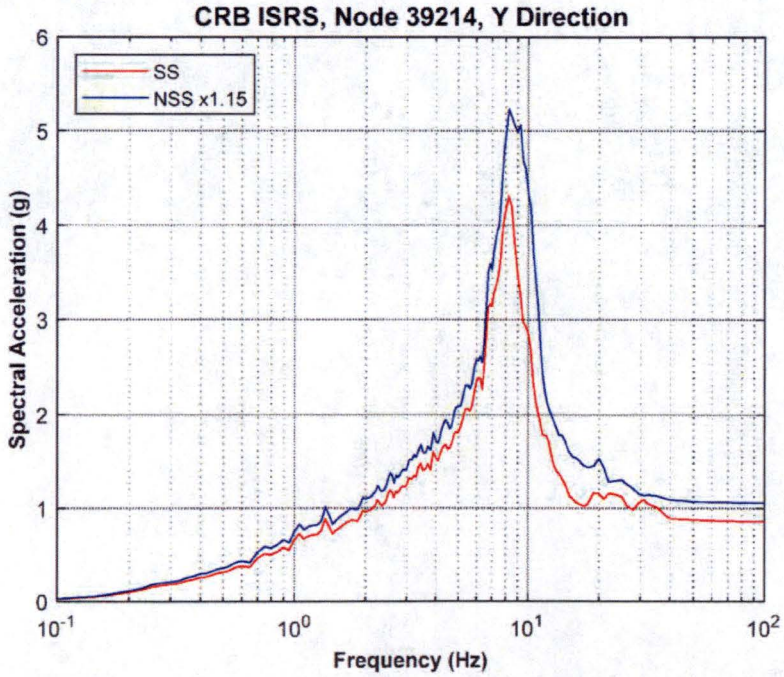

Figure 148. Control Building In-Structure Response Spectra Comparison, Node 39214, Y-Direction

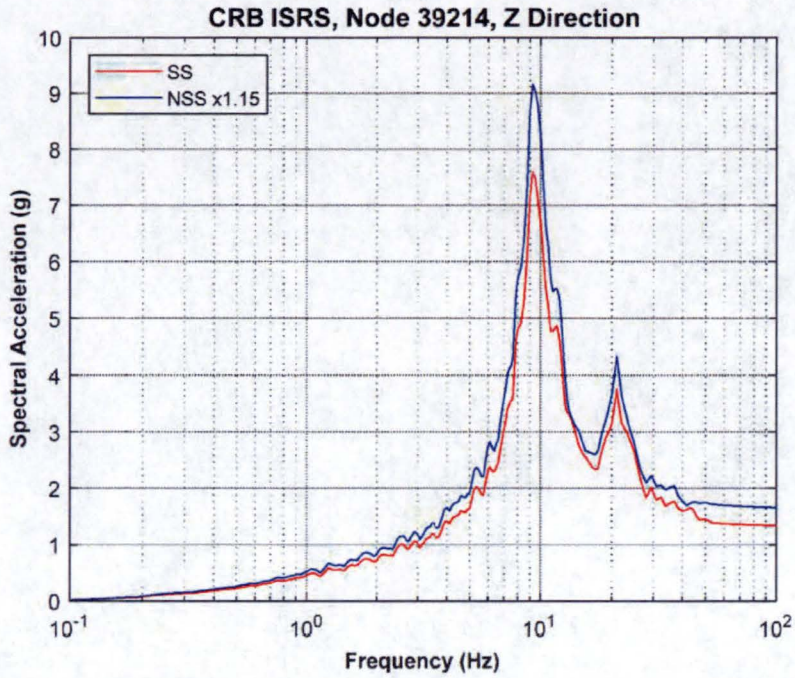

Figure 149. Control Building In-Structure Response Spectra Comparison, Node 39214, Z-Direction

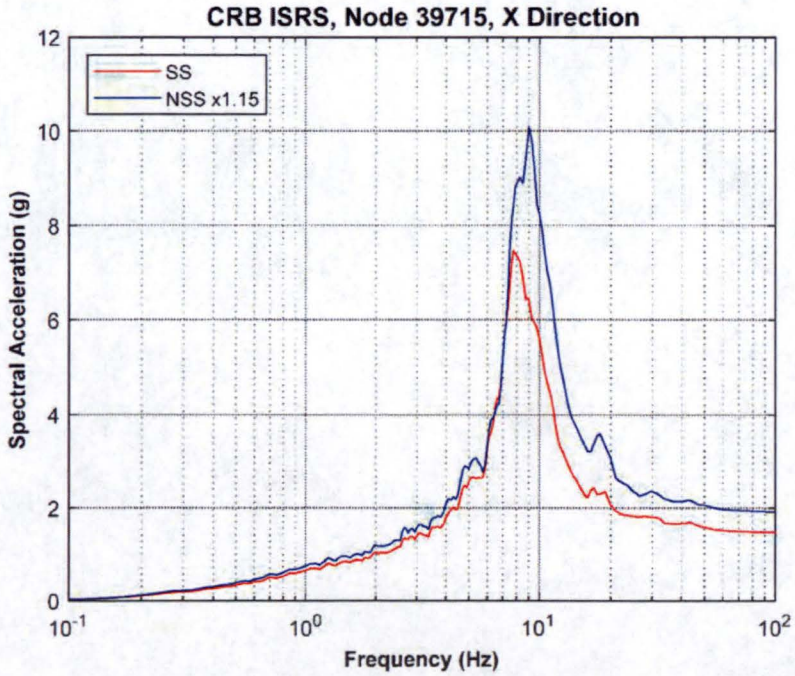

Figure 150. Control Building In-Structure Response Spectra Comparison, Node 39715, X-Direction (a)

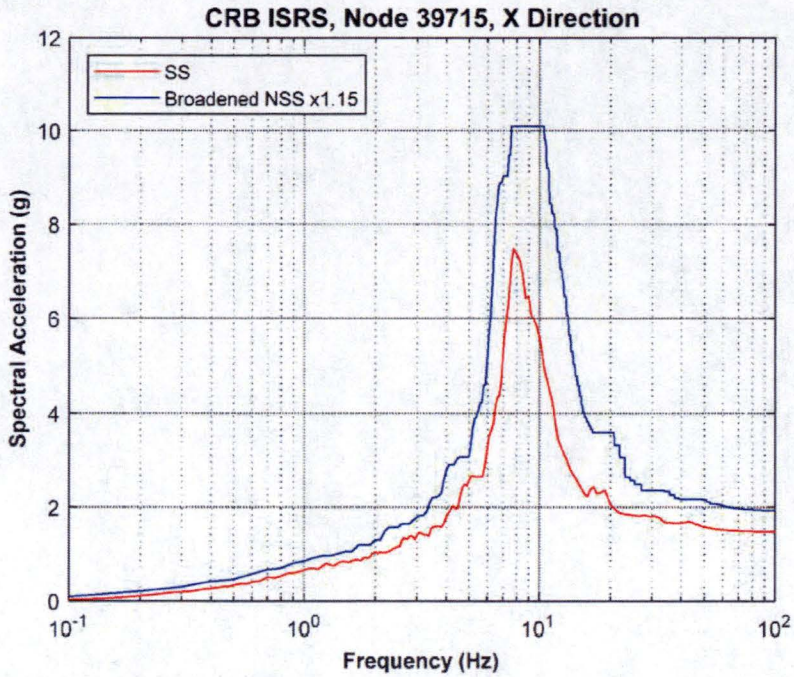

Figure 151. Control Building In-Structure Response Spectra Comparison, Node 39715, X-Direction (b)

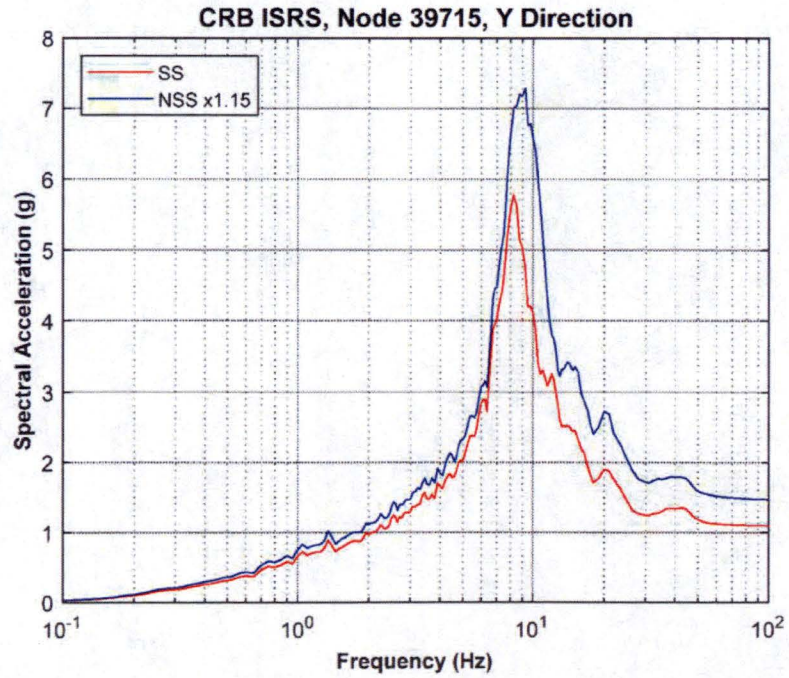

Figure 152. Control Building In-Structure Response Spectra Comparison, Node 39715, Y-Direction

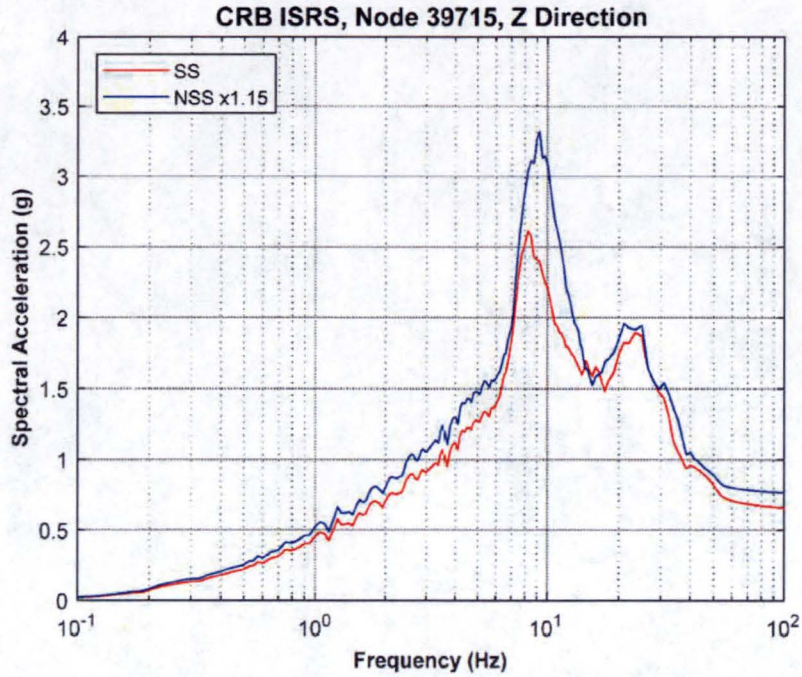

Figure 153. Control Building In-Structure Response Spectra Comparison, Node 39715, Z-Direction (a)

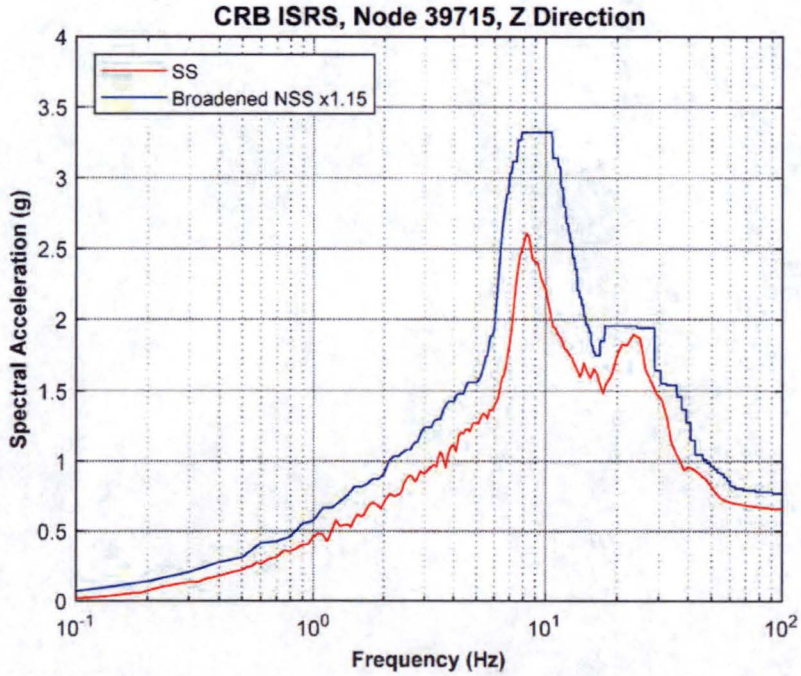

Figure 154. Control Building In-Structure Response Spectra Comparison, Node 39715, Z-Direction (b)

Updated Design Basis In-Structure Response Spectra for Floor Elevations

The updated design basis ISRS for floor elevations 63'-3" and 76'-6" are provided in this section. As shown in Figure 119 and Figure 131, the 5 percent damped design basis ISRS for floor elevations 63'-3" and 76'-6" was updated to account for identified exceedances. A frequency-dependent scale factor, α_{fi} , is presented to modify the ISRS plots for other damping ratios, as shown below:

$$\alpha_{f_i} = \left(\frac{Updated\ Design\ Basis\ ISRS, 5\%\ Damping)}{Design\ Basis\ ISRS, 5\%\ Damping}\right)_{f_i} \qquad \text{Equation 6}$$

Where, for each frequency point, f_i, scale factor α_{f_i} is calculated by dividing the updated 5% damped design basis ISRS by 5% damped design basis ISRS. Then, ISRS plots for each damping ratio is scaled in accordance with Equation 7:

Where ξ = 2%, 3%, 4%, 7%, and 10% damping ratio.

$$Updated\ Design\ Basis\ ISRS, \xi\ Damping = \alpha_{f_i}(Design\ Basis\ ISRS, \xi\ \ Damping) \qquad \text{Equation 7}$$

The following figures show the updated design basis ISRS for all damping ratios for floor elevations 63'-3" and 76'-6".

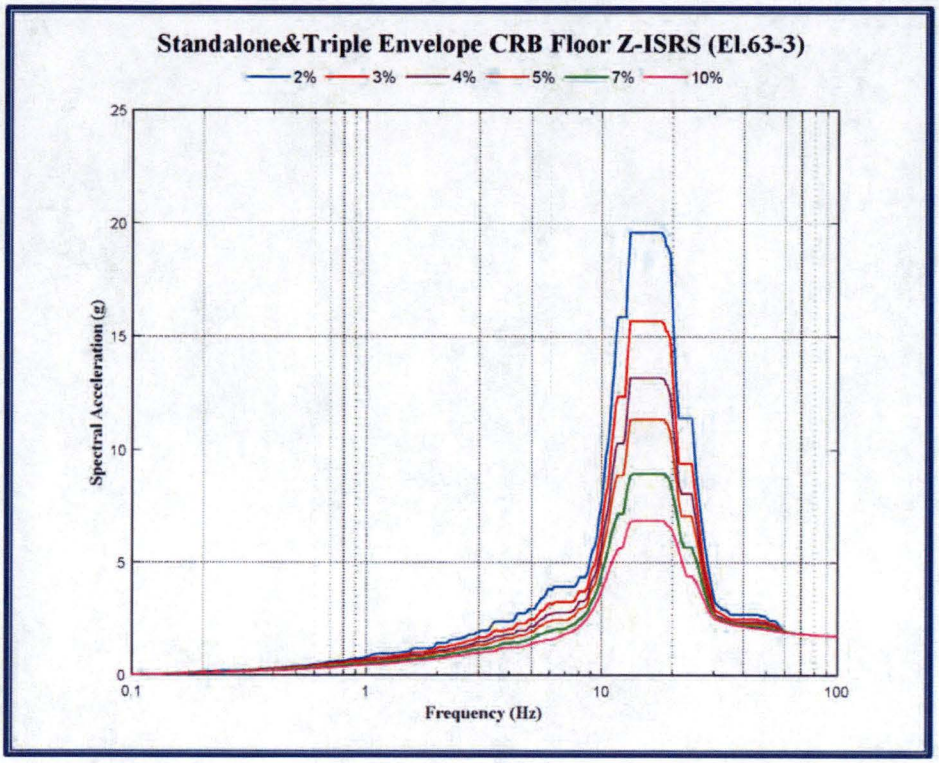

Figure 155. Updated Design Basis In-Structure Response Spectra for Floor El. 63'-3"

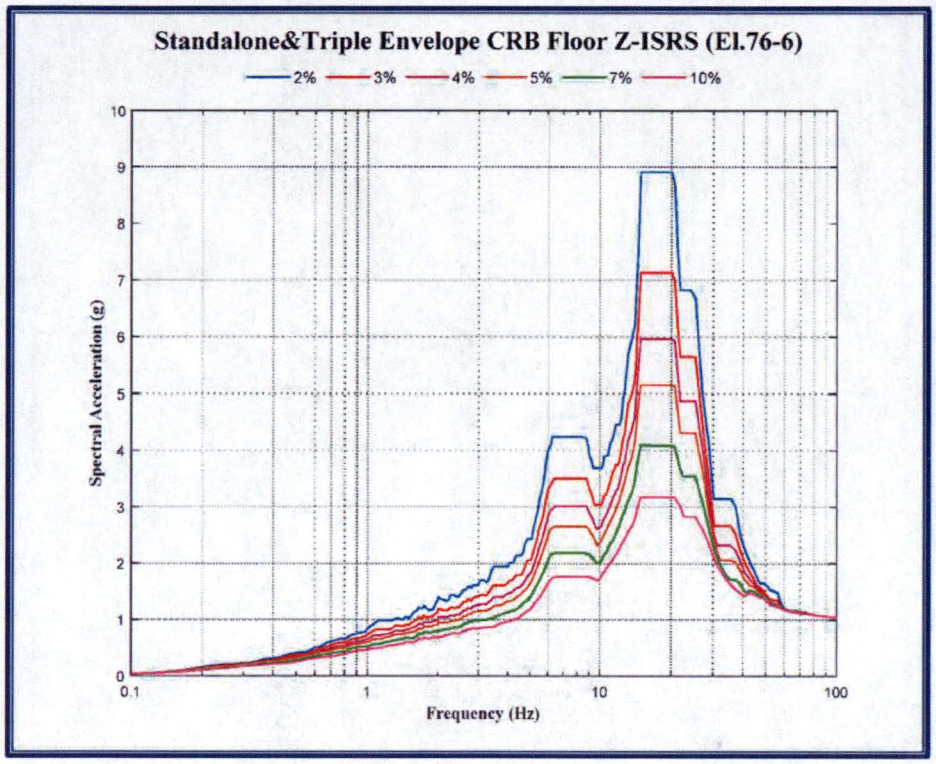

Figure 156. Updated Design Basis In-Structure Response Spectra for Floor El. 76'-6"

Response to Questions 3, 4, and 5

3. The information has been provided in the response to Questions 1 and 2 above.

4. As discussed with the NRC on February 26, 2019, in lieu of providing tables, NuScale has provided plots of 1.15 times the NSS case to show where exceedances greater than 15 percent occur. This allows for clear inspection of the data.

5. The following describes the analysis cases involved in the sensitivity study.

   Two models were used for the RXB. Model A is the RXB SASSI model without soil separation and Model B is the RXB SASSI model with soil separation. The two models are identical, except the backfill soil properties in the separation zone in Model B are reduced. To account for the effect of partial soil separation in the analysis model for the study, the Young's moduli of the backfill elements down to a depth of 25 ft, the top four layers of backfill elements, was factored by 0.01. The soil moduli of the top four backfill soil layers are reduced for the full width of the backfill soil, 25 ft. Both models were then analyzed for Soil Type 7 with cracked concrete properties and 7 percent concrete material damping. Soil Type 7 was chosen because that is the model that generally produced the highest ISRS, forces, and moments. Cracked concrete properties were chosen to be consistent with the use of 7 percent damping for the concrete material. Because the effects of soil separation are being investigated, all comparisons were made with results from Soil Type 7, cracked concrete, and 7 percent concrete damping.

   Similarly, two models were used for the CRB. The original CRB SASSI model without soil separation is designated as Model A and the CRB SASSI model with the reduced backfill soil properties to account for the soil separation effect is designated as Model B. The two models are identical except that the backfill soil properties in the separation zone in Model B are reduced. To account for the effect of partial soil separation in the analysis model for the study, the Young's moduli of the backfill soil solid elements down to one-third of the embedment, which is approximately equal to the total thickness of the top three layers of backfill soil to a depth of 18.75 ft, were factored by 0.01. This factor was applied to all backfill elements outside the exterior walls, a total width of 25 ft. The CRB was analyzed for Soil Type 7 with cracked concrete properties and 7 percent concrete material damping. Soil Type 7 was chosen because that is the model that produces the highest ISRS, forces, and moments. Cracked concrete properties were chosen to be consistent with the use of 7 percent damping for the concrete material. Because the effects of soil separation are being investigated, all comparisons are made with results from Soil Type 7, cracked concrete, and

7 percent concrete damping.

This is described in FSAR Section 3.7.2.1.1.3.

Reference

Rezaeian, S., Bozorgnia, Y., Idriss, I.M., Abrahamson, N., Campbell, K., and Silva, W., "Damping Scaling Models for Elastic Response Spectra," presentation at NGA-West2 Preliminary Results Workshop. November 15, 2012.

Impact on DCA:

The FSAR Section 3.7.2, Tables 1.8-2 and 3.7.2-56, and Figures 3.72-114, 3.7.2-118a and 3.7.2-119a have been revised as described in the response above and as shown in the markup provided in this response.

RAI 01-61, RAI 02.04.13-1, RAI 03.04.01-4, RAI 03.04.02-1, RAI 03.04.02-2, RAI 03.04.02-3, RAI 03.05.01.03-1, RAI 03.05.01.04-1, RAI 03.05.02-2, RAI 03.05.03-4, RAI 03.06.02-6, RAI 03.06.02-15, RAI 03.06.03-11, RAI 03.07.01-2, RAI 03.07.01-3, RAI 03.07.02-4S3, RAI 03.07.02-6S1, RAI 03.07.02-6S2, RAI 03.07.02-8, RAI 03.07.02-12, RAI 03.07.02-15S5, RAI 03.07.02-16S1, RAI 03.07.02-23S1, RAI 03.07.02-26, RAI 03.08.04-1S1, RAI 03.08.04-3S2, RAI 03.08.04-23S1, RAI 03.08.04-23S2, RAI 03.08.04-23S3, RAI 03.08.05-14S1, RAI 03.09.02-15, RAI 03.09.02-48, RAI 03.09.02-67, RAI 03.09.02-69, RAI 03.09.03-12, RAI 03.09.06-5, RAI 03.09.06-6, RAI 03.09.06-16, RAI 03.09.06-16S1, RAI 03.09.06-27, RAI 03.11-8, RAI 03.11-14, RAI 03.11-14S1, RAI 03.11-18, RAI 03.13-3, RAI 04.02-1S2, RAI 05.02.03-19, RAI 05.02.05-8, RAI 05.04.02.01-13, RAI 05.04.02.01-14, RAI 05.04.02.01-19, RAI 06.02.01.01.A-18, RAI 06.02.01.01.A-19, RAI 06.02.06-22, RAI 06.02.06-23, RAI 06.04-1, RAI 09.01.01-20, RAI 09.01.02-4, RAI 09.01.05-3, RAI 09.01.05-6, RAI 09.03.02-3, RAI 09.03.02-4, RAI 09.03.02-5, RAI 09.03.02-6, RAI 09.03.02-8, RAI 10.02-1, RAI 10.02-2, RAI 10.02-3, RAI 10.02.03-1, RAI 10.02.03-2, RAI 10.03.06-1, RAI 10.03.06-5, RAI 10.04.06-1, RAI 10.04.06-2, RAI 10.04.06-3, RAI 10.04.10-2, RAI 11.01-2, RAI 11.01-2S2, RAI 12.03-55S1, RAI 13.01.01-1, RAI 13.01.01-1S1, RAI 13.02.02-1, RAI 13.03-4, RAI 13.05.02.01-2, RAI 13.05.02.01-2S1, RAI 13.05.02.01-3, RAI 13.05.02.01-3S1, RAI 13.05.02.01-4, RAI 13.05.02.01-4S1, RAI 14.02-7, RAI 19-31, RAI 19-31S1, RAI 19-38, RAI 20.01-13

Table 1.8-2: Combined License Information Items

Item No.	Description of COL Information Item	Section
COL Item 1.1-1:	A COL applicant that references the NuScale Power Plant design certification will identify the site-specific plant location.	1.1
COL Item 1.1-2:	A COL applicant that references the NuScale Power Plant design certification will provide the schedules for completion of construction and commercial operation of each power module.	1.1
COL Item 1.4-1:	A COL applicant that references the NuScale Power Plant design certification will identify the prime agents or contractors for the construction and operation of the nuclear power plant.	1.4
COL Item 1.7-1:	A COL applicant that references the NuScale Power Plant design certification will provide site-specific diagrams and legends, as applicable.	1.7
COL Item 1.7-2:	A COL applicant that references the NuScale Power Plant design certification will list additional site-specific piping and instrumentation diagrams and legends as applicable.	1.7
COL Item 1.8-1:	A COL applicant that references the NuScale Power Plant design certification will provide a list of departures from the certified design.	1.8
COL Item 1.9-1:	A COL applicant that references the NuScale Power Plant design certification will review and address the conformance with regulatory criteria in effect six months before the docket date of the COL application for the site-specific portions and operational aspects of the facility design.	1.9
COL Item 1.10-1:	A COL applicant that references the NuScale Power Plant design certification will evaluate the potential hazards resulting from construction activities of the new NuScale facility to the safety-related and risk significant structures, systems, and components of existing operating unit(s) and newly constructed operating unit(s) at the co-located site per 10 CFR 52.79(a)(31). The evaluation will include identification of management and administrative controls necessary to eliminate or mitigate the consequences of potential hazards and demonstration that the limiting conditions for operation of an operating unit would not be exceeded. This COL item is not applicable for construction activities (build-out of the facility) at an individual NuScale Power Plant with operating NuScale Power Modules.	1.10
COL Item 2.0-1:	A COL applicant that references the NuScale Power Plant design certification will demonstrate that site-specific characteristics are bounded by the design parameters specified in Table 2.0-1. If site-specific values are not bounded by the values in Table 2.0-1, the COL applicant will demonstrate the acceptability of the site-specific values in the appropriate sections of its combined license application.	2.0
COL Item 2.1-1:	A COL applicant that references the NuScale Power Plant design certification will describe the site geographic and demographic characteristics.	2.1
COL Item 2.2-1:	A COL applicant that references the NuScale Power Plant design certification will describe nearby industrial, transportation, and military facilities. The COL applicant will demonstrate that the design is acceptable for each potential accident, or provide site-specific design alternatives.	2.2
COL Item 2.3-1:	A COL applicant that references the NuScale Power Plant design certification will describe the site-specific meteorological characteristics for Section 2.3.1 through Section 2.3.5, as applicable.	2.3
COL Item 2.4-1:	A COL applicant that references the NuScale Power Plant design certification will investigate and describe the site-specific hydrologic characteristics for Section 2.4.1 through Section 2.4.14, except Section 2.4.8 and Section 2.4.10.	2.4

Table 1.8-2: Combined License Information Items (Continued)

Item No.	Description of COL Information Item	Section
COL Item 3.7-10:	A COL applicant that references the NuScale Power Plant design certification will perform a site-specific configuration analysis that includes the Reactor Building with applicable configuration layout of the desired NuScale Power Modules. The COL applicant will confirm the following are bounded by the corresponding design certified seismic demands: 1) The in-structure response spectra of the standard design at the foundation and roof. See FSAR Figure 3.7.2-107 and Figure 3.7.2-108 for foundation in-structure response spectra and Figure 3.7.2-113 for roof in-structure response spectra. 2) The maximum forces in the NuScale Power Module lug restraints and skirts. See Table 3B-28. 3) The site-specific in-structure response spectra for the NuScale Power Module at the skirt support will be shown to be bounded by the in-structure response spectra in Figure 3.7.2-156 and Figure 3.7.2-157. The site-specific in-structure response spectra for the NuScale Power Module at the lug restraints will be shown to be bounded by the in-structure response spectra in Figure 3.7.2-158 through Figure 3.7.2-163. 4) The maximum forces and moments in the ~~east and~~ west wing wall~~s~~ and pool wall~~s~~. See ~~FSAR Table 3.7.2-32~~Table 3B-22b and Table 3B-23b. 5) Not used.~~The site-specific in-structure response spectra for the fuel storage racks will be shown to be bounded by the in-structure response spectra in Figure 3-6 through Figure 3-14 of TR-0816-49833.~~ 6) The site-specific in-structure response spectra shown immediately below will be shown to be bounded by their corresponding certified in-structure response spectra: • Reactor Building north exterior wall at EL 75′-0″: bounded by in-structure response spectra in Figure 3.7.2-110 • Reactor Building west exterior wall at EL 126′-0″: bounded by in-structure response spectra in Figure 3.7.2-112 • Reactor Building crane wheels at EL 145′-6″: bounded by in-structure response spectra in Figure 3.7.2-114 • Control Building east wall at EL 76′-6″: bounded by in-structure response spectra in Figure 3.7.2-119a and Figure 3.7.2-119b • Control Building south wall at EL 120′-0″: bounded by in-structure response spectra in Figure 3.7.2-121a and Figure 3.7.2-121b If not, the standard design will be shown to have appropriate margin or should be appropriately modified to accommodate the site-specific demands.	3.7
COL Item 3.7-11:	A COL applicant that references the NuScale Power Plant design certification will perform a site-specific analysis that~~, if applicable,~~ assesses the effects of soil separation. The COL applicant will confirm that the in-structure response spectra in the soil separation cases are bounded by the in-structure response spectra shown in FSAR Figure 3.7.2-107 through Figure 3.7.2-122.	3.7
COL Item 3.7-12:	A COL applicant that references the NuScale Power Plant design certification will perform an analysis that uses site-specific soil and time histories to confirm the adequacy of the fluid-structure interaction correction factor.	3.7
COL Item 3.7-13:	A COL applicant that references the NuScale Power Plant design certification will perform a site-specific analysis that assesses the effects of non-vertically propagating seismic waves on the free-field ground motions and seismic responses of Seismic Category I structures, systems, and components.	3.7
COL Item 3.7-14:	A COL applicant that references the NuScale Power Plant design certification will demonstrate that the site-specific seismic demand is bounded by the FSAR capacity for an empty dry dock condition.	3.7
COL Item 3.7-15:	A COL applicant that references the NuScale Power Plant design certification will determine the appropriate site-specific number of interaction planes for soil structure interaction.	3.7
COL Item 3.8-1:	A COL applicant that references the NuScale Power Plant design certification will describe the site-specific program for monitoring and maintenance of the Seismic Category I structures in accordance with the requirements of 10 CFR 50.65 as discussed in Regulatory Guide 1.160. Monitoring is to include below grade walls, groundwater chemistry if needed, base settlements and differential displacements.	3.8

model were similar and further confirms that the ESM approaches the DM in accuracy.

The comparison of 7P to 9P is accomplished by looking at the in-structure response spectra (ISRS) at three locations in the reactor building:

- The northeast corner on top of the basemat as shown in Figure 3.7.2-5.
- The NPM1 East bay wall at the lug support as shown in Figure 3.7.2-6.
- The center of the roof slab as shown in Figure 3.7.2-7.

RAI 03.07.02-4S2

In addition, bending moments at the center of the roof are compared to investigate if the moment responses calculated by the analysis using the 7P interaction nodes are close to those from the analysis using the 9P interaction nodes. These comparisons are performed with the CSDRS and all five CSDRS-compatible time histories for Soil Type 11 (soft soil) and Soil Type 7 (rock) using cracked concrete and 4 percent damping.

The 7P versus 9P ISRS comparisons for the Capitola time histories are provided in Figure 3.7.2-8, Figure 3.7.2-9, and Figure 3.7.2-10. The corresponding results for the other time histories are similar. As can be seen in these figures, there is very close correlation between the 7P and 9P models, with the larger variation occurring in the soft soil. This level of agreement justifies using a 7P versus a 9P model and, because the results are similar, demonstrates the acceptability of using the extended subtraction method as an alternative to the direct method.

While the results are similar, they are not exact. This difference is not a concern because of the methodology used in developing accelerations and forces in the structures. Each building is evaluated with several soil types and two stiffnesses. In addition, for the CSDRS, five separate time histories are evaluated, and the results are averaged.

RAI 03.07.02-4S3

COL Item 3.7-15: A COL applicant that references the NuScale Power Plant design certification will determine the appropriate site-specific number of interaction planes for soil structure interaction.

Cracked Model Stiffness

For SASSI2010 analyses, the plate stiffnesses are only controlled by two input parameters. The two parameters are the Young's modulus and the plate thickness. It is not possible to reduce the bending stiffness by 50 percent for cracked concrete while preserving the axial stiffness at 100 percent for in-plane forces by modifying Young's modulus. A compromise approach is used by reducing the thickness by a factor equal to cubic root of 0.5, or 0.7937 to reduce the bending stiffness in half for the cracked concrete condition. In this approach, the uncracked axial stiffness is reduced by a factor of 0.7937.

For convenience in design of components and supports that need to be Seismic Category I or Seismic Category II, ISRS at multiple nodes at each floor are combined to develop a single ISRS for each floor. The ISRS corresponding to each main floor of the RXB identified below are provided in the listed figures. Although ISRS are provided at the NPM base (floor at EL. 25' 0"), time histories were used as input for the evaluation of the NPMs as described in Appendix 3A. The governing ISRS envelop the ISRS taken from node locations on the corners of the buildings to capture the torsional and rocking components. See Table 3.7.2-53 for a list of nodes enveloped at each floor to produce the floor ISRS. Figure 3.7.2-142 through Figure 3.7.2-148 show the locations of the nodes selected for floor ISRS generation.

Floor	Figure
24'-0"	Figure 3.7.2-107
25'-0"	Figure 3.7.2-108
50'-0"	Figure 3.7.2-109
75'-0"	Figure 3.7.2-110
100'-0"	Figure 3.7.2-111
126'-0"	Figure 3.7.2-112
181'-0"	Figure 3.7.2-113

3.7.2.5.4 Reactor Building Crane In-Structure Response Spectra

RAI 03.07.02-4S3, RAI 03.08.04-23S3

The seismic analysis of the RBC uses ISRS for input. The ISRS are generated at four selected individual crane wheel locations. These locations are on the reactor pool wall at the crane rail slab at ~~elevation 145' 6"~~El. 145'-6", see Table 3.7.2-56. The enveloping ISRS for these four locations are provided in Figure 3.7.2-114. In addition to these four nodes, a fifth node located on the crane rail slab is used to generate the ISRS in the vertical direction. This node is used because when soil separation effects are considered, the vertical direction is not bounded by the enveloped ISRS of the other four nodes. The seismic analysis of the RBC is completed per ASME NOG-1 (Reference 3.7.2-4).

RAI 03.08.04-23S3

3.7.2.5.5 ~~NuScale Power Module Bay Wall In-Structure Response Spectra~~Not Used

RAI 03.08.04-23S3

~~The NPM lug restraints transfer the horizontal forces between the NPMs and the walls of the bay. These restraints ensure that the NPM will not fall as a result of a seismic event. Because of the significance of the restraints, bounding ISRS are provided. These ISRS are not used for the design of any of the restraints, nor any specific components. However they are used in Section 3.8.4.8 to confirm acceptability of the site independent Reactor Building for use at specific sites.~~

RAI 03.08.04-23S3

RAI 03.07.02-4S3, RAI 03.08.04-23S3

Table 3.7.2-56: Selected Crane Wheel Locations and a Crane Rail Slab Node for In-Structure Response Spectra Presentation

Location No.	Coordinates (inches)			Location Description
	X (E-W)	Y (N-S)	Z (VT)	
1	2215	-453	1548	SW Crane Wheel
2	2215	453	1548	NW Crane Wheel
3	3067.25	-453	1548	SE Crane Wheel
4	3067.25	453	1548	NE Crane Wheel
5	420.0	453	1548	Crane Rail Slab at Grid Line RX-2 at El. 145'-6"

RAI 03.07.02-4S3, RAI 03.07.02-6S3

Figure 3.7.2-114: ~~ISRS~~In-Structure Response Spectra at Reactor Building Crane Wheels at El. 145′ 6″

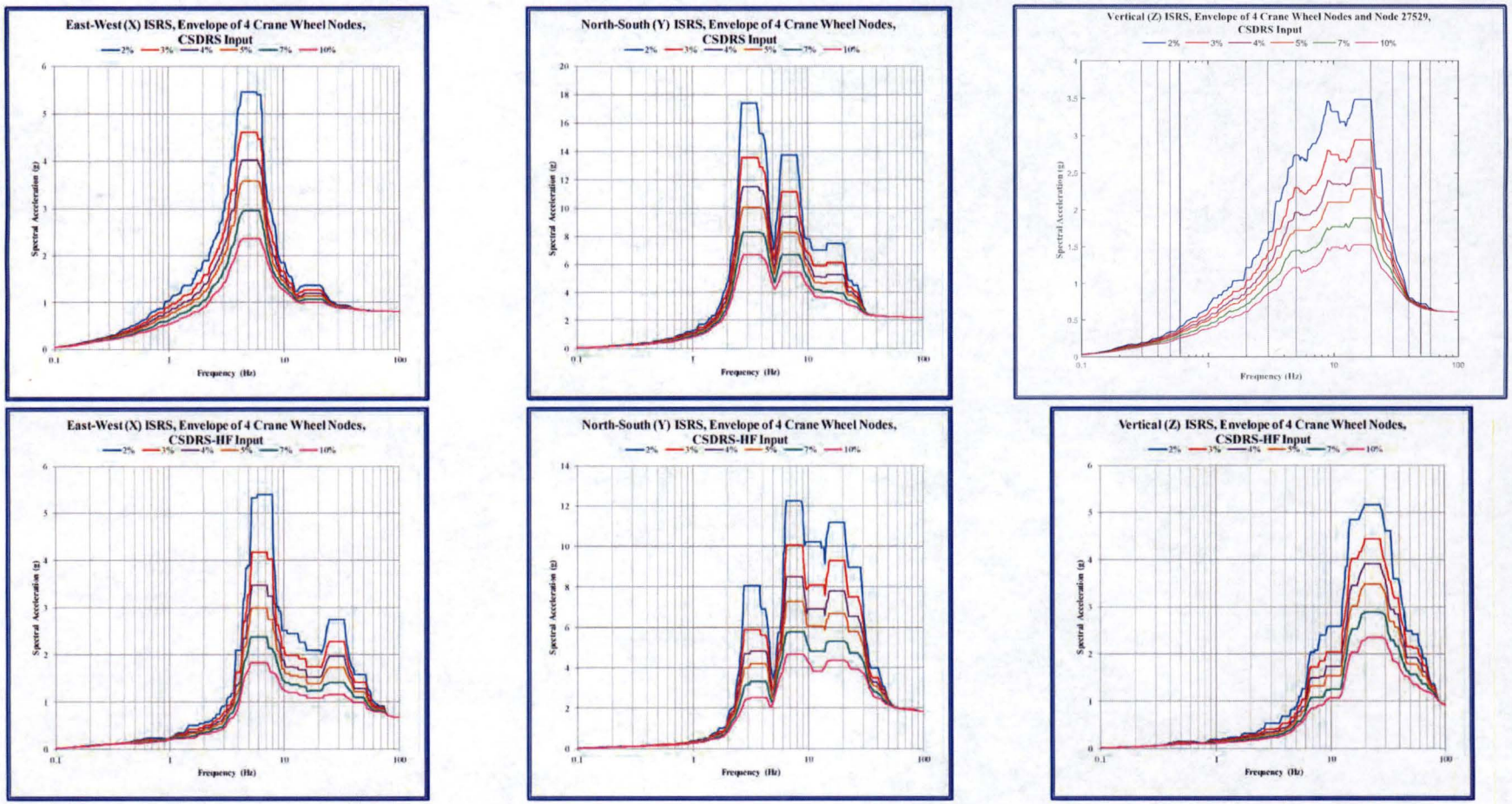

RAI 03.07.02-4S3, RAI 03.07.02-6S3, RAI 03.07.02-26

Figure 3.7.2-118a: Control Building - In-Structure Response Spectra at El. 63'-3" (Z=570"), 5 CSDRS Inputs

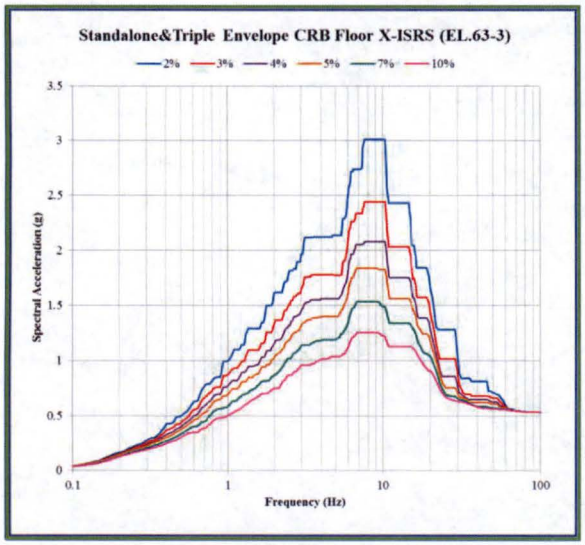

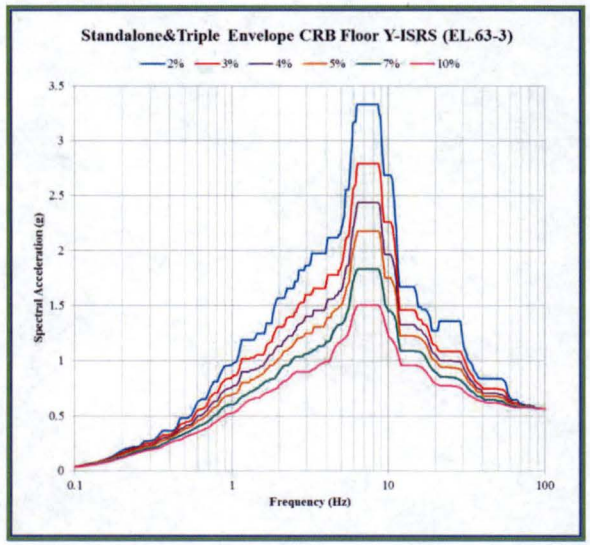

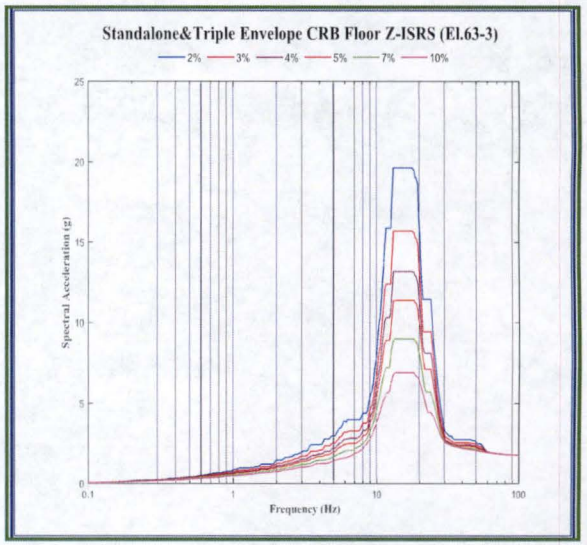

RAI 03.07.02-4S3, RAI 03.07.02-6S3, RAI 03.07.02-26
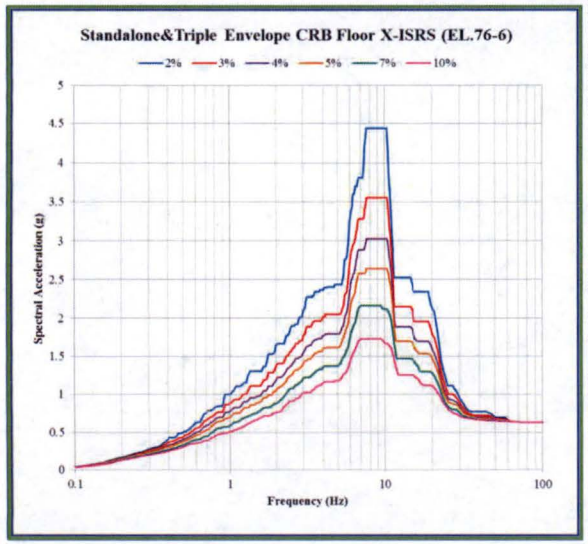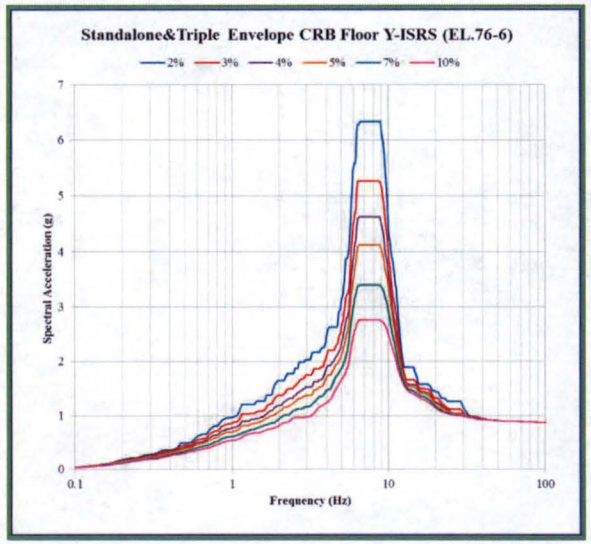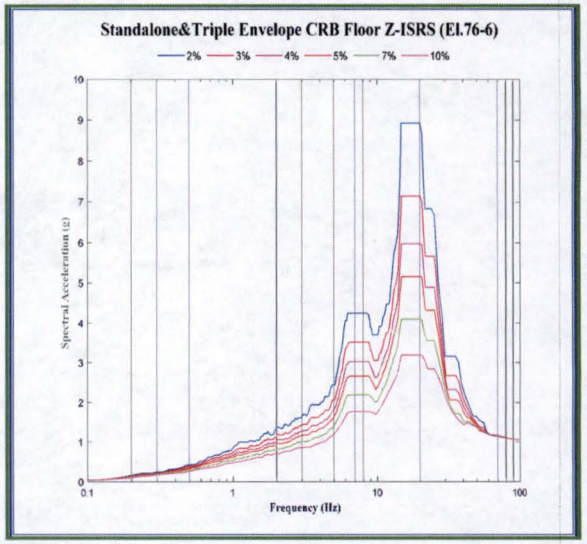
Figure 3.7.2-119a: Control Building - In-Structure Response Spectra at El. 76'-6" (Z=720"), 5 CSDRS Inputs